FIGURES

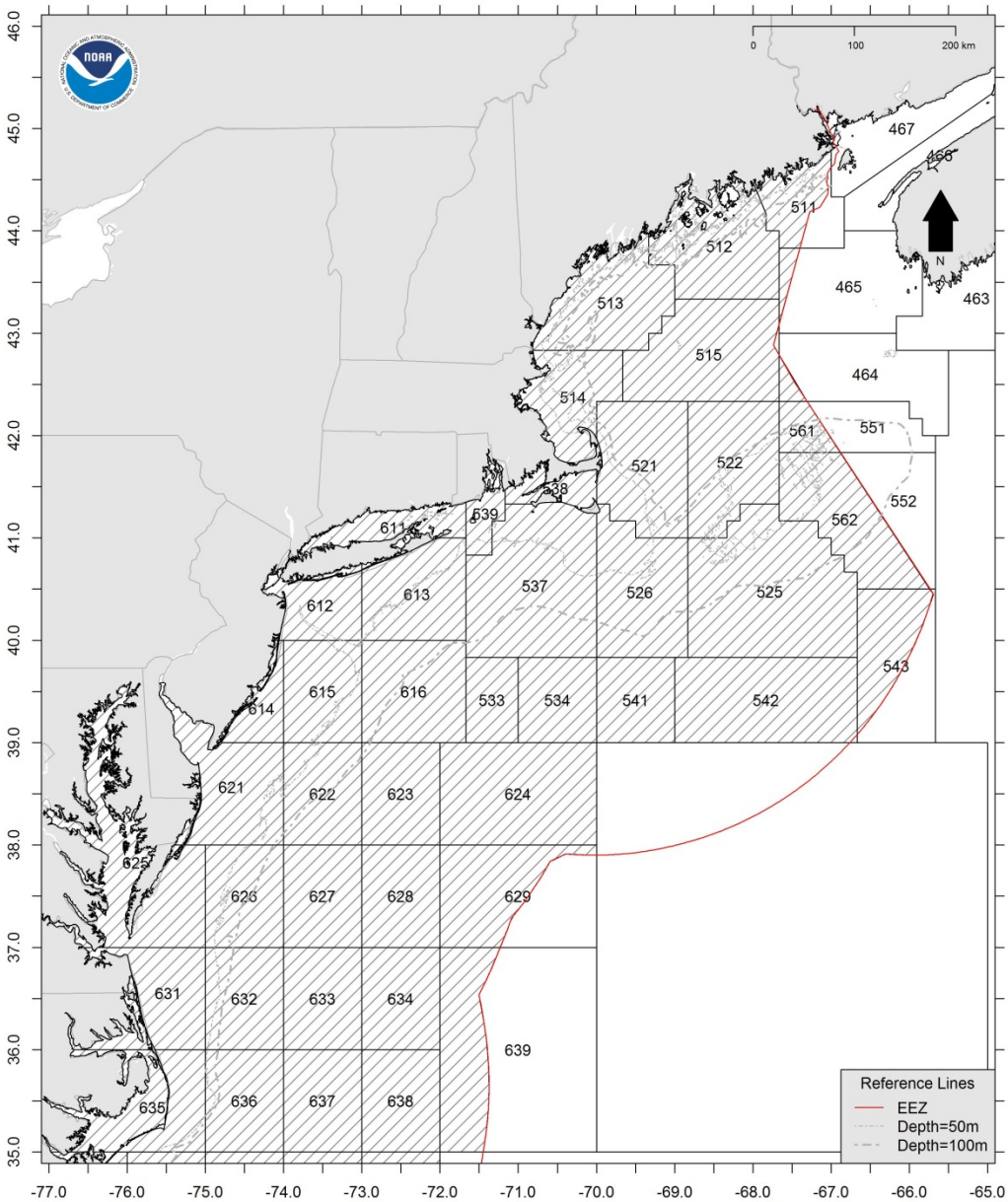

Figure B1. Statistical areas used for reporting commercial fishery statistics. Prior to 1985, statistical areas 551 and 561 comprised statistical area 523 and statistical areas 552 and 562 comprised statistical area 524. Shaded statistical areas delineate witch flounder stock area; Red line represents the U.S. Exclusive Economic Zone.

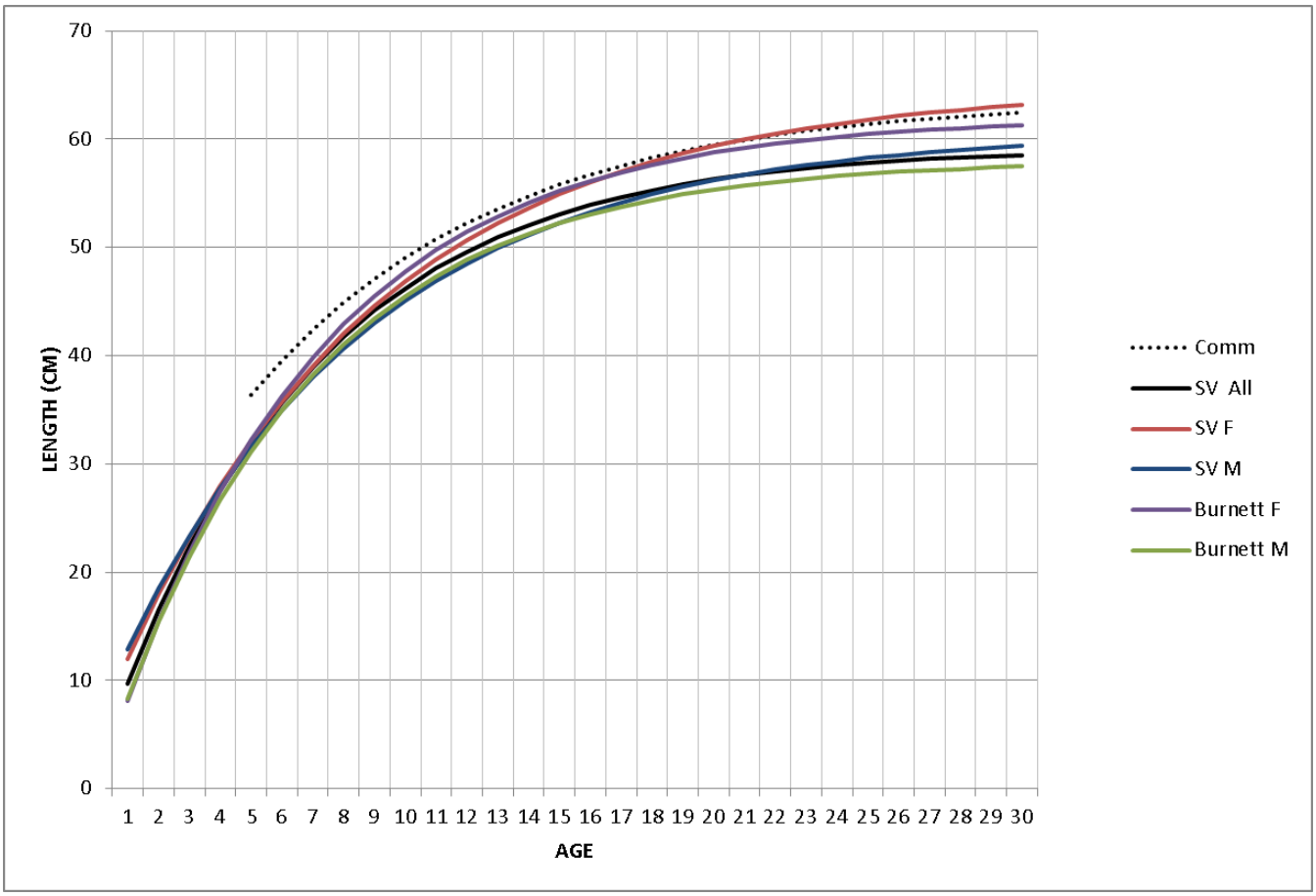

Figure B2. Von Bertalanffy growth curves based on witch flounder length and age data from commercial port sampling (Comm; black dotted line) in which sexes are combined from 1982-2015; Northeast Fisheries Science Center (NEFSC) survey sampling for females (SV F; red solid line), males (SV M; blue solid line) and all sexes combined (SV All; black solid line) from 1982-2015; and NEFSC survey sampling data 1980-1984 via Burnett (MS 1987) for females (Burnett F; purple solid line) and males (Burnett M; green solid line).

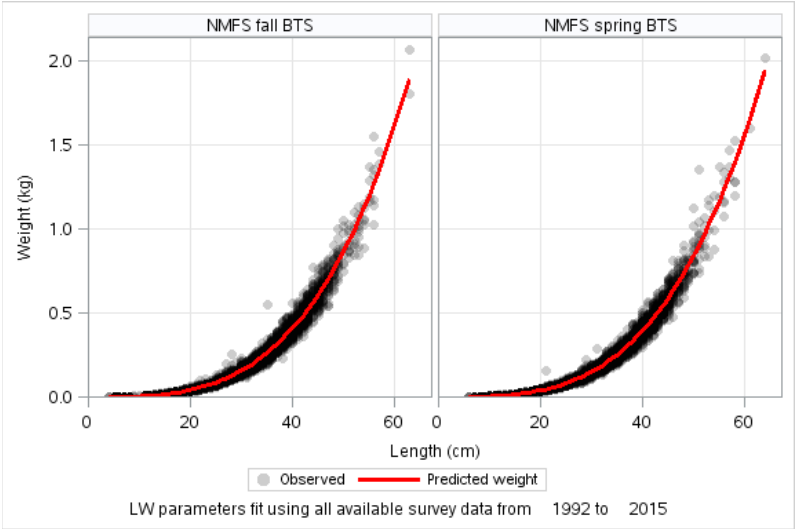

Figure B3. Length-weight relationships of witch flounder based on Northeast Fisheries Science Center research vessel bottom trawl survey for fall (left) and spring (right) for 1992 to 2015.

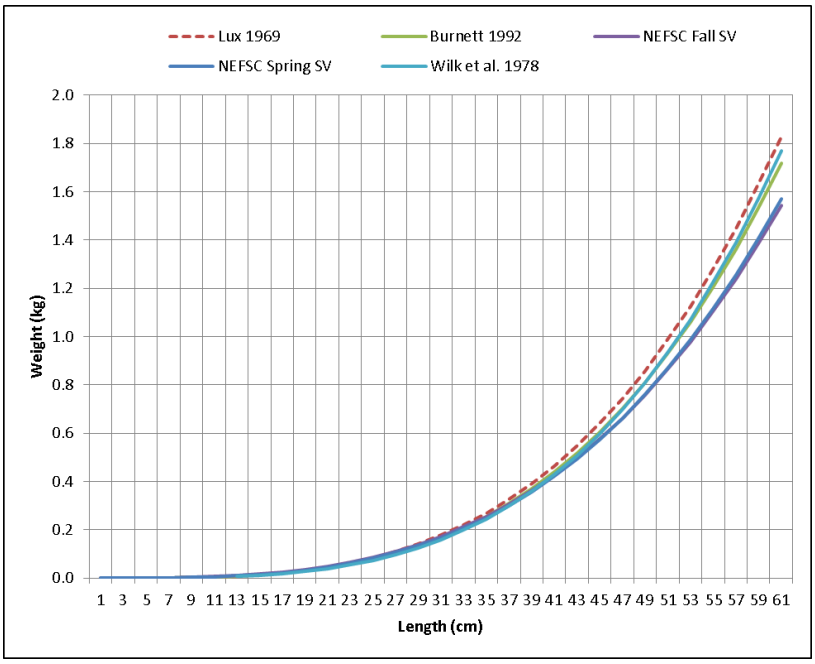

Figure B4. Length-weight relationships of witch flounder from Lux (1969; red dashed line), Burnett et al. (1992; green line), Wilk et al. (1978; light blue line), and1992-2015 Northeast Fisheries Science Center spring survey (blue line) and fall survey (purple line) derived in the current assessment.

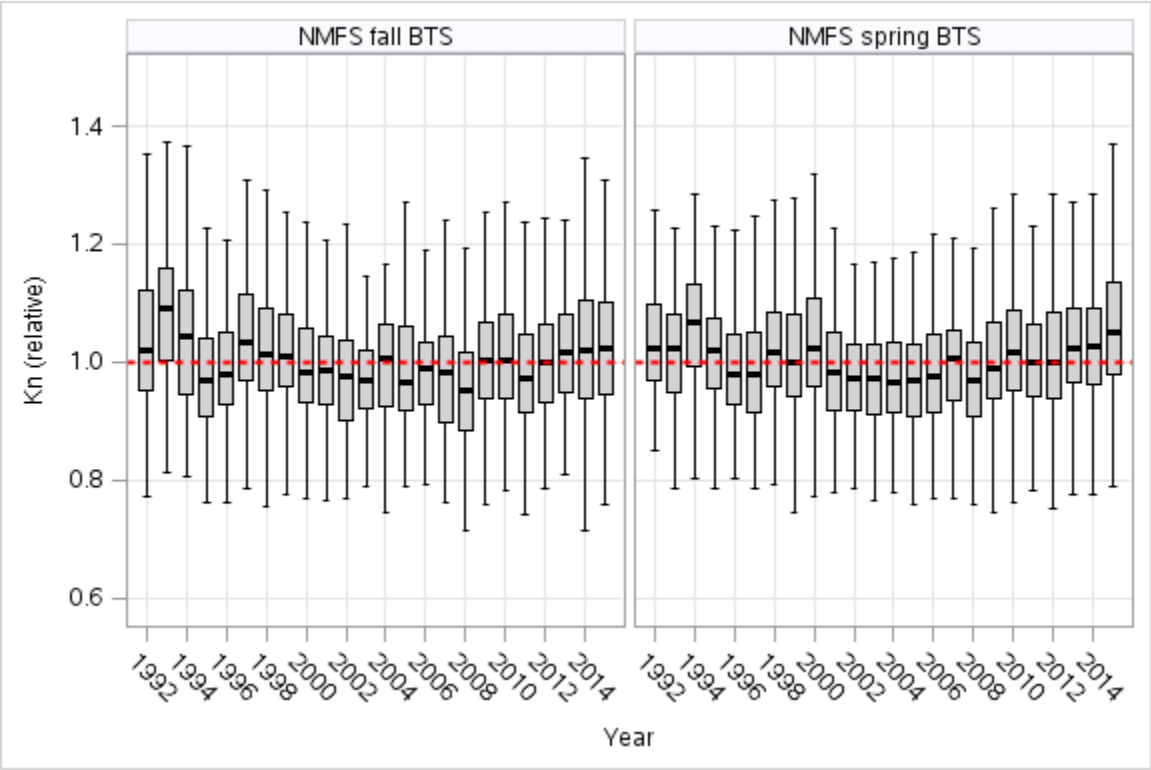

Figure B5. Annual trends in relative condition factor of witch flounder based on length and weight data from the Northeast Fisheries Science Center bottom trawl survey, spring and fall, 1982- 2015.

.

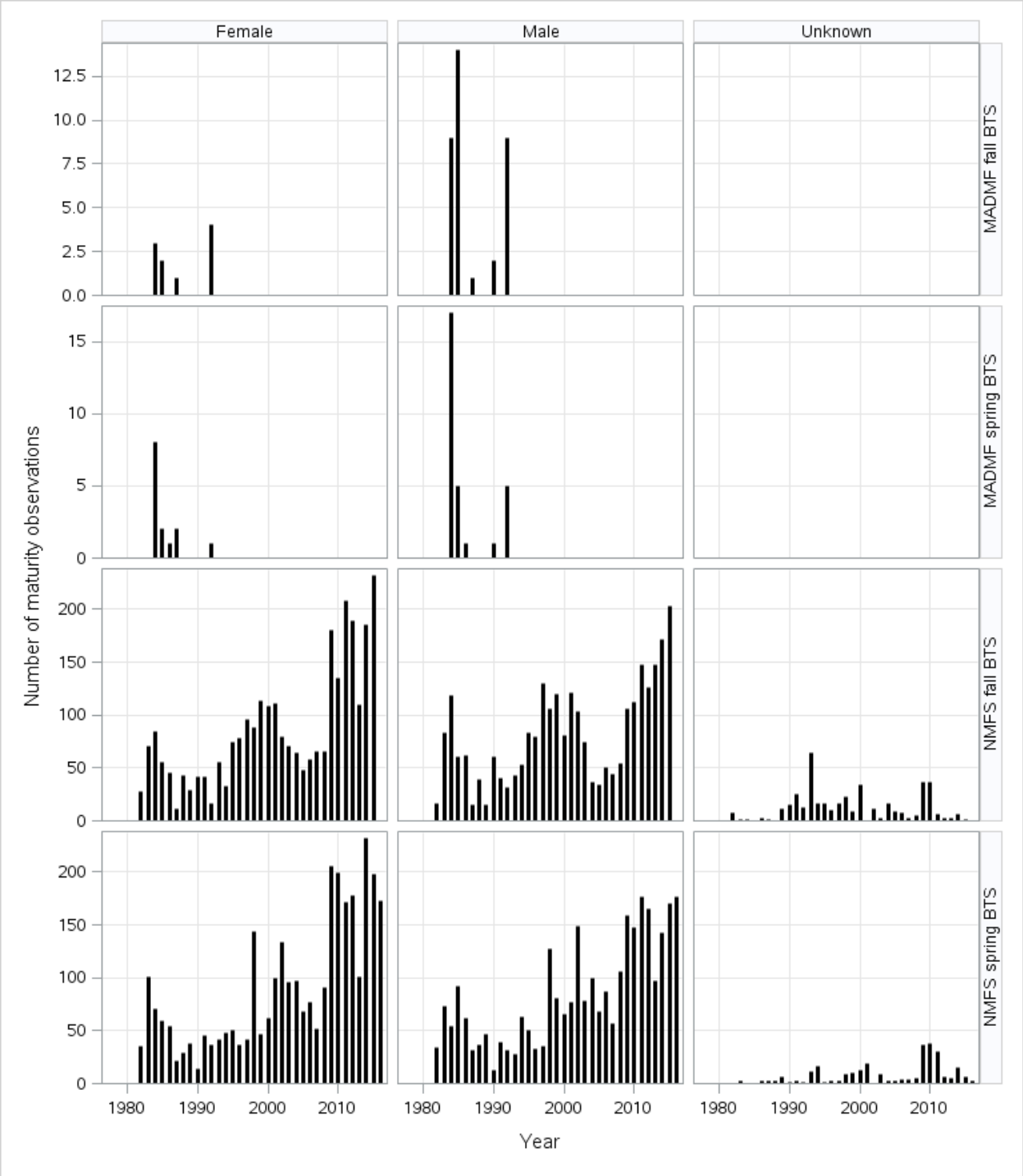

Figure B6. Number of fish with maturity observations, by year and sex, taken during Northeast Fisheries Science Center bottom trawl surveys (spring and fall), Massachusetts Division of Marine Fisheries (spring and fall).

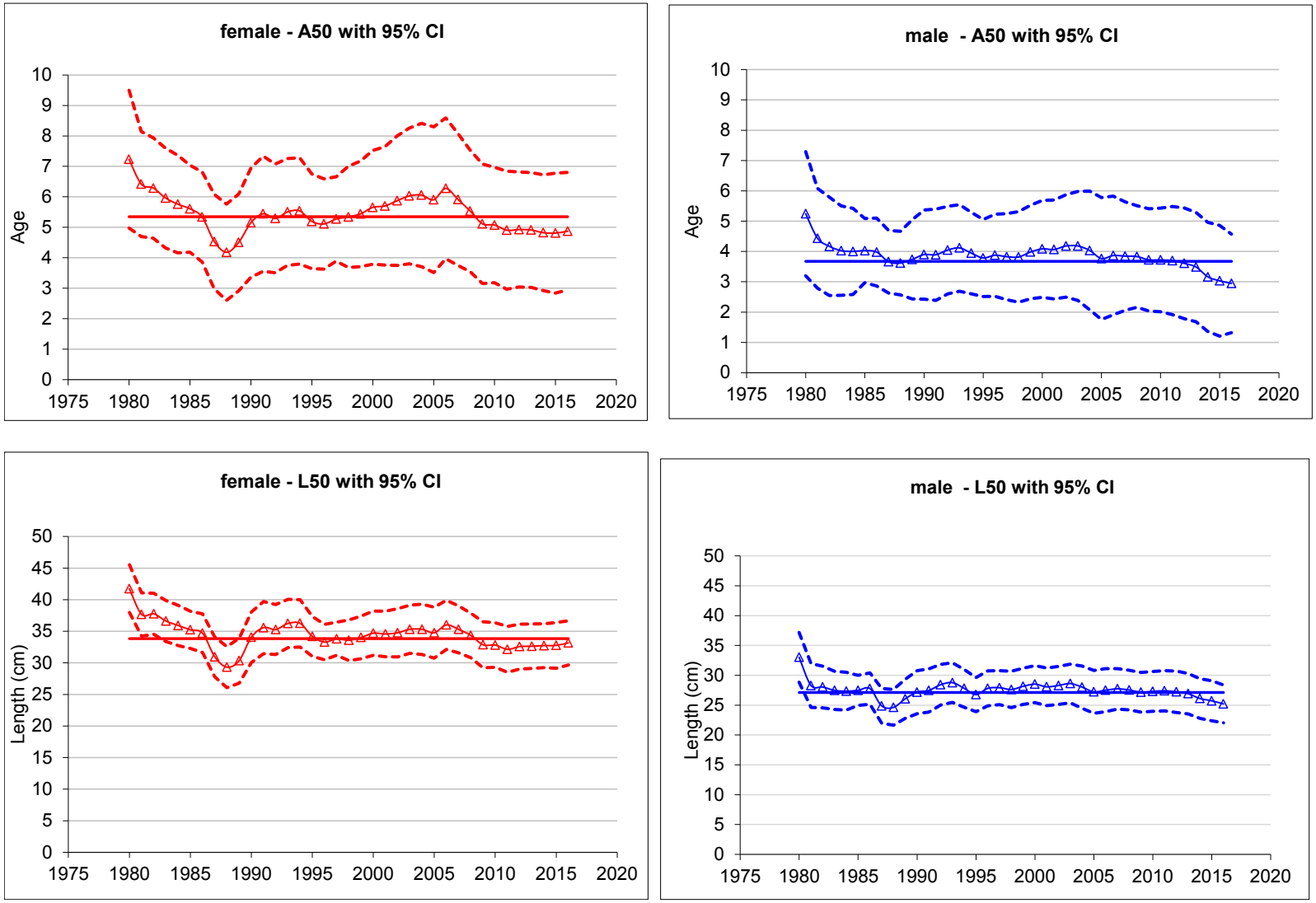

Figure B7. Annual estimates of median age (A50; top) and length (L50; bottom) of female (left) and male (right) witch flounder maturity derived from a five-year moving time block of maturity observations collected during the Northeast Fisheries Science Center spring survey, 1980 – 2016. Time series average is indicated in solid line; dash lines indicate 95% confidence intervals.

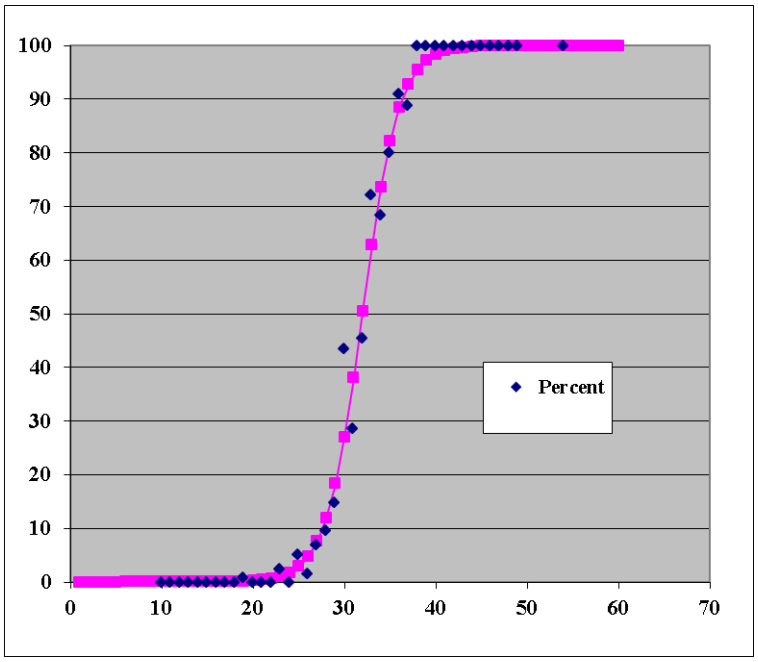

Figure B8. Percent mature at length (cm) of female witch flounder derived from data collected during spring and fall Maine-New Hampshire inshore trawl survey (strata 1-4; regions 1-5). (S. Sherman, ME DMR, pers comm. July 2016)

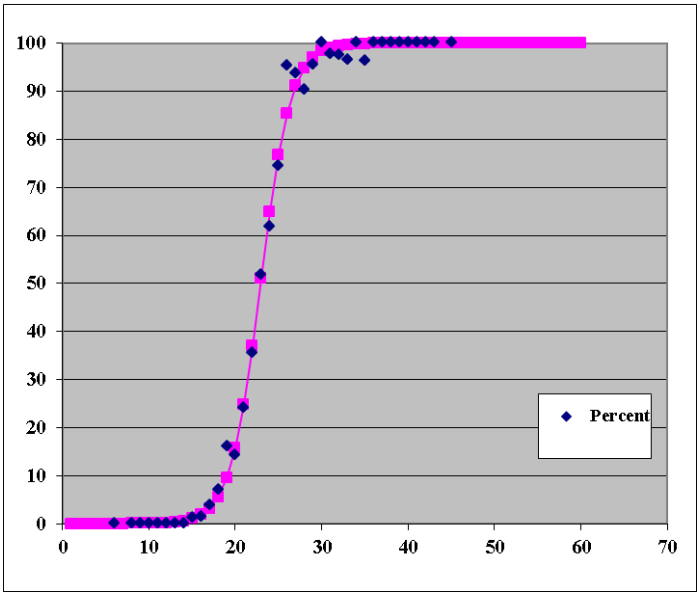

Figure B9. Percent mature at length (cm) of male witch flounder from data collected during spring and fall Maine-New Hampshire inshore trawl survey (strata 1-4; regions 1-5). (S. Sherman, ME DMR, pers comm July 2016)

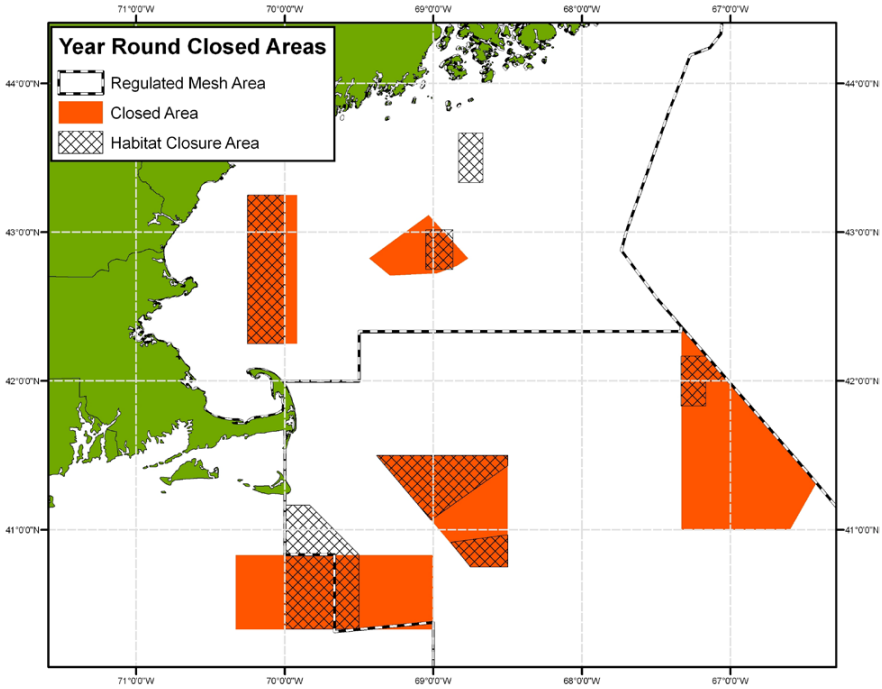

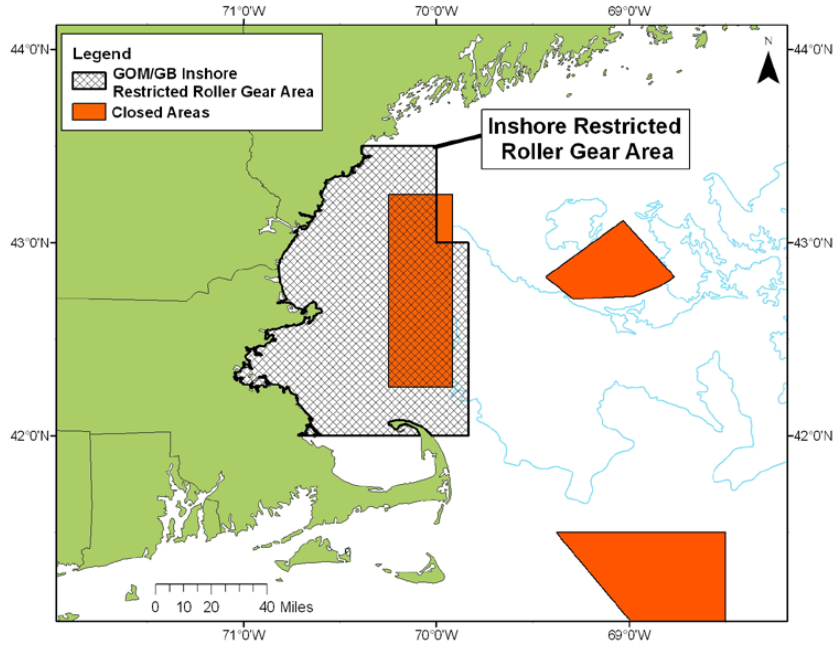

Figure B10. Current (fishing year 2016) year around closed areas (Western Gulf of Maine, Cashes Ledge, Closed Area I, II and Nantucket Lightship Closed Area shown in orange and essential fish habitat areas shown in hatched shading) in the Gulf of Maine and Georges Bank region. Taken from Northeast Multispecies Information Sheet" Closed Area Regulations (April 29, 2016); available online at .
https://www.greateratlantic.fisheries.noaa.gov/regs/infodocs/multsclosedareas.pdf
http://www.greateratlantic.fisheries.noaa.gov/sustainable/species/multispecies/
https://www.greateratlantic.fisheries.noaa.gov/sustainable/species/multispecies/index.html

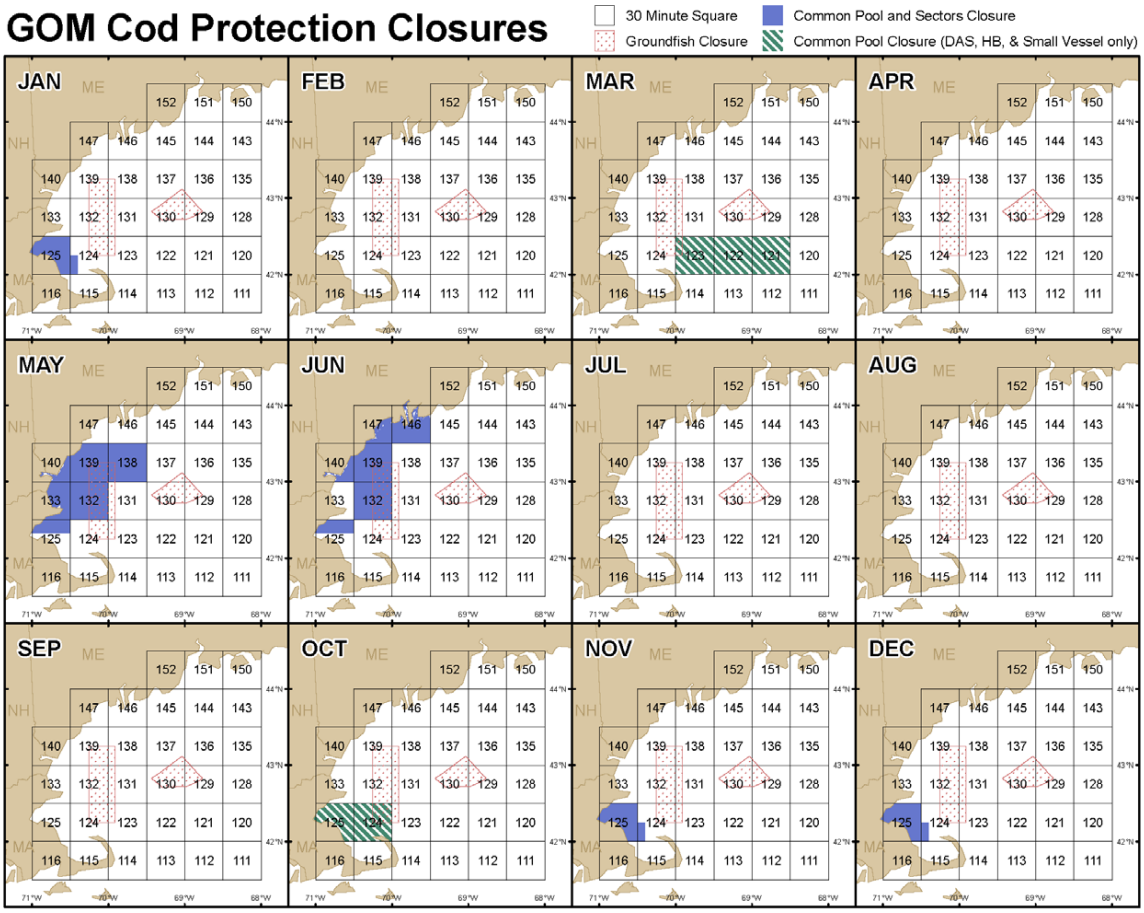

Figure B11. Gulf of Maine cod protection closures in fishing year 2016 to the Northeast Multispecies fishery management plan.

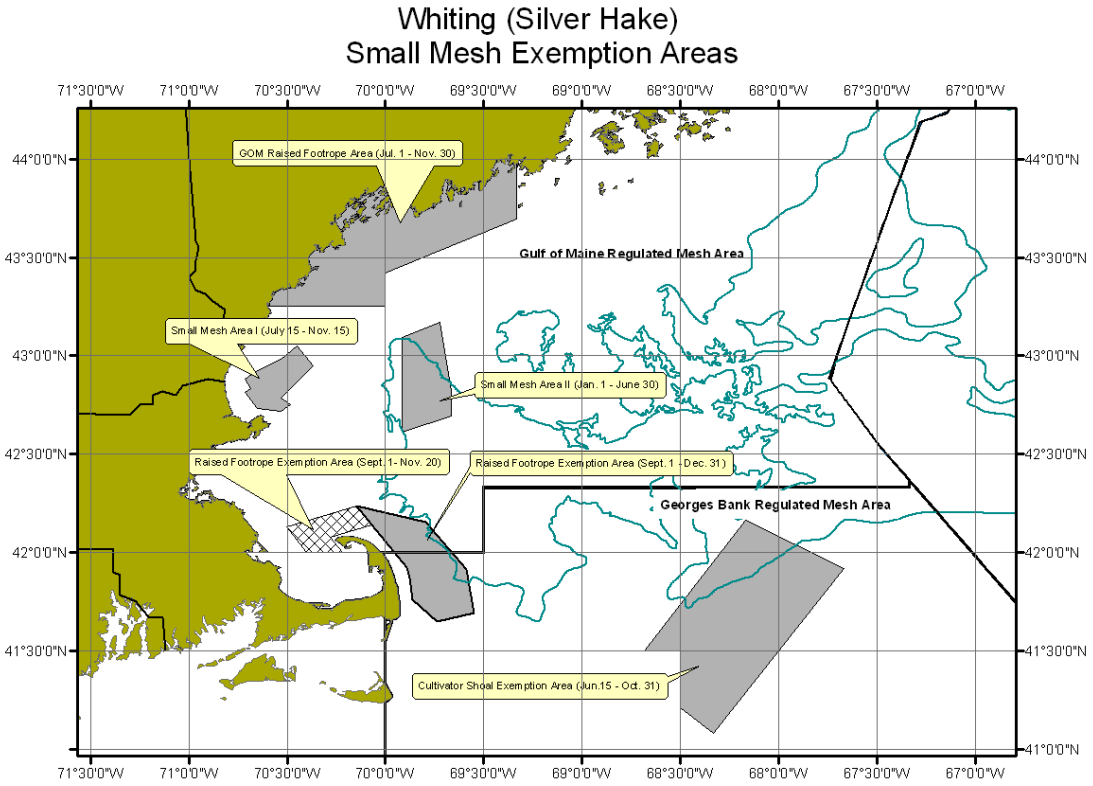

Figure B12. Small mesh exemption area in the Gulf of Maine – Georges Bank region.

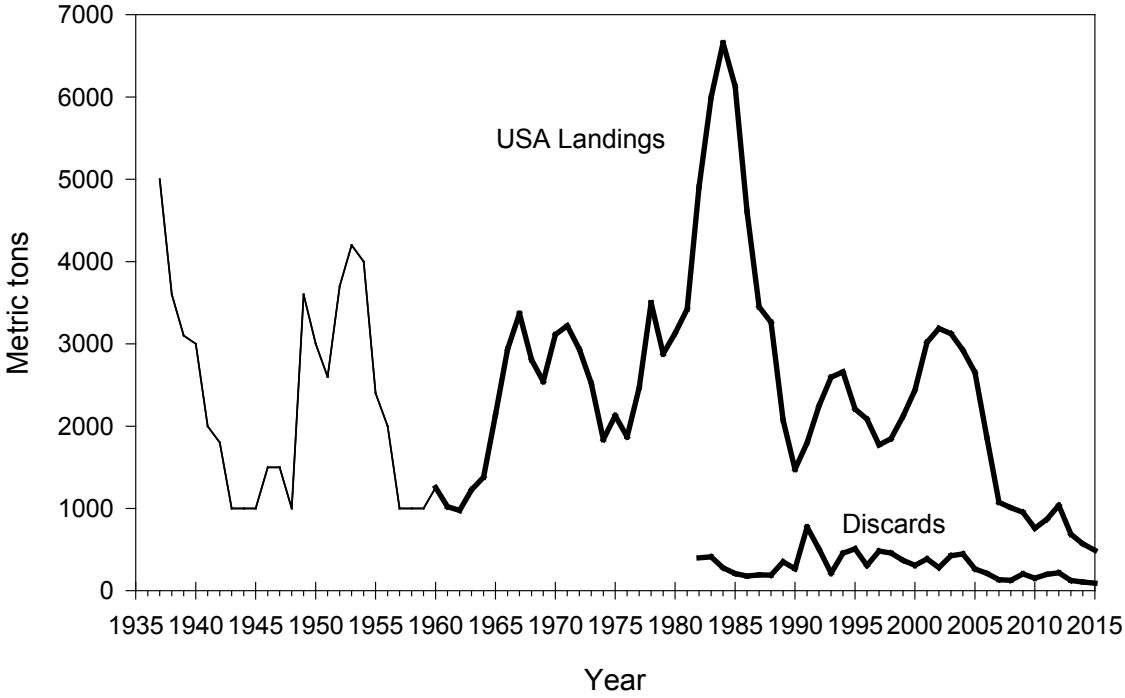

Figure B13. USA witch flounder landings (mt), excluding USA landings from the Grand Banks in the mid-1980's. The thin line represents provisional landings data taken from Lange and Lux (1978). Discards are from the Gulf of Maine shrimp trawl, scallop dredge, gillnet, haddock separator trawl, small-mesh (<5.5 inch) otter trawl and large-mesh (>5.5 inch) otter trawl fisheries.

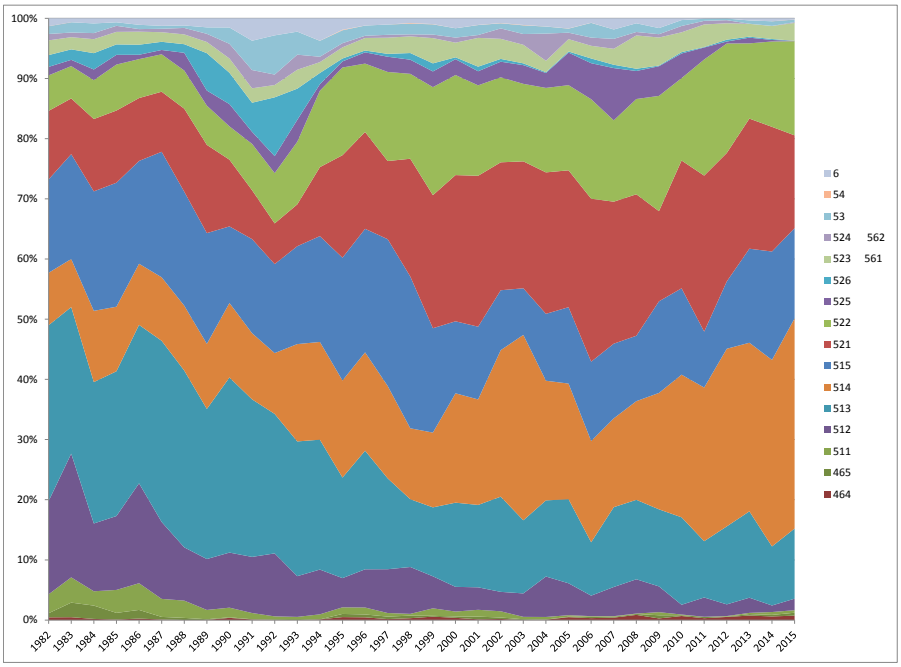

Figure B14. Percentage of witch flounder landings by statistical area, 1982 to 2015.

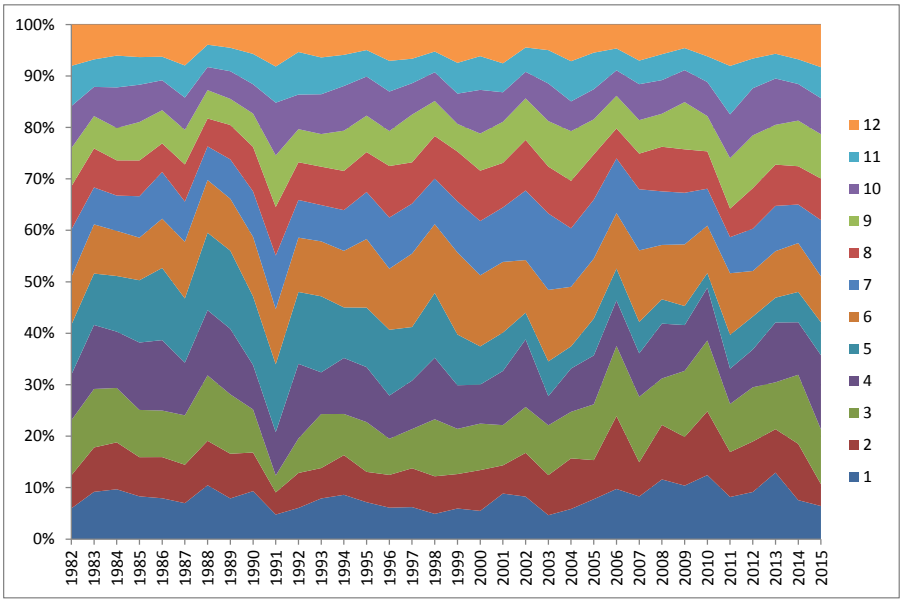

Figure B15. Percentage of witch flounder landings by month, 1982 to 2015.

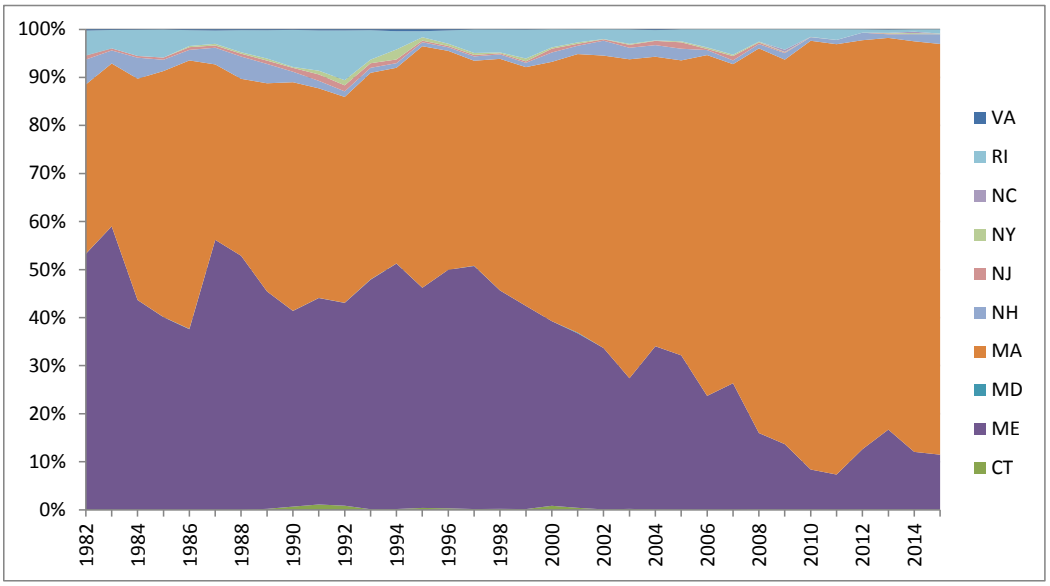

Figure B16. Percentage of witch flounder landings by state, 1982 to 2015.

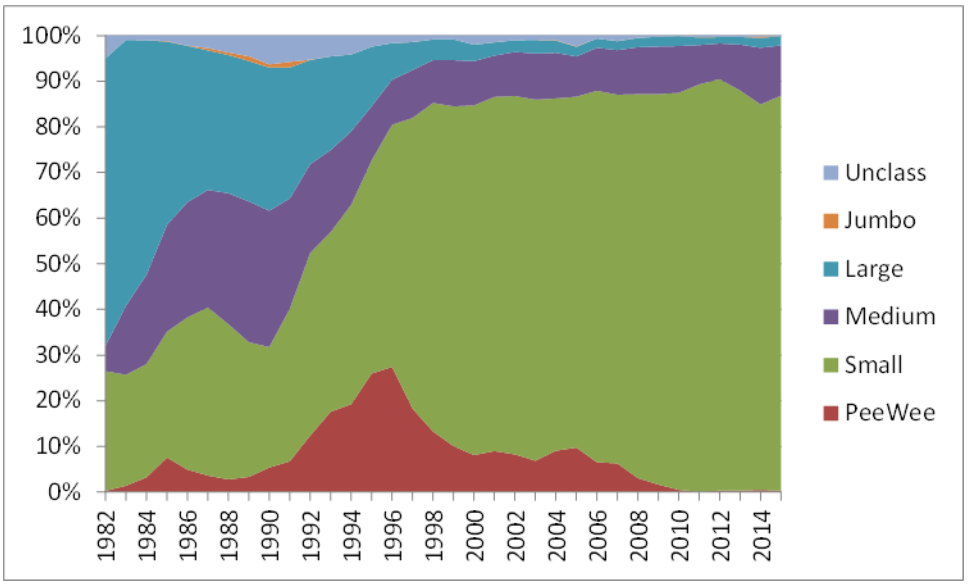

Figure B17. Percentage of witch flounder landings by market category, 1982 to 2015.

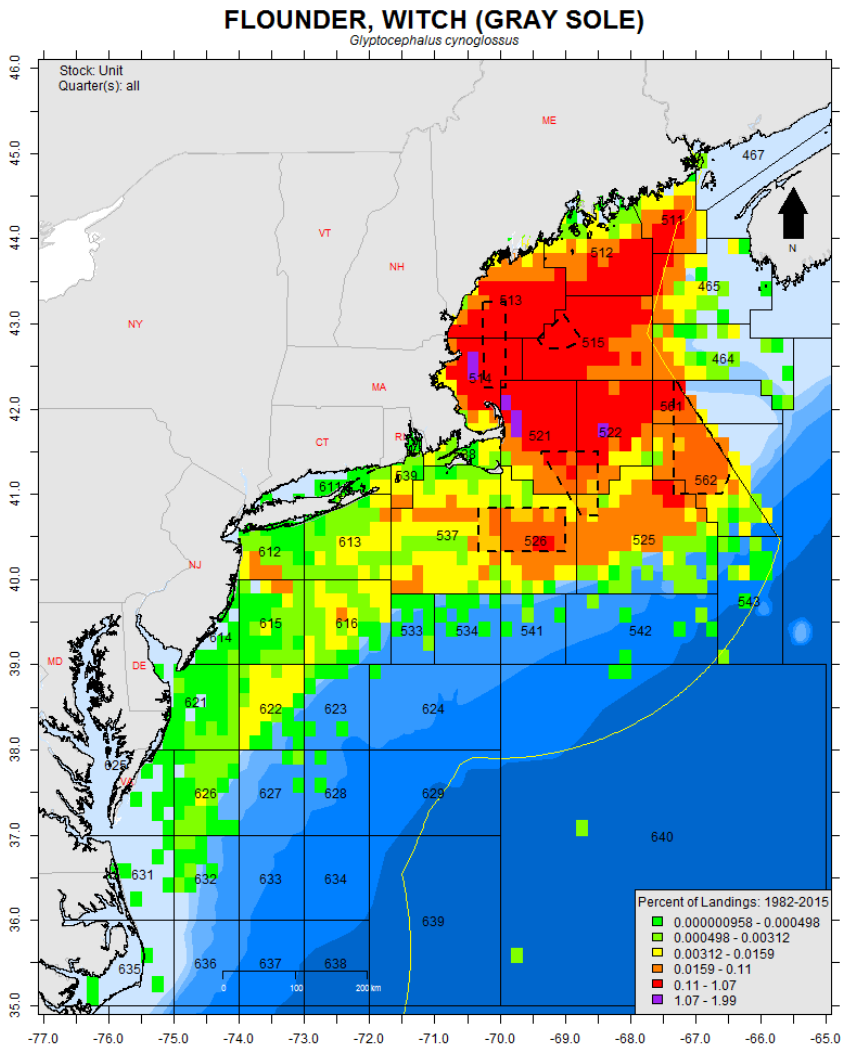

Figure B18. Distribution of commercial landings by ten minute square of latitude/longitude from 1982 – 2015.

This map represents commercial landings for FLOUNDER, WITCH (GRAY SOLE), *Glyptocephalus cynoglossus*. Landings were reported via Dealer reports. Data from 1982 - 1993, have been restricted to interviewed weighout trips (INTV=1), and data from 1994 - 2015 have been restricted to dealer trips matched to a Vessel Trip Report (VTR) (ALEVEL=A) to ensure gear and area information is as accurate as possible.

Landings from all quarters are displayed.

Due to incomplete location data, the map depicts 56.81% of the total catch reported for the species and time frame noted.

Northeast Fisheries Science Center statistical areas are represented by numbered polygons and bathymetry is depicted in blue shading. Groundfish closed areas (dashed borders), and the Exclusive Economic Zone (yellow line) have been overlaid for your reference.

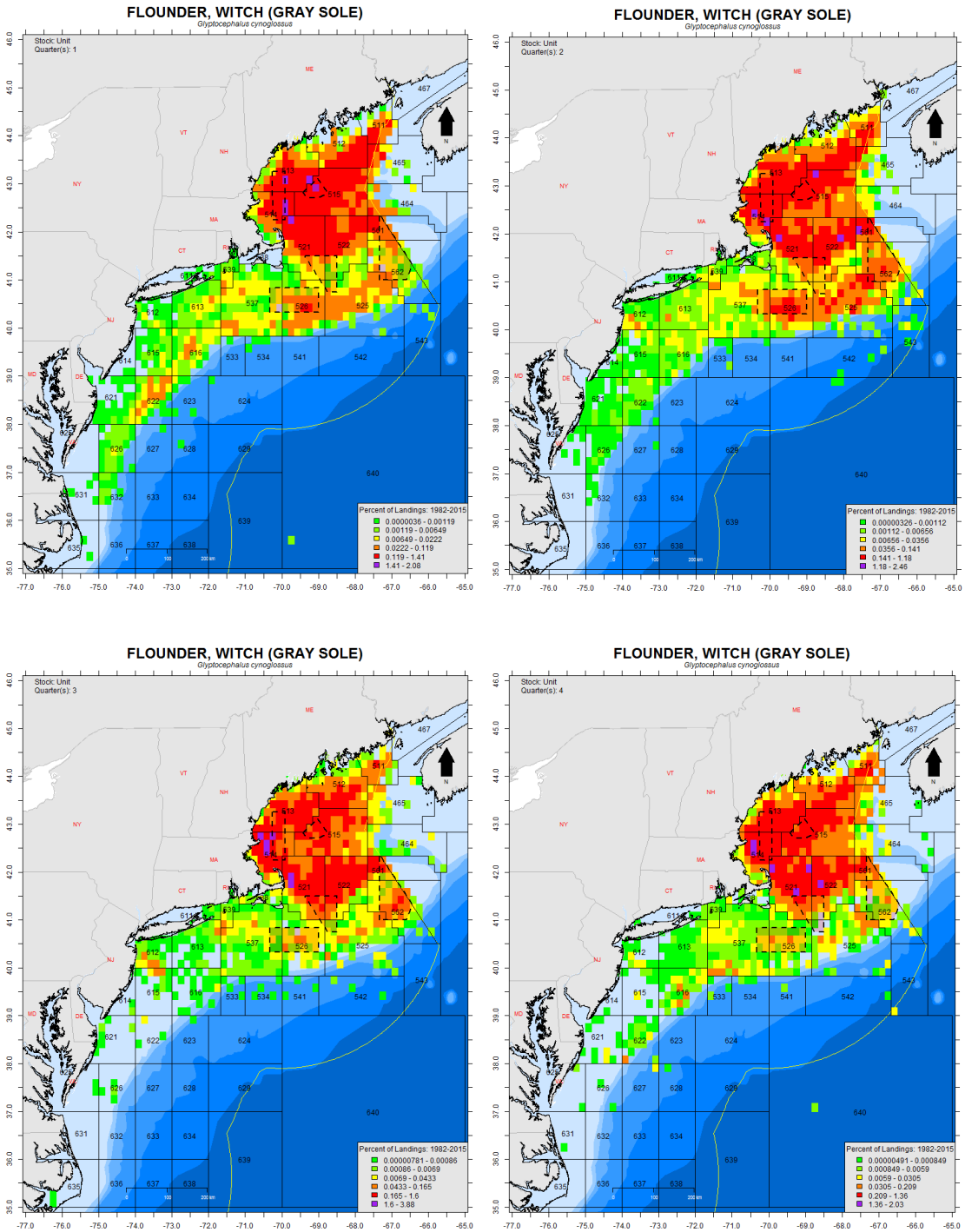

Figure B19. Distribution of witch flounder landing by calendar quarter and ten minute square latitude/longitude with Quarter 1 (top left), Qtr 2 (top right), Qtr 3 (lower left), and Qtr 4 (lower right).

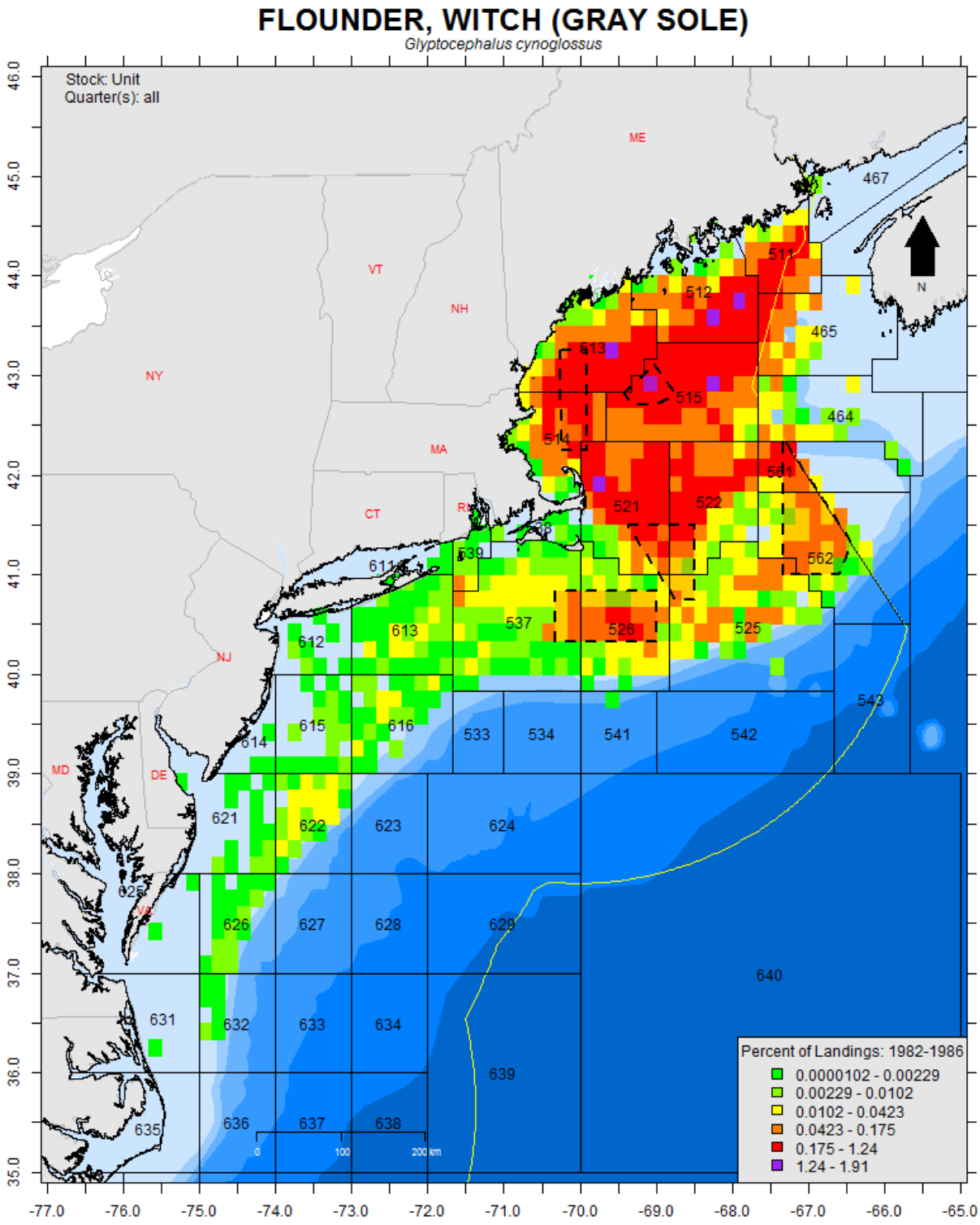

Figure B20. Distribution of witch flounder landing by ten minute square latitude/longitude , 1982 – 1986.

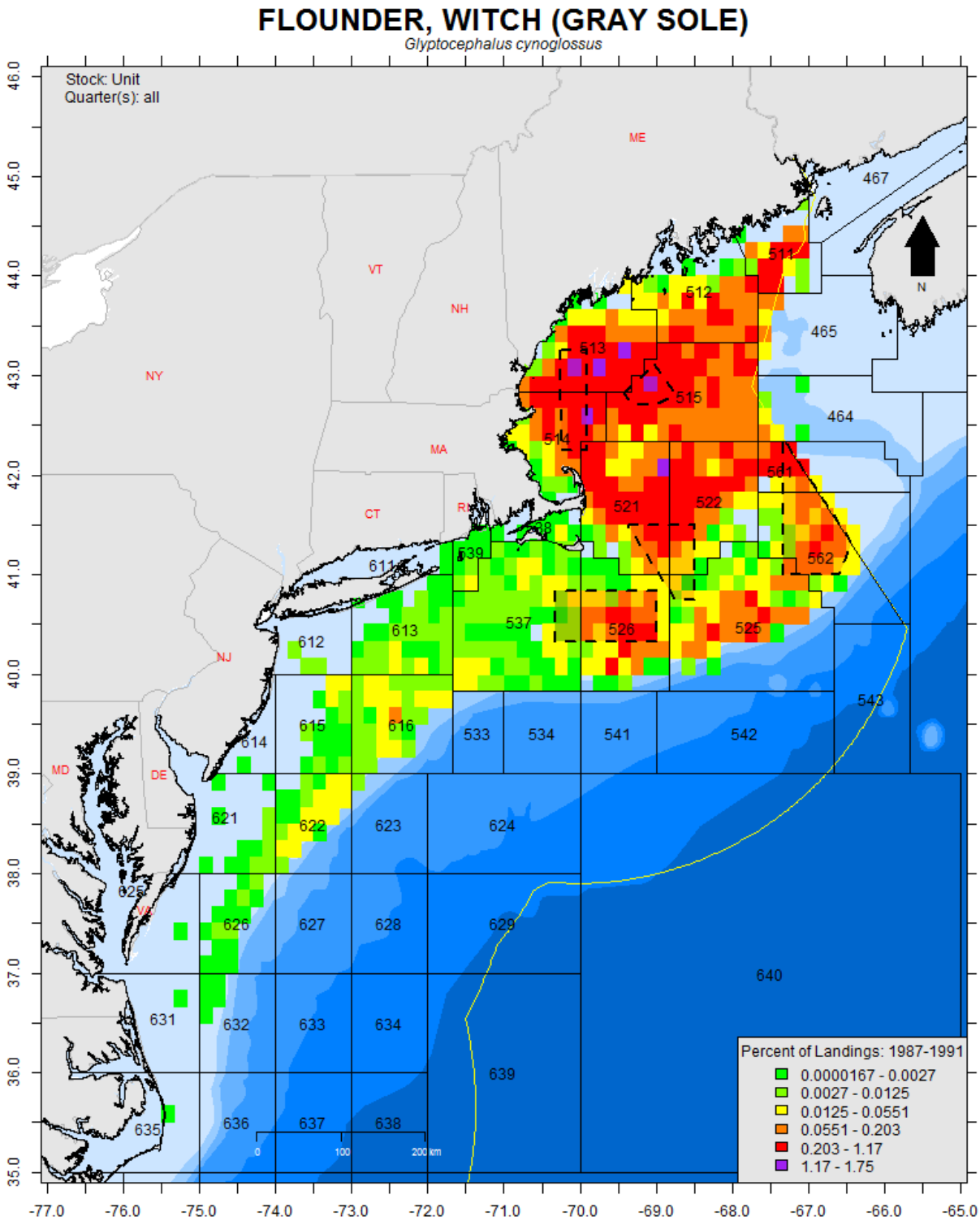

Figure B20 continued. Distribution of witch flounder landing by ten minute square latitude/longitude, 1987 - 1991

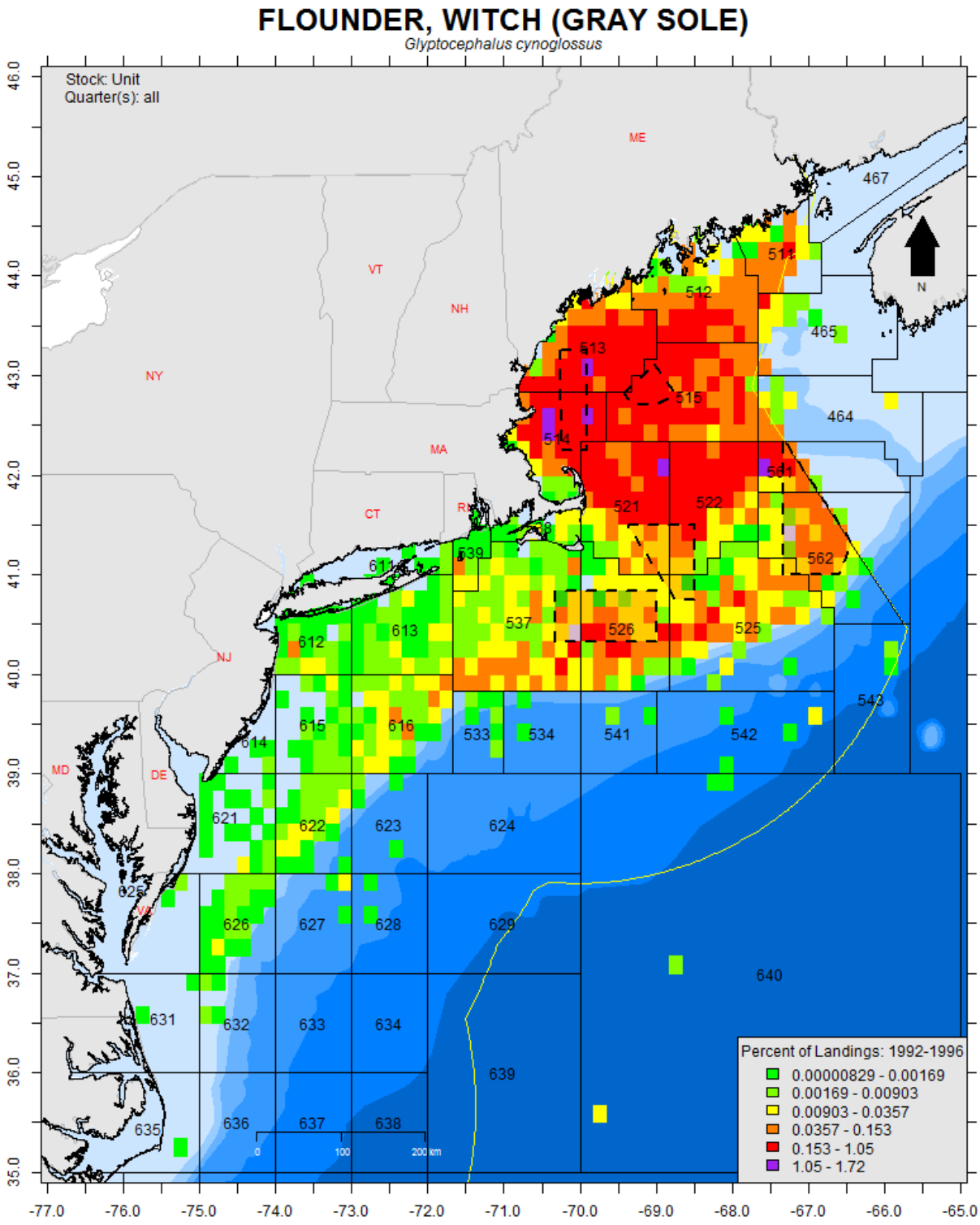

Figure B20 continued. Distribution of witch flounder landing by ten minute square latitude/longitude, 1992 – 1996

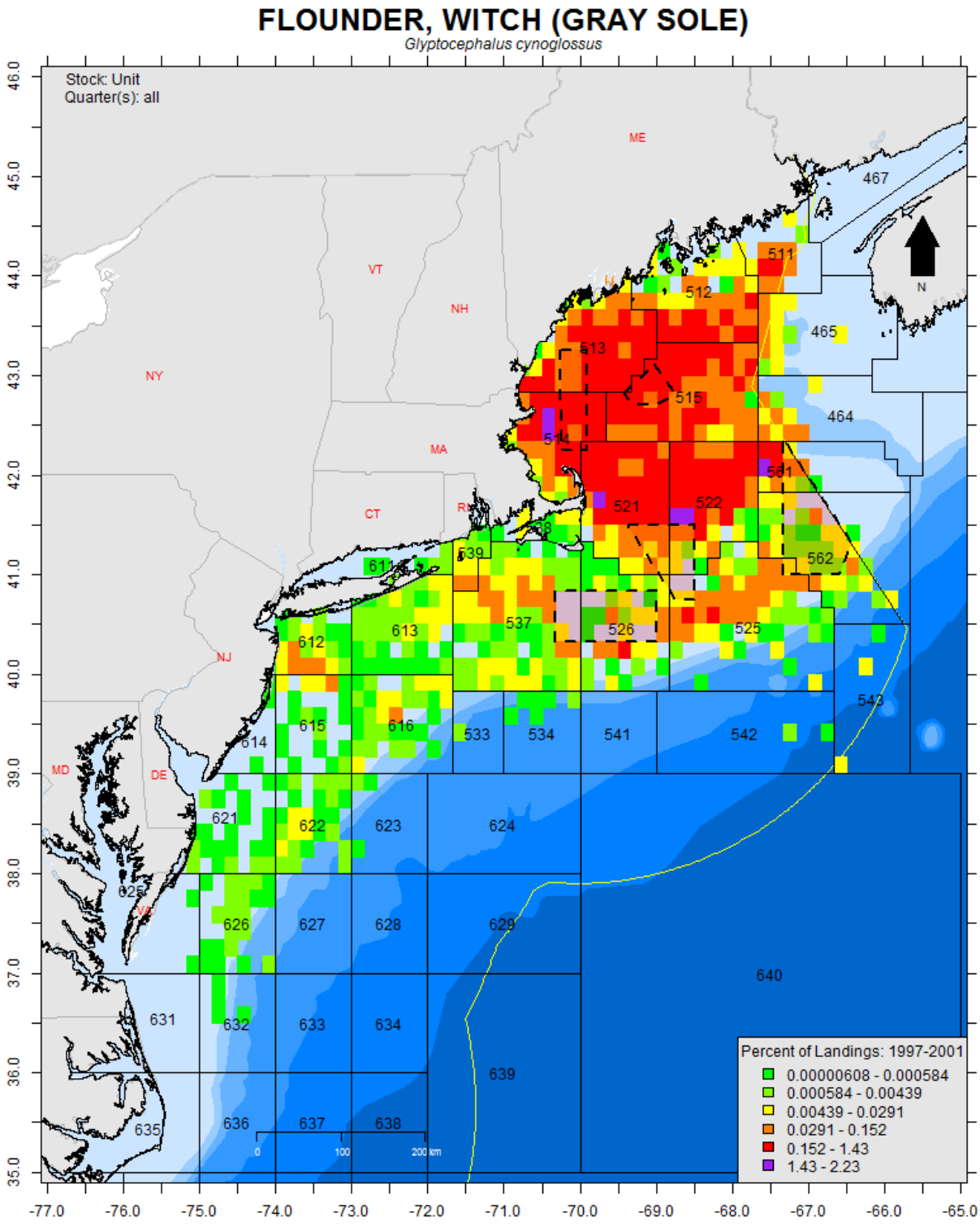

Figure B20 continued. Distribution of witch flounder landing by ten minute square latitude/longitude 1997- 2001.

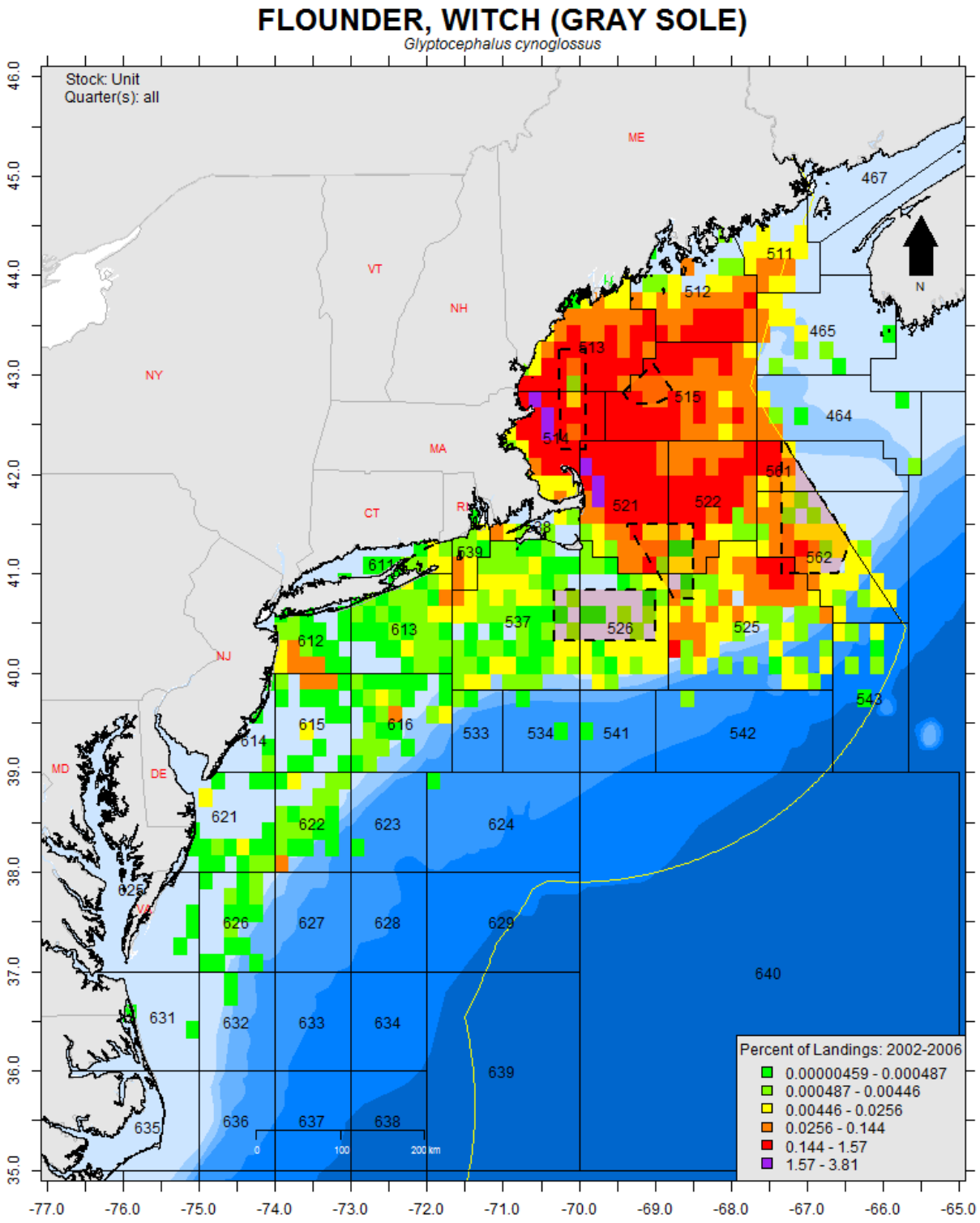

Figure B20 continued. Distribution of witch flounder landing by ten minute square latitude/longitude, 2002-2006.

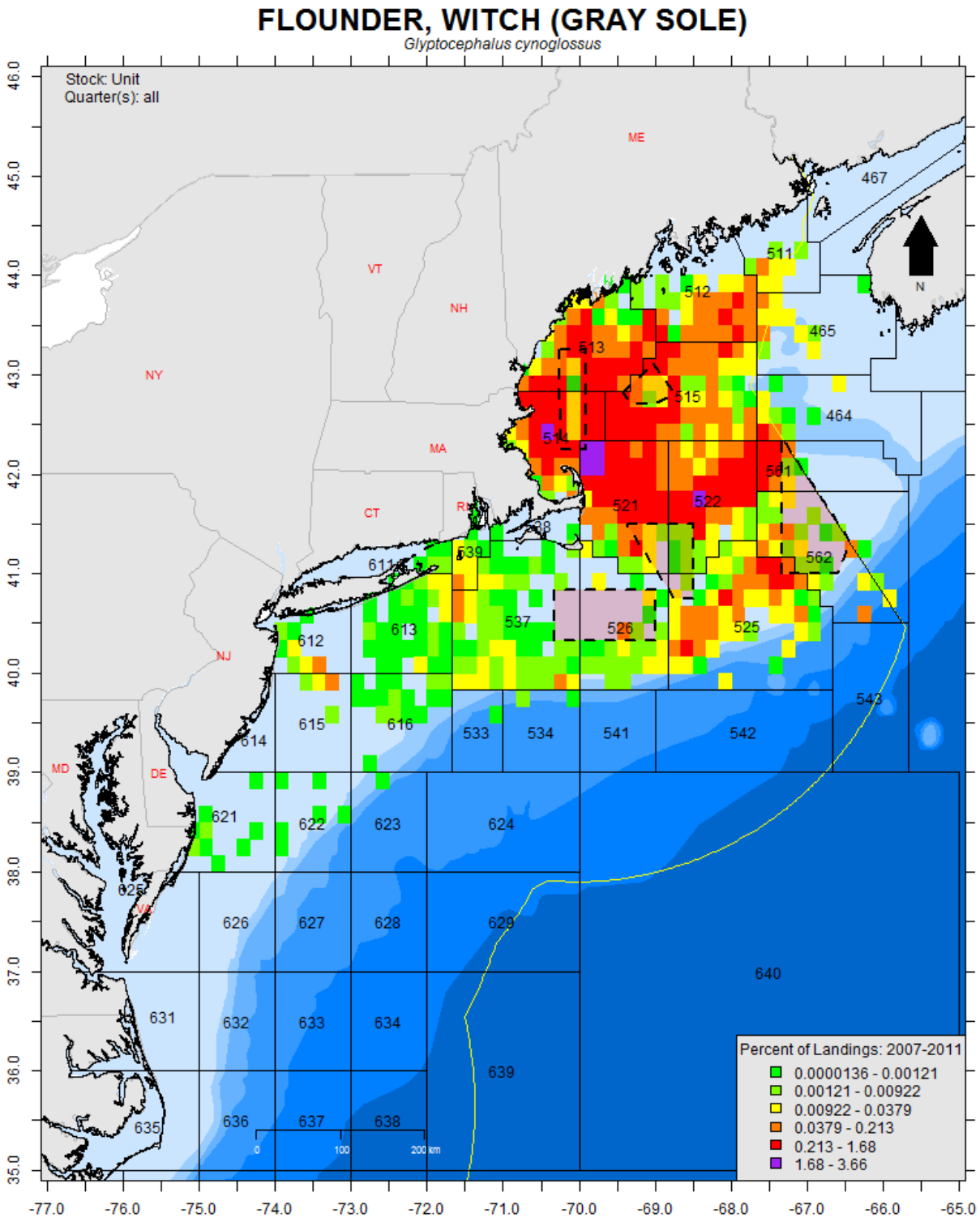

Figure B20 continued. Distribution of witch flounder landing by ten minute square latitude/longitude, 2007-2011.

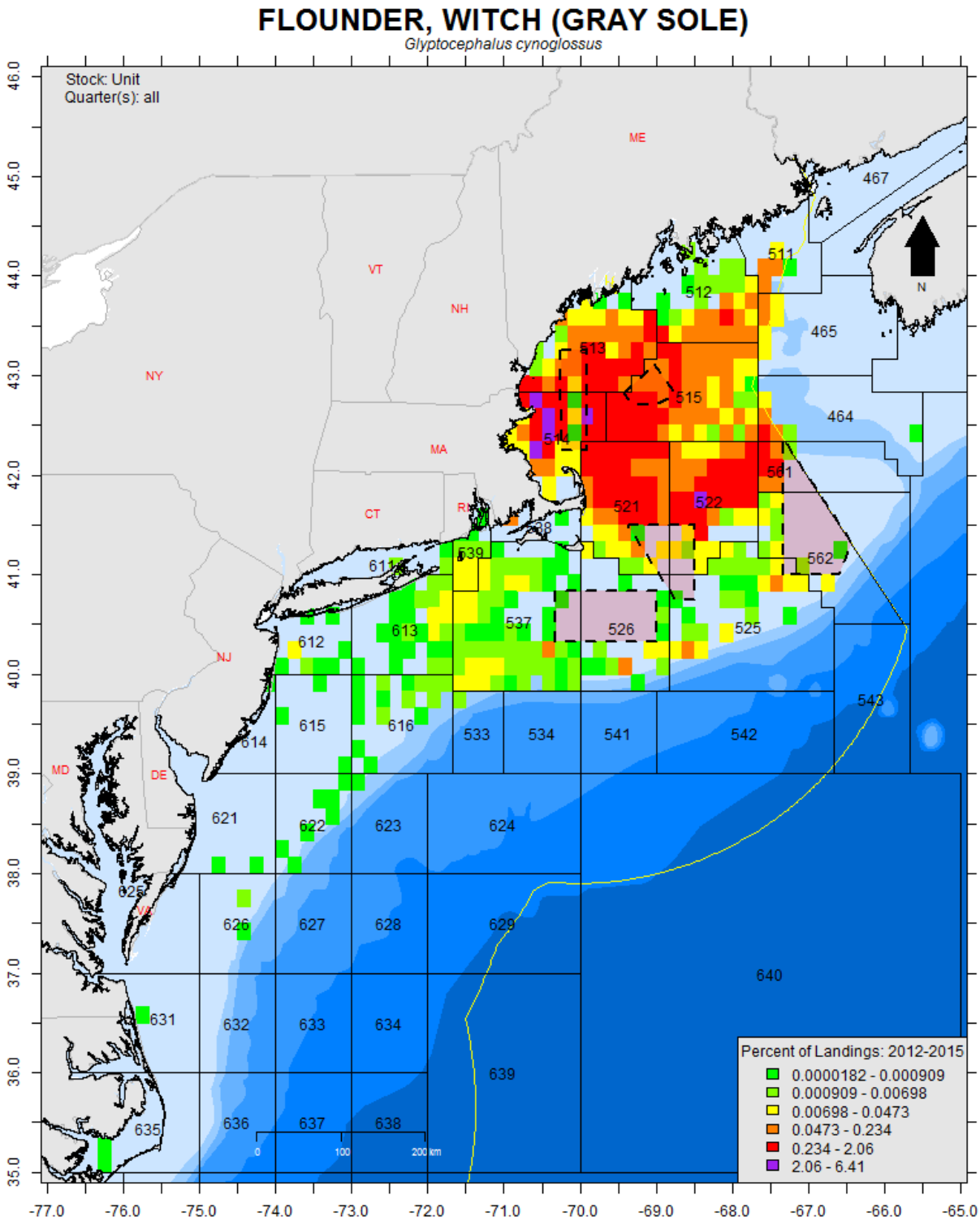

Figure B20 continued. Distribution of witch flounder landing by ten minute square latitude/longitude, 2012 – 2015.

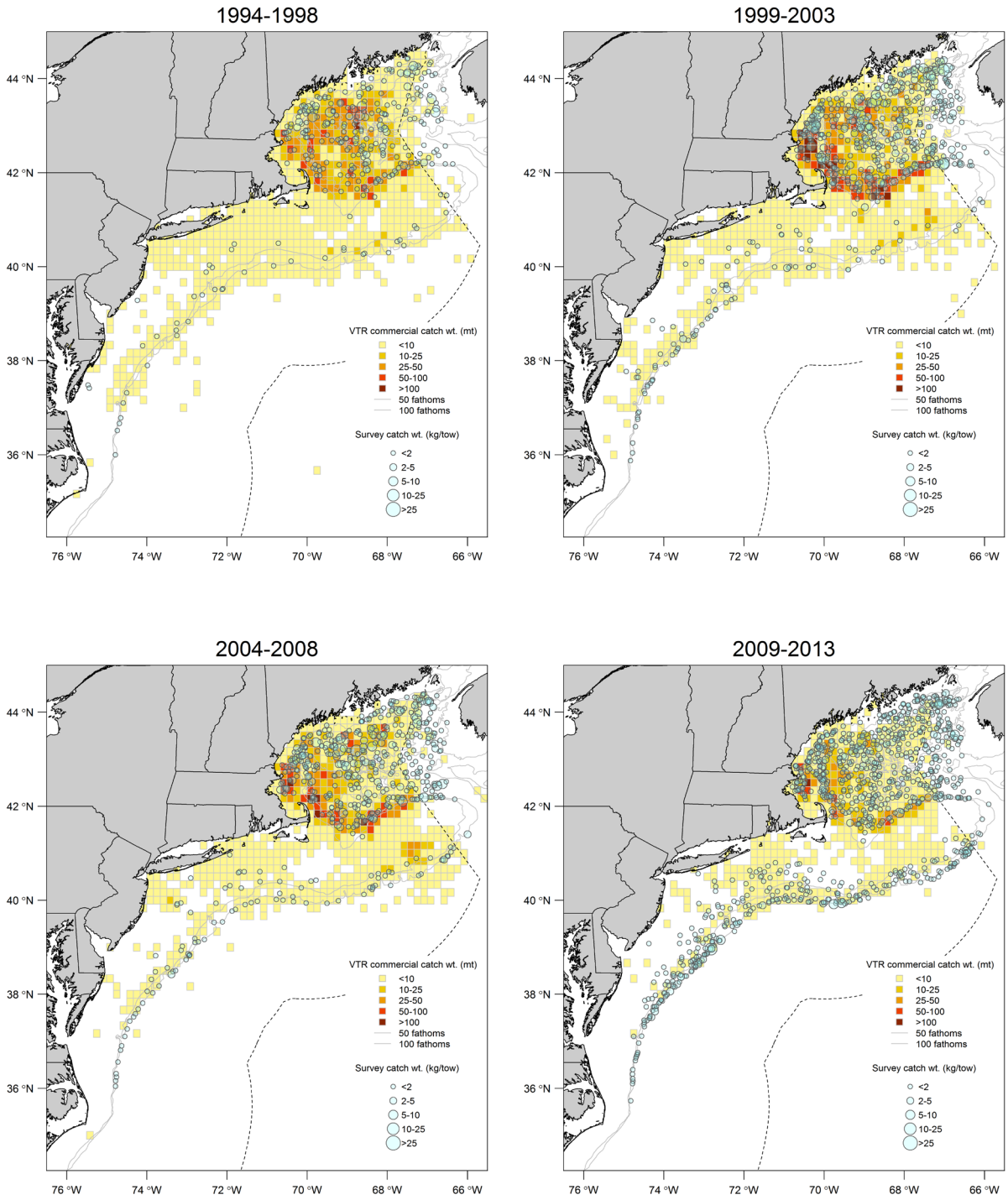

Figure B21. Distribution of commercial trawl catch (landings and discards per trip) as recorded in Vessel Trip Report (VTR) compared with annual Northeast Fisheries Science Center survey catches (kg/tow), by 5-year time blocks (1994-1998, 1999-2003, 2004-2008, 2009-2013; and 2-year block 2014-2015).

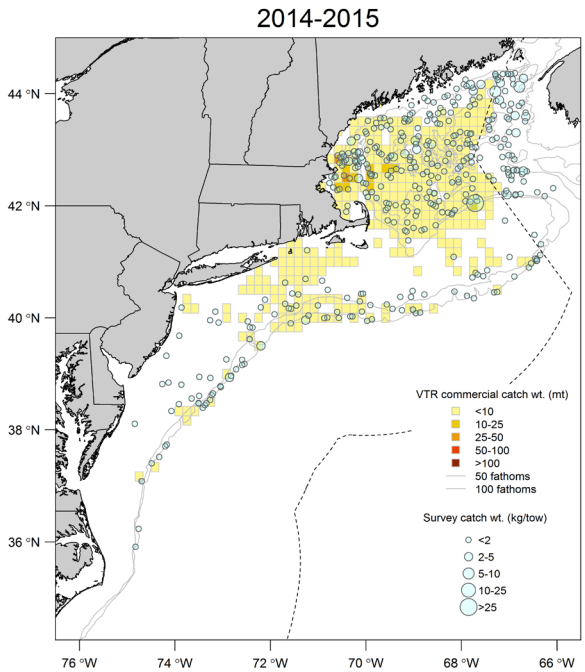

Figure B21, continued. Distribution of commercial trawl catch (landings and discards per trip) as recorded in Vessel Trip Report (VTR) compared with annual Northeast Fisheries Science Center survey catches (kg/tow), by 5-year time blocks.

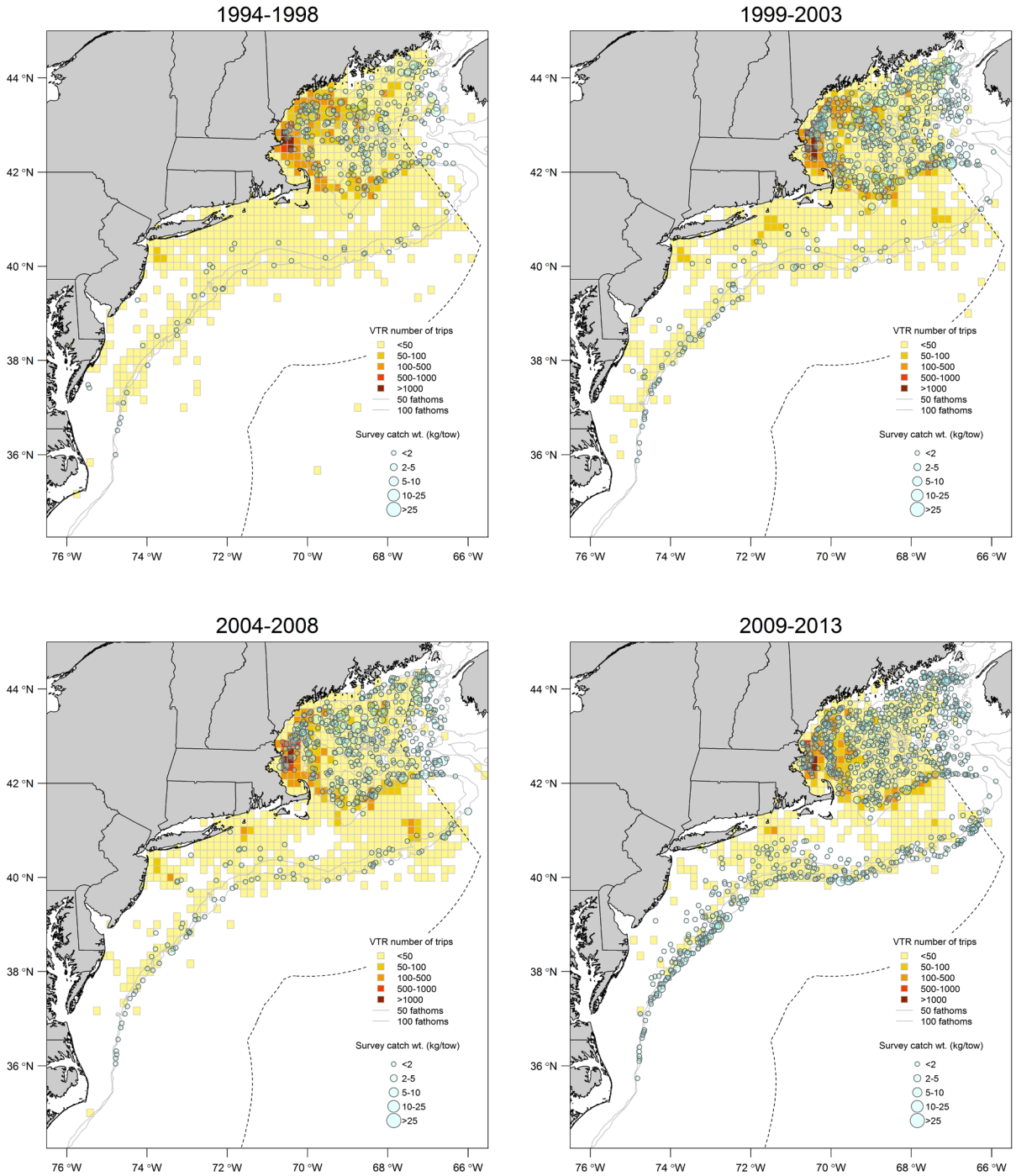

Figure B22. Distribution of commercial trawl trips as recorded in Vessel Trip Report (VTR) compared with annual Northeast Fisheries Science Center survey catches (kg/tow), by 5-year time blocks, (1994-1998, 1999-2003, 2004-2008, 2009-2013; and 2-year block 2014-2015).

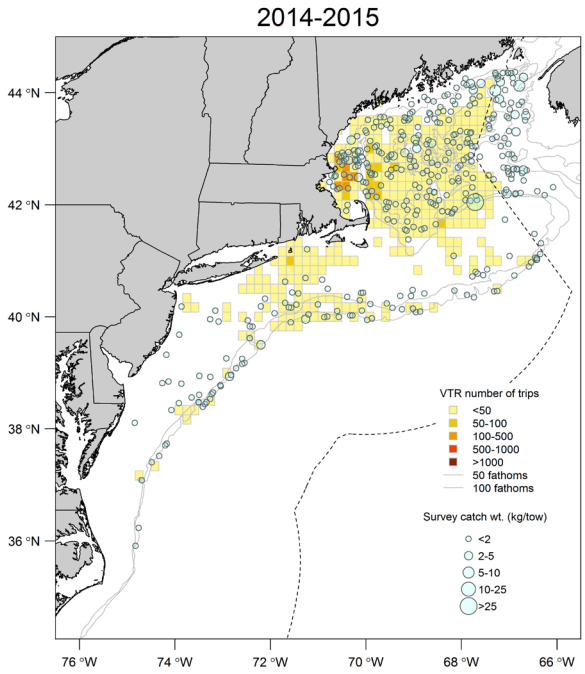

Figure B22, continued. Distribution of commercial trawl trips as recorded in Vessel Trip Report (VTR) compared with annual Northeast Fisheries Science Center survey catches (kg/tow), by 5-year time blocks.

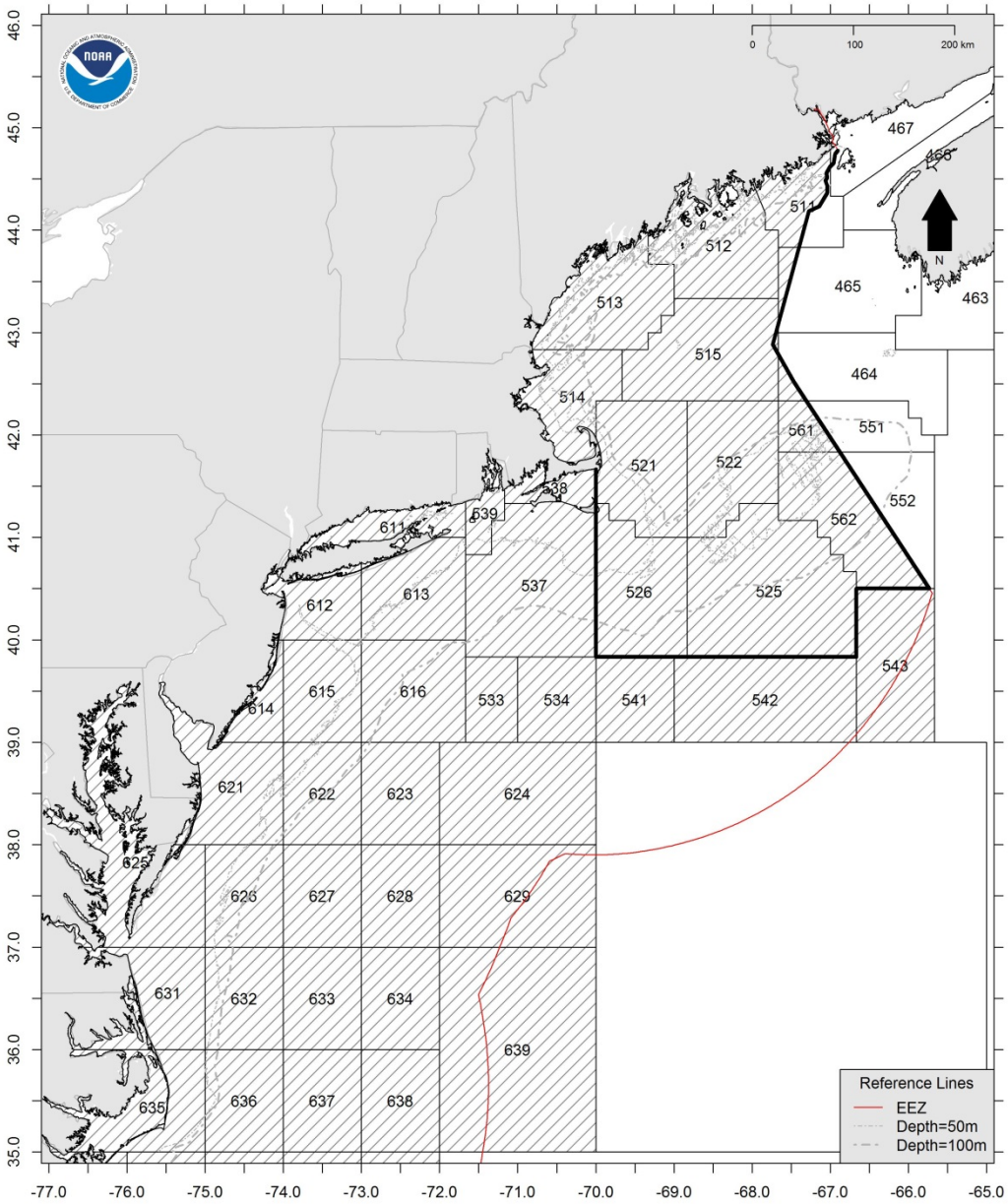

Figure B23. Statistical areas used for reporting commercial fishery statistics. Prior to 1985, statistical areas 551 and 561 comprised statistical area 523 and statistical areas 552 and 562 comprised statistical area 524. Shaded statistical areas indicate witch flounder stock area; Red line represents the U.S. Exclusive Economic Zone; the Gulf of Maine- Georges Bank region (CORE region) is outlined with a bold black line.

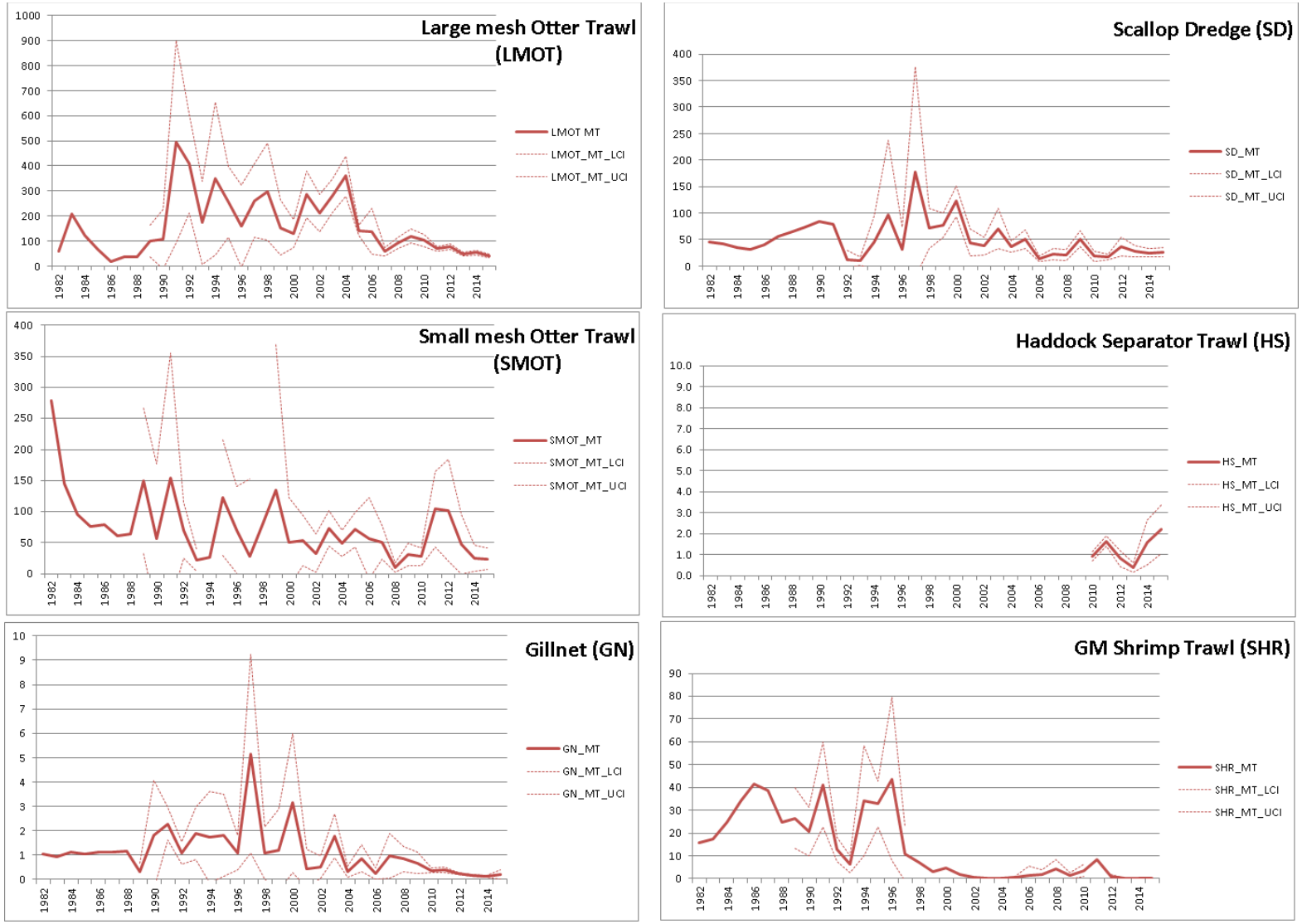

Figure B24. Witch flounder discards, with 95% confidence intervals, for six gear type/mesh groups, 1982 – 2015.

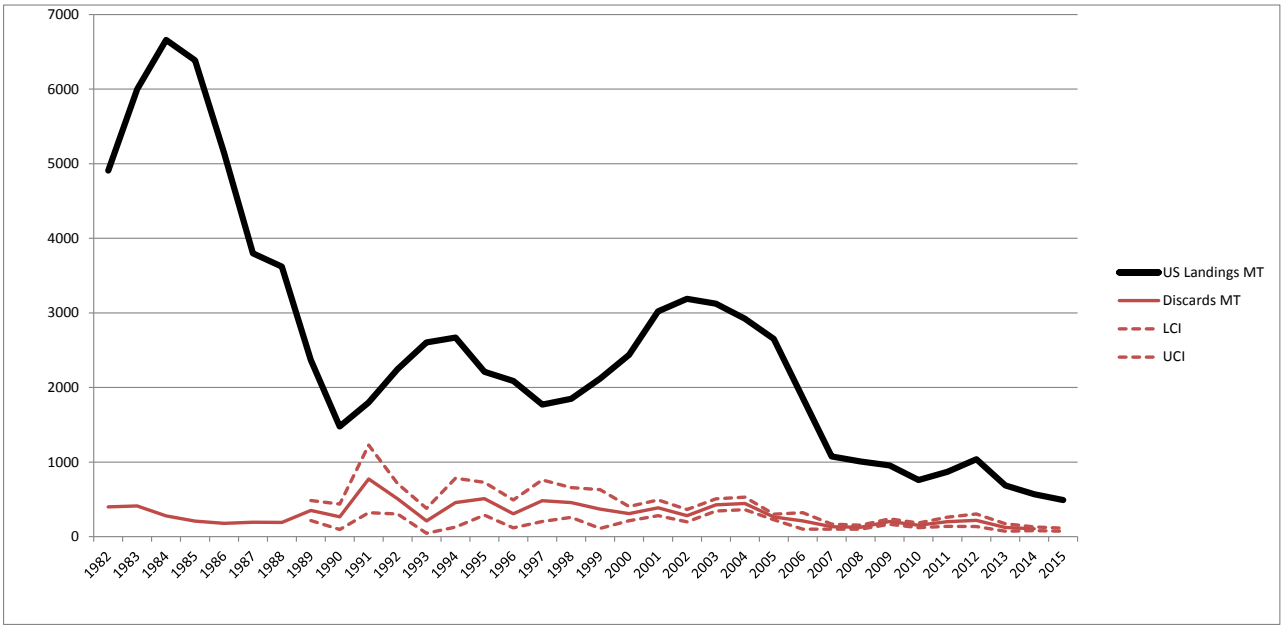

Figure B25. USA landings (mt), excluding USA landings from the Grand Banks in the mid-1980s, and estimated discards with 95% confidential intervals, 1982 - 2015.

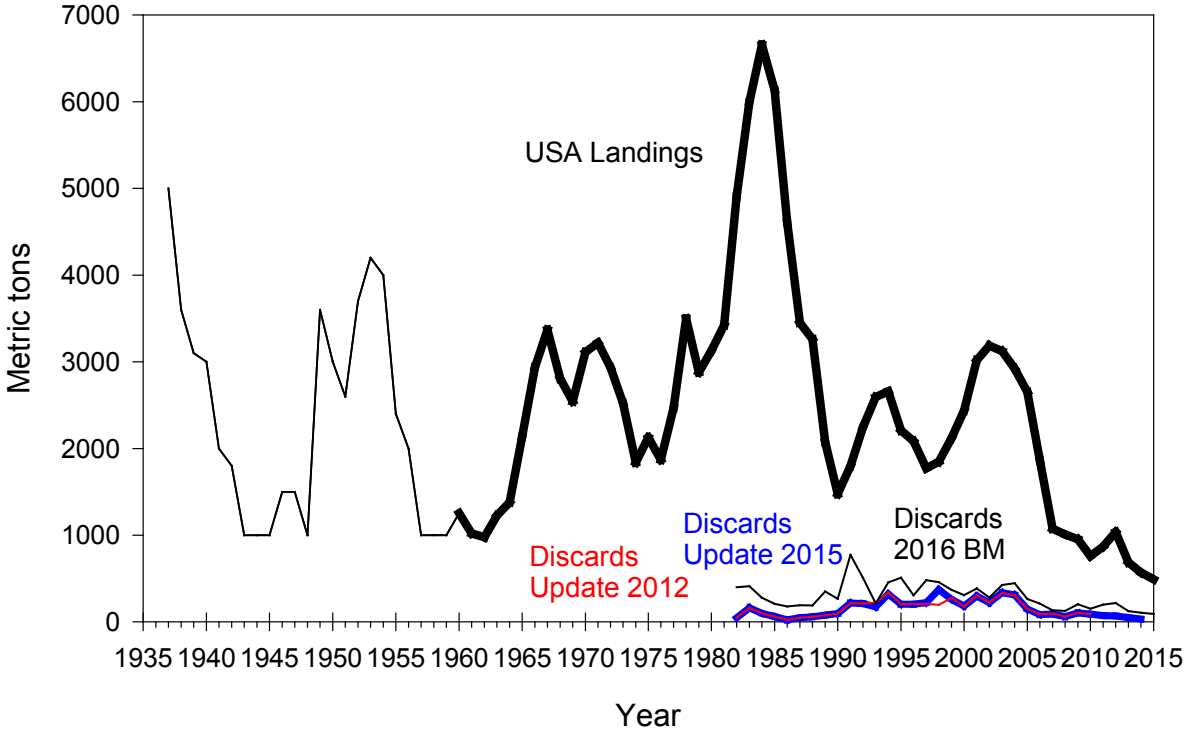

Figure B26. USA witch flounder landings (mt), excluding USA landings from the Grand Banks in the mid-1980's. The thin line represents provisional landings data taken from Lange and Lux (1978). Discards estimated in 2016 (black line) are from six fisheries: shrimp trawl, scallop dredge, gillnet, haddock separator trawl, small-mesh (<5.5 inch) otter trawl and large-mesh (>5.5 inch) otter trawl fisheries; discards estimated for the 2012 Update (red), 2015 Update (blue) are from three fisheries: large mesh otter trawl, small mesh otter trawl and shrimp trawl.

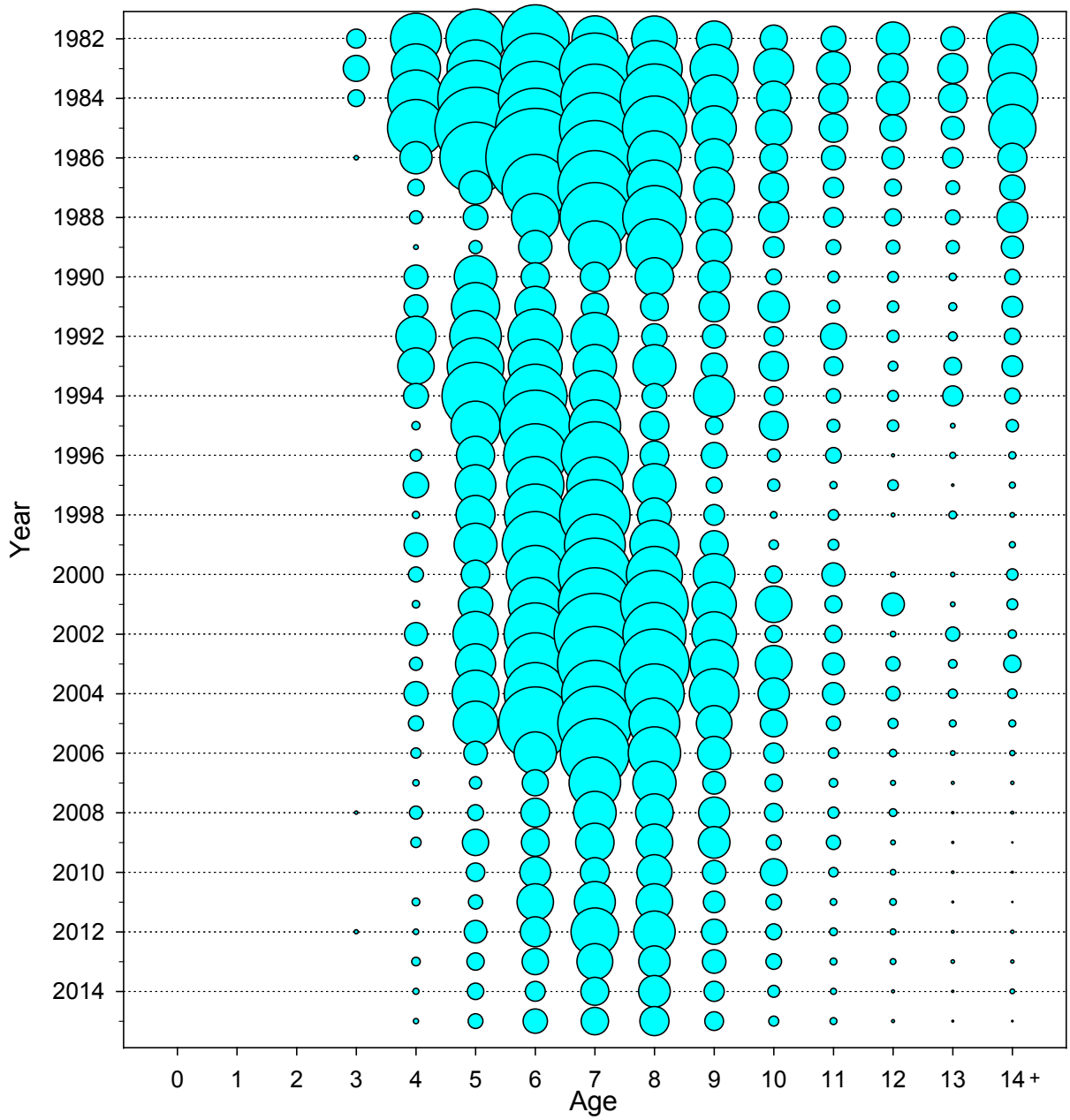

Figure B27. Witch flounder commercial landings at age (in numbers) ages 0 to 14 plus, 1982 to 2015.

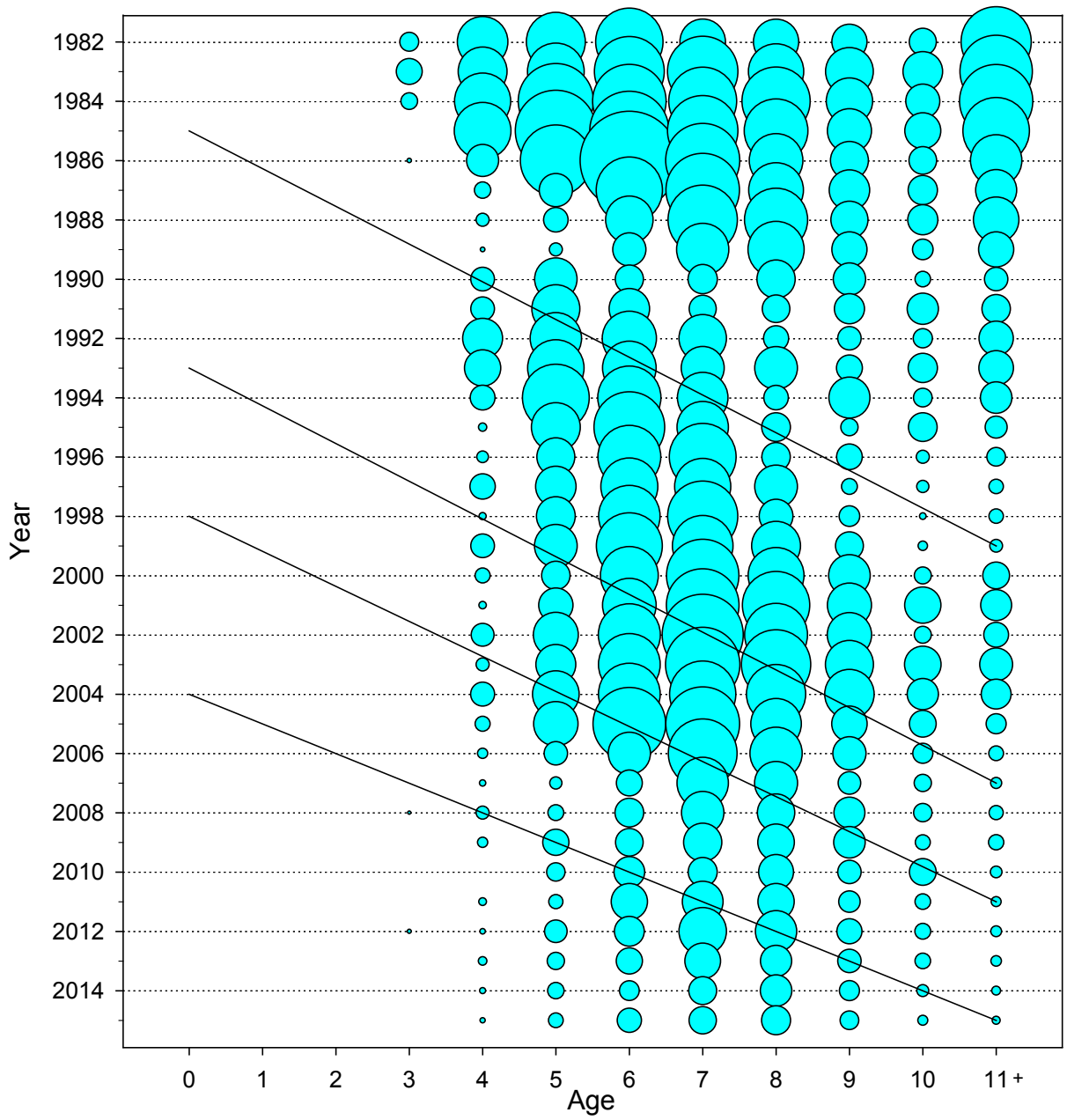

Figure B28. Witch flounder commercial landings at age (in numbers), ages 0 to 11 plus, 1982 to 2015; selected cohorts (1985, 1993, 1998, and 2004 year classes) are indicated with diagonal lines.

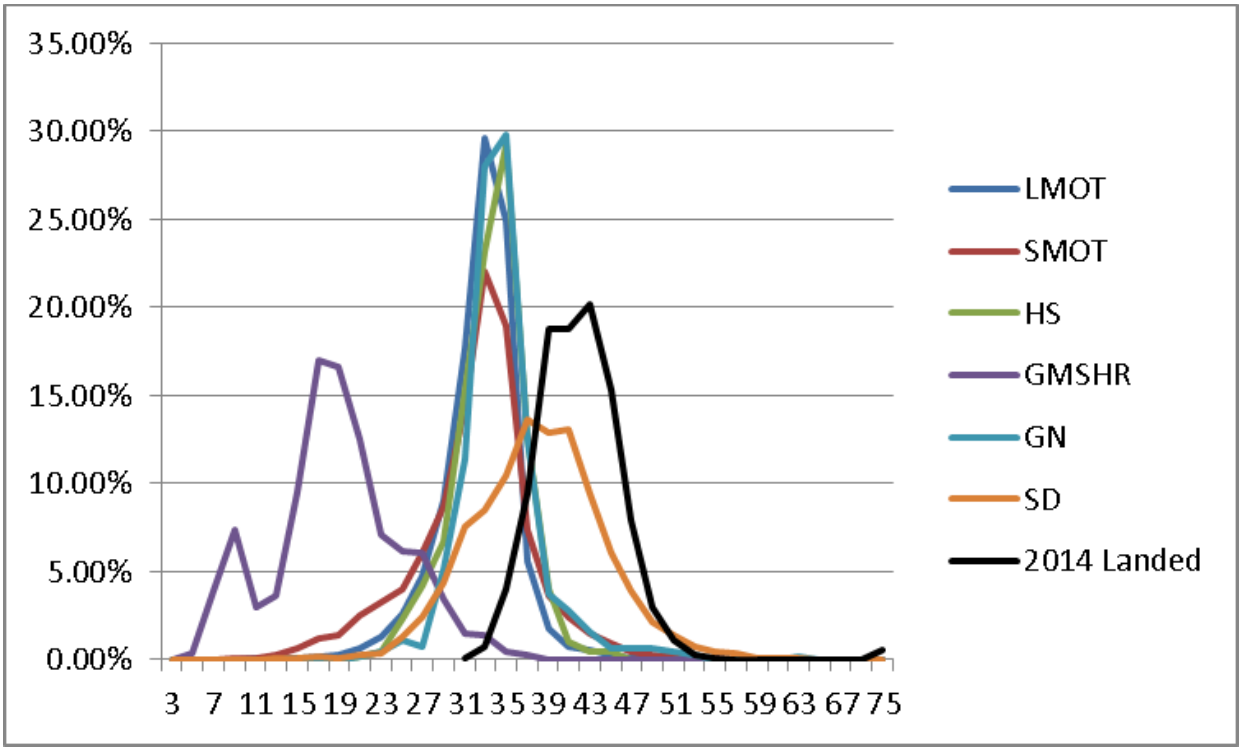

Figure B29. Northeast Fisheries Observer Program proportion at length (cm) of discarded witch flounder for statistical areas in the stock area by six gear types for all years combined. The gear types are: large mesh otter trawl (LMOT), small mesh otter trawl (SMOT), haddock separator trawl (HS), shrimp trawl (GMSHR), gillnet (GN) and scallop dredge (SD). The proportion at length of 2014 landed witch flounder from commercial port sampling is included for reference.

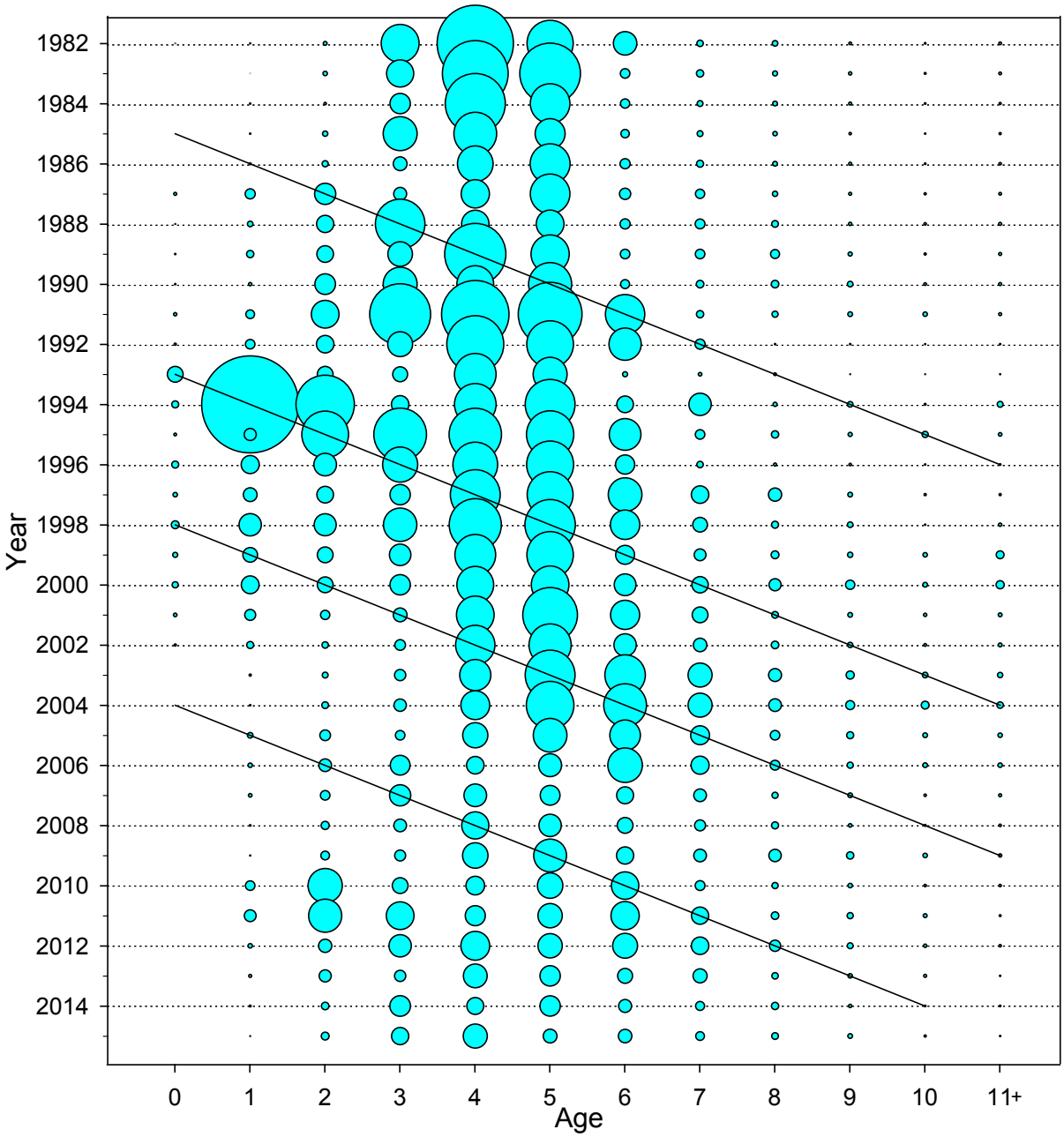

Figure B30. Witch flounder discards at age (in numbers) from six fisheries (large-mesh otter trawl, small mesh otter trawl, Gulf of Maine shrimp trawl, scallop dredge, gillnet, and haddock separator trawl), 1982 to 2015; selected cohorts (1985, 1993, 1998, and 2004 year classes) are indicated with diagonal lines.

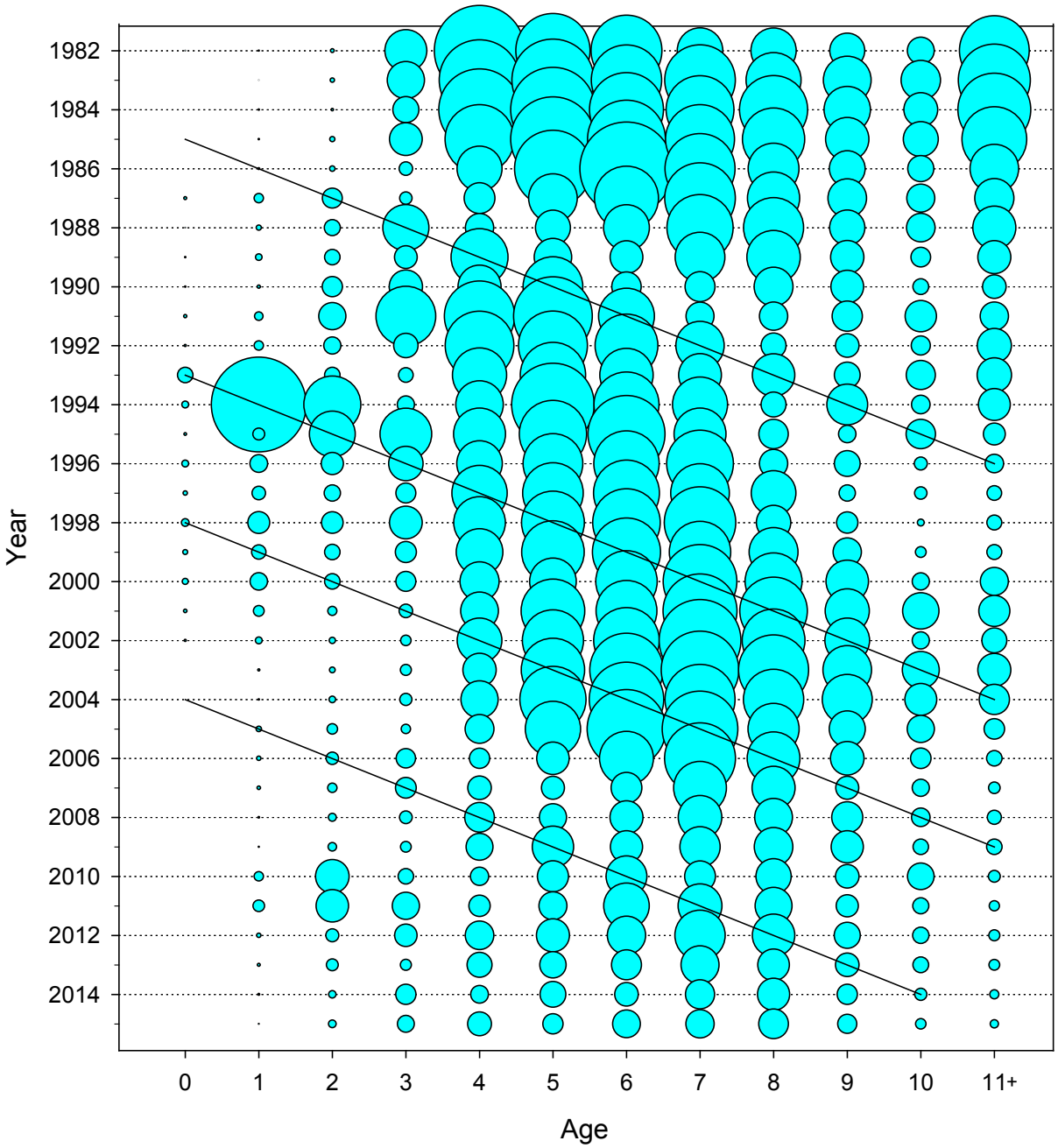

Figure B31. Witch flounder catch at age (in numbers), 1982-2015; selected cohorts (1985, 1993, 1998, and 2004 year classes) are indicated with diagonal lines.

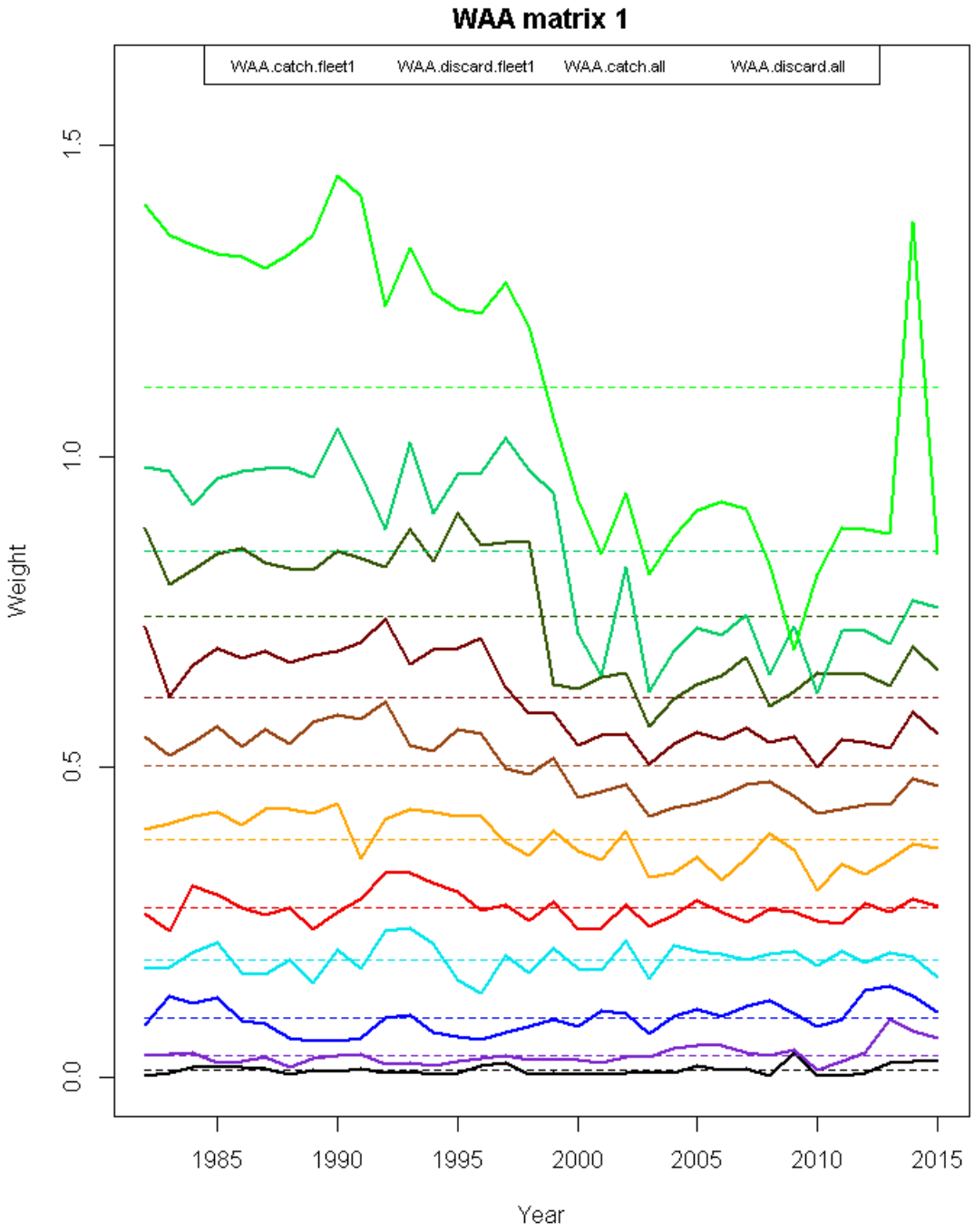

Figure B32. Witch flounder mean weight at age in the catch for ages 1 to 11+, 1982 -2015.

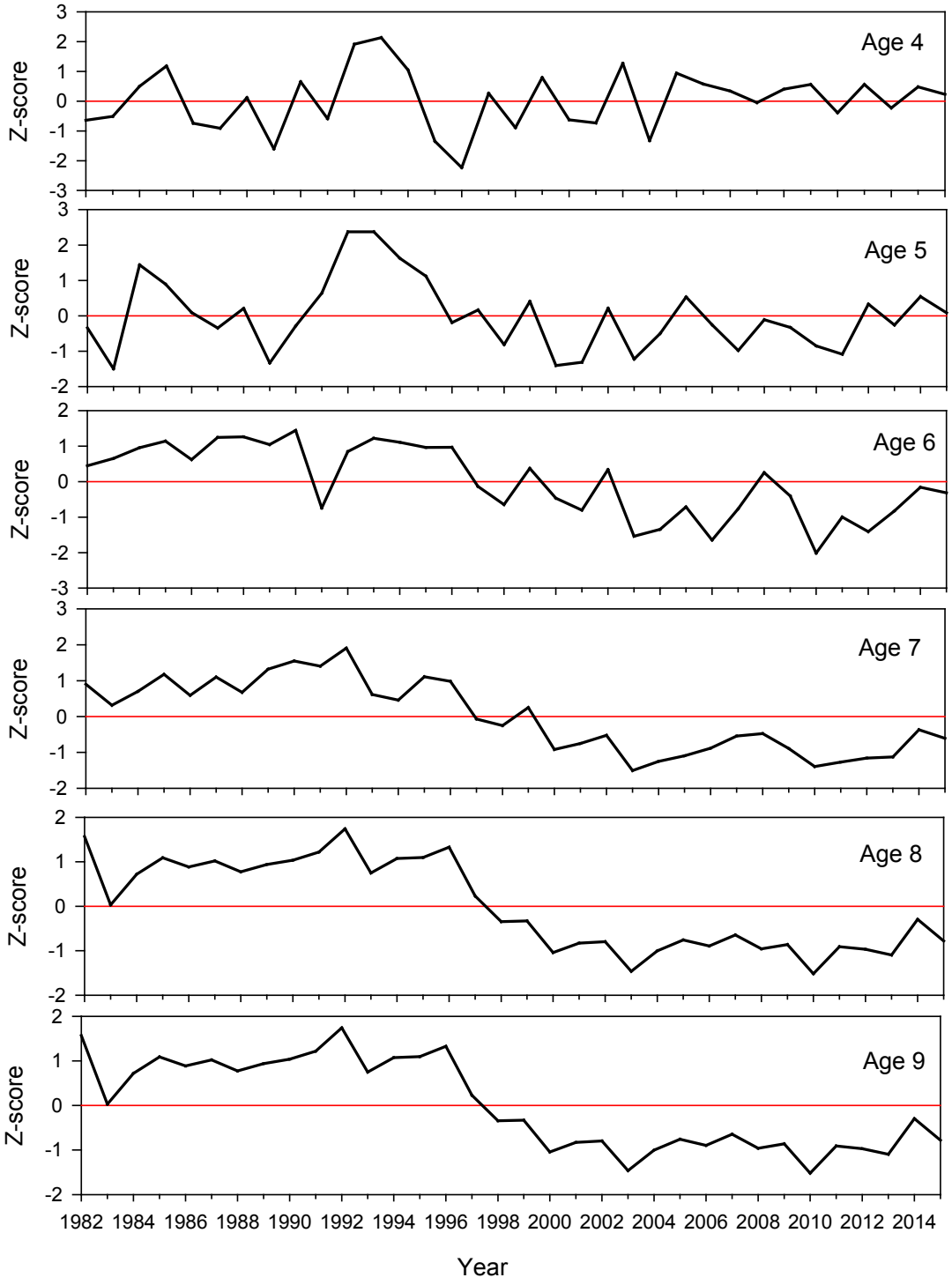

Figure B33. Z-scores of witch flounder mean weight at age in the catch for ages 4 to 9, 1982 - 2015.

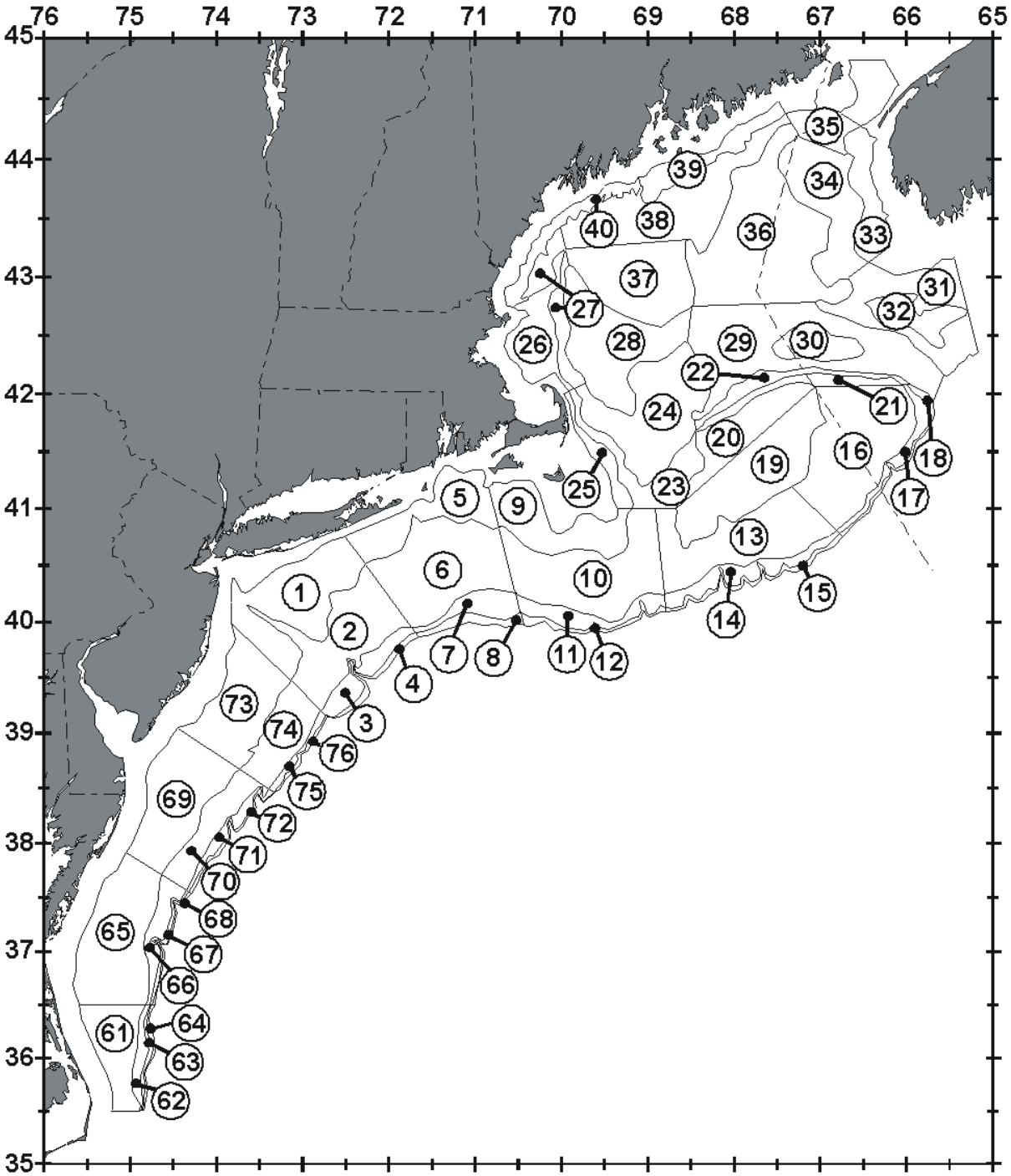

Figure B34. Northeast Fisheries Science Center bottom trawl survey offshore strata 1-76 (depth range 27 to 200 meters).

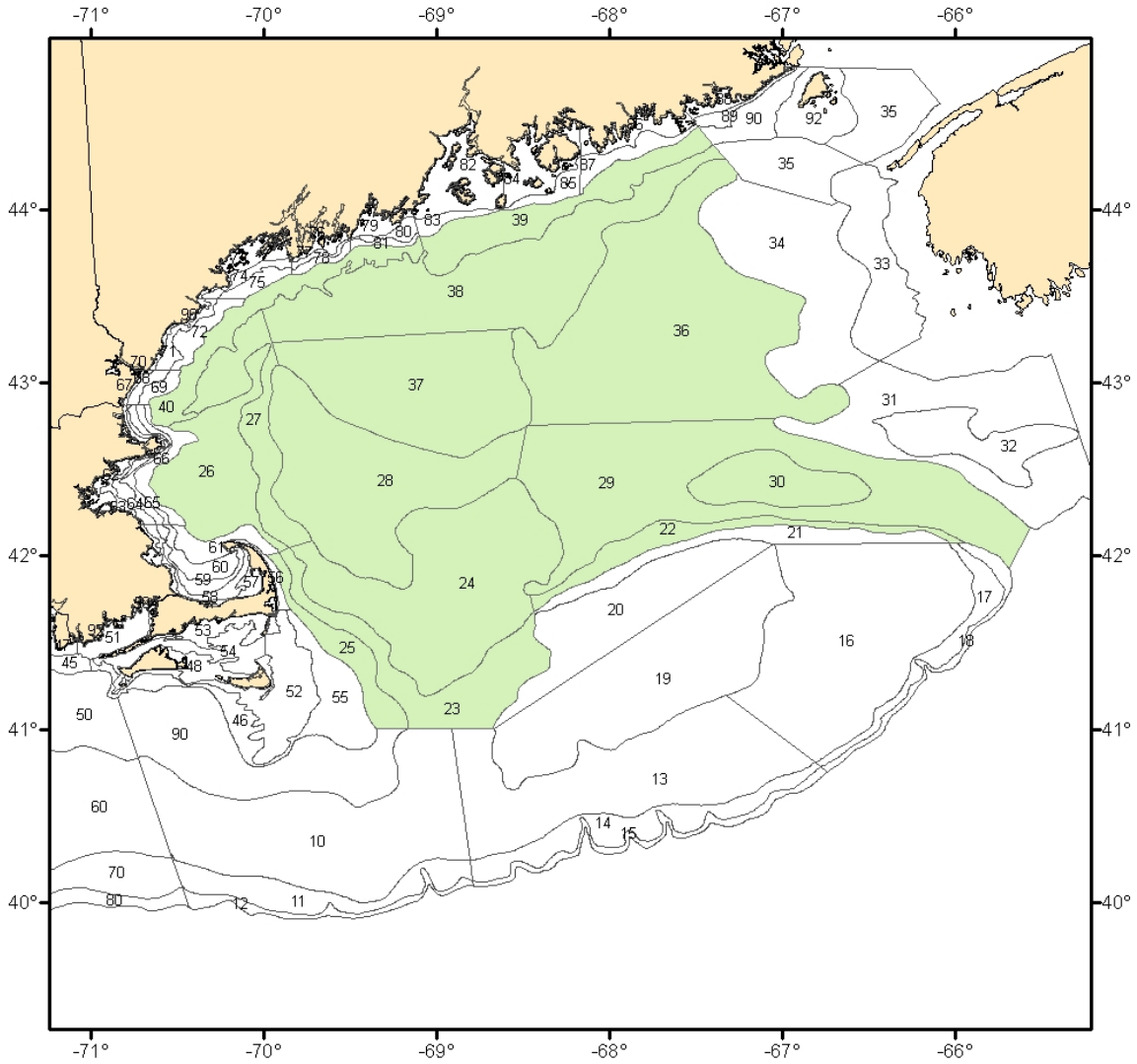

Figure B35. Northeast Fisheries Science Center bottom trawl survey strata (offshore strata 22-30; 36-40) used in the witch flounder stock assessment.

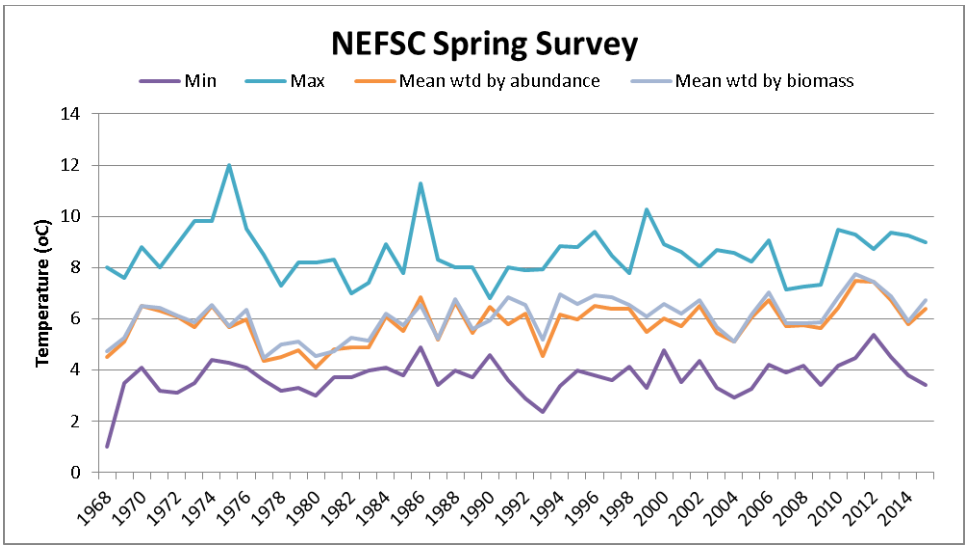

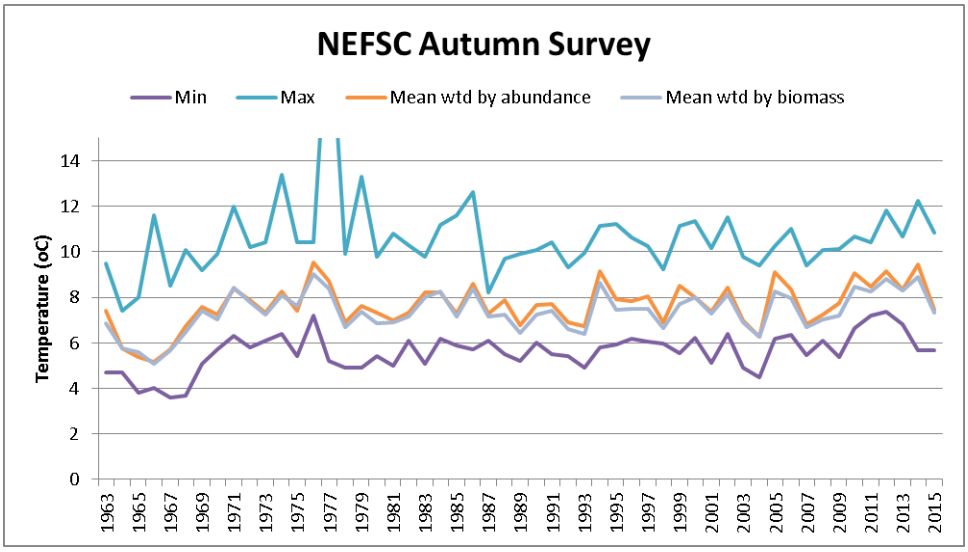

Figure B36. Minimum and maximum bottom temperature (degrees Celsius) of Northeast Fisheries Science Center (NEFSC) spring (top) and autumn (bottom) survey Gulf of Maine–Georges Bank region (strata 22-30, 36-40) and the weighted mean depth (weighted by witch flounder abundance and biomass).

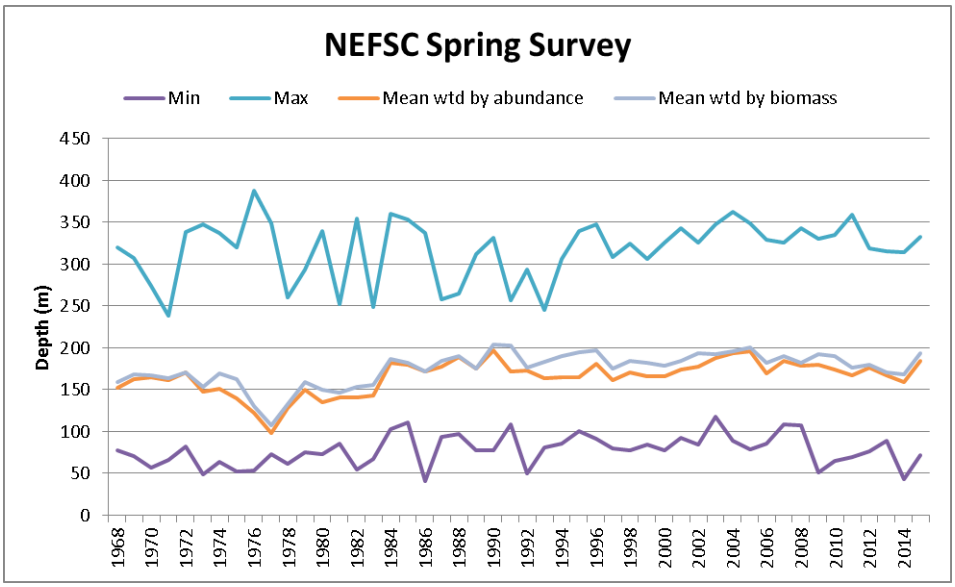

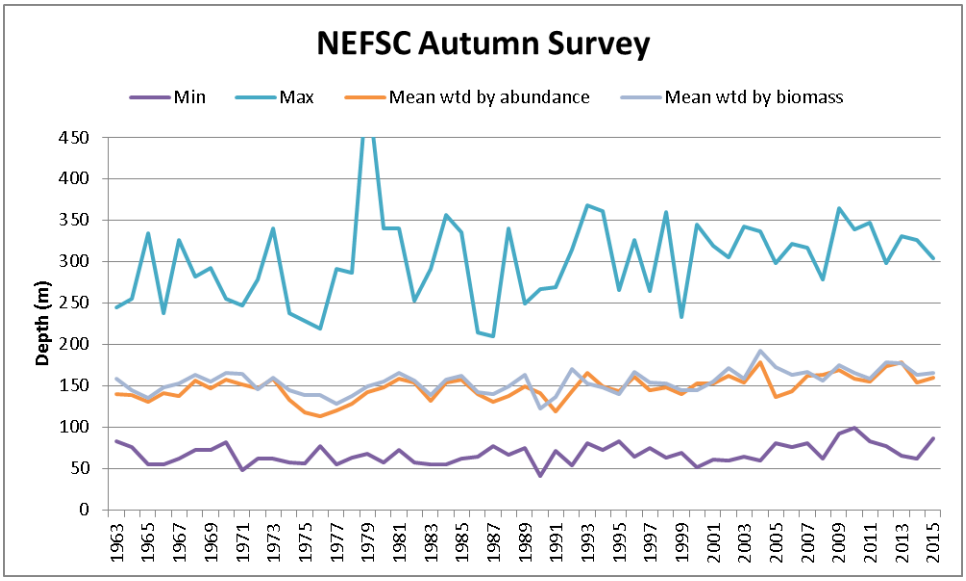

Figure B37. Minimum and maximum depth (m) of Northeast Fisheries Science Center (NEFSC) spring (top) and autumn (bottom) survey in the Gulf of Maine–Georges Bank region (strata 22-30, 36-40) and the weighted mean depth (weighted by witch flounder abundance and biomass).

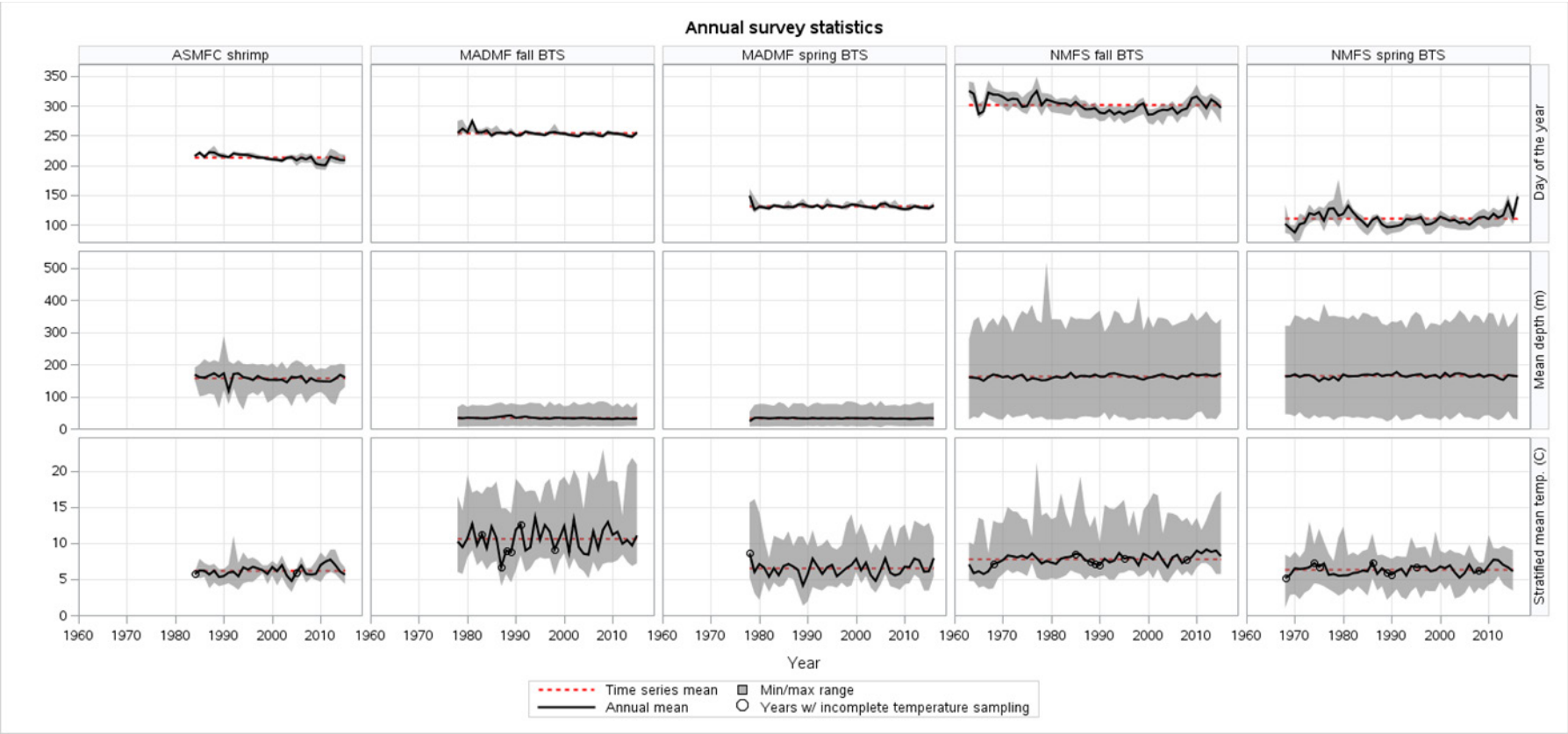

Figure B38. Annual timing (day of year; top row), mean depth (m; middle row), and stratified mean bottom temperature (C; bottom row) for the Atlantic States Marine Fisheries Commission (ASMFC) shrimp survey, Massachusetts Division of Marine Fisheries (MADMF) fall and spring , and Northeast Fisheries Science Center (NEFSC) fall and spring bottom trawl survey (from left to right, respectively). Annual means values (black line), time series mean (red dash line) and minimum/maximum values (gray shading).

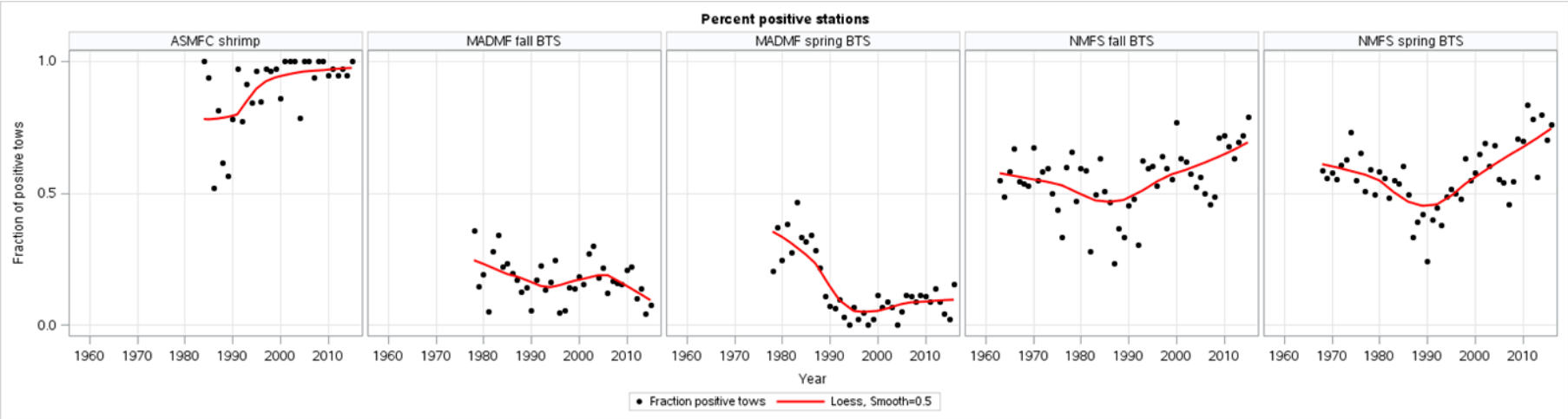

Figure B39. Fraction of survey stations with positive catch of witch flounder in the Atlantic States Marine Fisheries Commission (ASMFC) shrimp survey, Massachusetts Division of Marine Fisheries (MADMF) fall and spring, and Northeast Fisheries Science Center (NEFSC) fall and spring bottom trawl survey (from left to right, respectively). Annual fraction of positive stations (black circles) and loess smooth (0.5; red line) are shown.

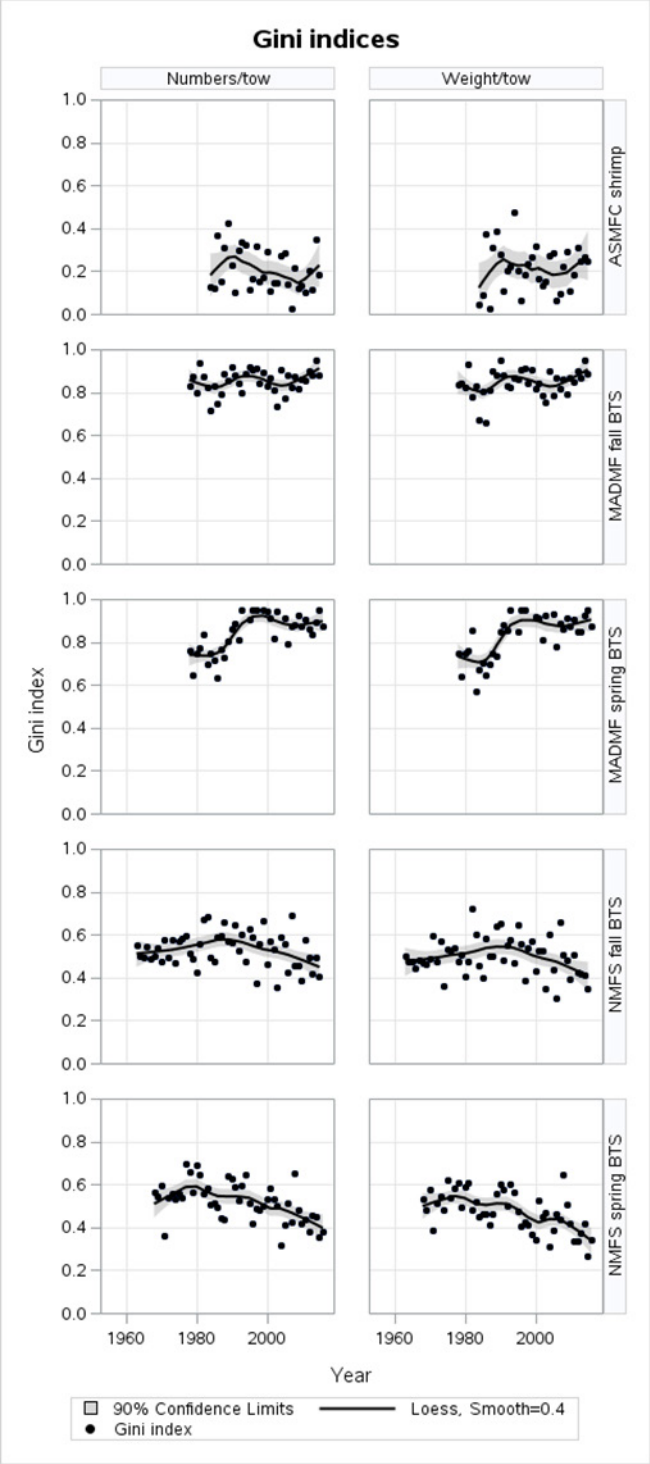

Figure B40. Concentration index (Gini index) of witch flounder (in numbers per tow and weight per tow) in the Atlantic States Marine Fisheries Commission (ASMFC) shrimp survey, Massachusetts Division of Marine Fisheries (MADMF) fall and spring , and Northeast Fisheries Science Center (NEFSC) fall and spring bottom trawl survey (from top to bottom, respectively) . Annual concentration values (black circles) and loess smooth (0.4; black line) are shown.
.

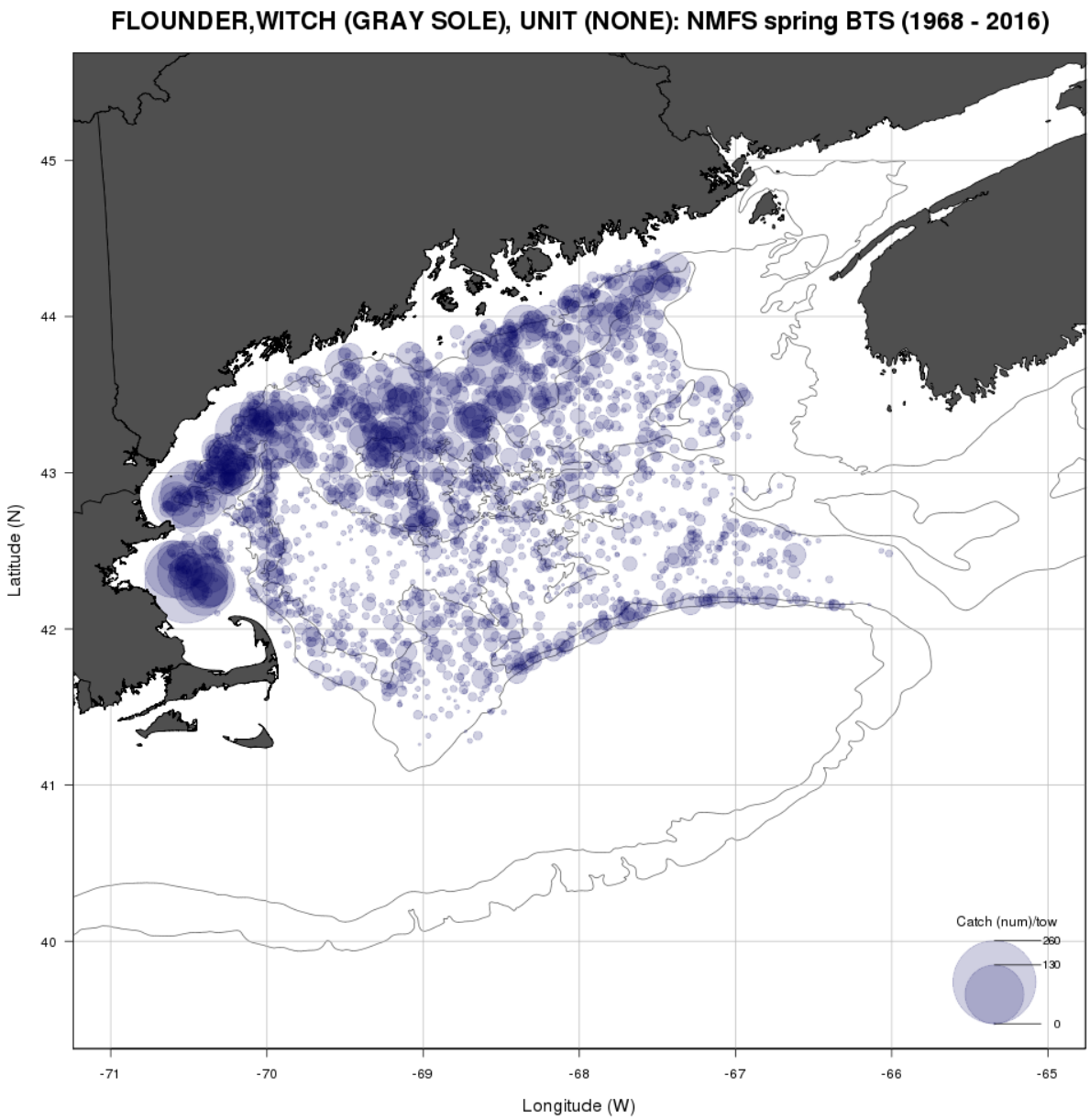

Figure B41. Number per tow of witch flounder in the Northeast Fisheries Science Center spring bottom trawl survey (strata 22-30, 36-40), 1968-2016.

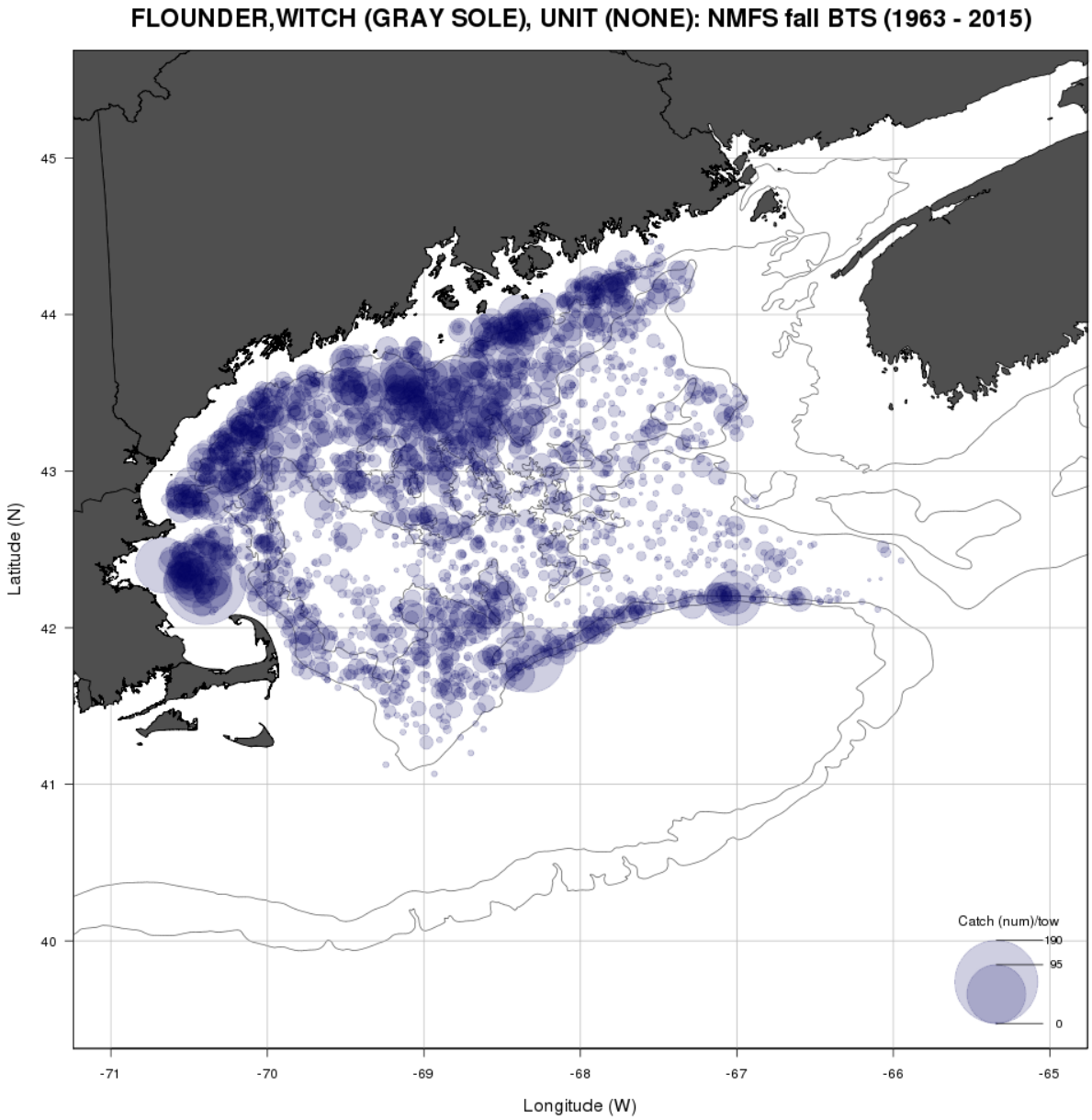

Figure B42. Number per tow of witch flounder in the Northeast Fisheries Science Center autumn bottom trawl survey (strata 22-30, 36-40), 1963-2015.

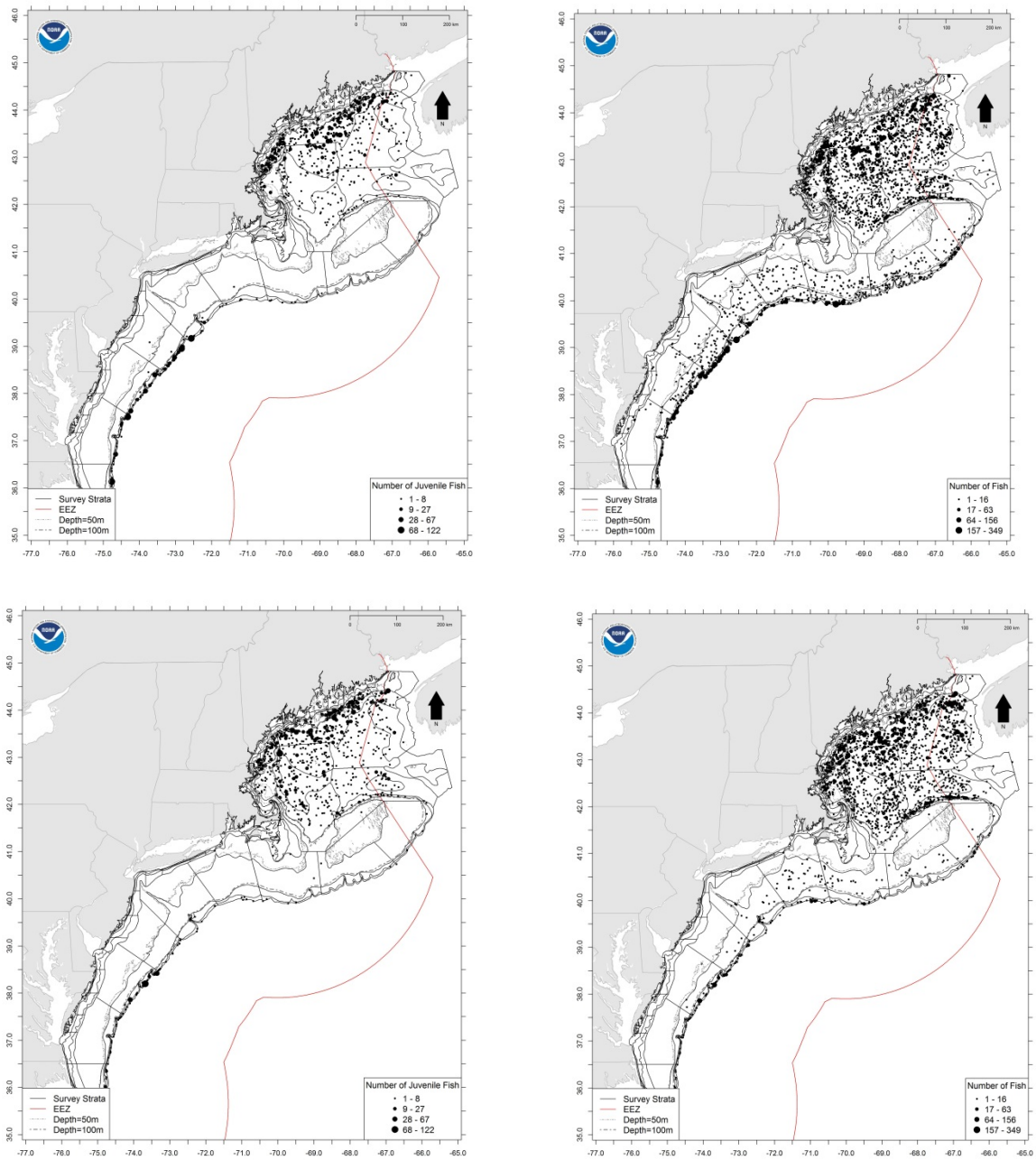

Figure B43. Distribution of juvenile (<25 cm) witch flounder in the Northeast Fisheries Science Center (NEFSC) 1968-2016 spring (top right) and 1963-2015 autumn (bottom right) survey. Distribution of all witch flounder in the NEFSC spring (top left) and autumn (bottom left) survey are also shown.

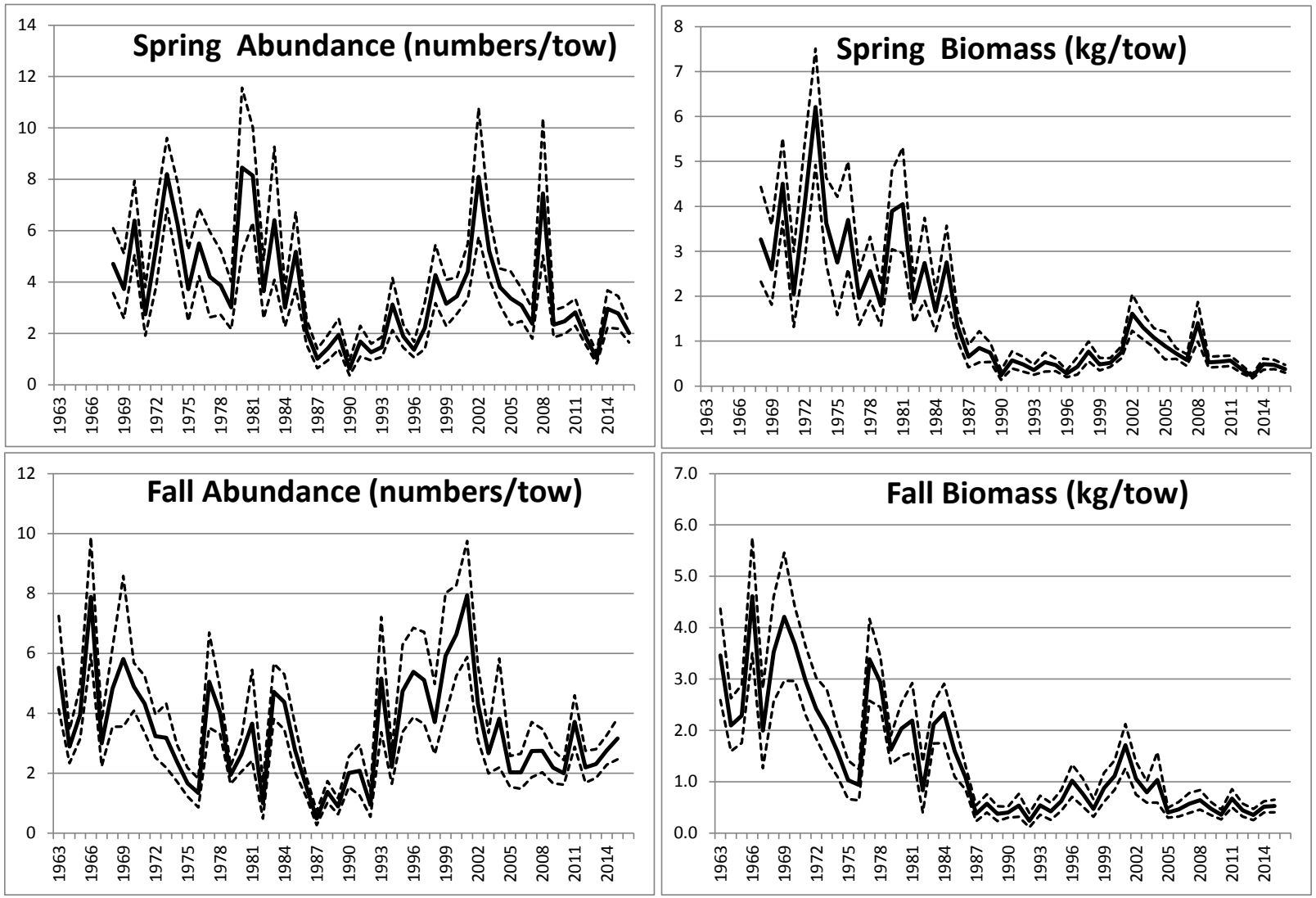

Figure B44. Stratified mean number (left) and weight (kg; right) per tow of witch flounder in the Northeast Fisheries Science Center autumn (bottom) and spring (top) bottom trawl surveys, 1963-2015, spring 2016.

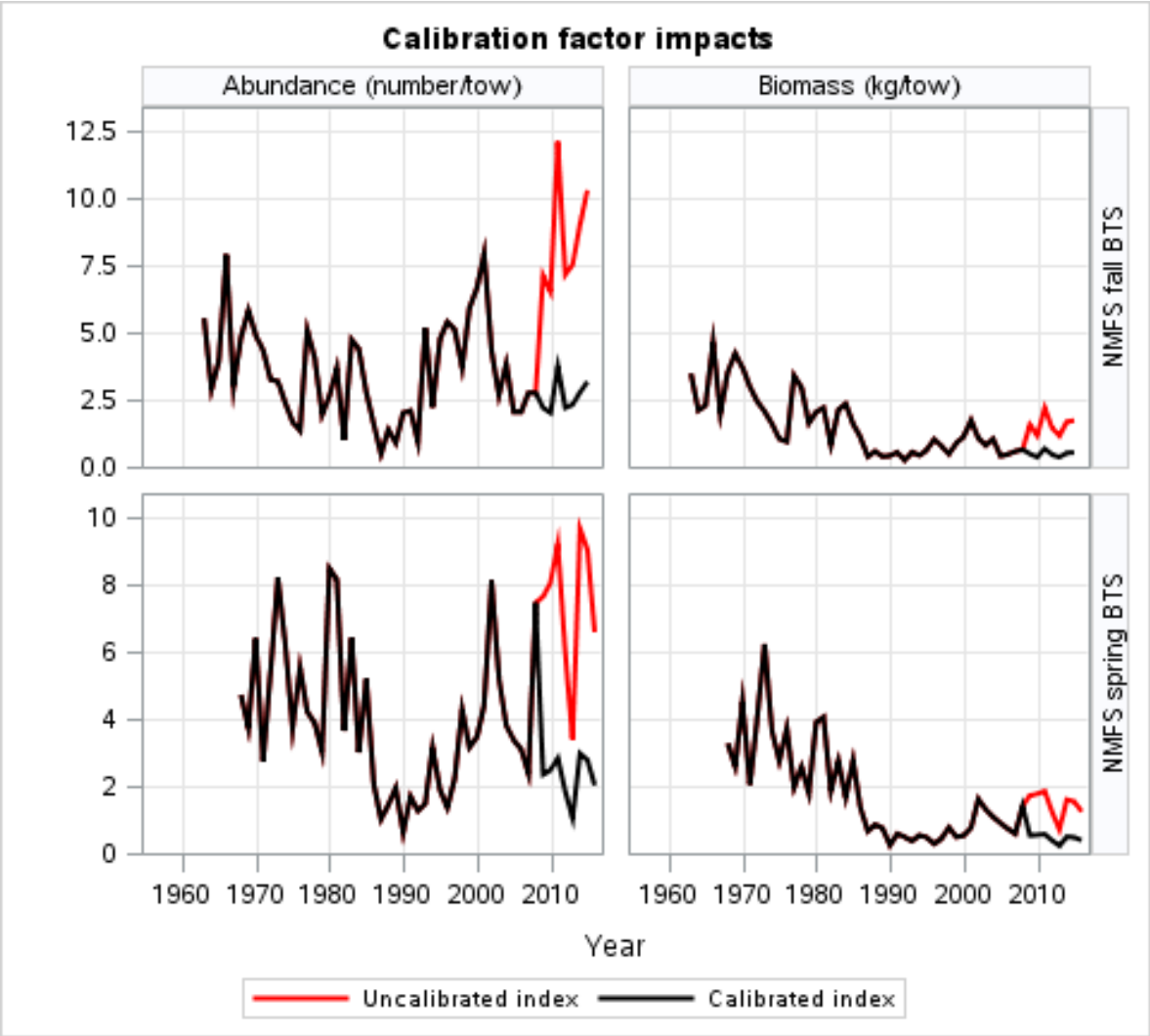

Figure B45. Stratified mean number (left) and weight (kg; right) per tow of witch flounder in the Northeast Fisheries Science Center autumn (top) and spring (bottom) bottom trawl surveys, 1963-2015, spring 2016. Red lines indicate Bigelow uncalibrated indices.

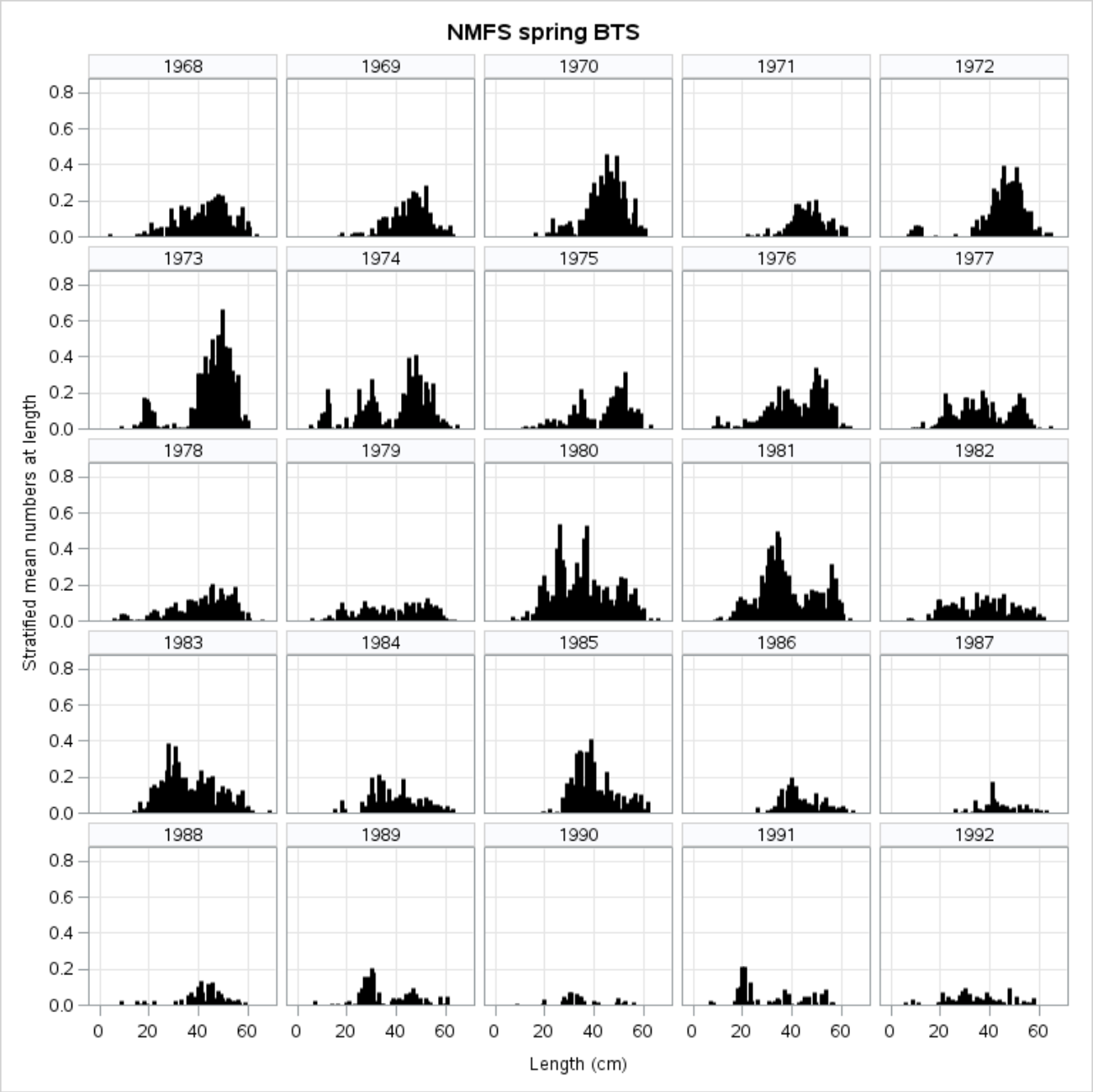

Figure B46. Stratified mean number of witch flounder per tow at length from Northeast Fisheries Science Center spring survey (strata 22-30, 36-40), 1968 – 2016.

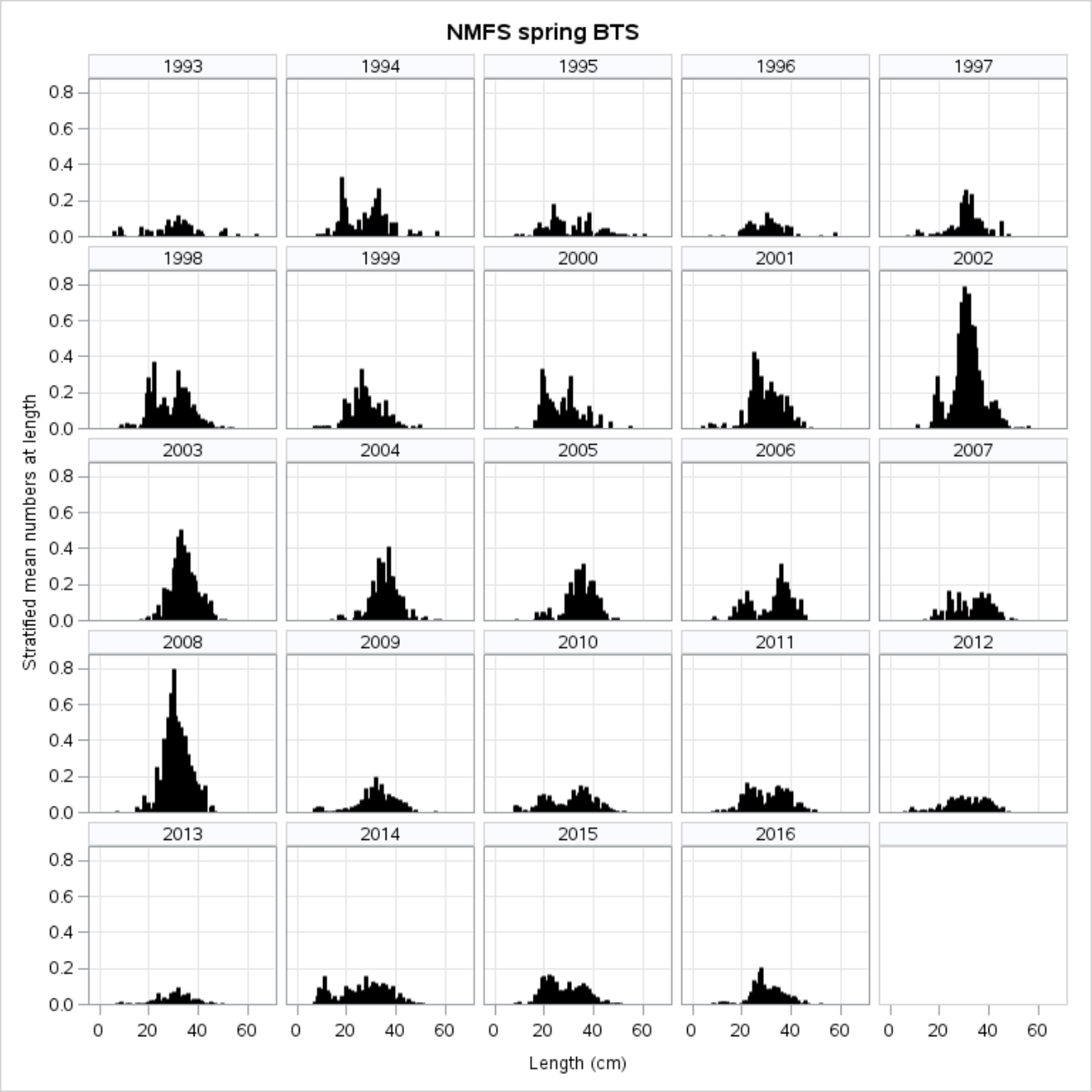

Figure B46, continued. Stratified mean number of witch flounder per tow at length from Northeast Fisheries Science Center spring survey (strata 22-30, 36-40), 1968 – 2016.

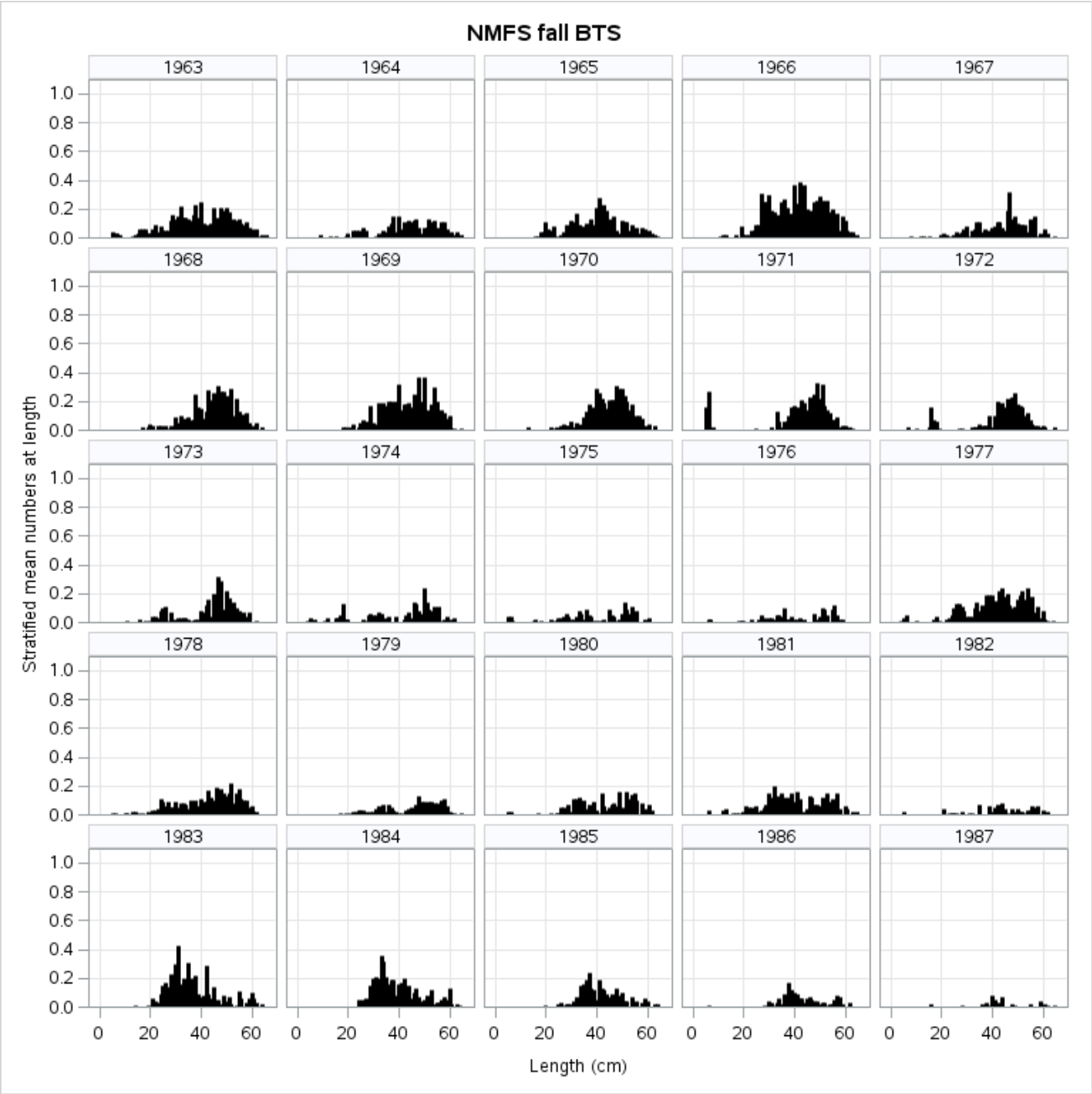

Figure B47. Stratified mean number of witch flounder per tow at length from Northeast Fisheries Science Center autumn survey (strata 22-30, 36-40), 1963 – 2015.

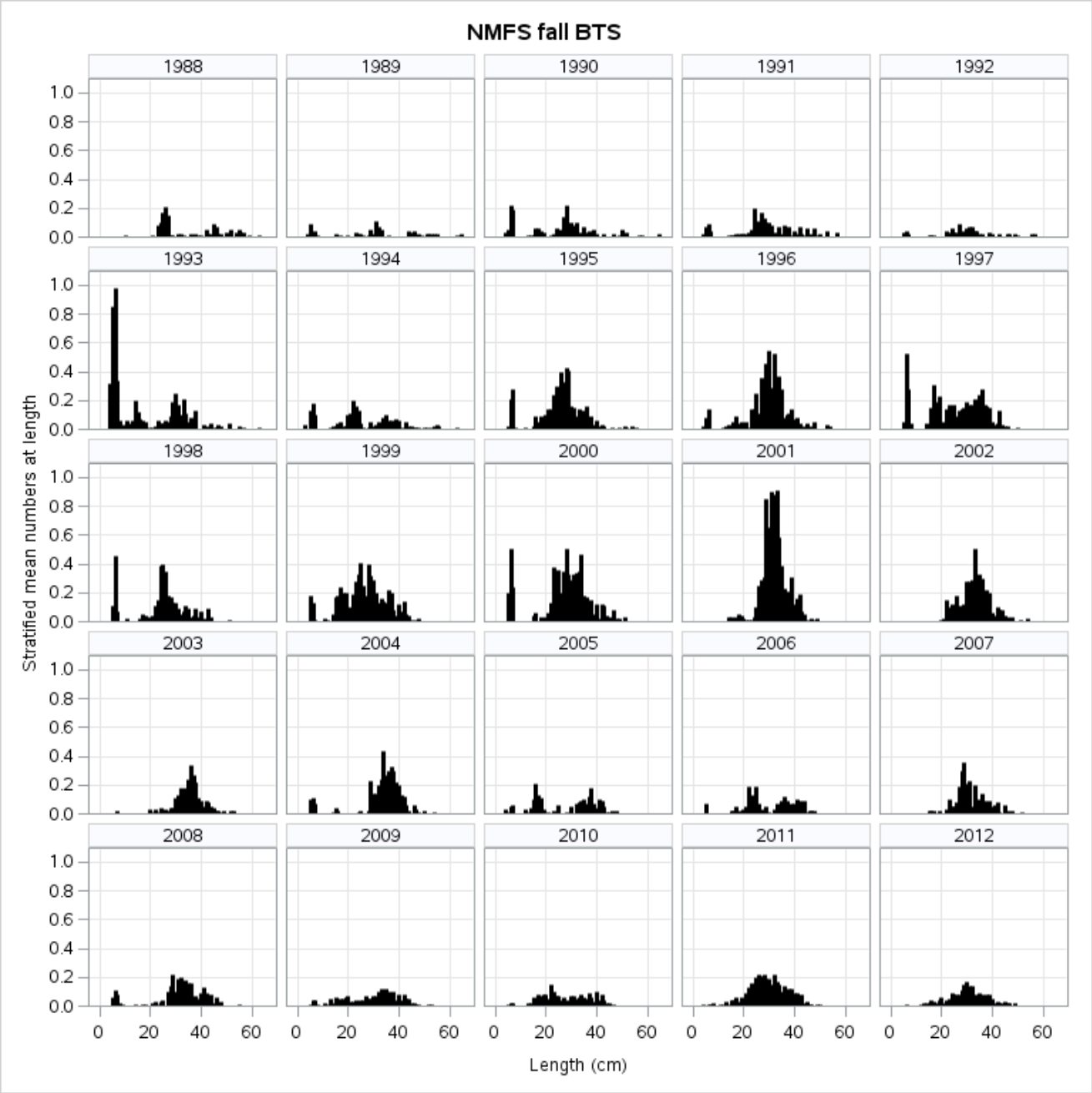

Figure B47, continued. Stratified mean number of witch flounder per tow at length from Northeast Fisheries Science Center autumn survey (strata 22-30, 36-40), 1963 – 2015.

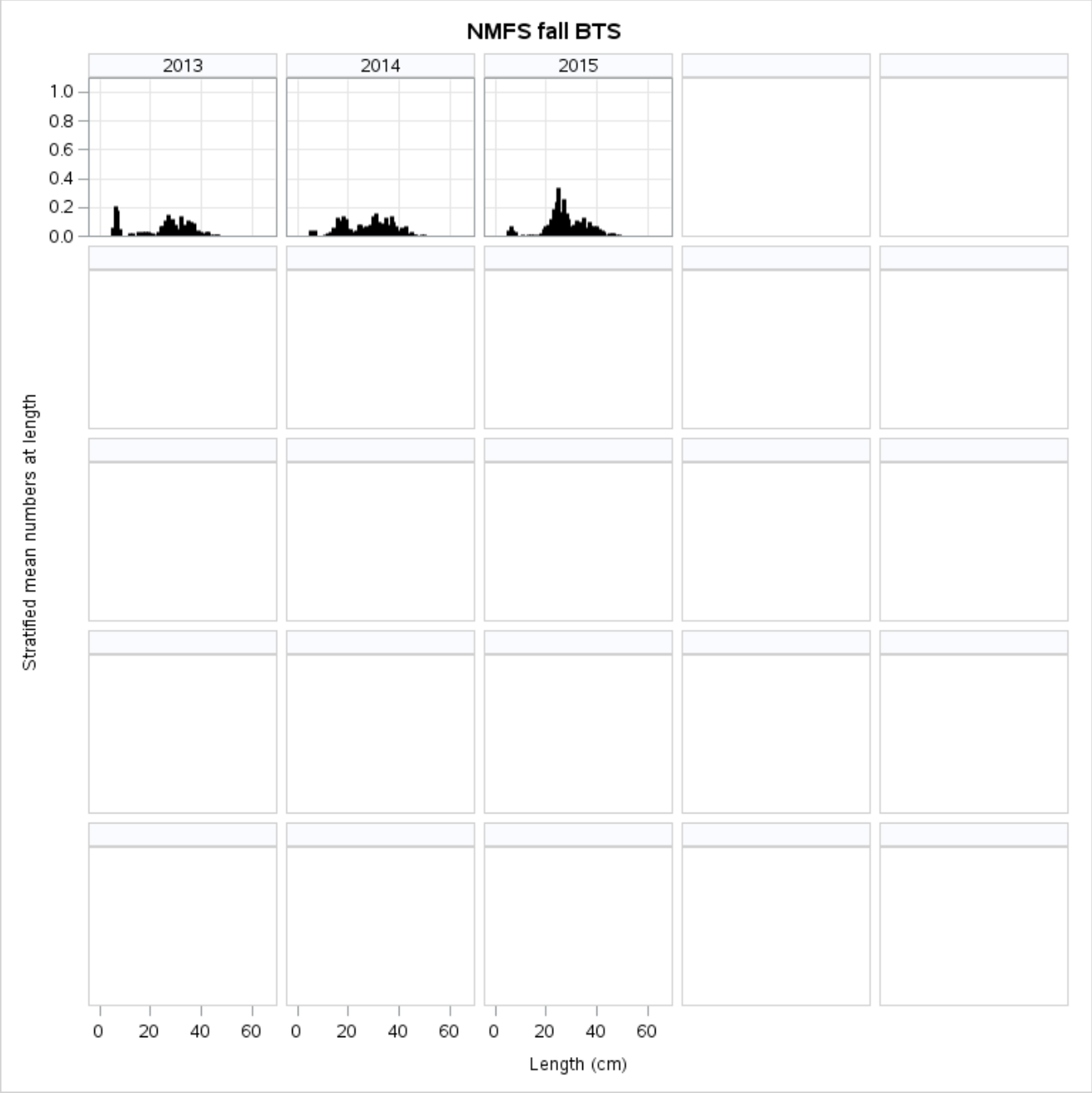

Figure B47, continued. Stratified mean number of witch flounder per tow at length from Northeast Fisheries Science Center autumn survey (strata 22-30, 36-40), 1963 – 2015.

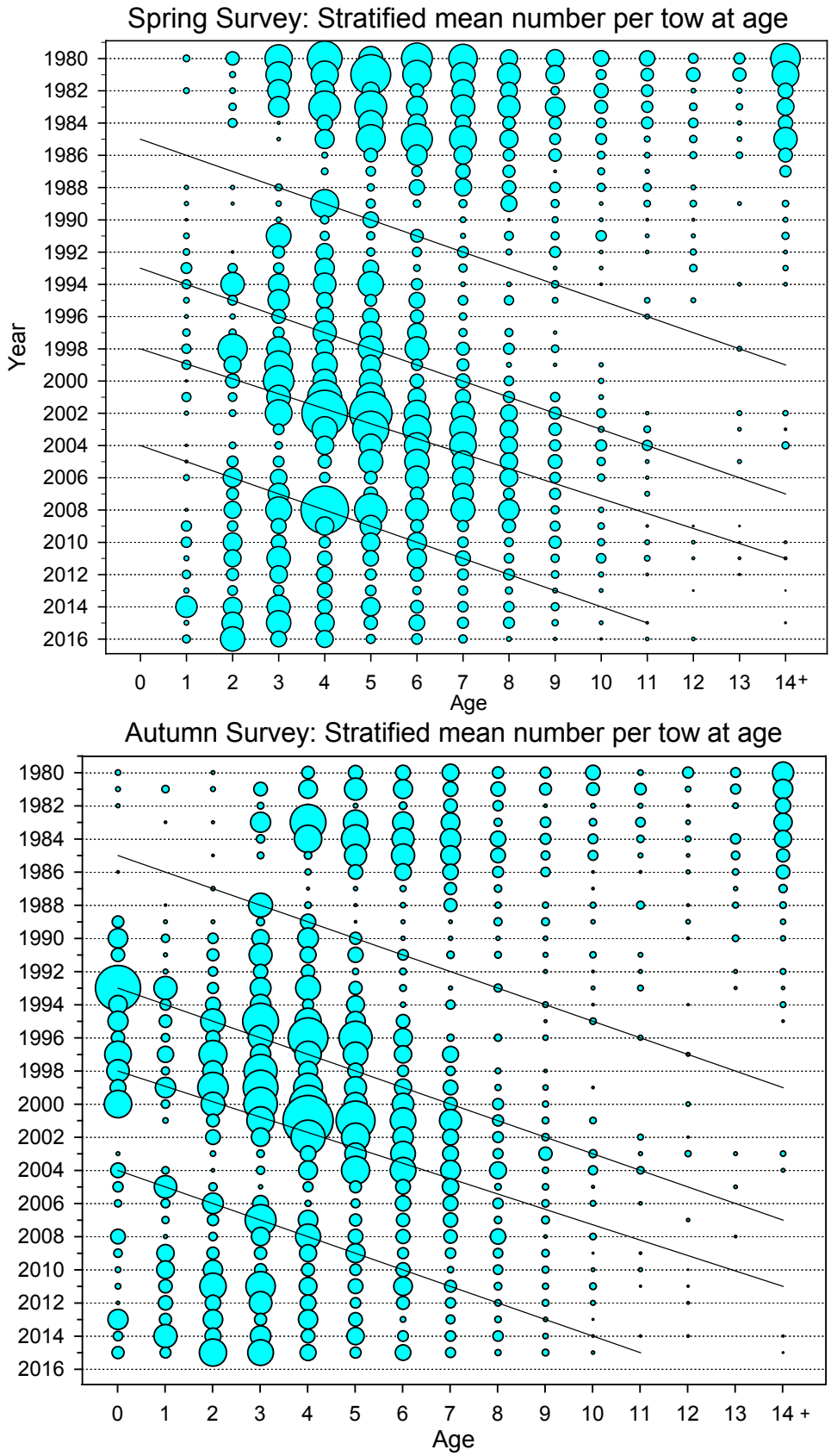

Figure B48. Stratified mean number of witch flounder per tow at age from Northeast Fisheries Science Center spring (top) and autumn (bottom) surveys, 1980 – 2015; spring 2016. Selected cohorts (1985, 1993, 1998, and 2004 year classes) are indicated with diagonal lines.

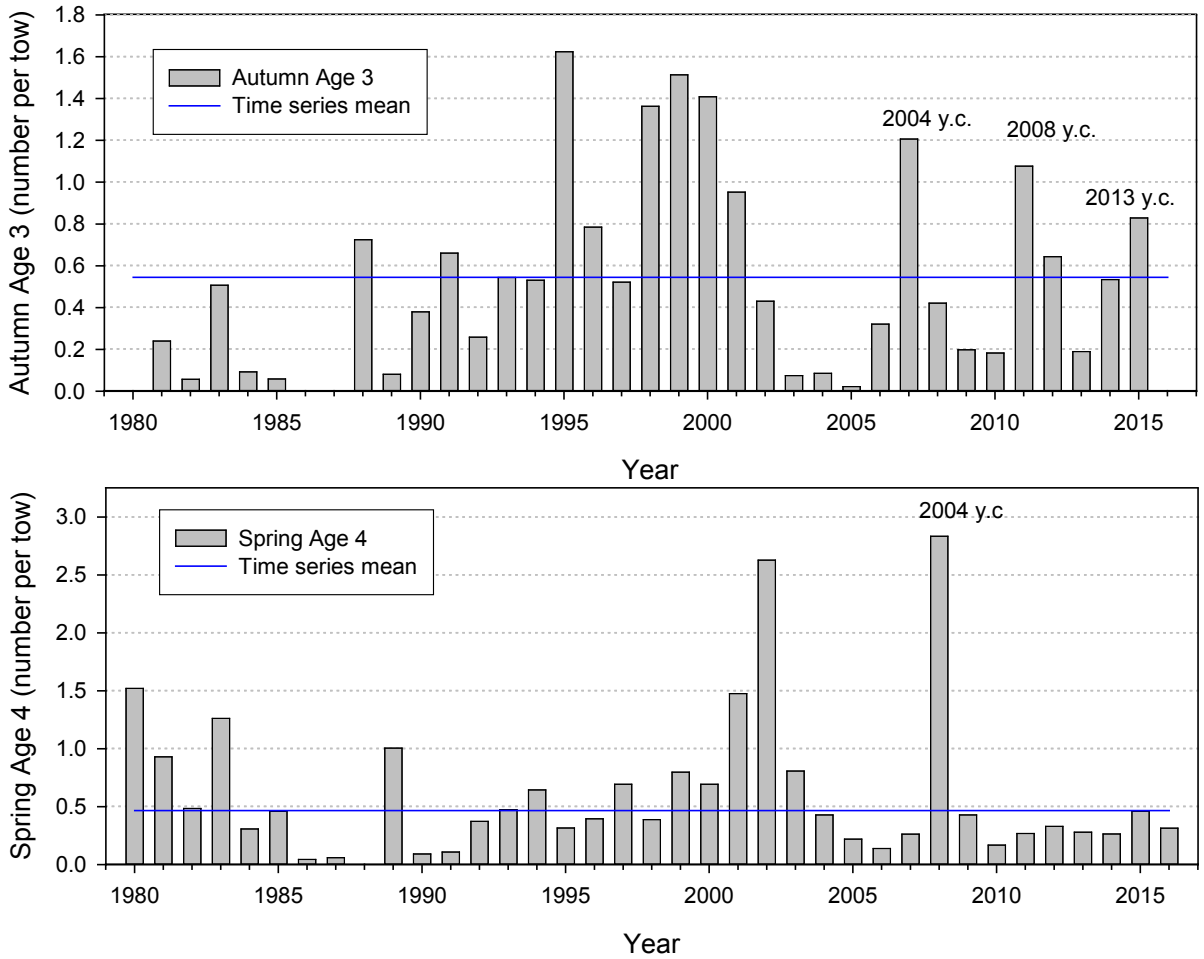

Figure B49. Stratified mean number per tow of age 3 witch flounder in the Northeast Fisheries Science Center autumn survey, 1980- 2015 (top), and age 4 witch flounder in the spring survey, 1980 -2016 (bottom). Constant conversion factor of 3.2572 applied to 2009 – 2016 surveys.

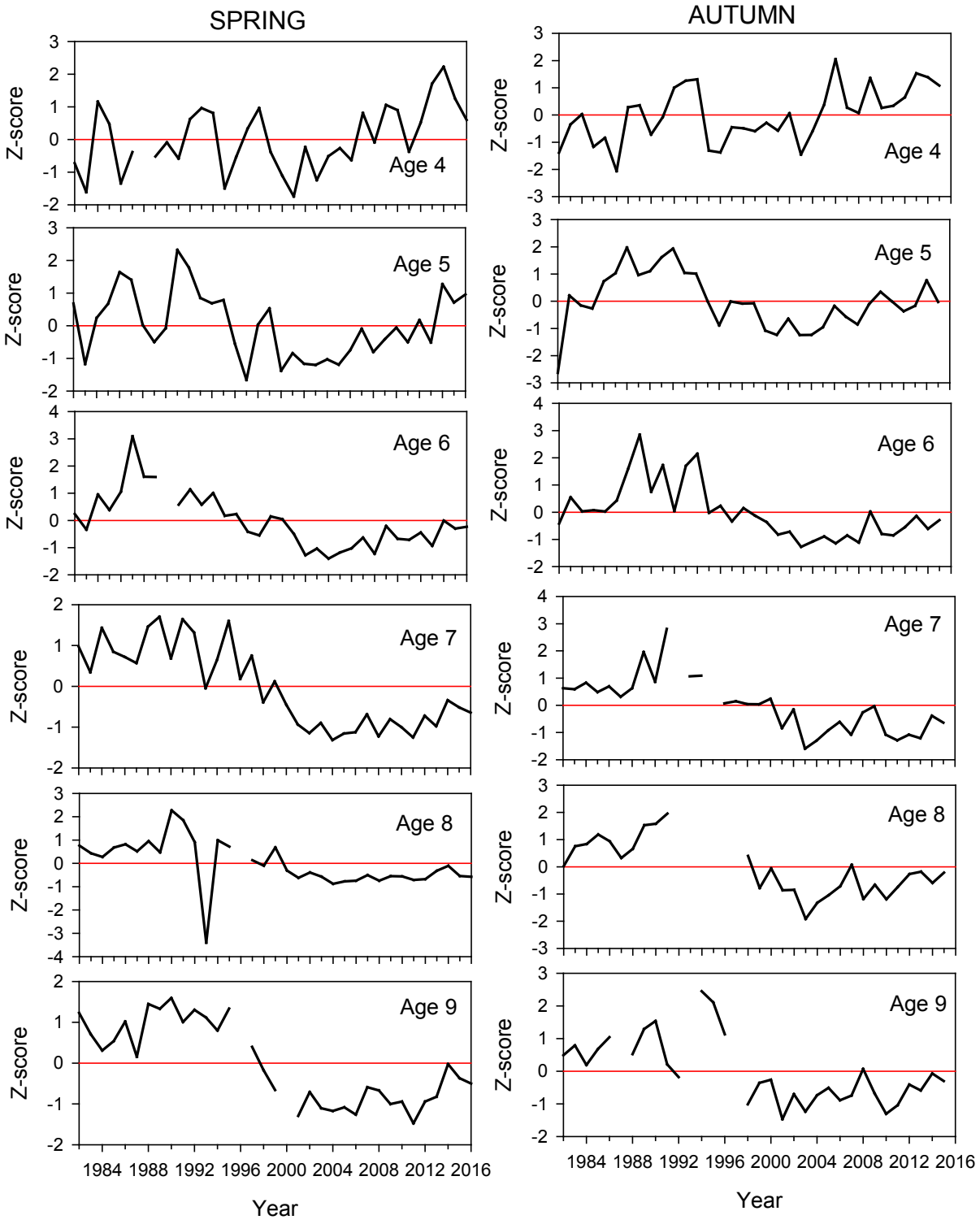

Figure B50. Z-scores of witch flounder mean weight at age (age groups 4 – 9) in the Northeast Fisheries Science Center spring survey (left), 1982-2016 and autumn survey 1982 -2015 (right).

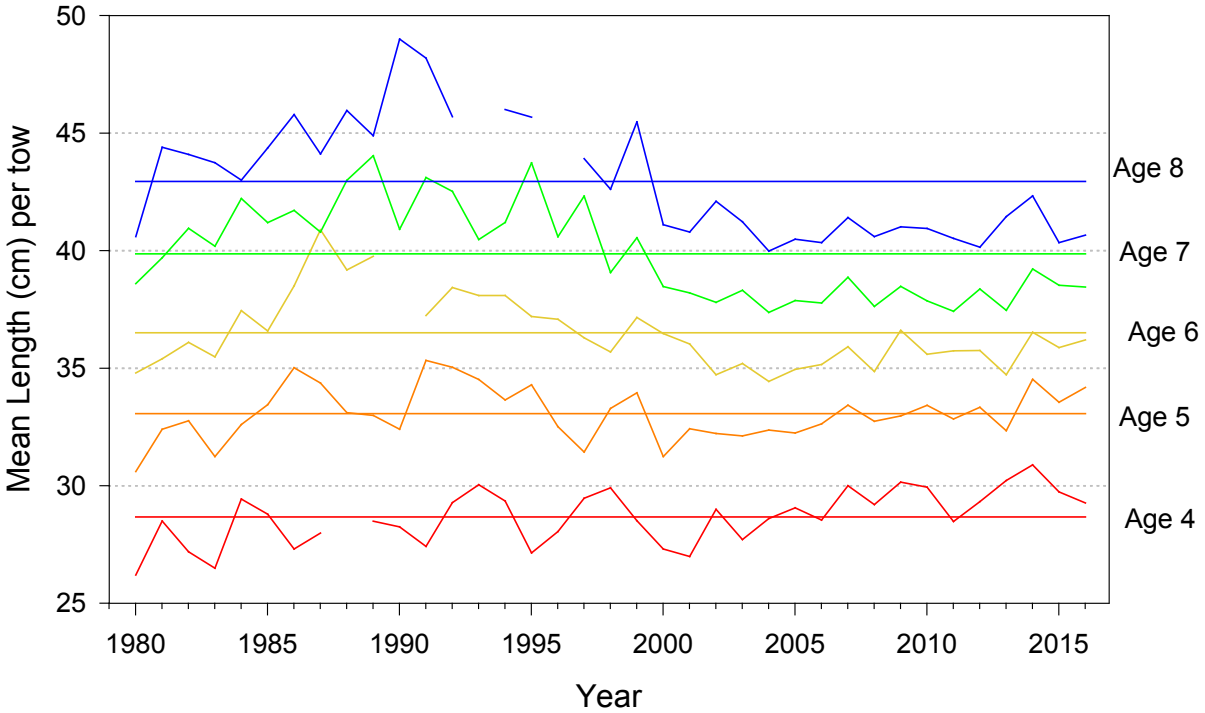

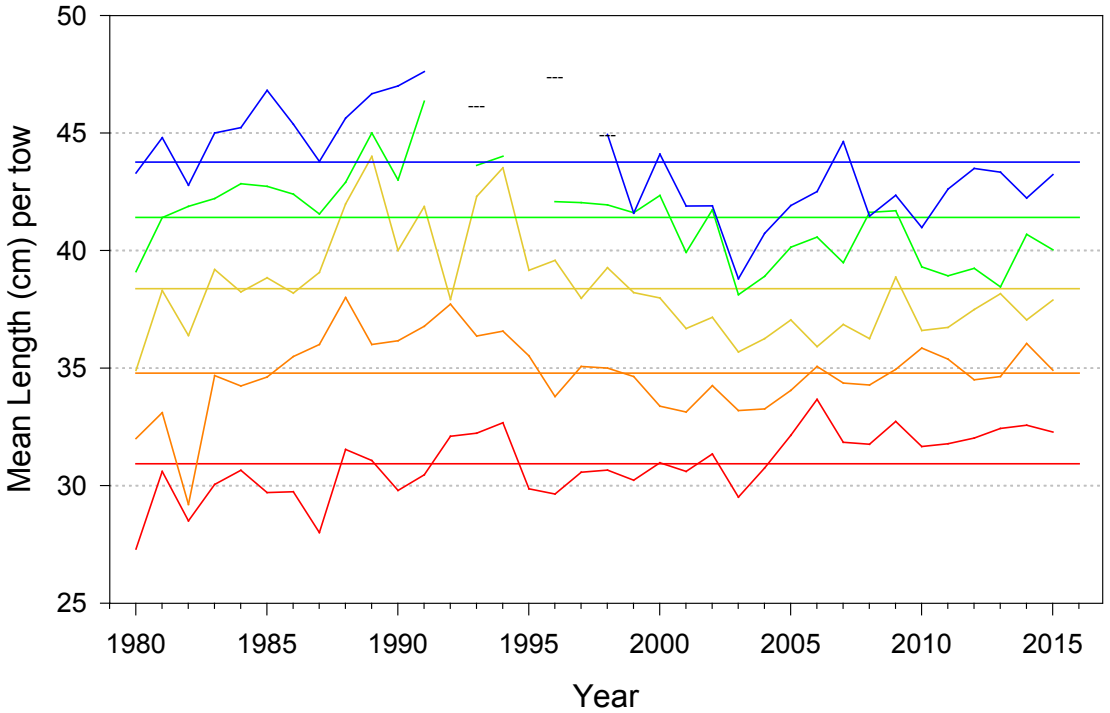

Figure.B51. Stratified mean length (cm) per tow at age of witch flounder in Northeast Fisheries Science Center bottom trawl spring (top) and autumn (bottom) surveys (strata 22-30, 36-40), 1980 – 2016.

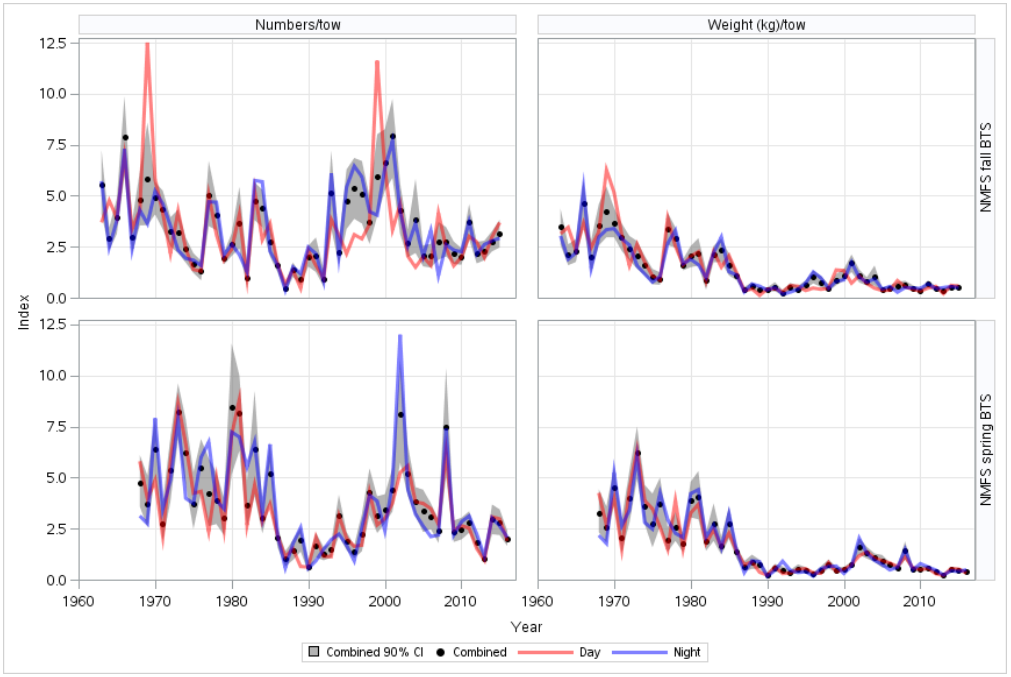

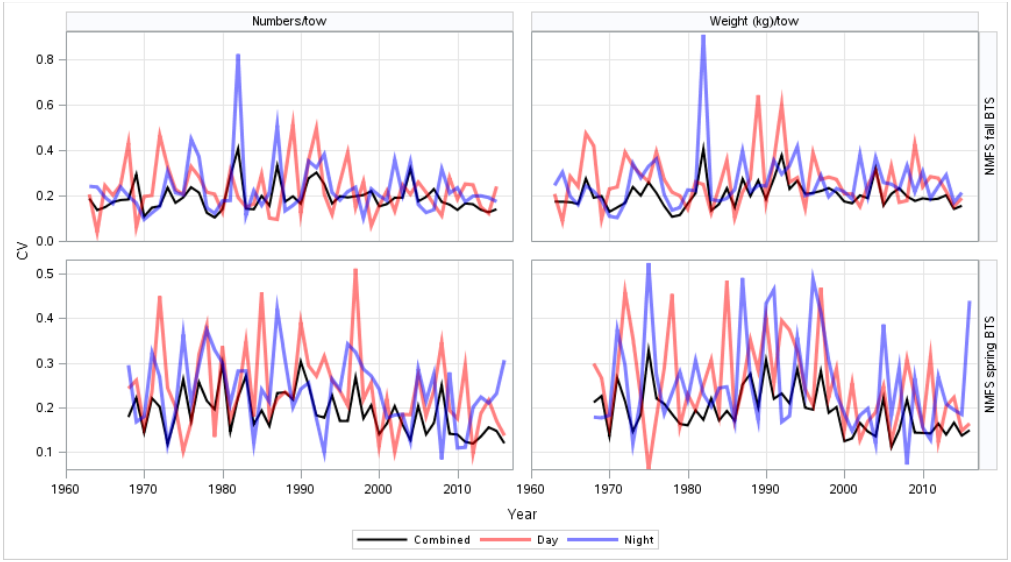

Figure B52. Stratified mean indices (number and weight per tow) of witch flounder from the Northeast Fisheries Science Center surveys broken out by day/night sampling compared with combined mean indices. CV are given in bottom plot.

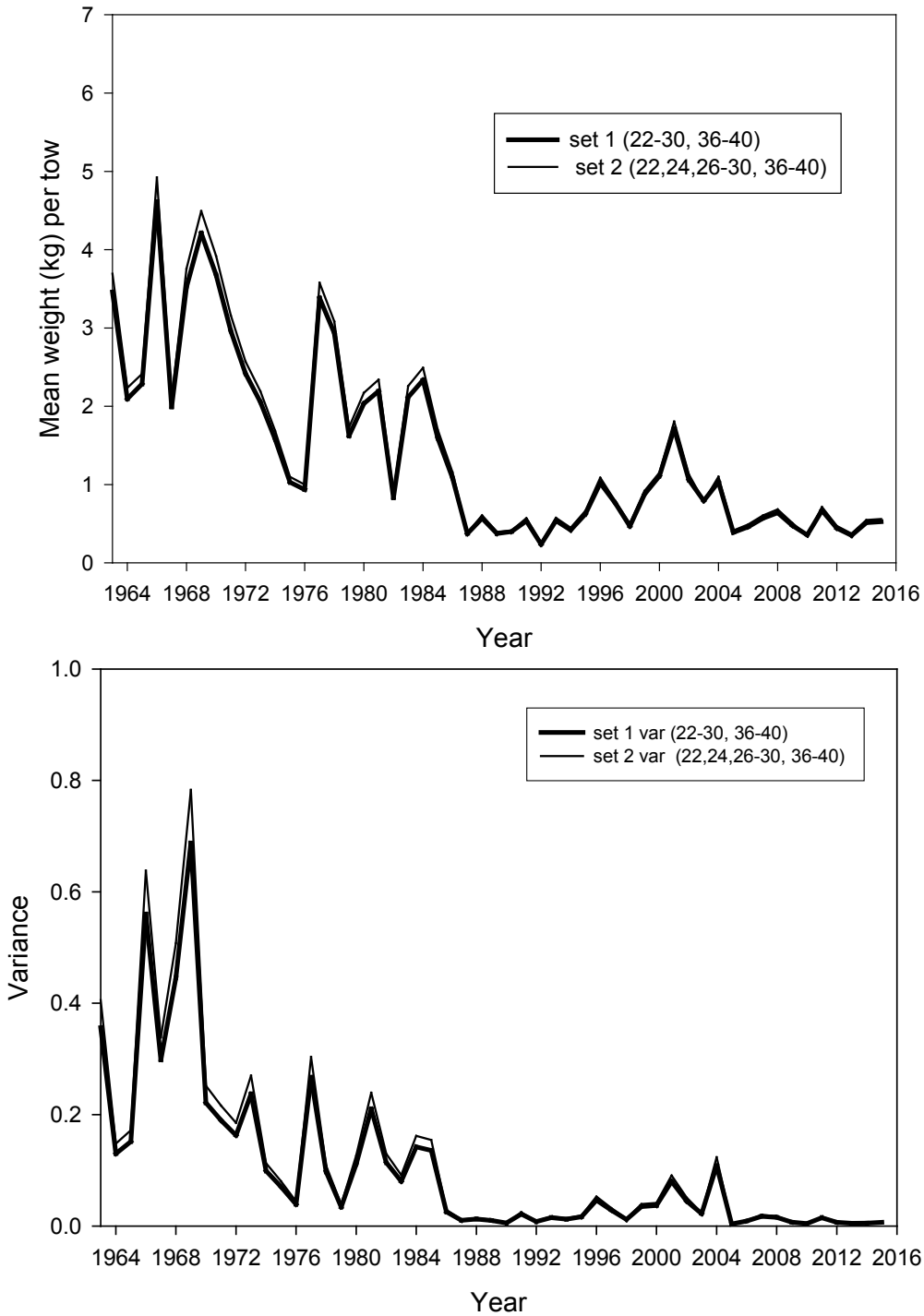

Figure B53. Stratified mean weight per tow (kg; top) and variance (bottom) of witch flounder in the Northeast Fisheries Science Center autumn bottom trawl survey for 2 strata sets in the Gulf of Maine-Georges Bank region, 1963-2015.

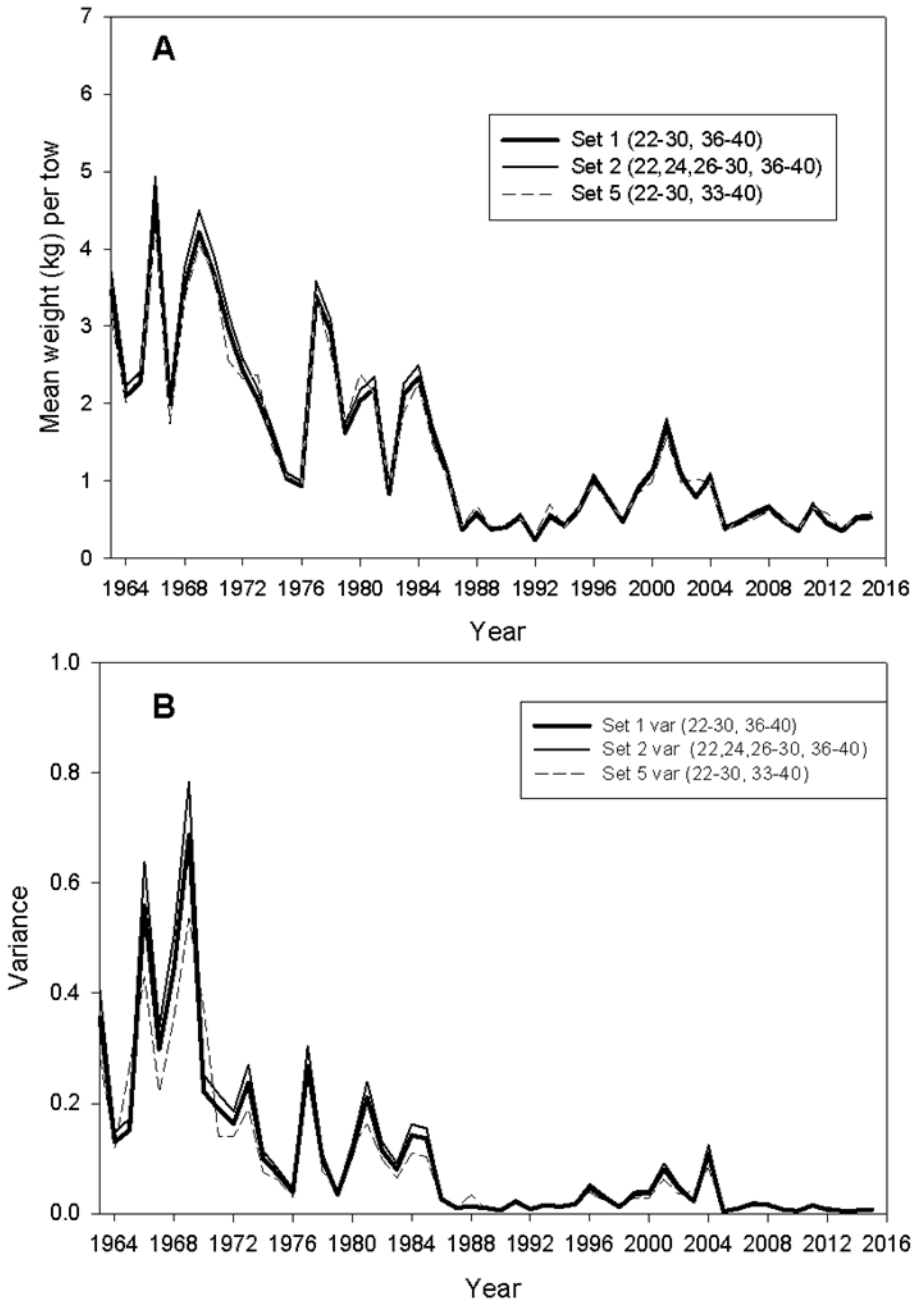

Figure B53a. Stratified mean weight per tow (kg; top) and variance (bottom) of witch flounder in the Northeast Fisheries Science Center autumn bottom trawl survey for 3 strata sets in the Gulf of Maine-Georges Bank region, 1963-2015. Strata set 5 includes strata 33, 34 and 351.

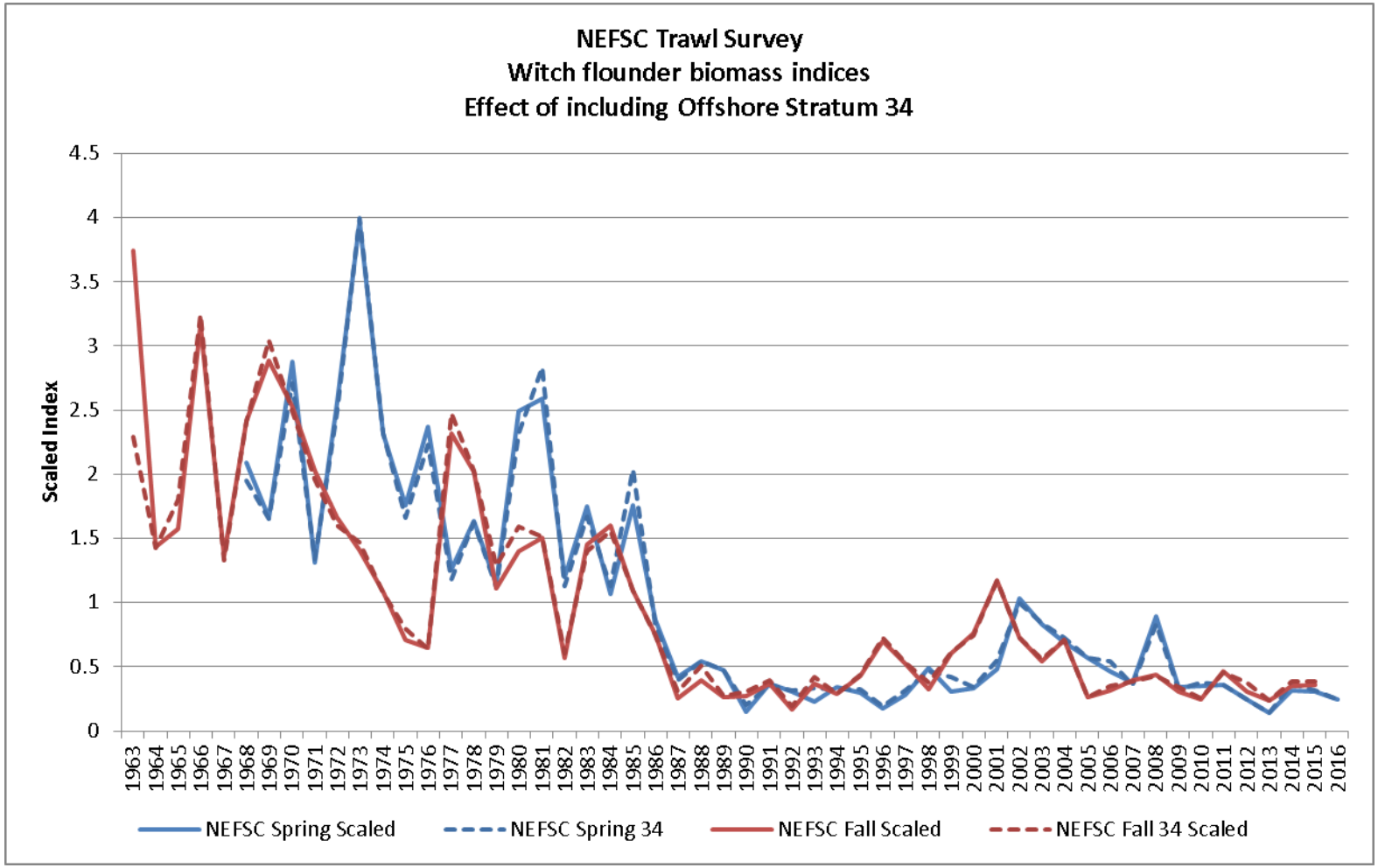

Figure B53b. Stratified mean weight per tow (kg) of witch flounder in the Northeast Fisheries Science Center spring (blue) and autumn (red) bottom trawl survey for 2 strata sets (solid line = set 22-30, 36-40; dashed line = 22-30, 34, 36-40) in the Gulf of Maine-Georges Bank region, 1963-2015.

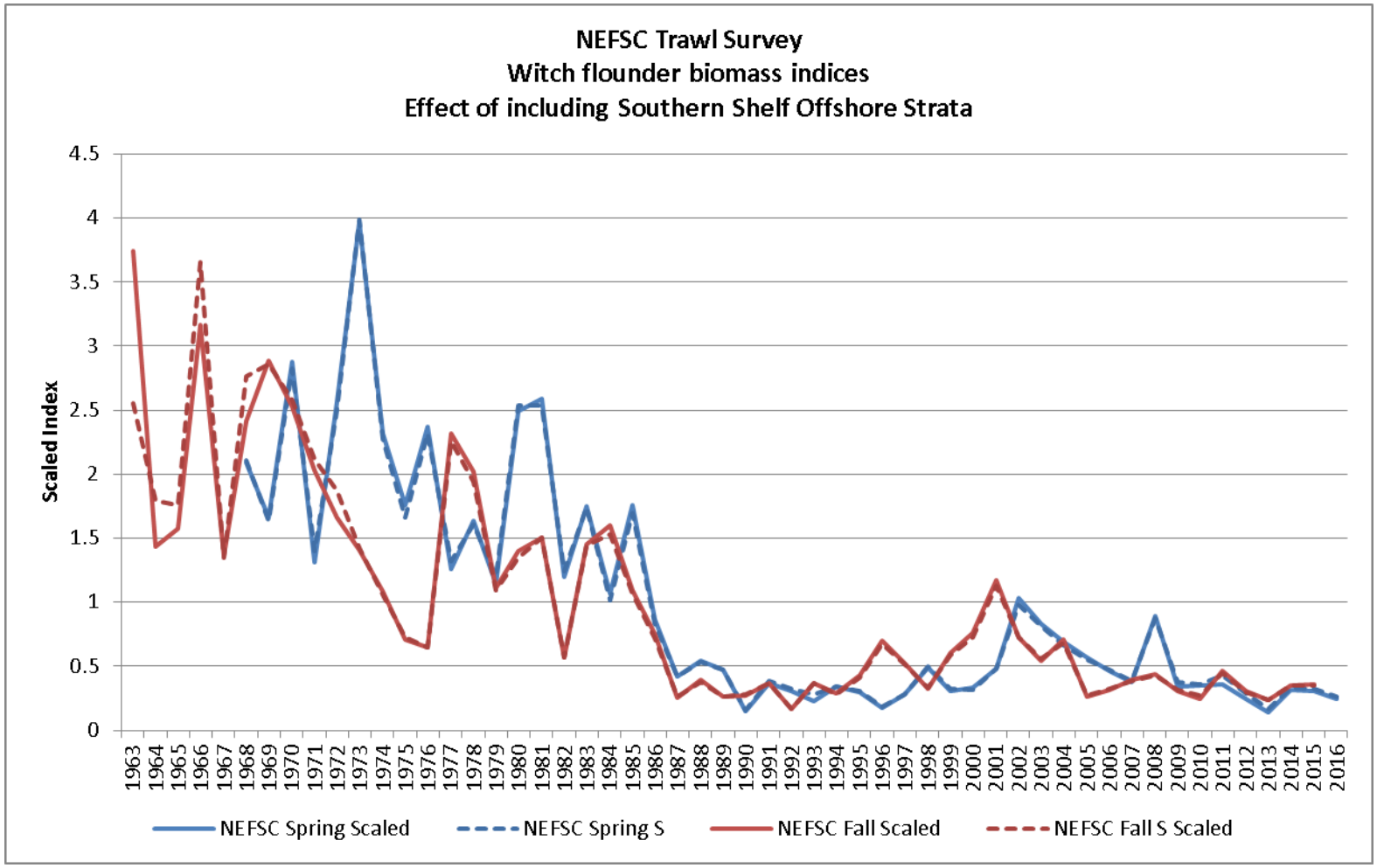

Figure B53c. Stratified mean weight per tow (kg) of witch flounder in the Northeast Fisheries Science Center spring (blue) and autumn (red) bottom trawl survey for 2 strata sets (solid line = set 22-30, 36-40; dashed line = 22-30, 34, 36-40 and southern offshore strata 2-4,6-8,10-18, 74-76) in the Gulf of Maine-Georges Bank and southward, 1963-2015.

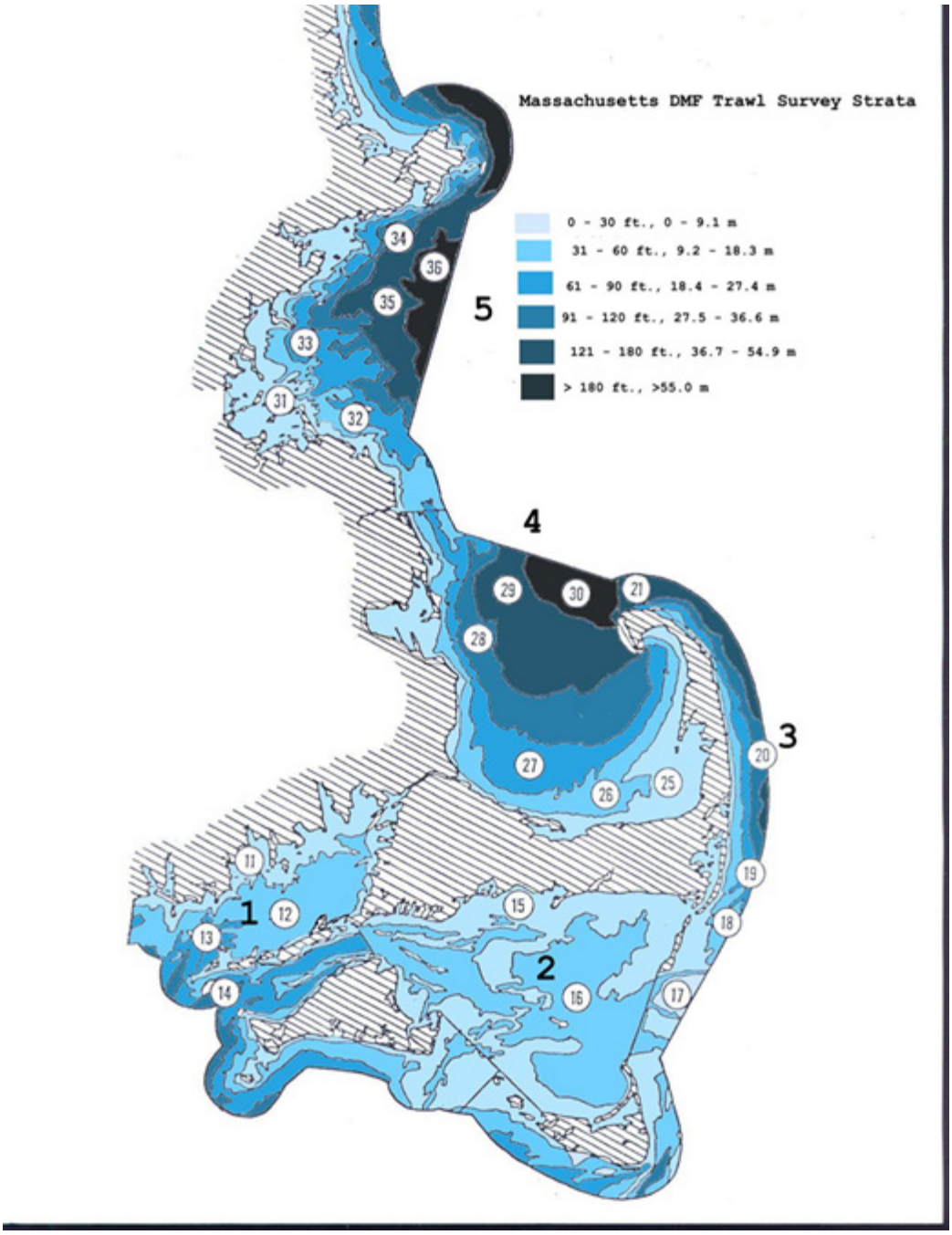

Figure B54. Massachusetts Division of Marine Fisheries inshore bottom trawl survey strata. Cape Cod Bay – Mass Bay region (Regions 4 and 5; strata 25 - 36) are used.

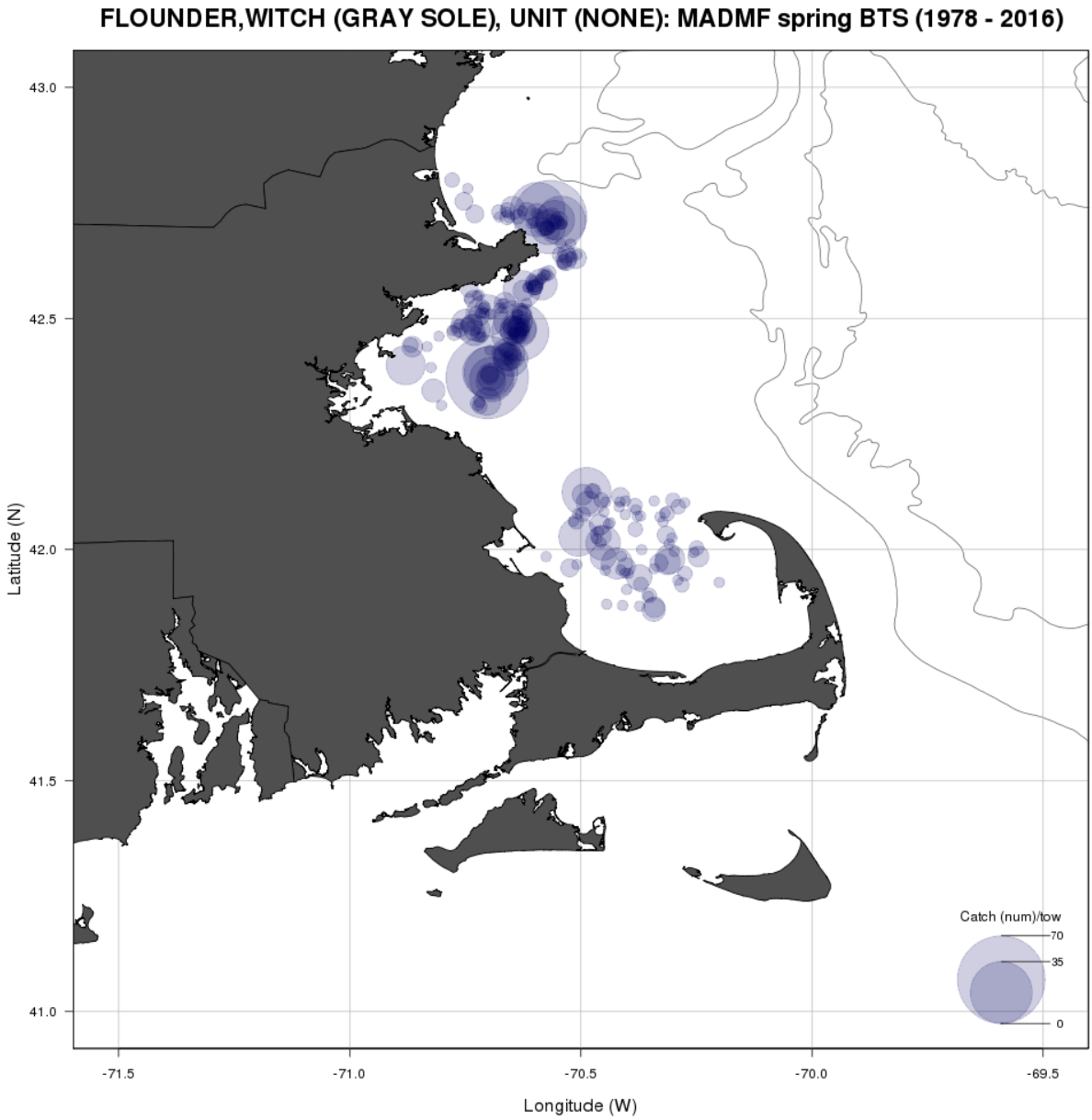

Figure B55. Number per tow of witch flounder in the Massachusetts Division of Marine Fisheries inshore bottom trawl survey strata. Cape Cod Bay – Mass Bay region (Regions 4 and 5; strata 25 - 36), spring 1978-2016.

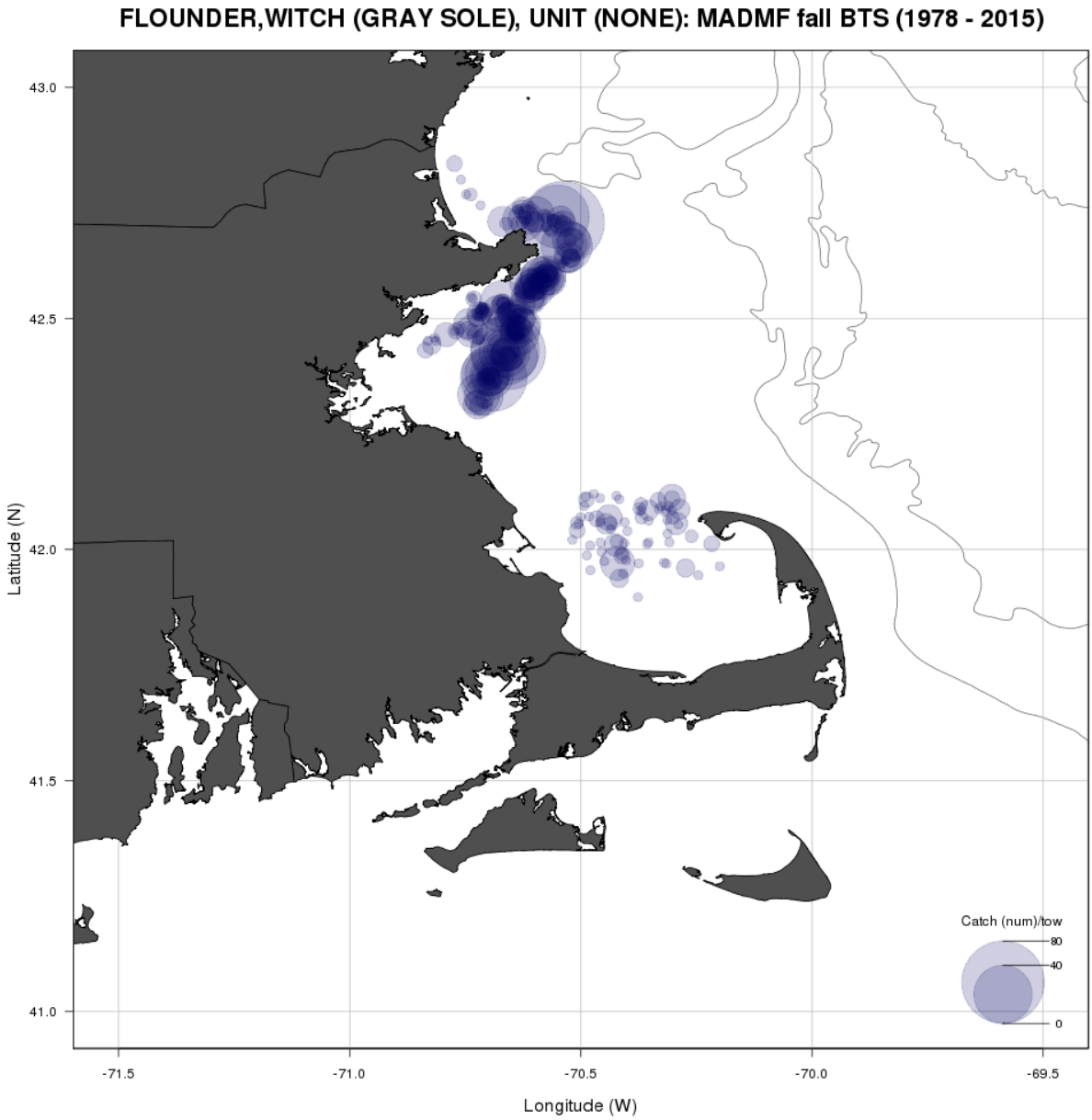

Figure B56. Number per tow of witch flounder in the Massachusetts Division of Marine Fisheries inshore bottom trawl survey strata. Cape Cod Bay – Mass Bay region (Regions 4 and 5; strata 25 - 36), autumn 1978-2015.

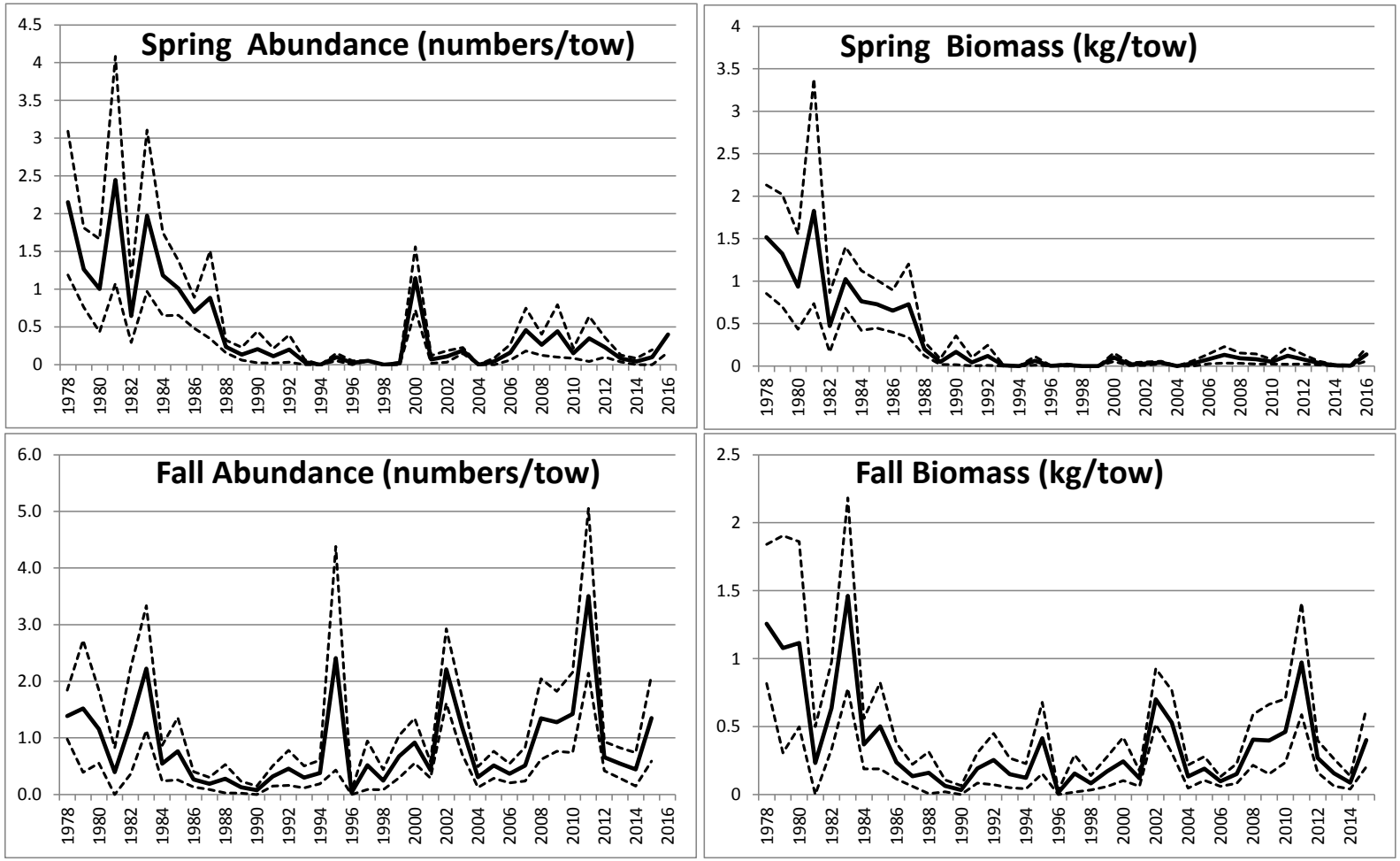

Figure B57. Stratified mean catch per tow, in numbers (left) and weight (right), of witch flounder in the Massachusetts Division of Marine Fisheries spring (top) and autumn (bottom) inshore trawl surveys in Cape Cod Bay – Mass Bay region (Regions 4 and 5), 1978 – 2016. Dashed line indicate the 90% confidence intervals.

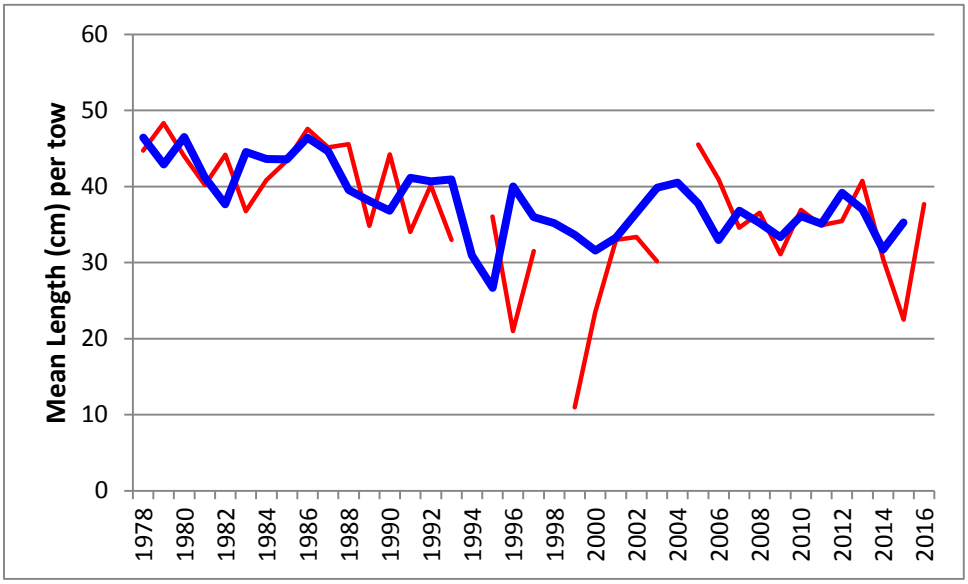

Figure B58. Stratified mean length (cm) per tow of witch flounder in the Massachusetts Division of Marine Fisheries spring (red line) and autumn (blue line) inshore trawl surveys in Cape Cod Bay – Mass Bay region (Regions 4 and 5), 1978 – 2016.

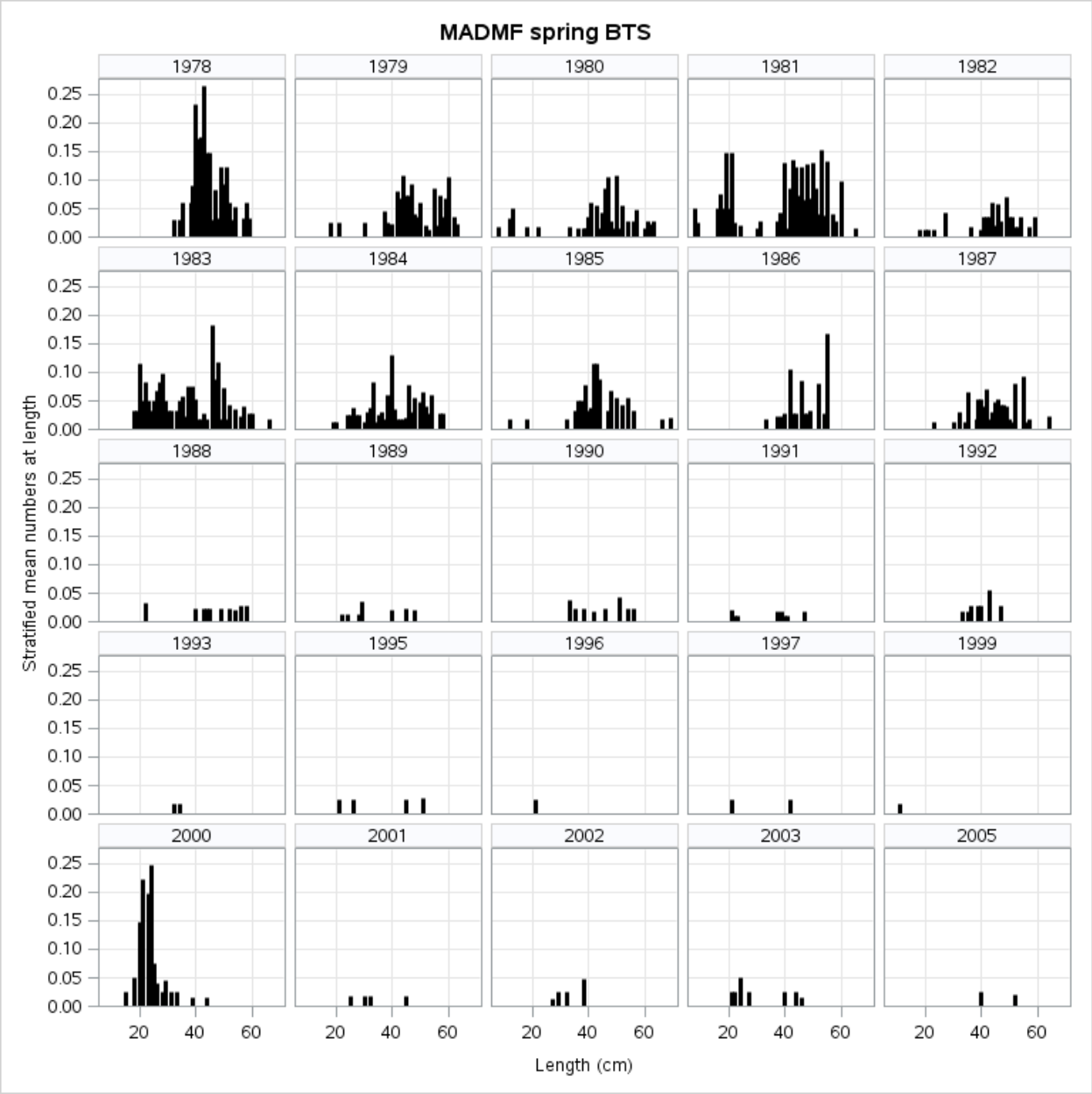

Figure B59. Stratified mean number per tow at length (cm) of witch flounder in the Massachusetts Division of Marine Fisheries spring bottom trawl surveys in Cape Cod Bay – Mass Bay region (Regions 4 and 5), 1978 – 2016.

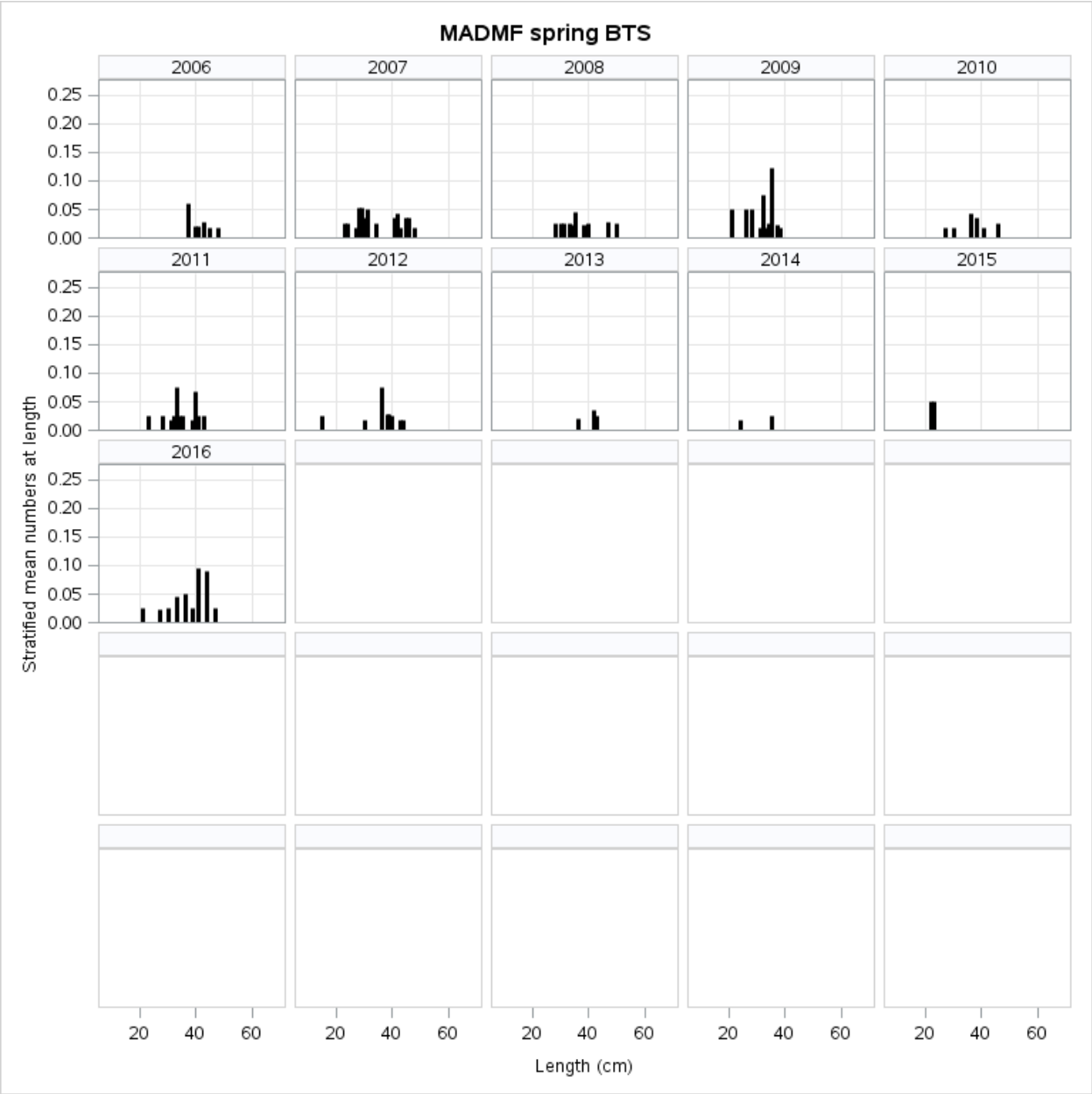

Figure B59, continued. Stratified mean number per tow at length (cm) of witch flounder in the Massachusetts Division of Marine Fisheries spring bottom trawl surveys in Cape Cod Bay – Mass Bay region (Regions 4 and 5), 1978 – 2016.

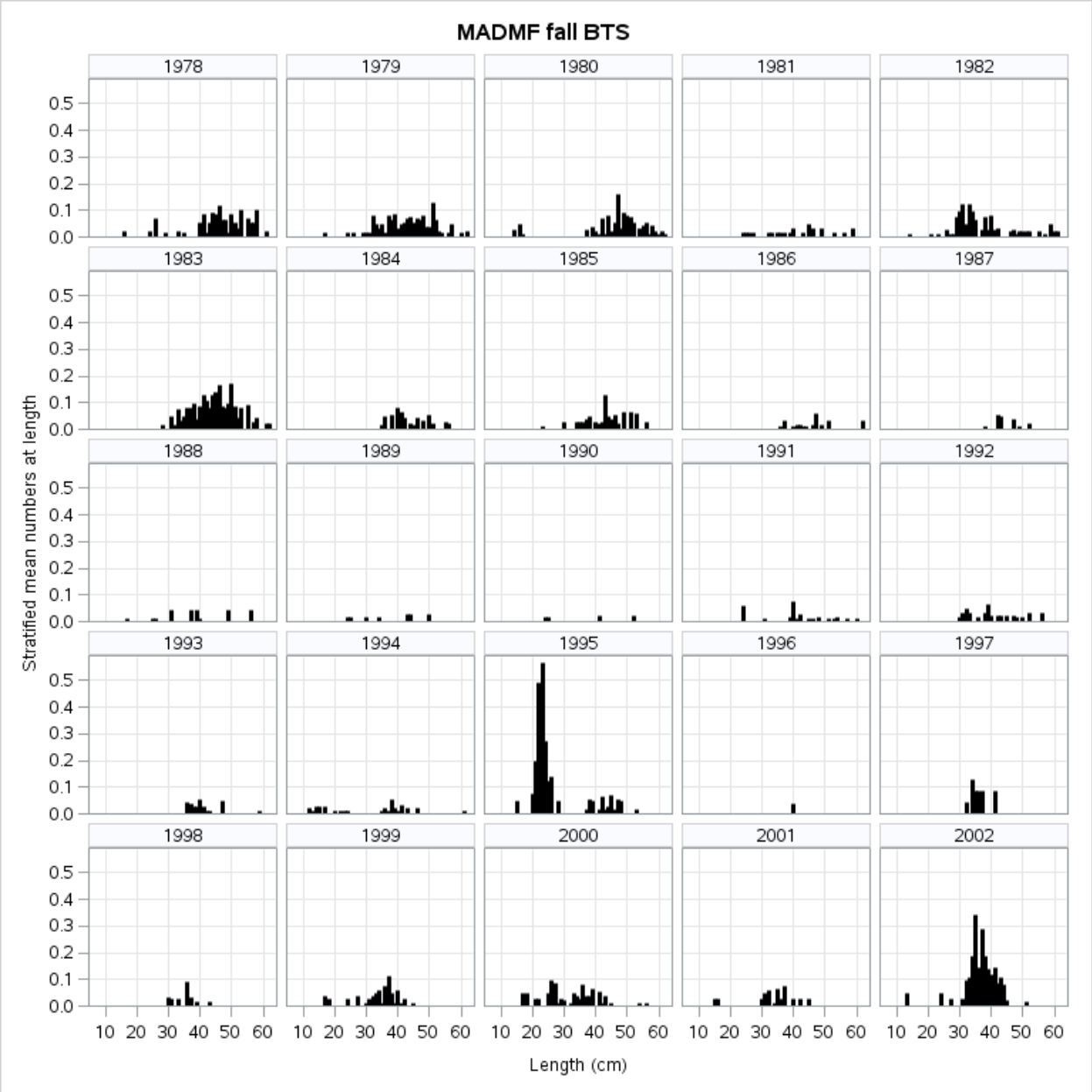

Figure B60. Stratified mean number per tow at length (cm) of witch flounder in the Massachusetts Division of Marine Fisheries autumn bottom trawl surveys in Cape Cod Bay – Mass Bay region (Regions 4 and 5), 1978 – 2015.

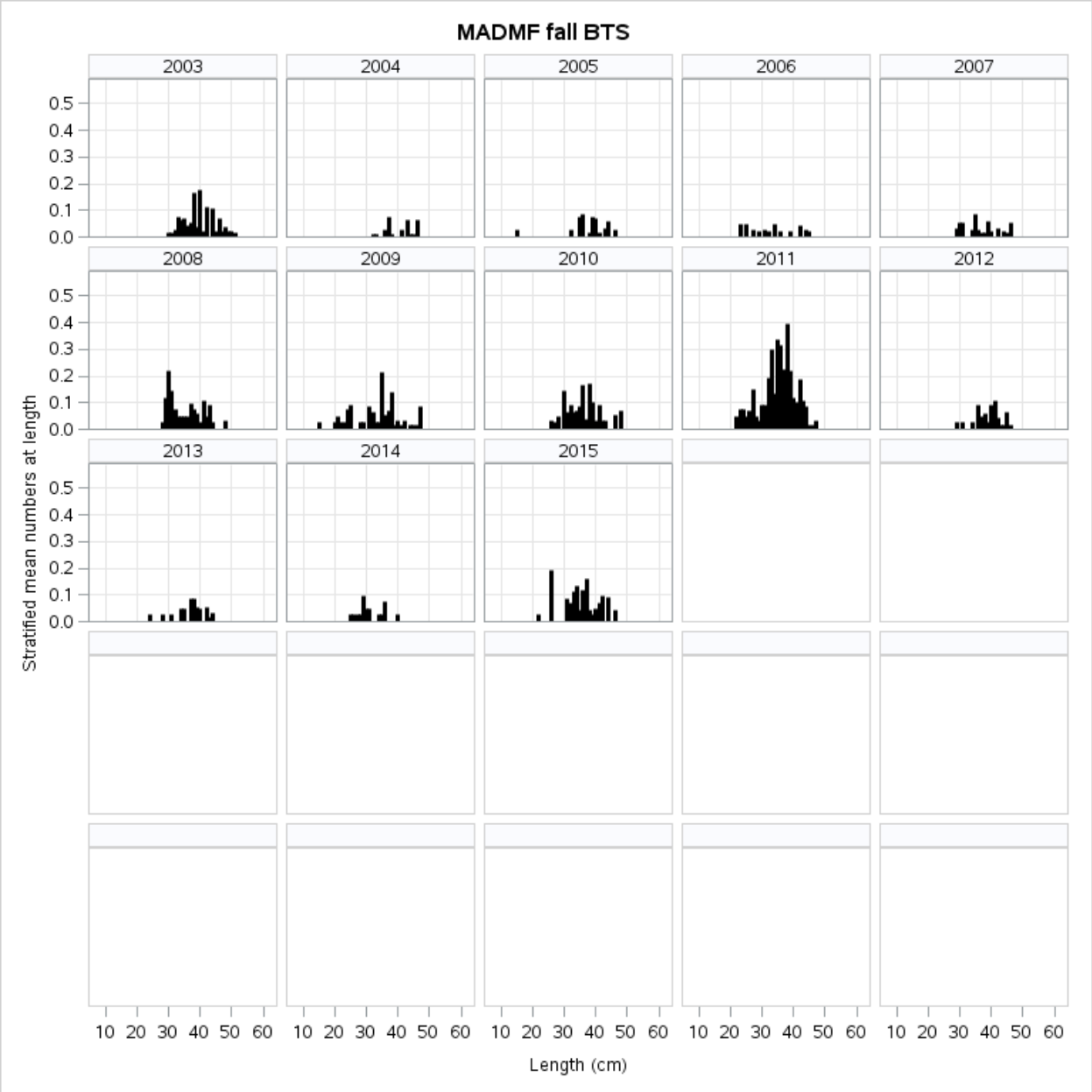

Figure B60, continued. Stratified mean number per tow at length (cm) of witch flounder in the Massachusetts Division of Marine Fisheries autumn bottom trawl surveys in Cape Cod Bay – Mass Bay region (Regions 4 and 5), 1978 – 2015.

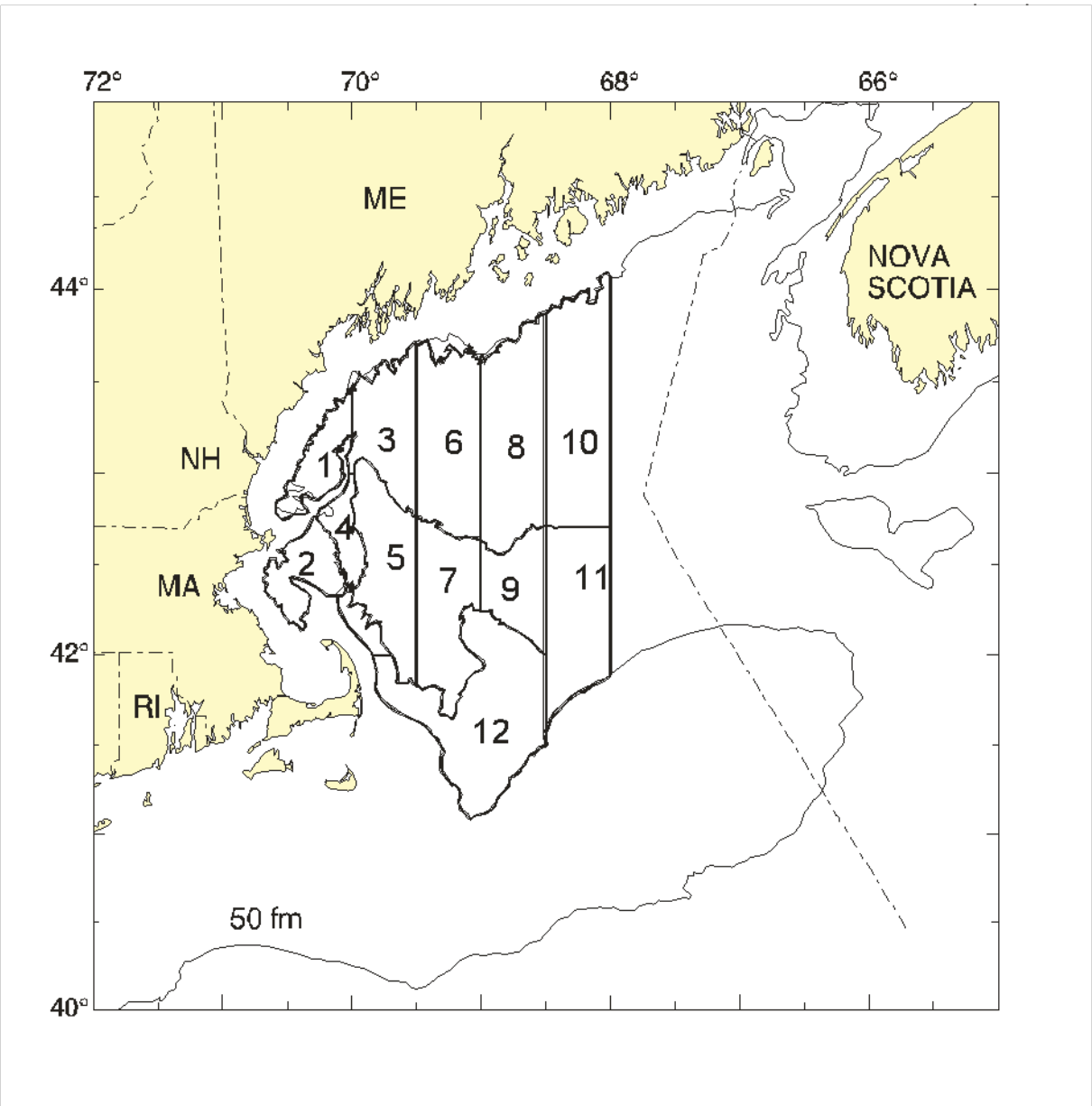

Figure B61. Sampling strata (1, 3, 6, 8) used during the Atlantic States Marine Fisheries Commission summer shrimp trawl survey.

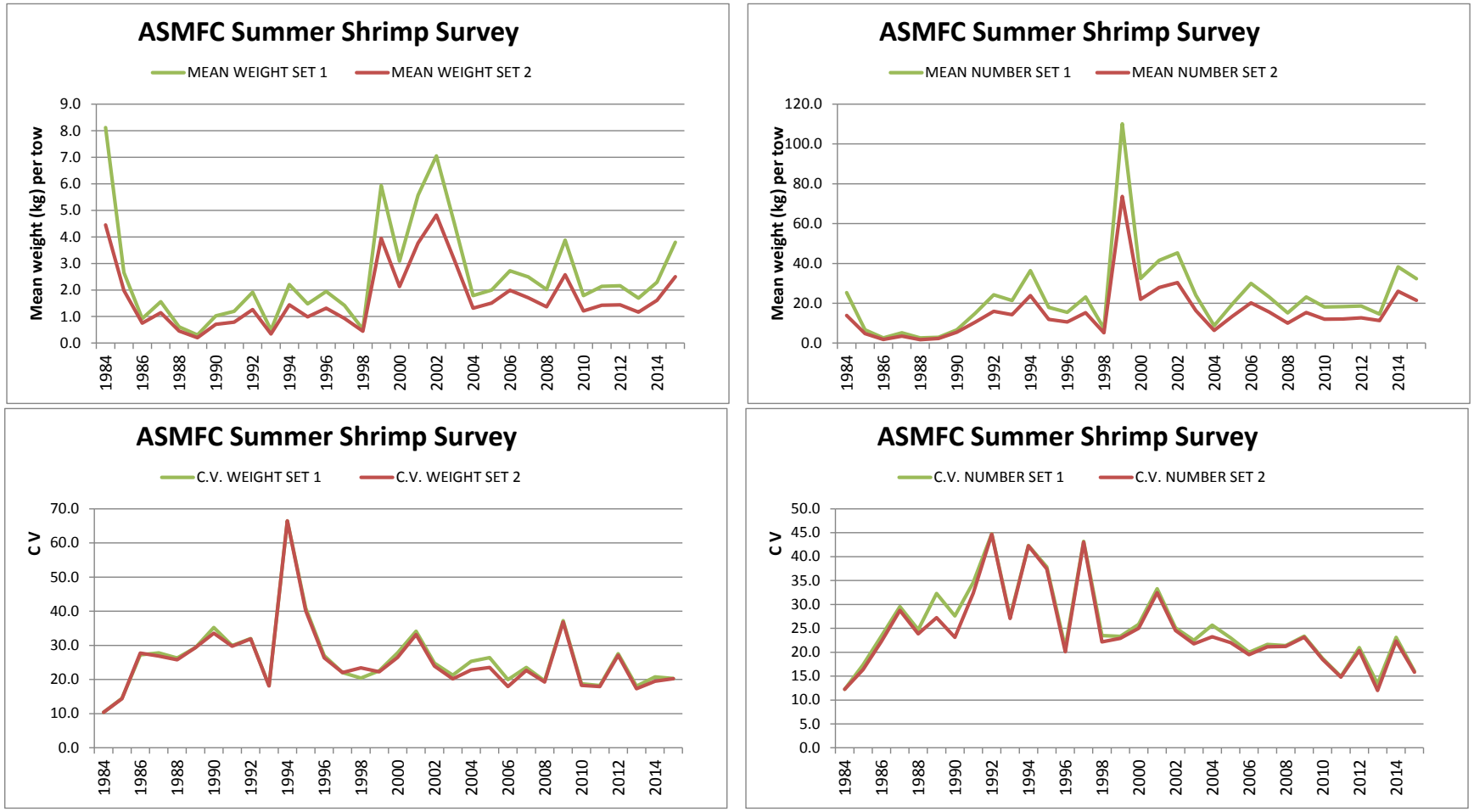

Figure B62. Comparison of stratified mean weight (left) and numbers (right) per tow and their associated coefficient of variation (CV) of two strata sets (set 1 = 1, 3, 6, 8 [green]; set 2 = 1, 3, 5, 6, 7, 8 [red]) in the Atlantic State Marine Fisheries Commission (ASMFC) summer shrimp survey in the Gulf of Maine, 1984 – 2015.

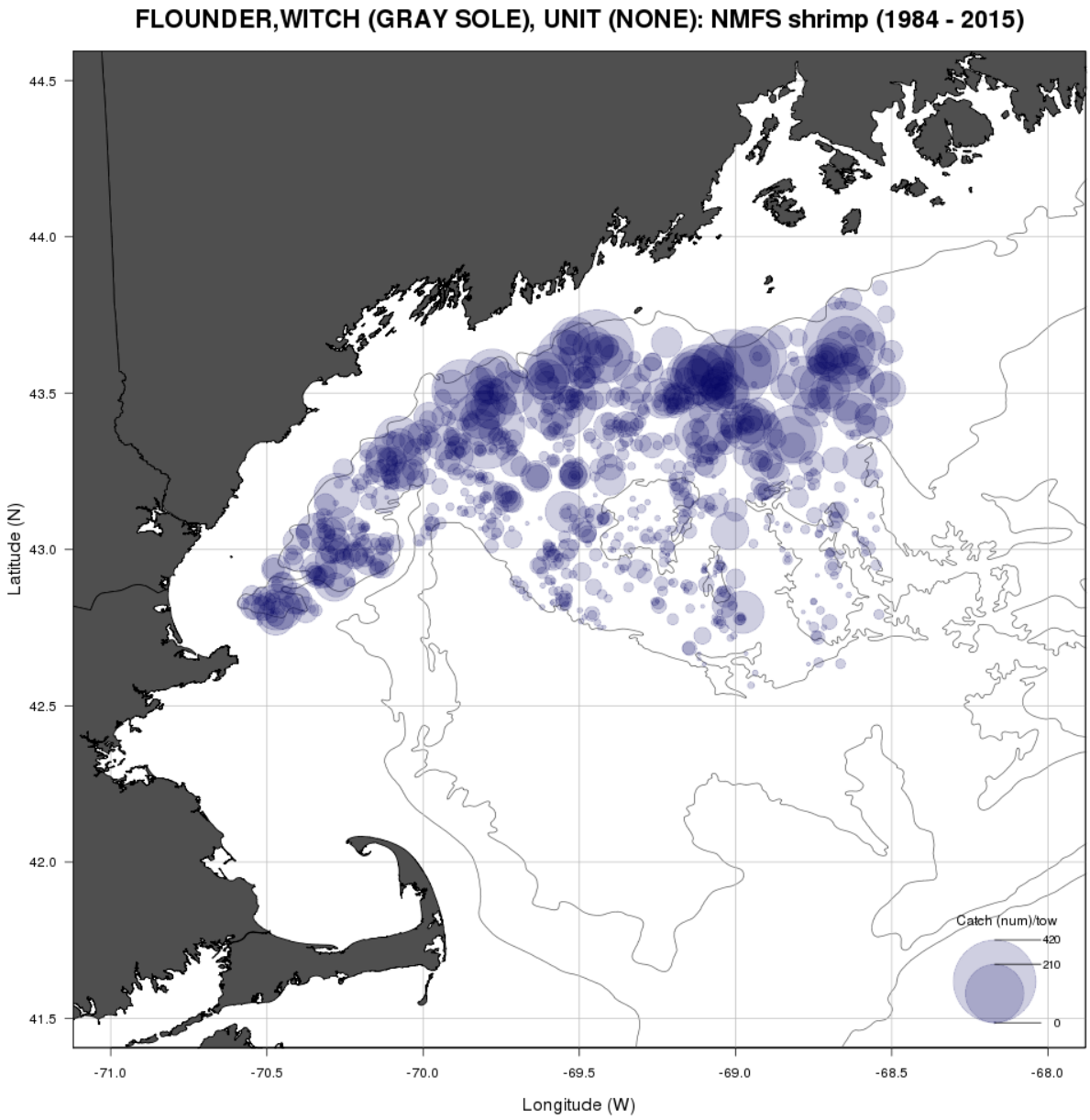

Figure B63. Number per tow of witch flounder in the in the Atlantic States Marine Fisheries Commission summer shrimp survey (strata set 1, 3, 6, 8), 1984 - 2015.

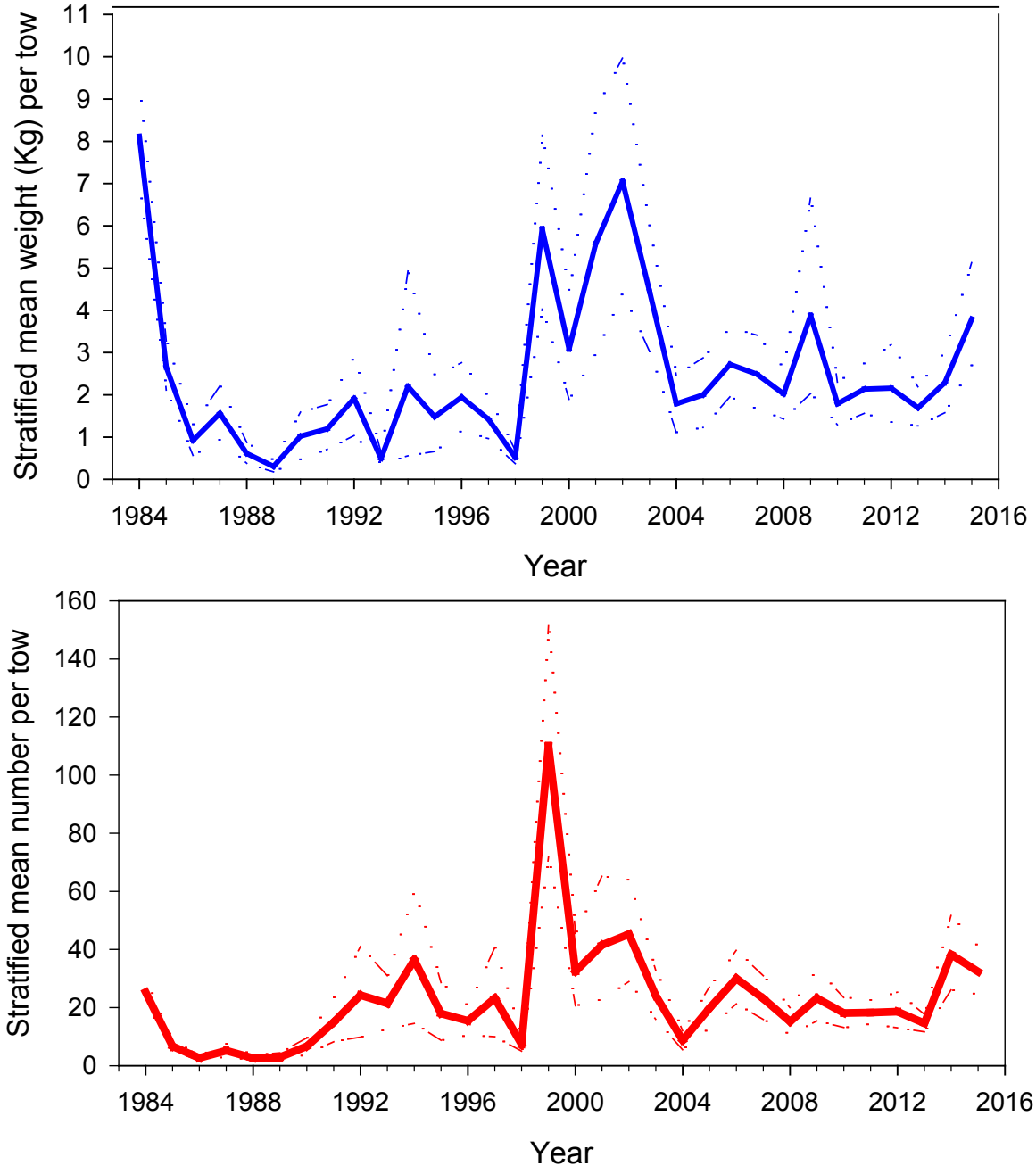

Figure B64. Stratified mean catch per tow, in weight (kg; top) and numbers (bottom), of witch flounder in the Atlantic States Marine Fisheries Commission summer shrimp survey (strata set 1, 3, 6, 8), 1984 - 2015. Dash lines represents 90% confidence intervals.

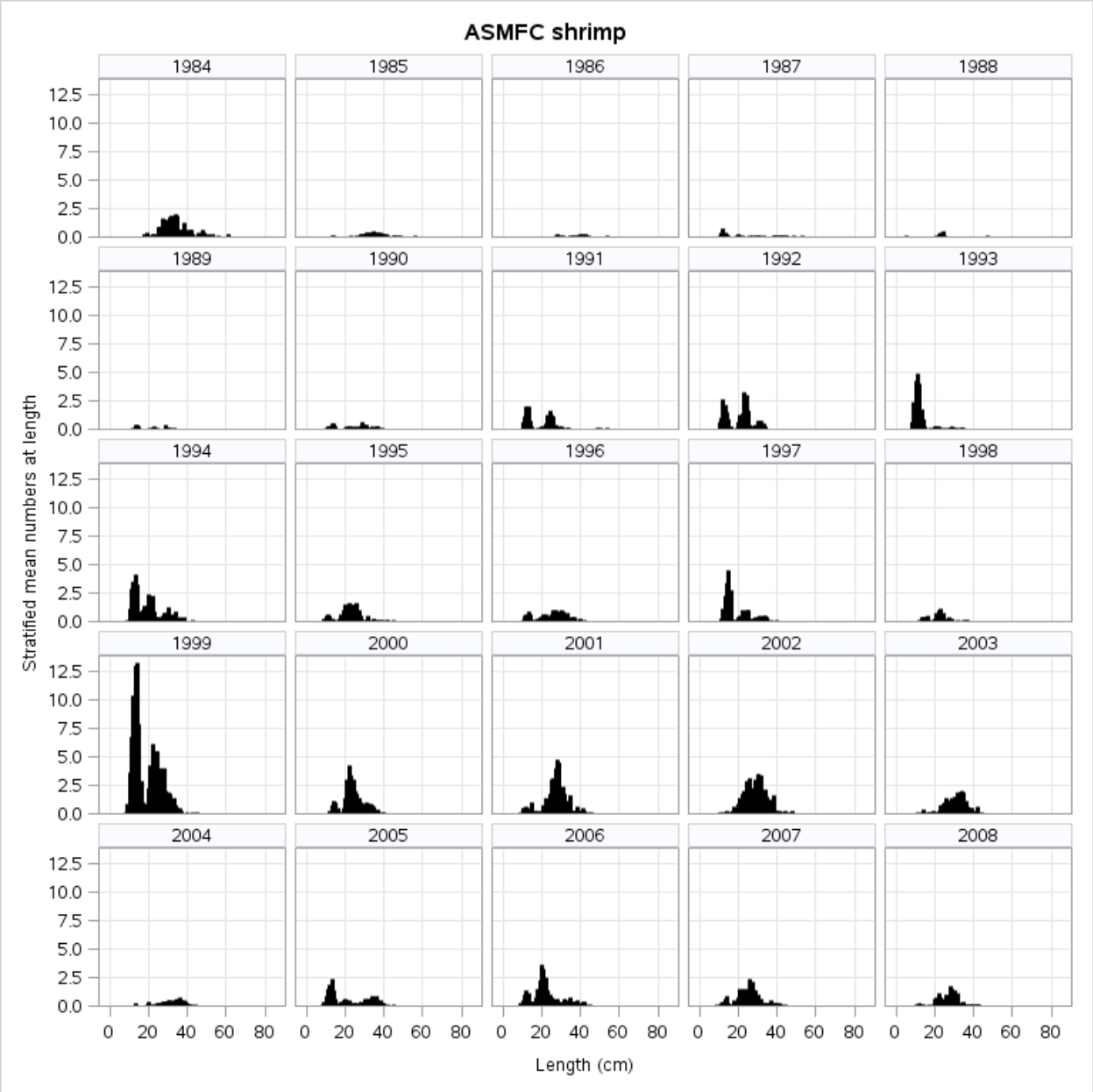

Figure B65. Stratified mean number per tow at length (cm), of witch flounder in the Atlantic States Marine Fisheries Commission summer shrimp survey (strata set 1, 3, 6, 8), 1984 - 2015.

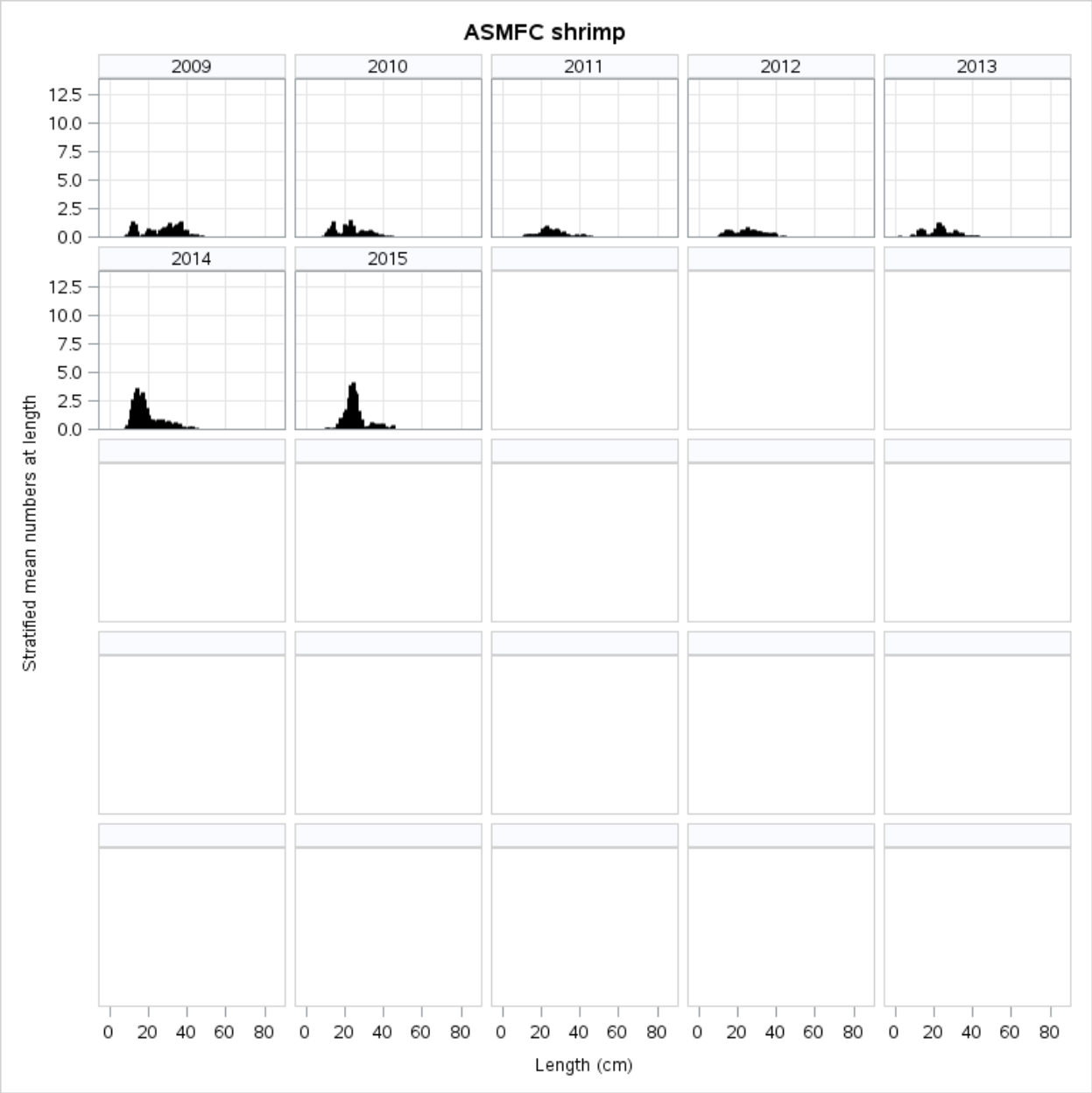

Figure B65, continued. Stratified mean number per tow at length (cm), of witch flounder in the Atlantic States Marine Fisheries Commission summer shrimp survey (strata set 1, 3, 6, 8), 1984 - 2015.

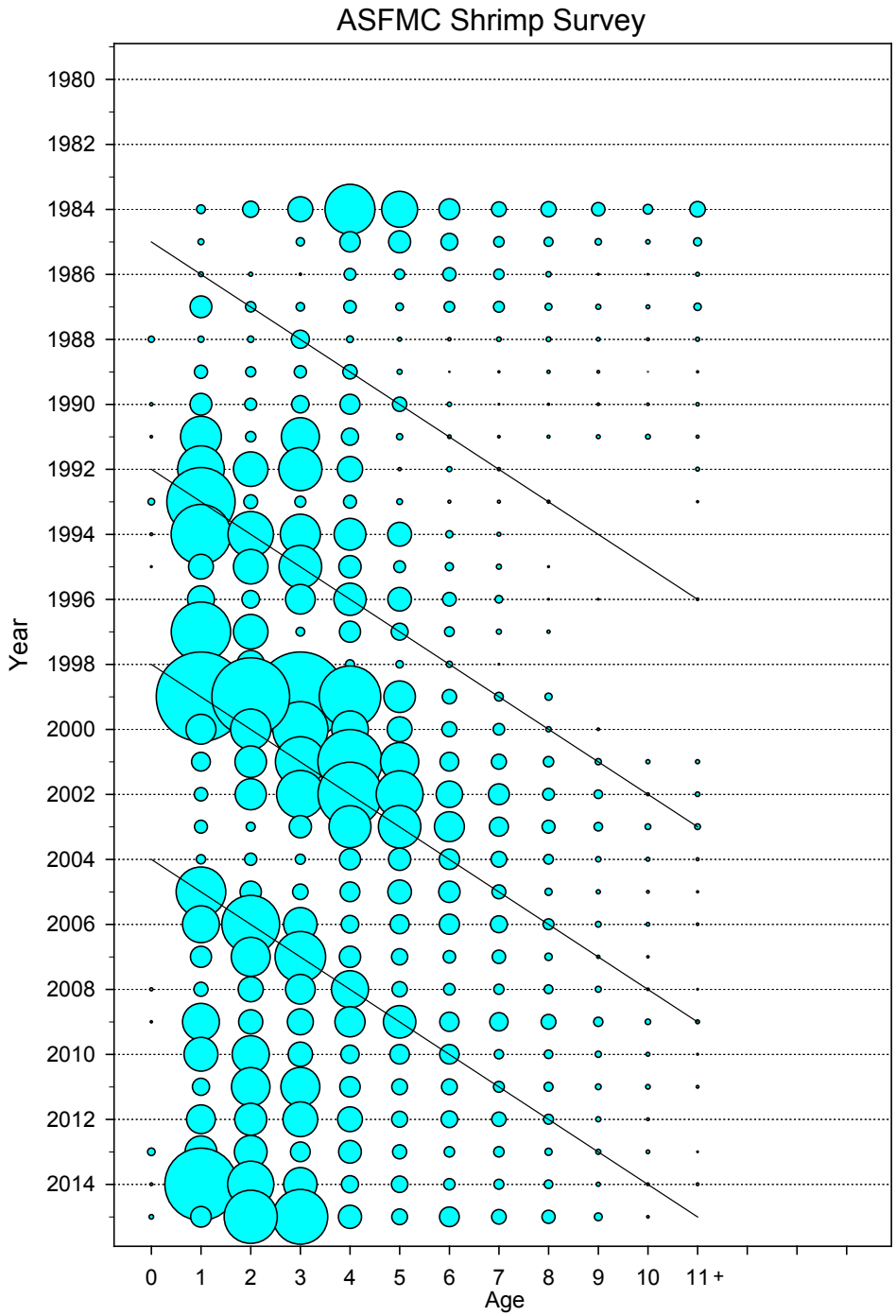

Figure B66. Stratified mean number per tow at age (cm), of witch flounder in the Atlantic States Marine Fisheries Commission summer shrimp survey (strata set 1, 3, 6, 8), 1984 - 2015.

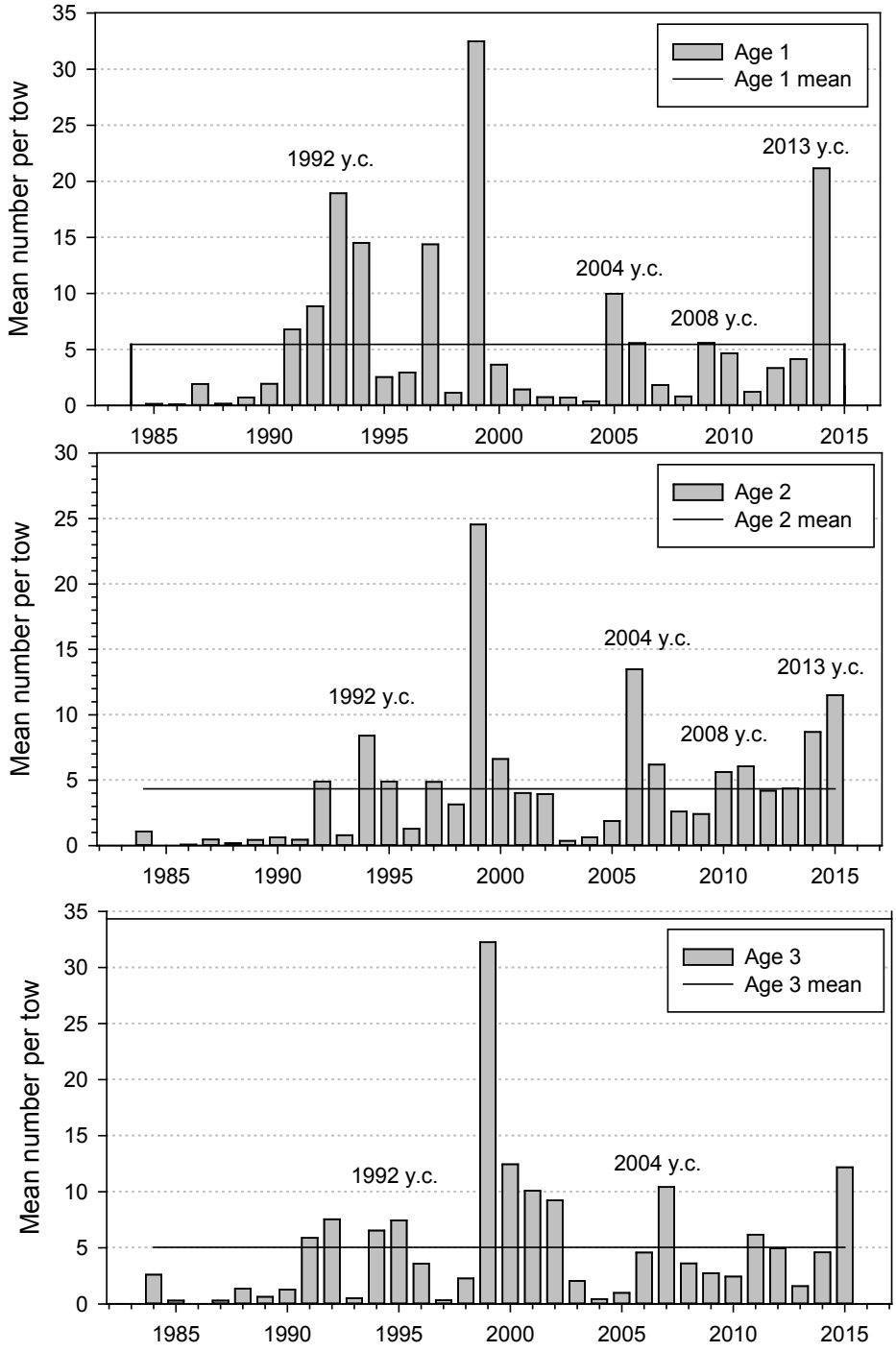

Figure B67. Stratified mean number per tow of age 1 (top), age 2 (middle) and age 3 (bottom) witch flounder in the Atlantic States Marine Fisheries Commission summer shrimp survey (strata set 1, 3, 6, 8), 1984 - 2015. Time series mean number per tow at age is also given.

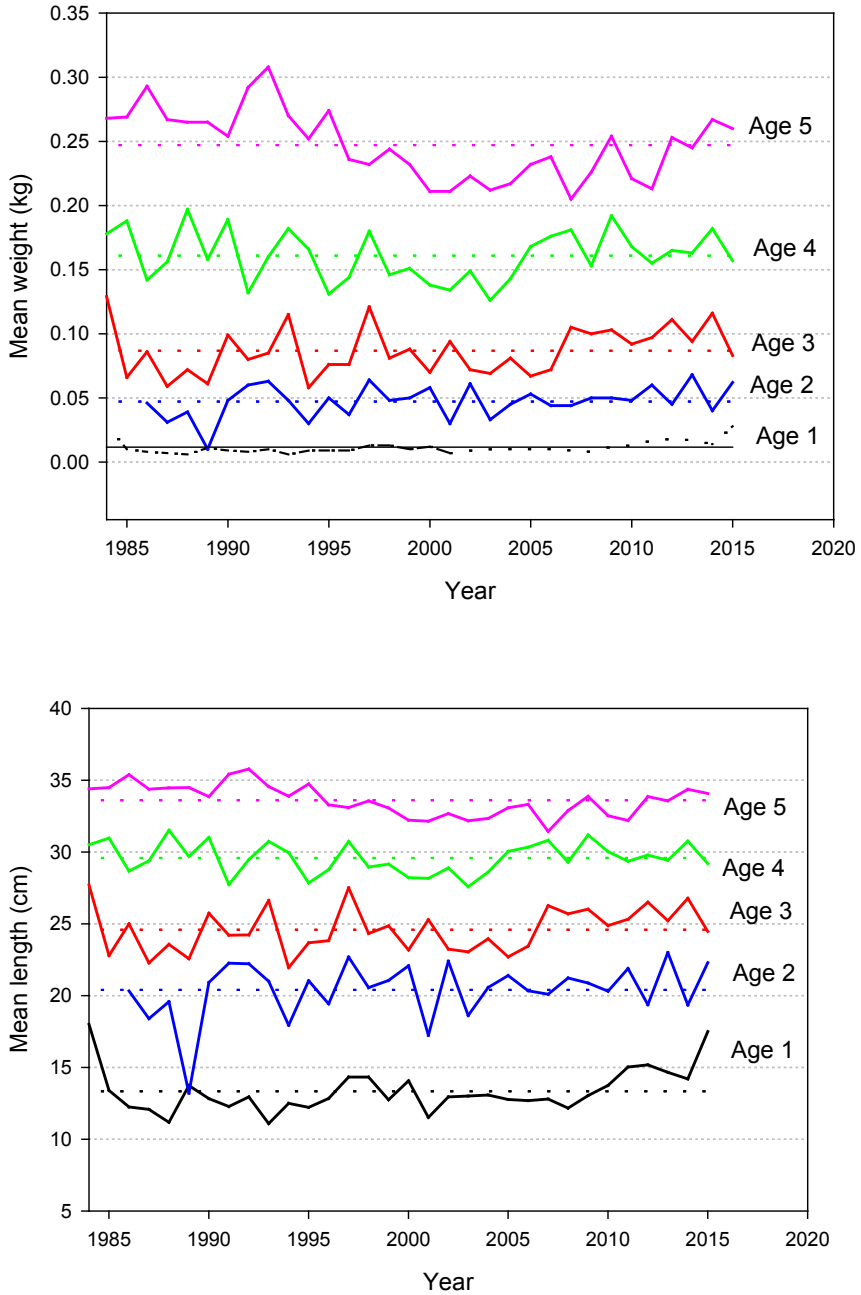

Figure B68. Stratified mean weight (kg; top) and length (cm; bottom) per tow of witch flounder in the Atlantic States Marine Fisheries Commission summer shrimp survey (strata set 1, 3, 6, 8), 1984 - 2015.

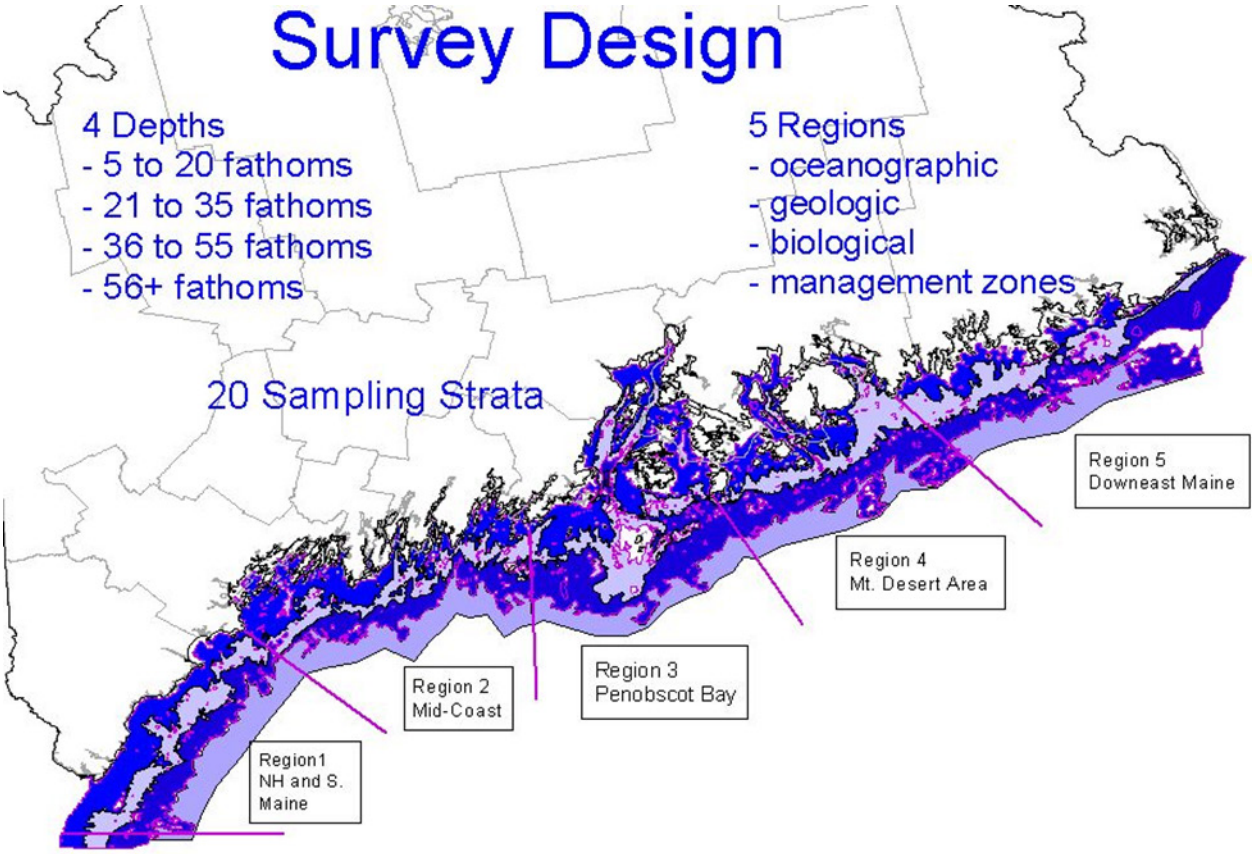

Figure B69. This map shows the 5 regions (each region is bounded by straight purple lines) and 4 depth strata (depicted in blue and purple shading) used in the Maine-New Hampshire Inshore Trawl Survey.

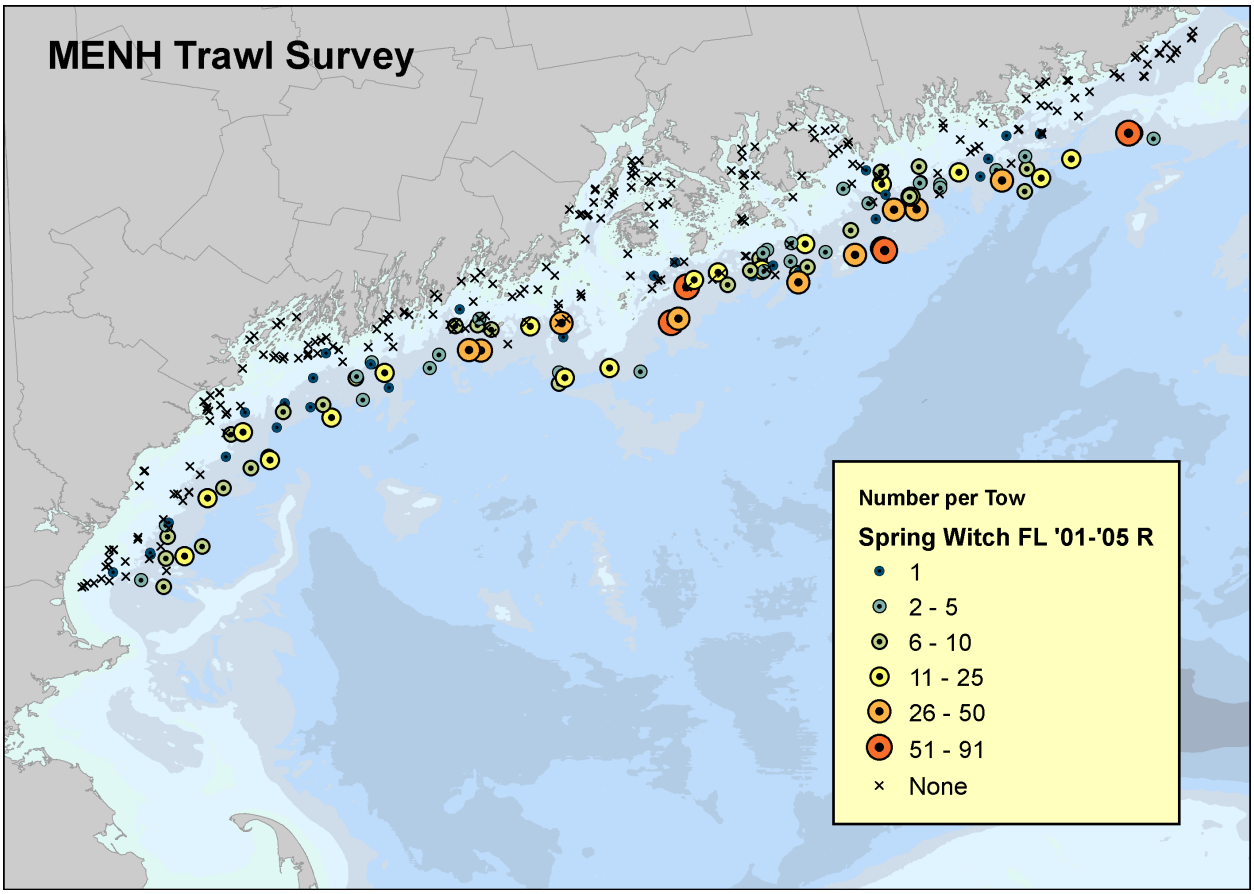

Figure B70. This map depicts survey catches for witch flounder (Glyptocephalus cynoglossus). The color-shaded circles represent number of fish per tow during the 2001-2005 (re-stratified) spring Maine-New Hampshire inshore trawl survey. The black '+' (plus symbol) represent no catch. Bathymetry is depicted in blue and gray shading.

Provided by Sally Sherman, Maine Department of Marine Resources, pers comm. July 28, 2016.

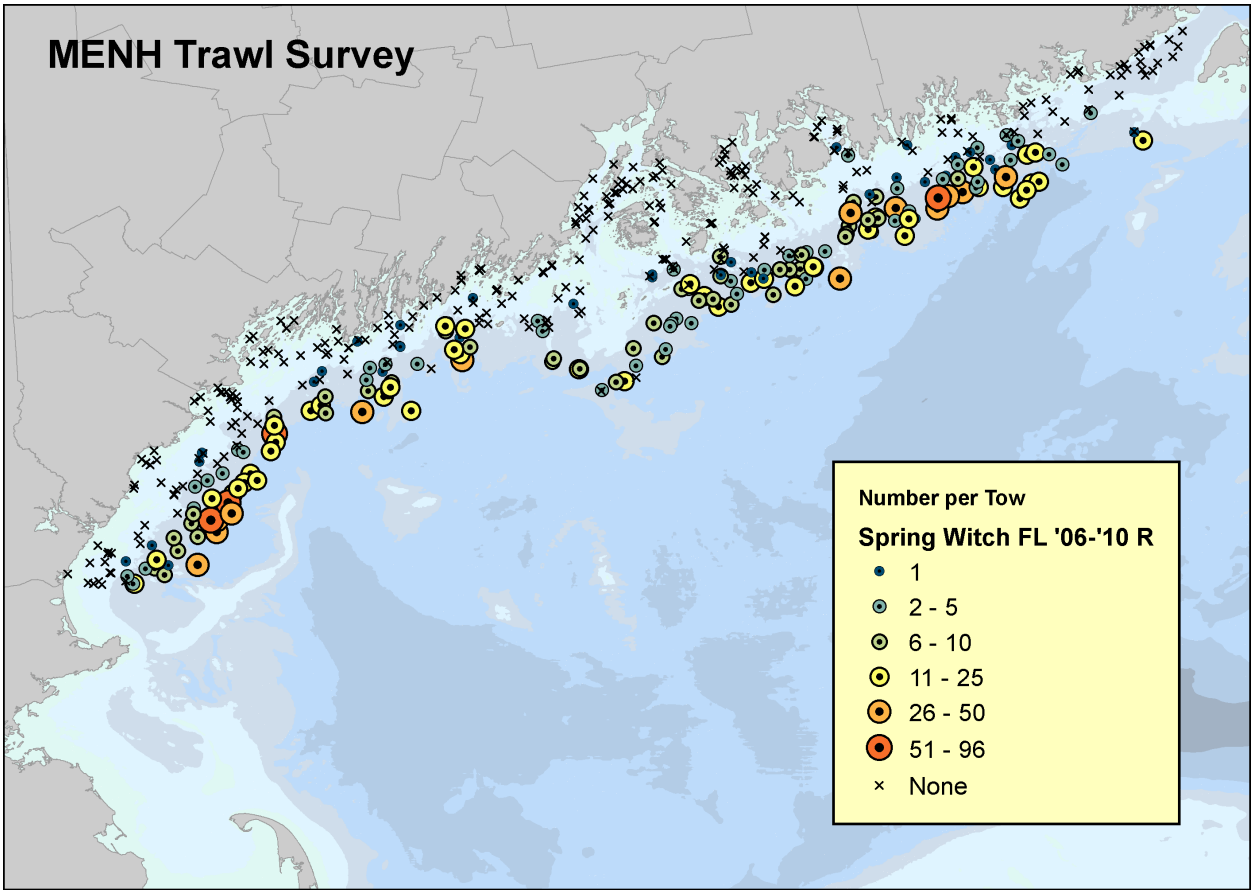

Figure B71. This map depicts survey catches for witch flounder (*Glyptocephalus cynoglossus*). The color-shaded circles represent number of fish per tow during the 2006-2010 (re-stratified) spring Maine-New Hampshire inshore trawl survey. The black '+' (plus symbol) represent no catch. Bathymetry is depicted in blue and gray shading.

Provided by Sally Sherman, Maine Department of Marine Resources, pers comm. July 28, 2016.

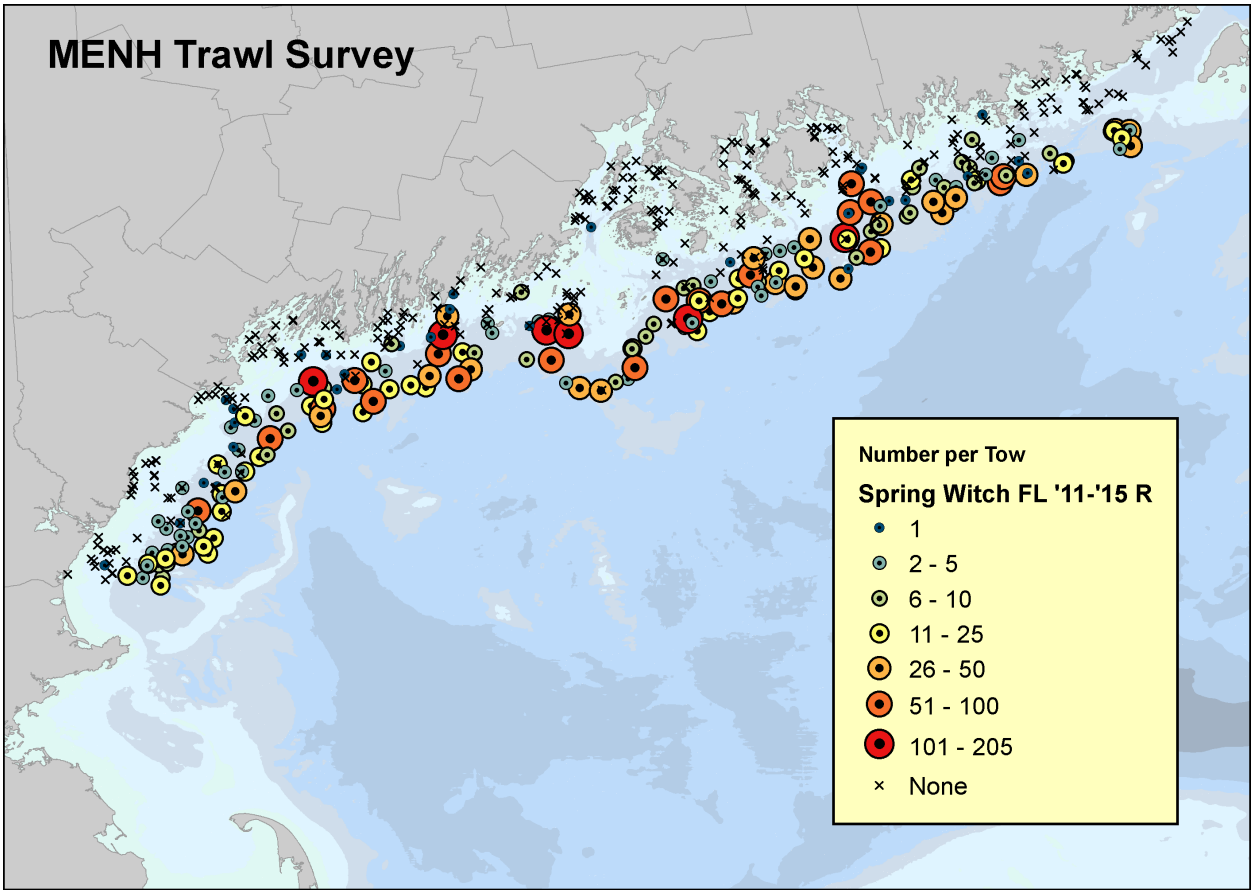

Figure B72. This map depicts survey catches for witch flounder (*Glyptocephalus cynoglossus*). The color-shaded circles represent number of fish per tow during the 2011-2015 (re-stratified) spring Maine-New Hampshire inshore trawl survey. The black '+' (plus symbol) represent no catch. Bathymetry is depicted in blue and gray shading.

Provided by Sally Sherman, Maine Department of Marine Resources, pers comm. July 28, 2016.

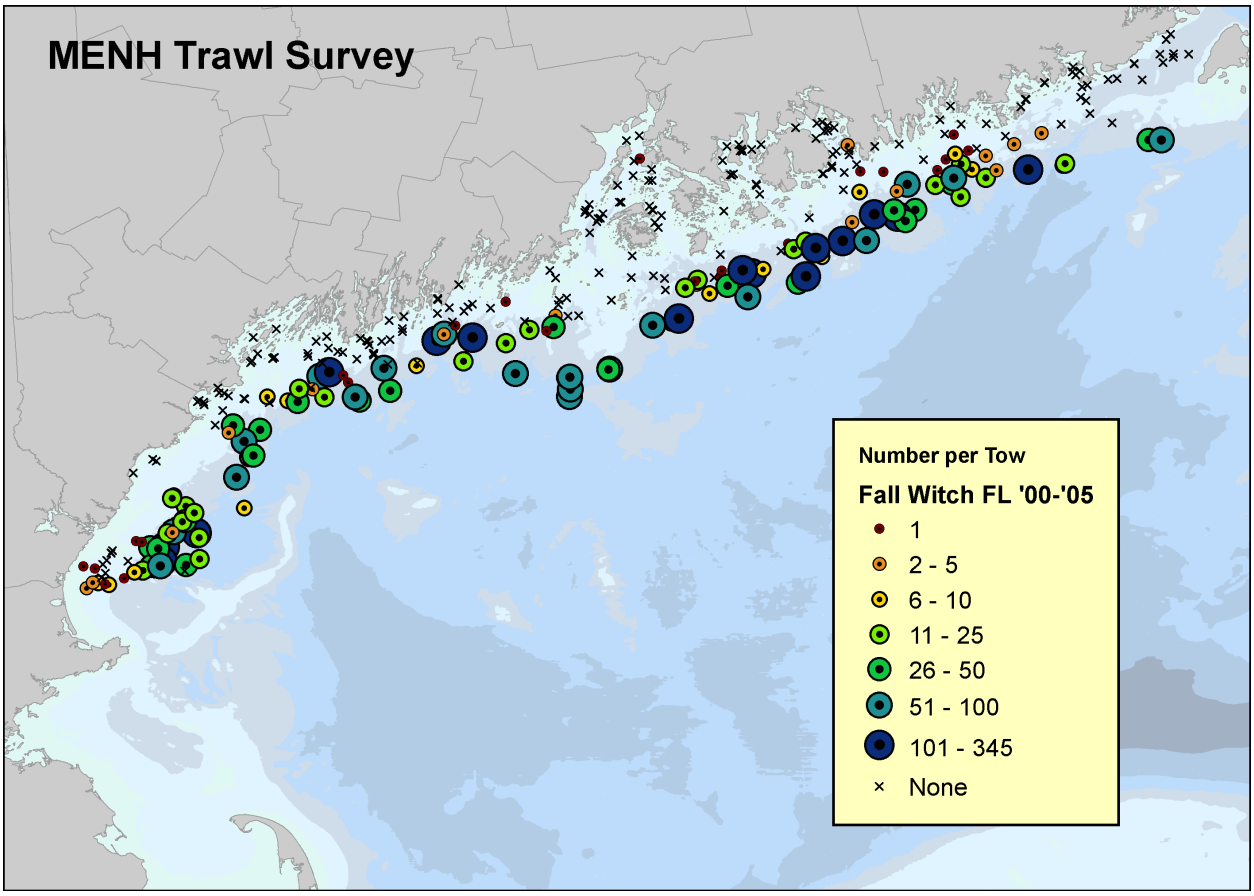

Figure B73. This map depicts survey catches for witch flounder (*Glyptocephalus cynoglossus*). The color-shaded circles represent number of fish per tow during the 2000-2005 (re-stratified) fall Maine-New Hampshire inshore trawl survey. The black '+' (plus symbol) represent no catch. Bathymetry is depicted in blue and gray shading.

Provided by Sally Sherman, Maine Department of Marine Resources, pers comm. July 28, 2016.

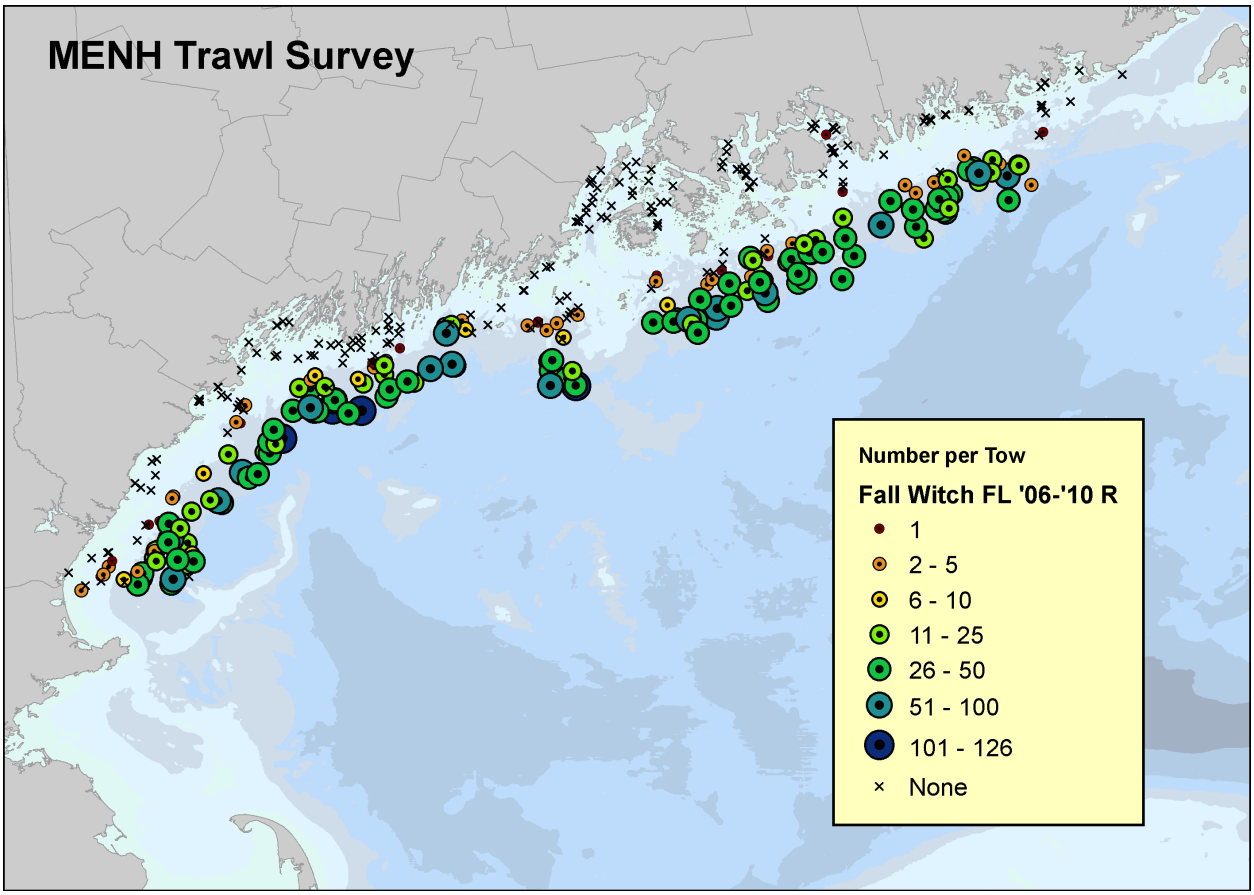

Figure B74. This map depicts survey catches for witch flounder (*Glyptocephalus cynoglossus*). The color-shaded circles represent number of fish per tow during the 2006-2010 (re-stratified) fall Maine-New Hampshire inshore trawl survey. The black '+' (plus symbol) represent no catch. Bathymetry is depicted in blue and gray shading.

Provided by Sally Sherman, Maine Department of Marine Resources, pers comm. July 28, 2016.

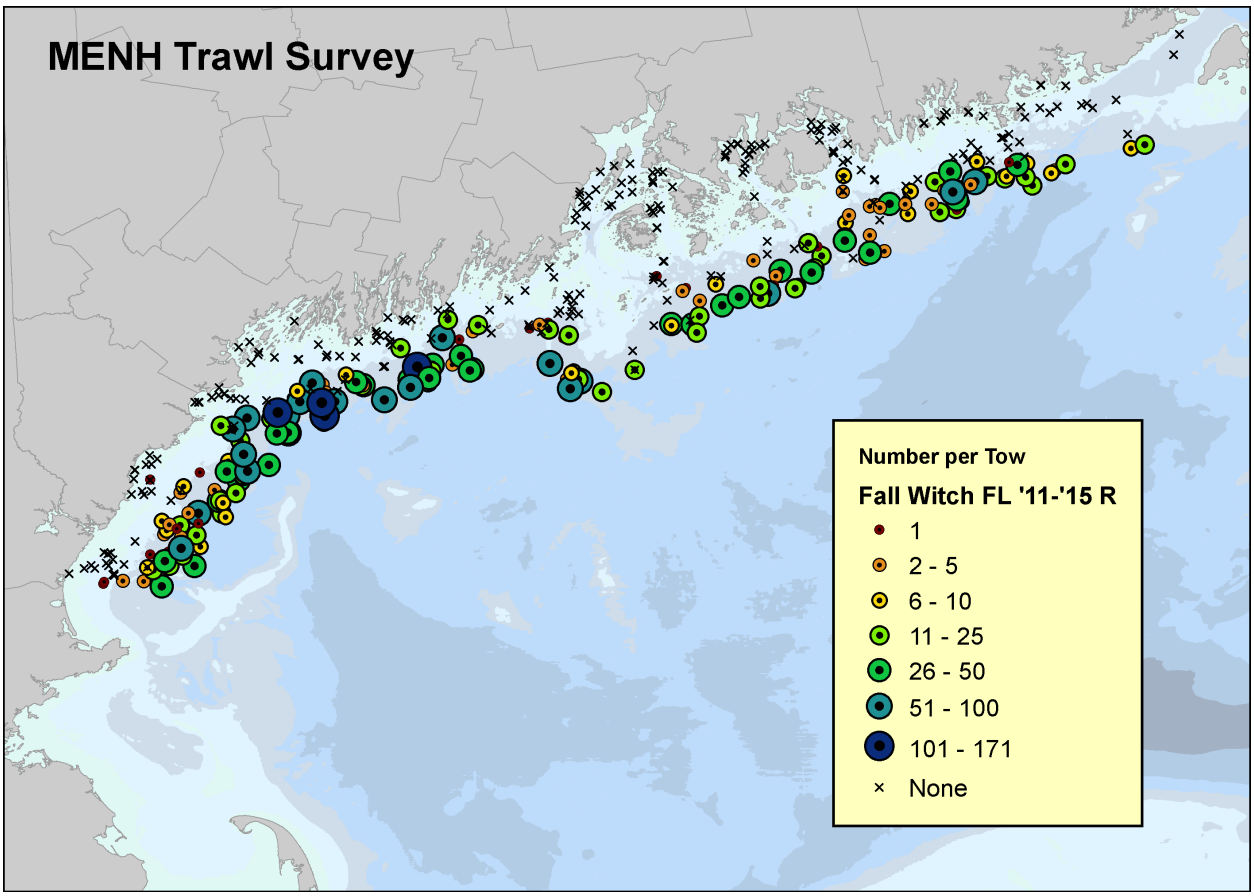

Figure B75. This map depicts survey catches for witch flounder (*Glyptocephalus cynoglossus*). The color-shaded circles represent number of fish per tow during the 2011-2015 (re-stratified) fall Maine-New Hampshire inshore trawl survey. The black '+' (plus symbol) represent no catch. Bathymetry is depicted in blue and gray shading.

Provided by Sally Sherman, Maine Department of Marine Resources, pers comm. July 28, 2016.

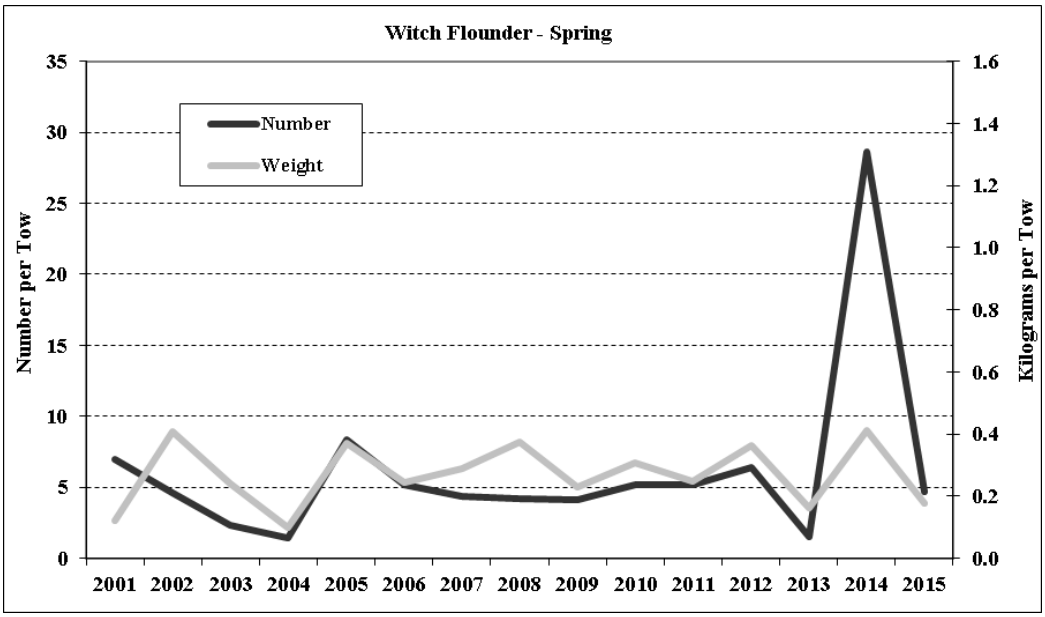

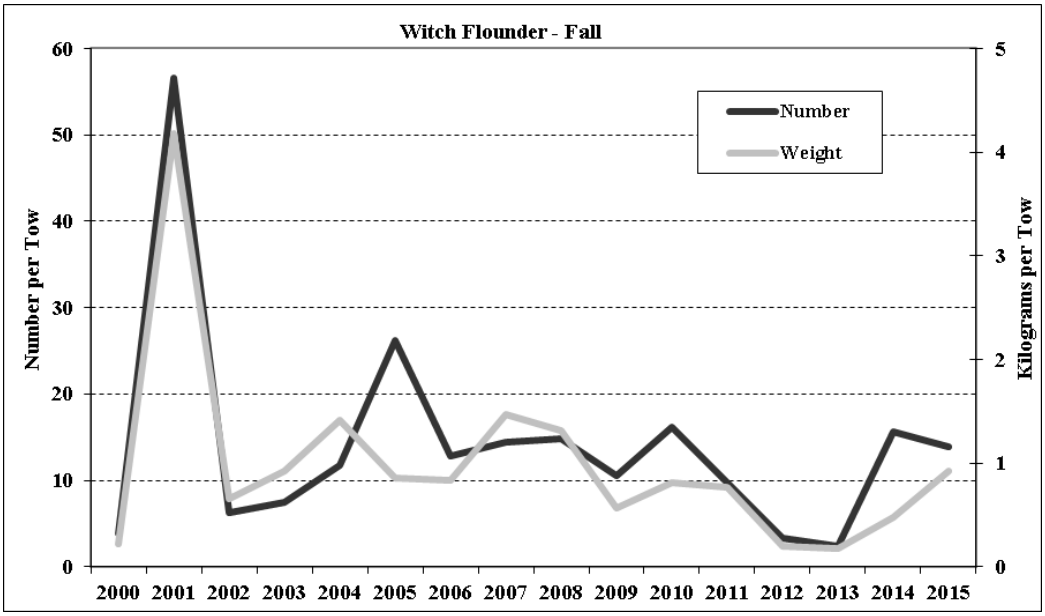

Figure B76. Stratified mean number per tow (black line) and weight (kg) per tow (gray line) of witch flounder in the Maine-New Hampshire inshore trawl survey spring (top) and fall (bottom) survey (strata 1 through 4; regions 1 to 5), 2000-2015. Indices for 2000-2002 were re-stratified; fixed stations are not included.

Survey indices have been provided by Sally Sherman, Maine Department of Marine Resources, pers comm. July 28, 2016. Annual reports and survey procedures and protocols of the Maine-New Hampshire Inshore Trawl Surve, are available online at http://www.maine.gov/dmr/rm/trawl/reports/index.htm

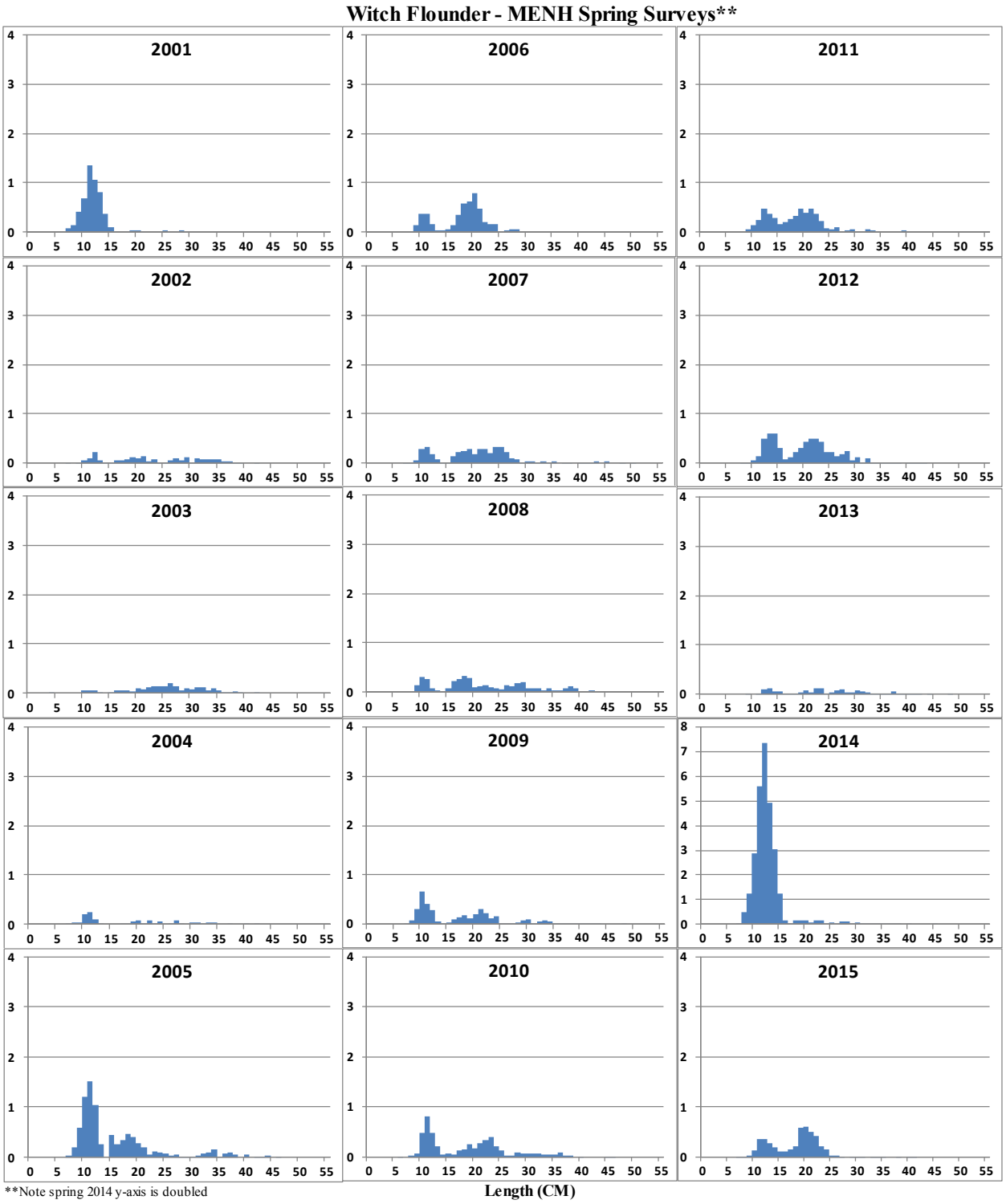

Figure B77. Stratified mean number of fish at length (cm; blue bars) for witch flounder from the 2000-2015 fall Maine-New Hampshire inshore trawl survey (regions 1 through 5; strata 1 through 4). Indices for 2000-2002 were re-stratified; fixed stations are not included.

Survey indices have been provided by Sally Sherman, Maine Department of Marine Resources, pers comm. July 28, 2016.

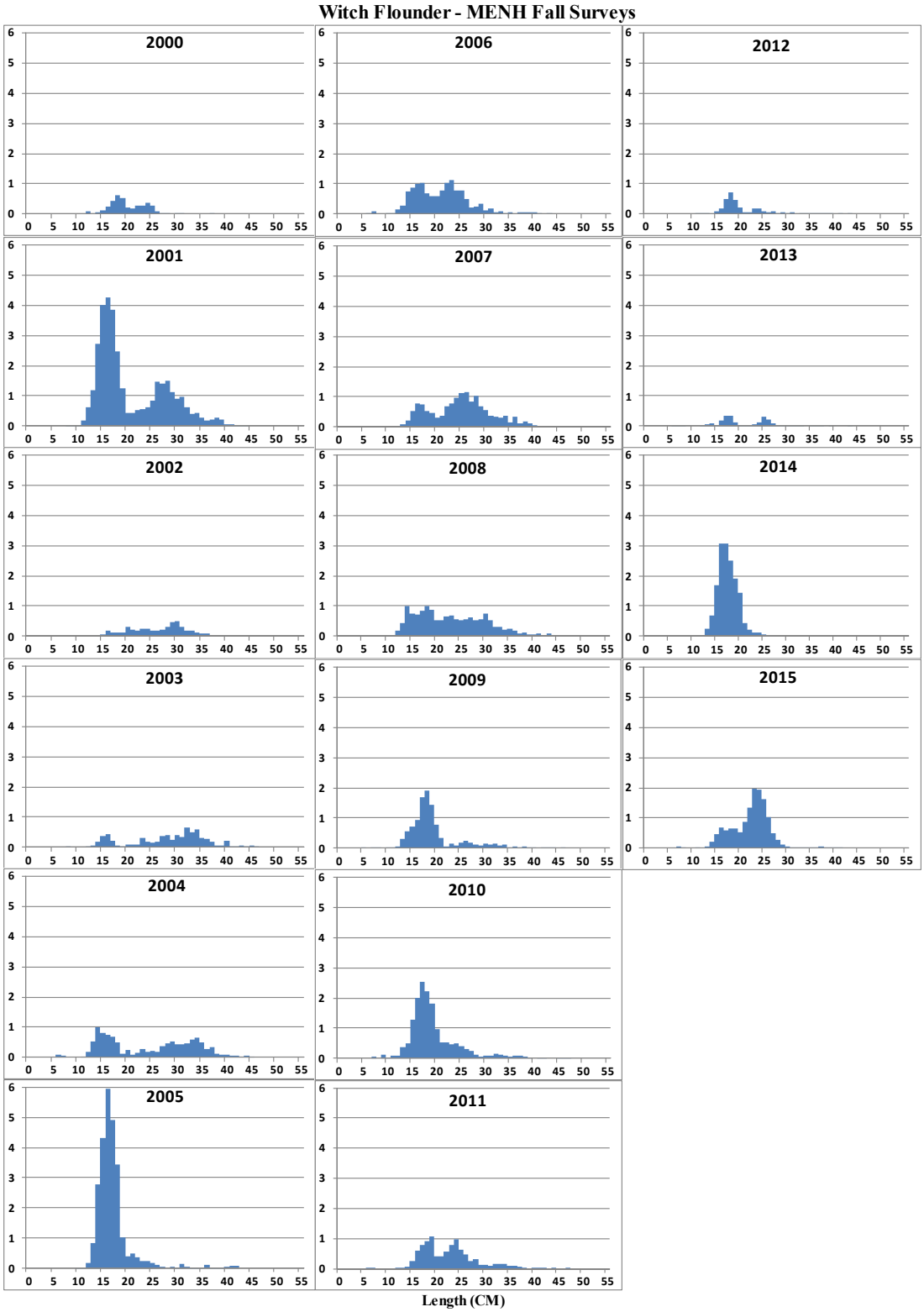

Figure B78. Stratified mean number of fish at length (cm; blue bars) for witch flounder from the 2000-2015 fall Maine-New Hampshire inshore trawl survey (regions 1 through 5; strata 1 through 4). Indices for 2000-2002 were re-stratified; fixed stations are not included.

Survey indices have been provided by Sally Sherman, Maine Department of Marine Resources, pers comm. July 28, 2016.

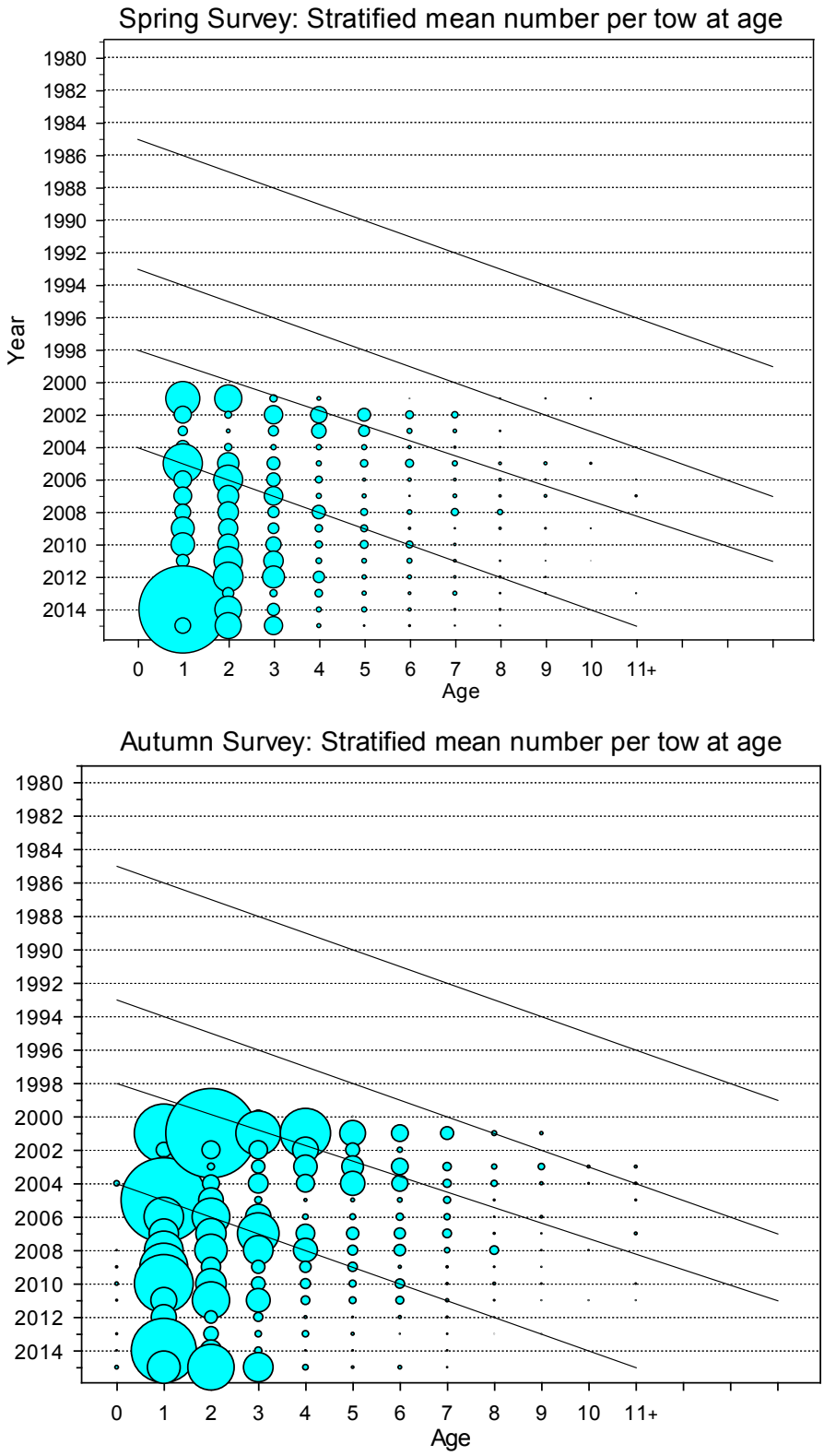

Figure B79. Stratified mean number of fish at age for witch flounder from the 2000-2015 spring (top) and autumn (bottom) Maine-New Hampshire inshore trawl survey (regions 1 through 5; strata 1 through 4). Indices for 2000-2002 were re-stratified; fixed stations are not included; seasonal Northeast Fisheries Science Center survey age/length keys used.

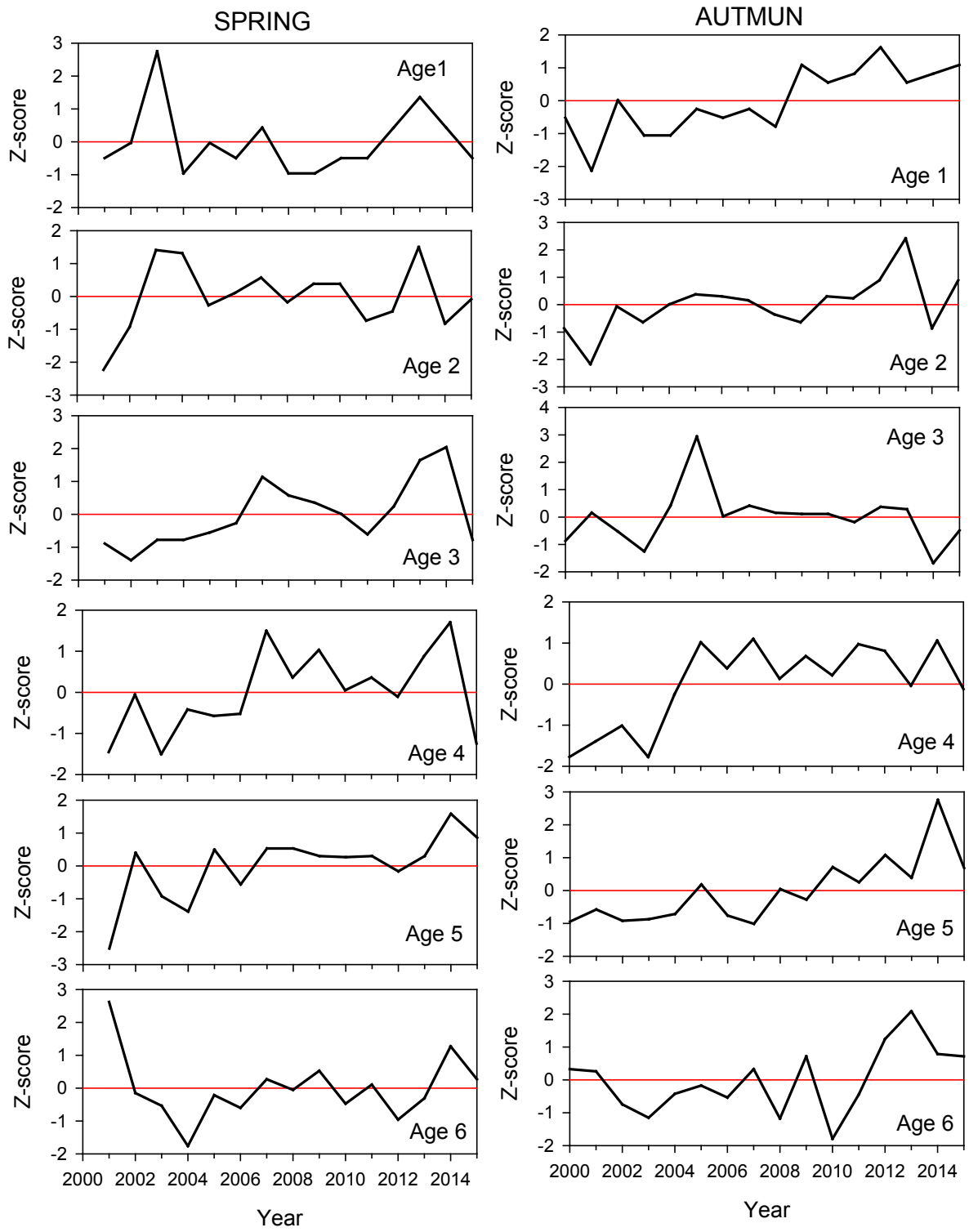

Figure B80. Z-scores of witch flounder mean weight at age (age groups 1-6) in the Maine-New Hampshire inshore trawl survey (regions 1 through 5; strata 1 through 4) spring survey (left), 2001-2016 and autumn survey 2000 -2015 (right).

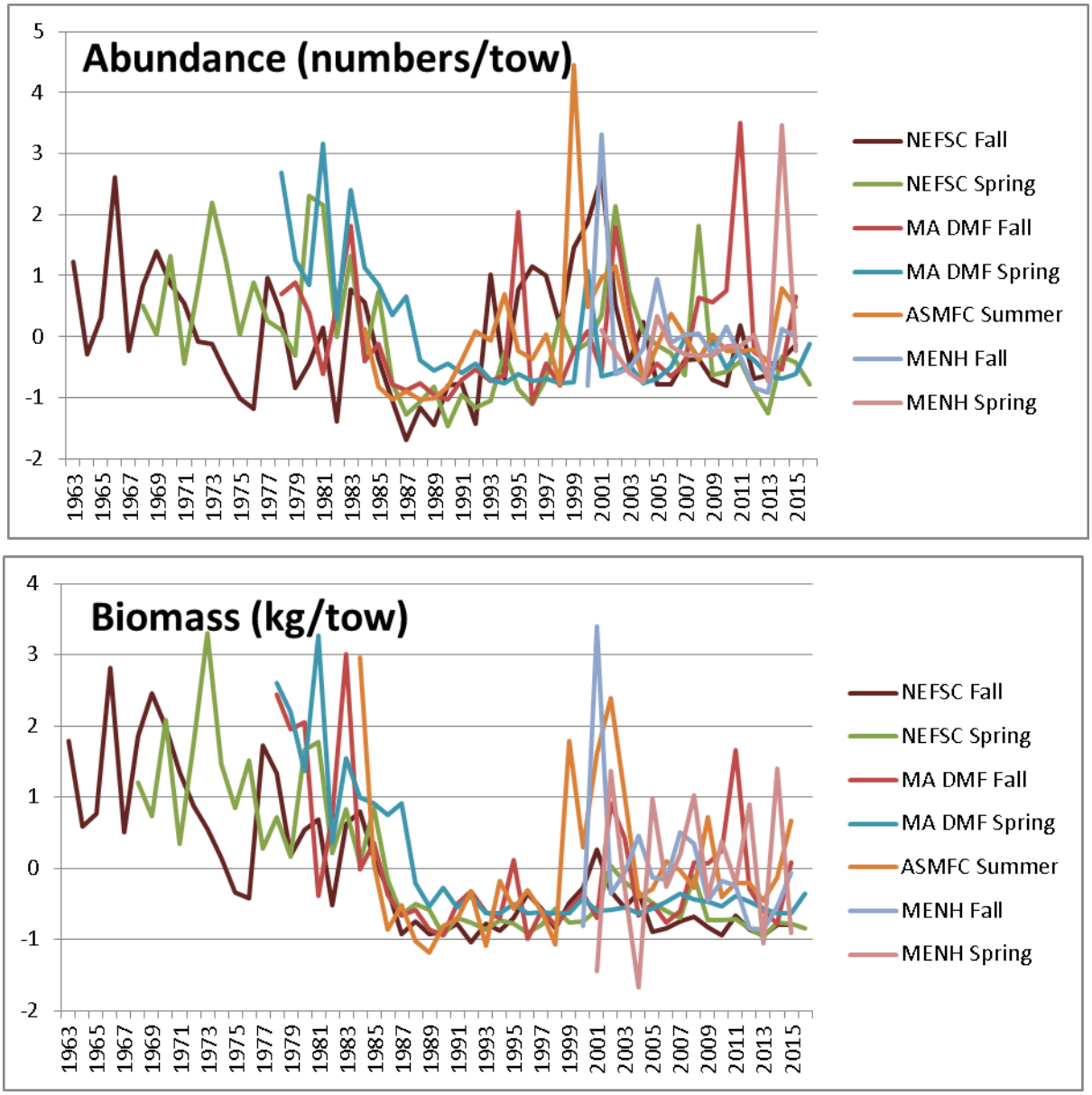

Figure B81. Normalized abundance (stratified mean number per tow; top) and biomass (stratified mean weight per tow; bottom) of witch flounder in the Northeast Fisheries Science Center (NEFSC), Massachusetts Division of Marine Fisheries (MA DMF), Maine-New Hampshire (ME-NH) spring and fall survey series and Atlantic States Marine Fisheries Commission (ASMFC) summer shrimp survey series.

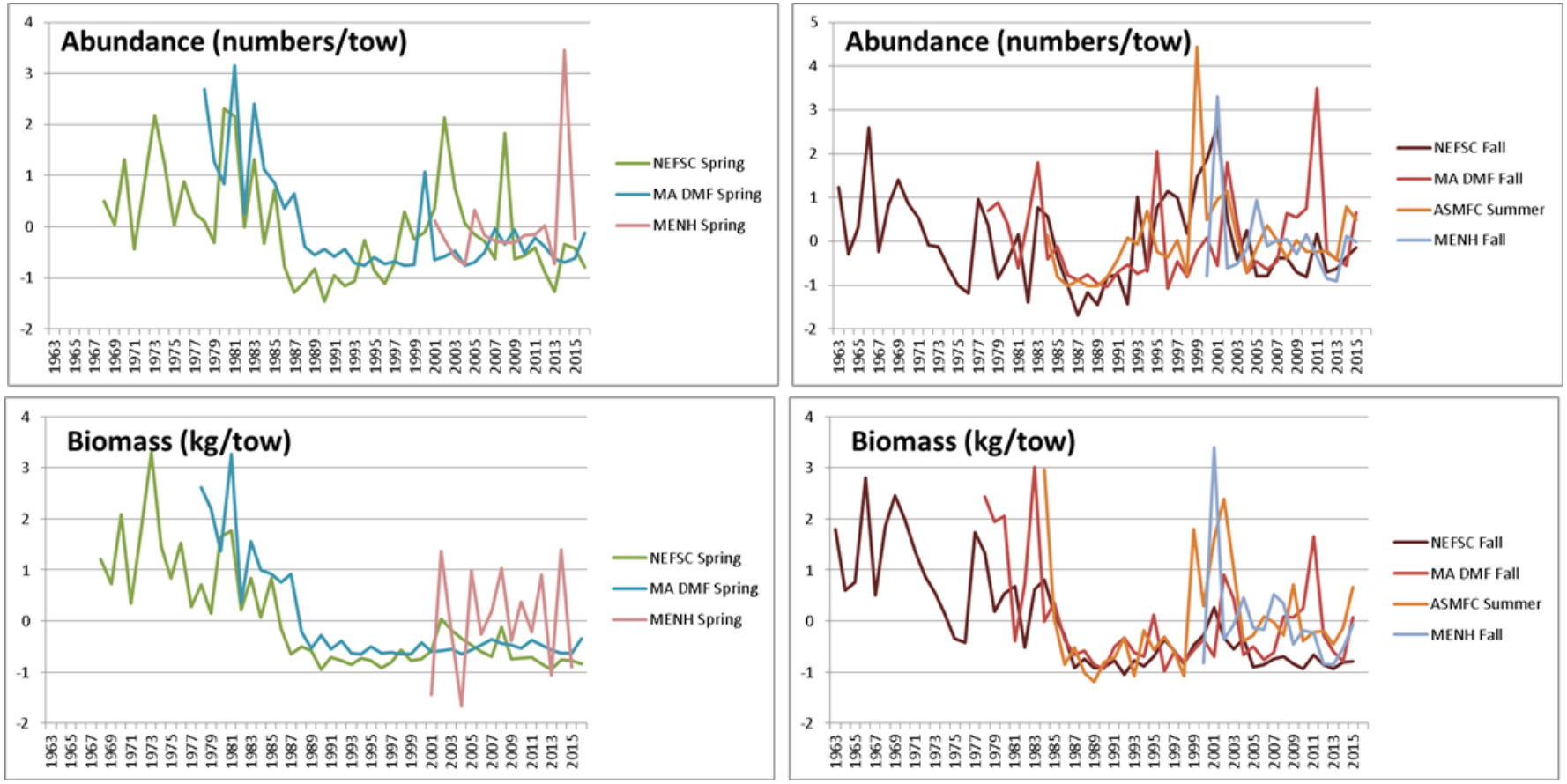

Figure B82. Normalized abundance (stratified mean number per tow; top) and biomass (stratified mean weight per tow; bottom) of witch flounder in the Northeast Fisheries Science Center (NEFSC), Massachusetts Division of Marine Fisheries (MA DMF), Maine-New Hampshire (ME-NH) spring (left) and fall survey series and Atlantic States Marine Fisheries Commission (ASMFC) summer shrimp survey series (right).

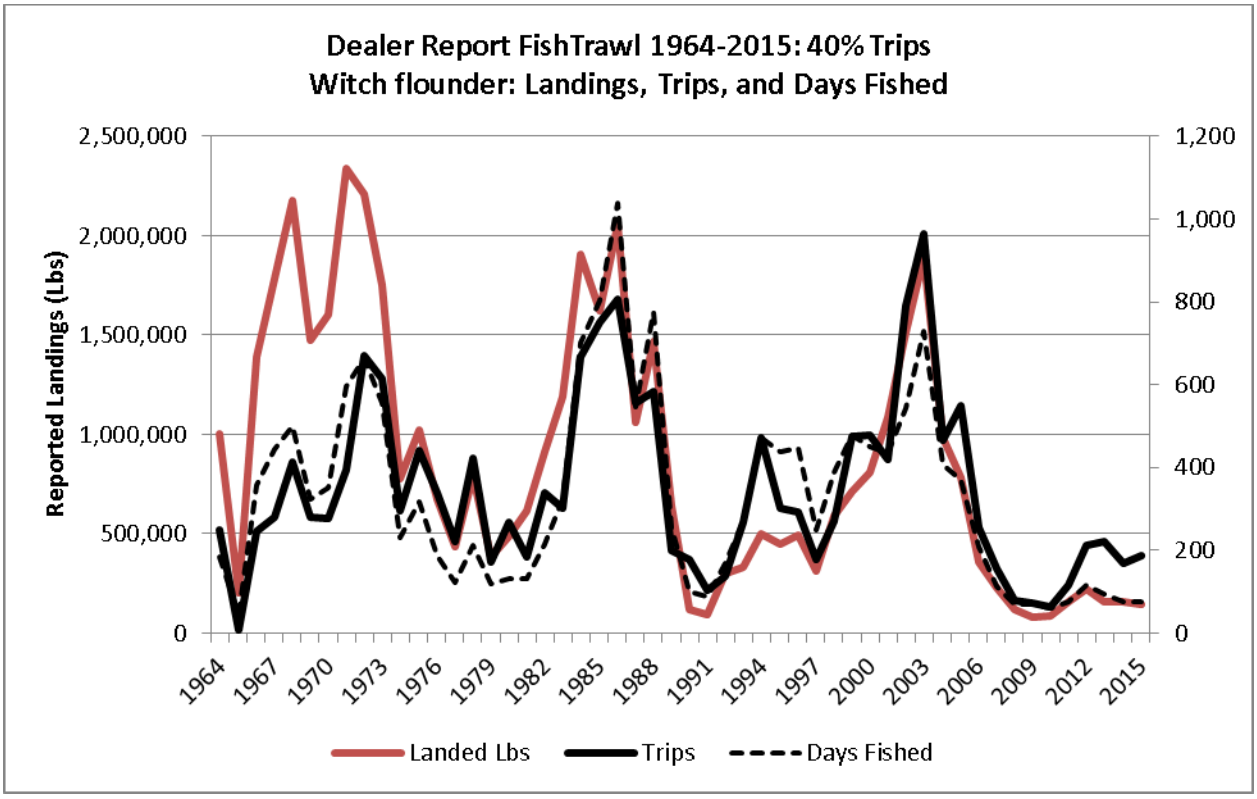

Figure B83. Dealer Report fish trawl gear landings, trips, and days fished for 'directed' (40%) trips.

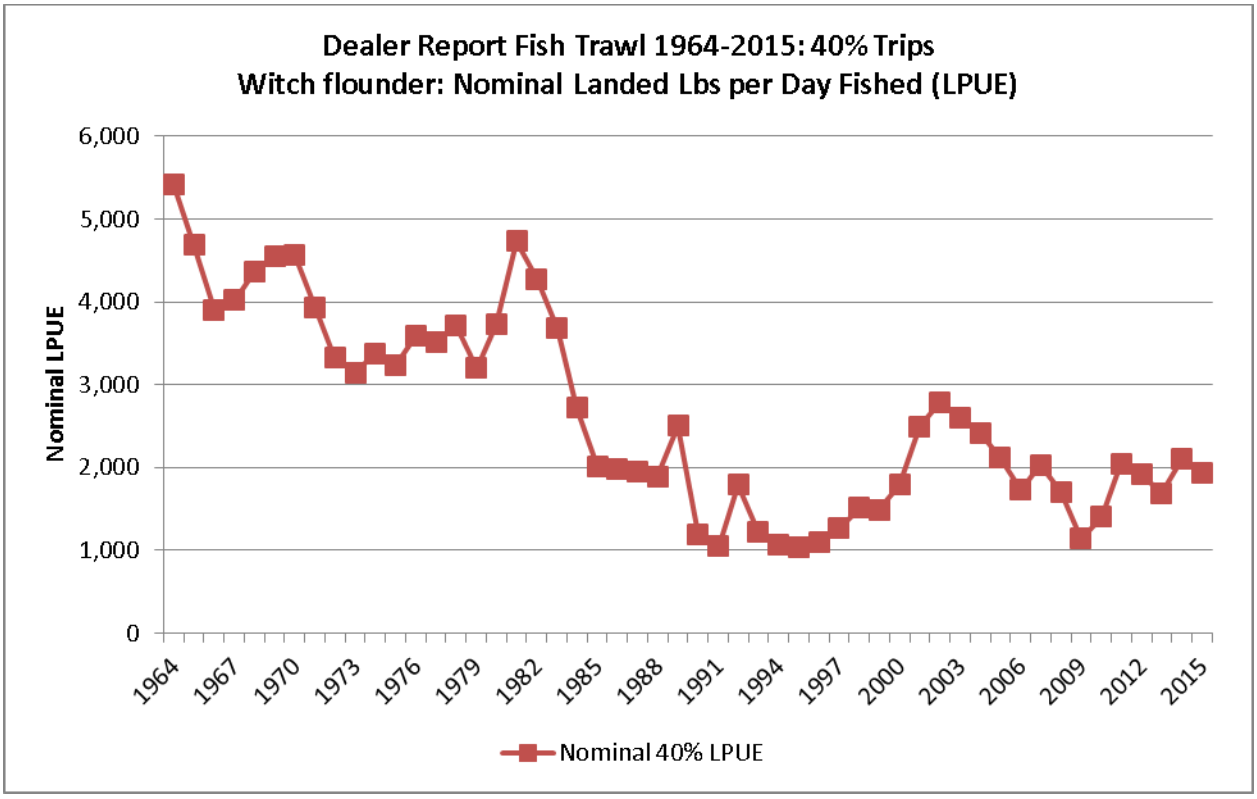

Figure B84. Dealer Report fish trawl gear landed lbs per day fished: nominal landed pounds per day fished (LPUE) for 'directed' (40%) trips.

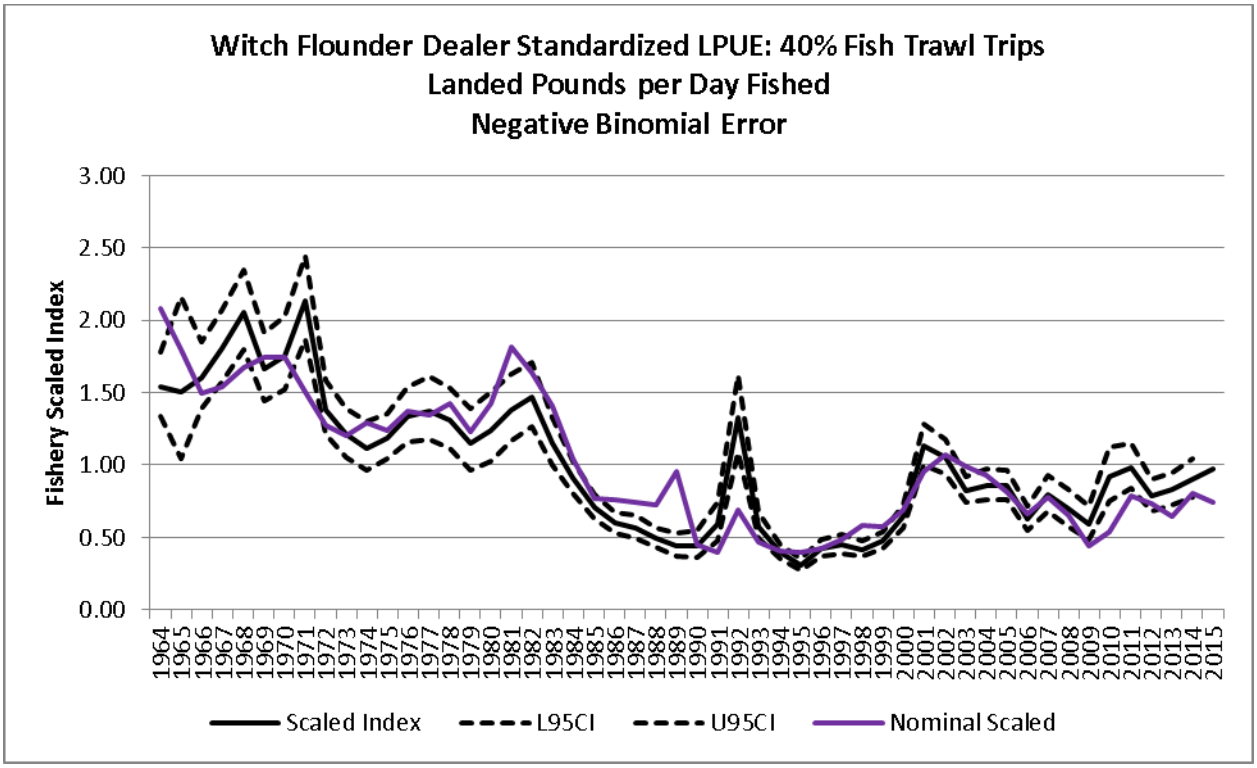

Figure B85. Comparison of the negative binomial model-based indices and the nominal index for fish trawl directed (40%) trips.

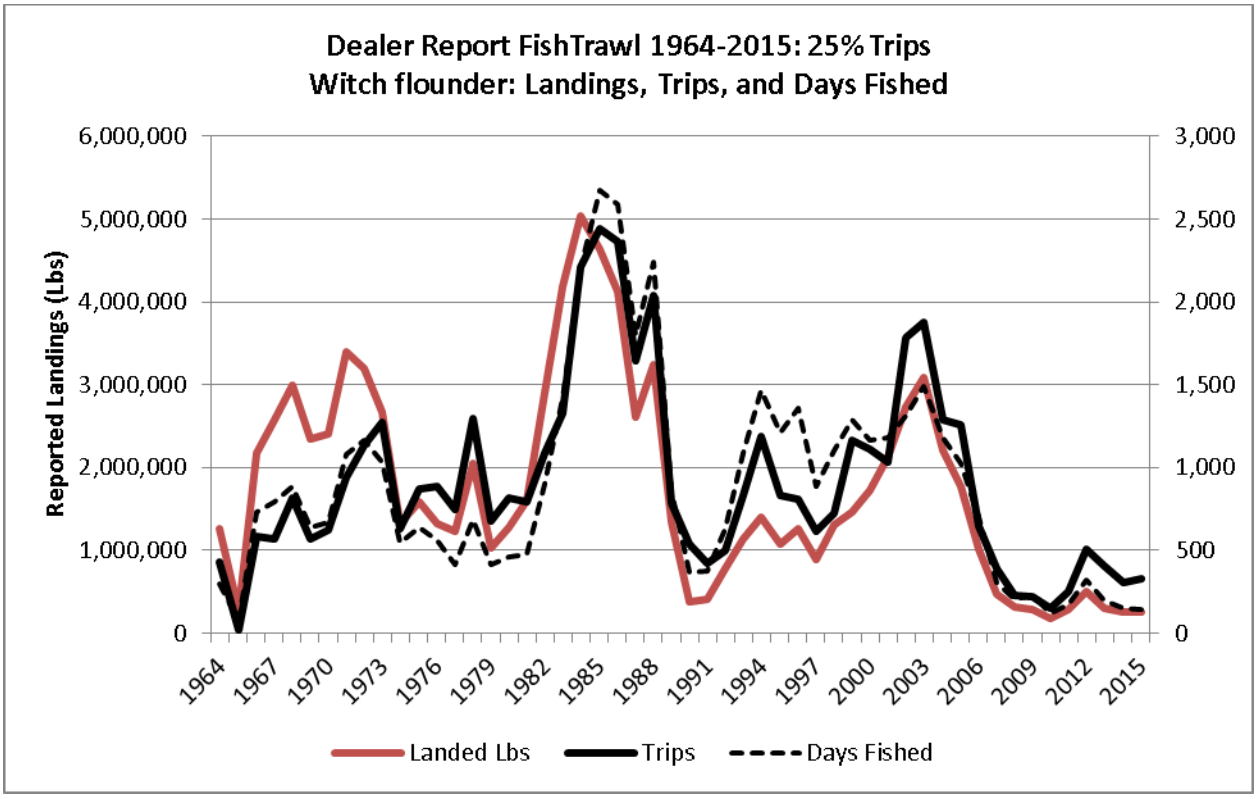

Figure B86. Dealer Report fish trawl gear landings, trips, and days fished for 'directed' (25%) trips.

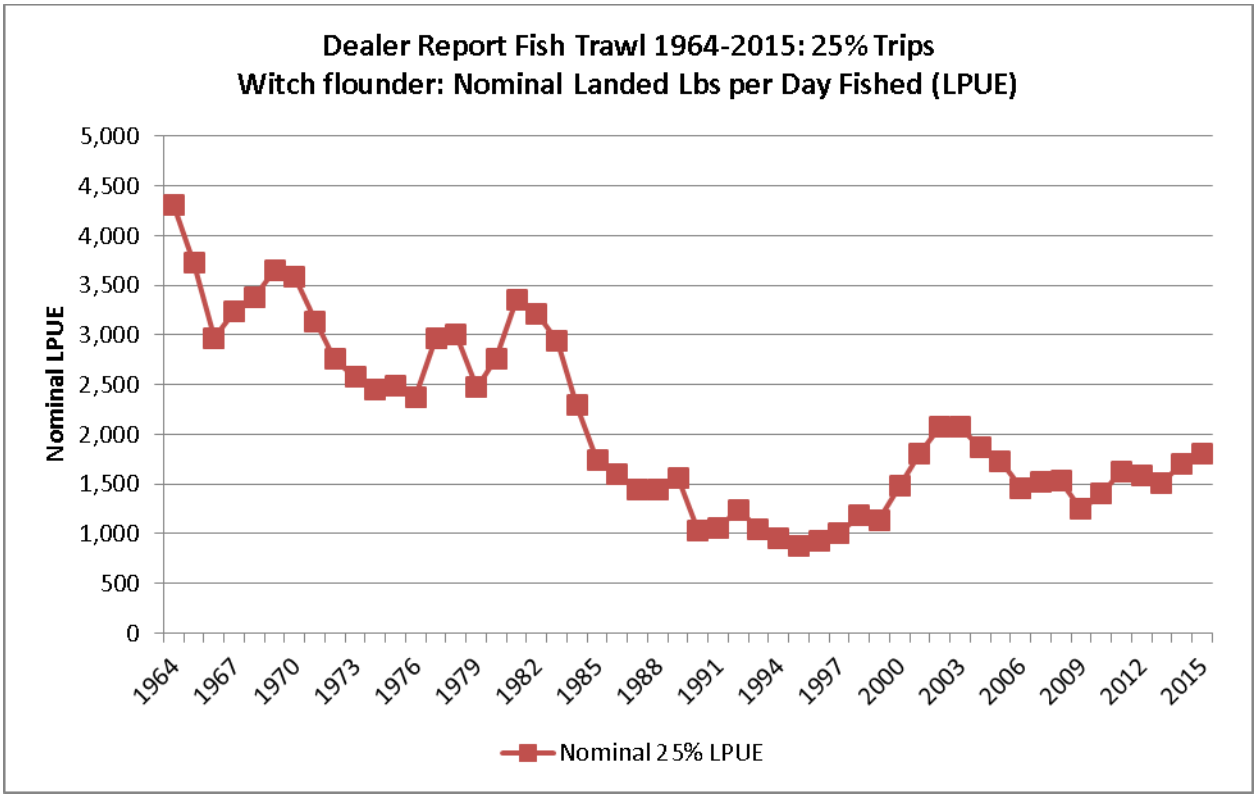

Figure B87. Dealer Report fish trawl gear landed lbs per day fished: nominal landed pounds per day fished (LPUE) for 'directed' (25%) trips.

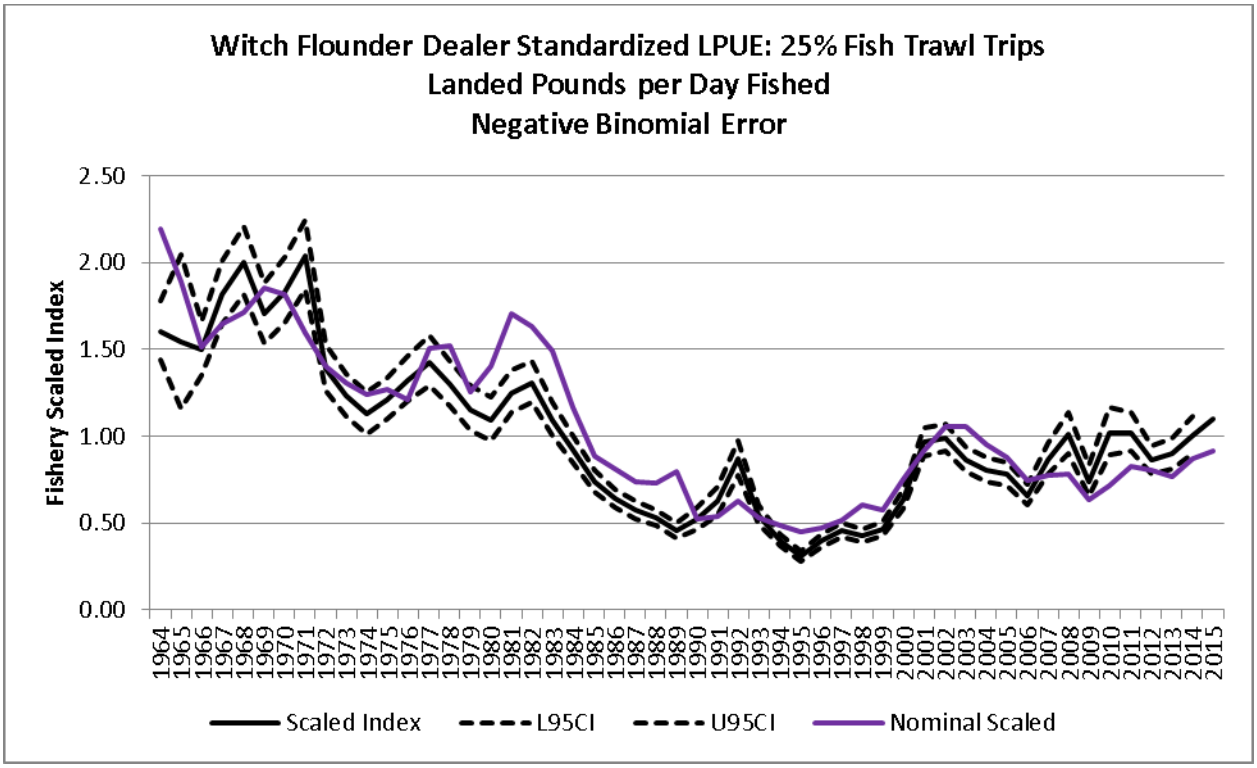

Figure B88. Comparison of the negative binomial model-based indices and the nominal index for fish trawl directed (25%) trips.

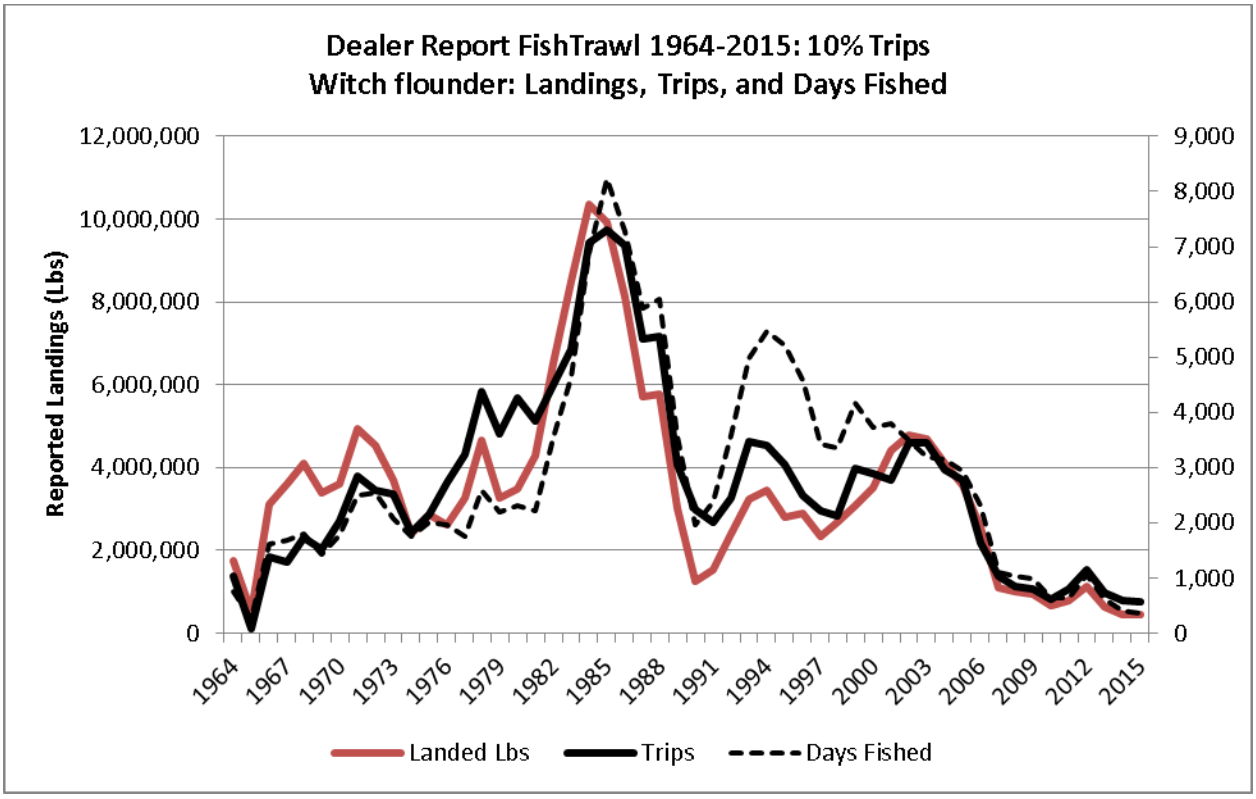

Figure B89. Dealer Report fish trawl gear landings, trips, and days fished for 'directed' (10%) trips.

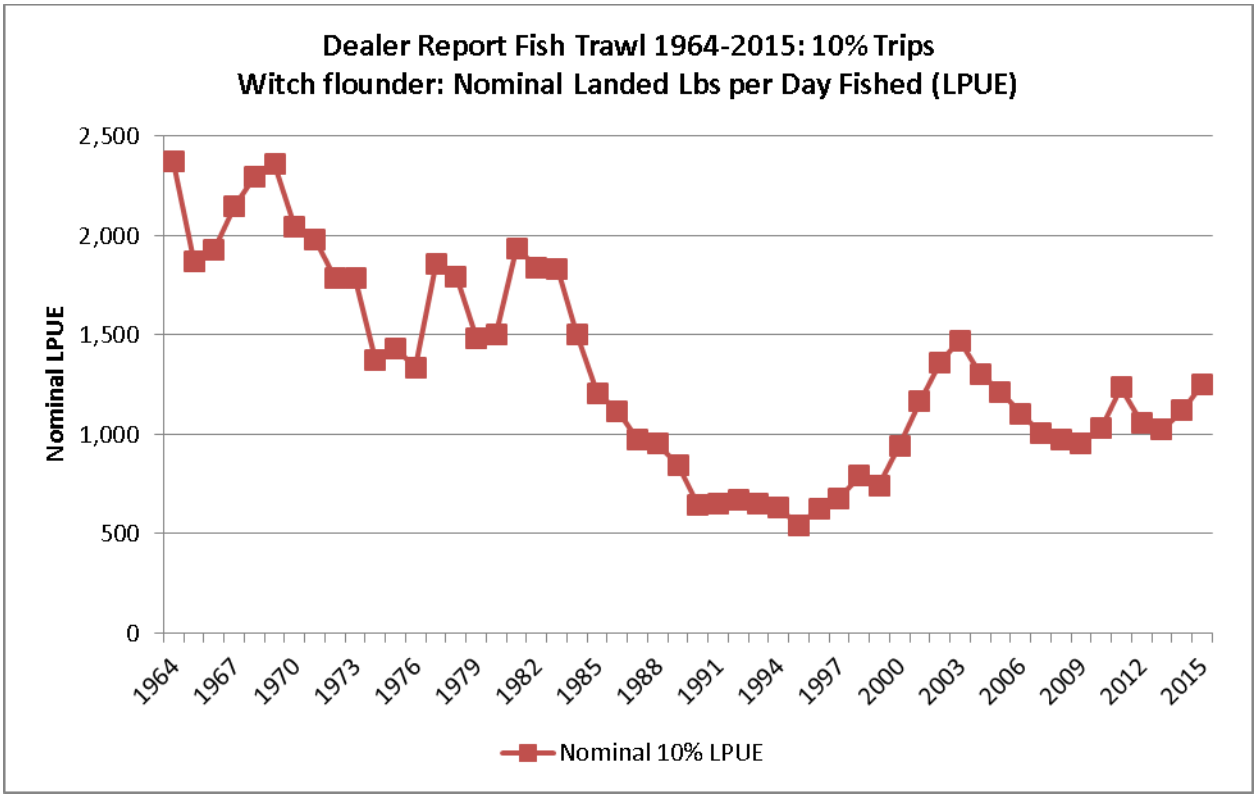

Figure B90. Dealer Report fish trawl gear landed lbs per day fished: nominal landed pounds per day fished (LPUE) for 'directed' (10%) trips.

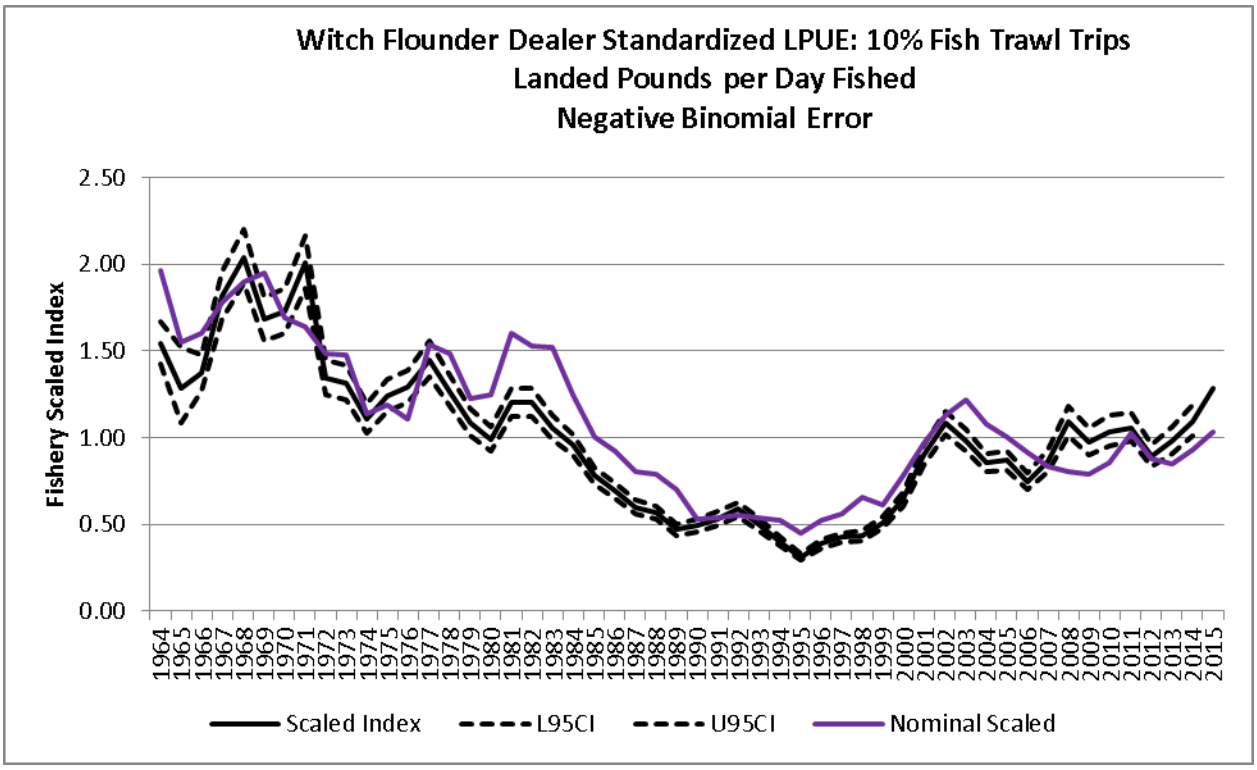

Figure B91. Comparison of the negative binomial model-based indices and the nominal index for fish trawl directed (10%) trips.

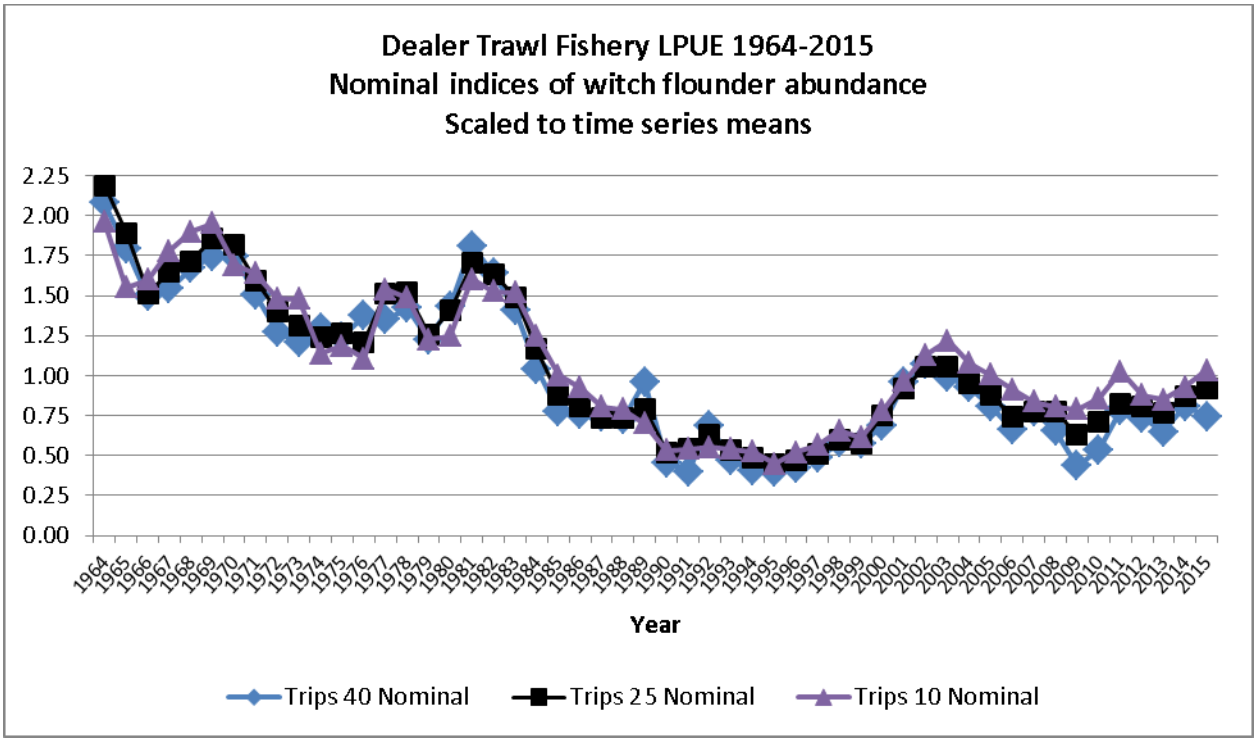

Figure B92. Comparison of nominal scaled landed pounds per day fished (LPUE) for fish trawl directed (10%, 25%, 40%) trips.

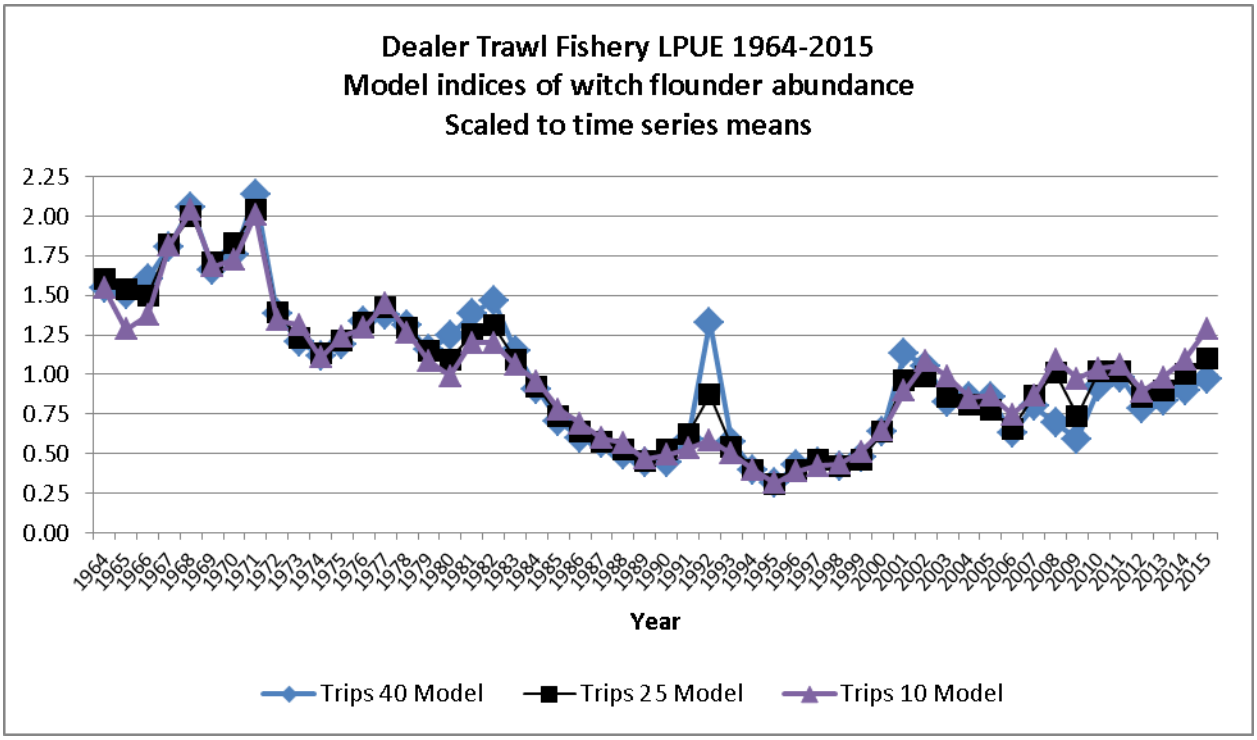

Figure B93. Comparison of negative binomial model scaled landed pounds per day fished (LPUE) for fish trawl directed trips (10%, 25%, 40%).

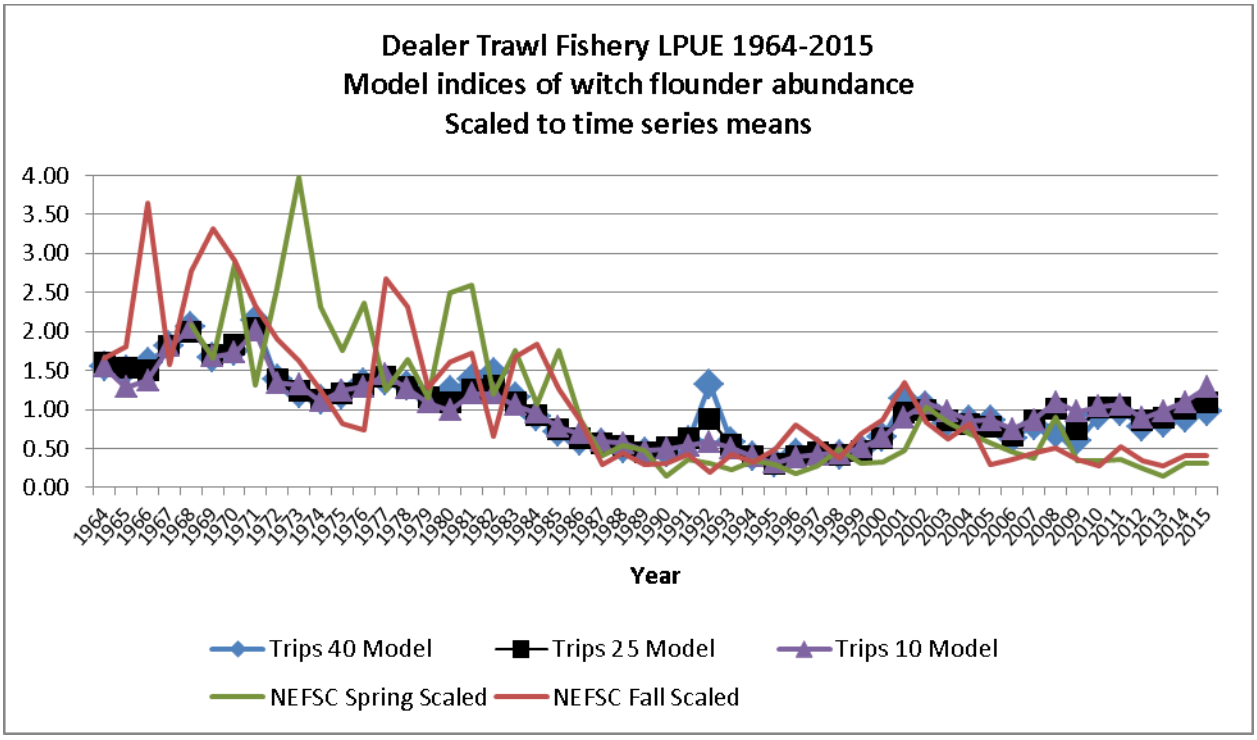

Figure B94. Comparison of negative binomial model scaled landed pounds per day fished (LPUE) for fish trawl directed trips (10%, 25%, 40%) with Northeast Fisheries Science Center (NEFSC) trawl survey Spring and Fall biomass indices.

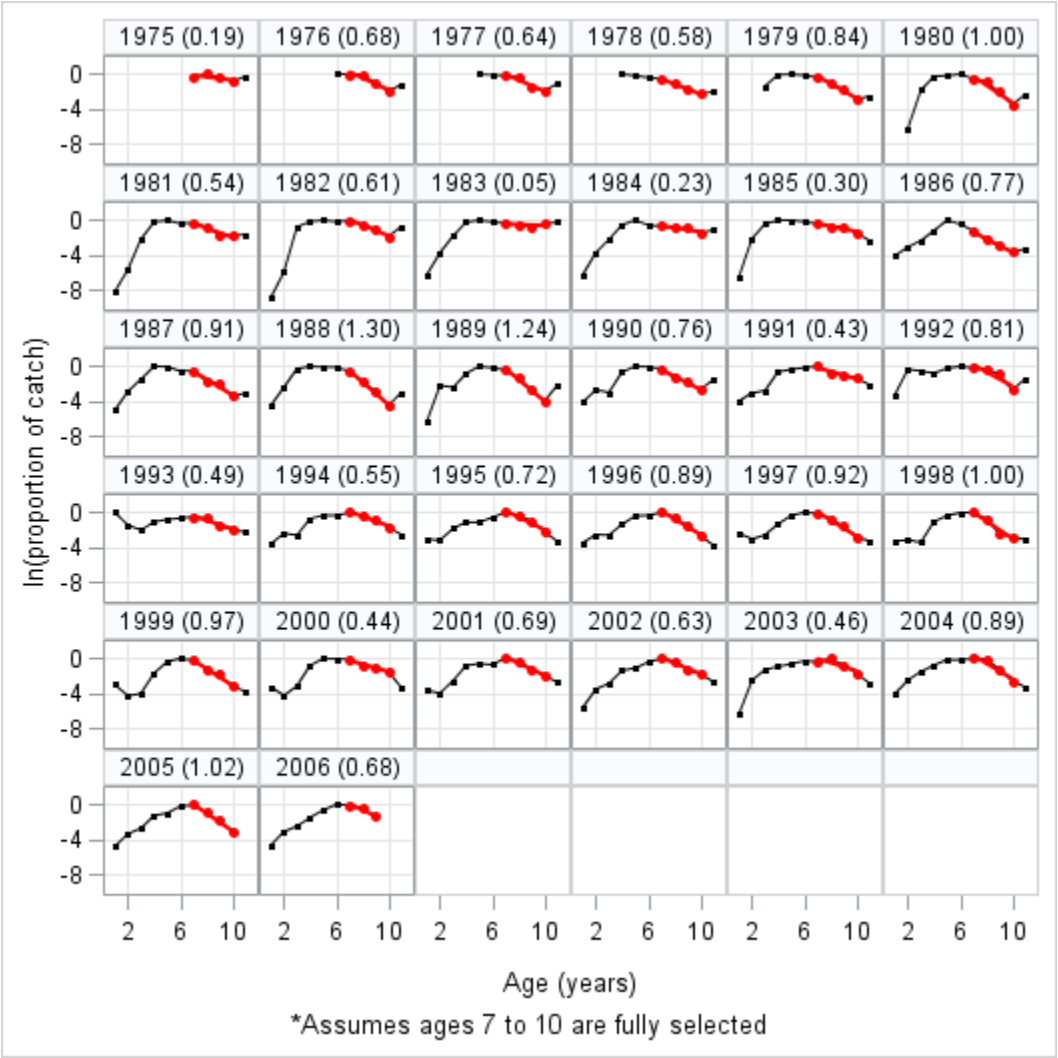

Figure B95. Witch flounder year class catch curves with a linear regression fitted to log-transformed age 7 to 10 (red circles) total fishery catch-at-age data (combined landings and discards). The corresponding slope of each regression line is shown next to the year class label above each plot. *Note that age 11 is a plus group.*

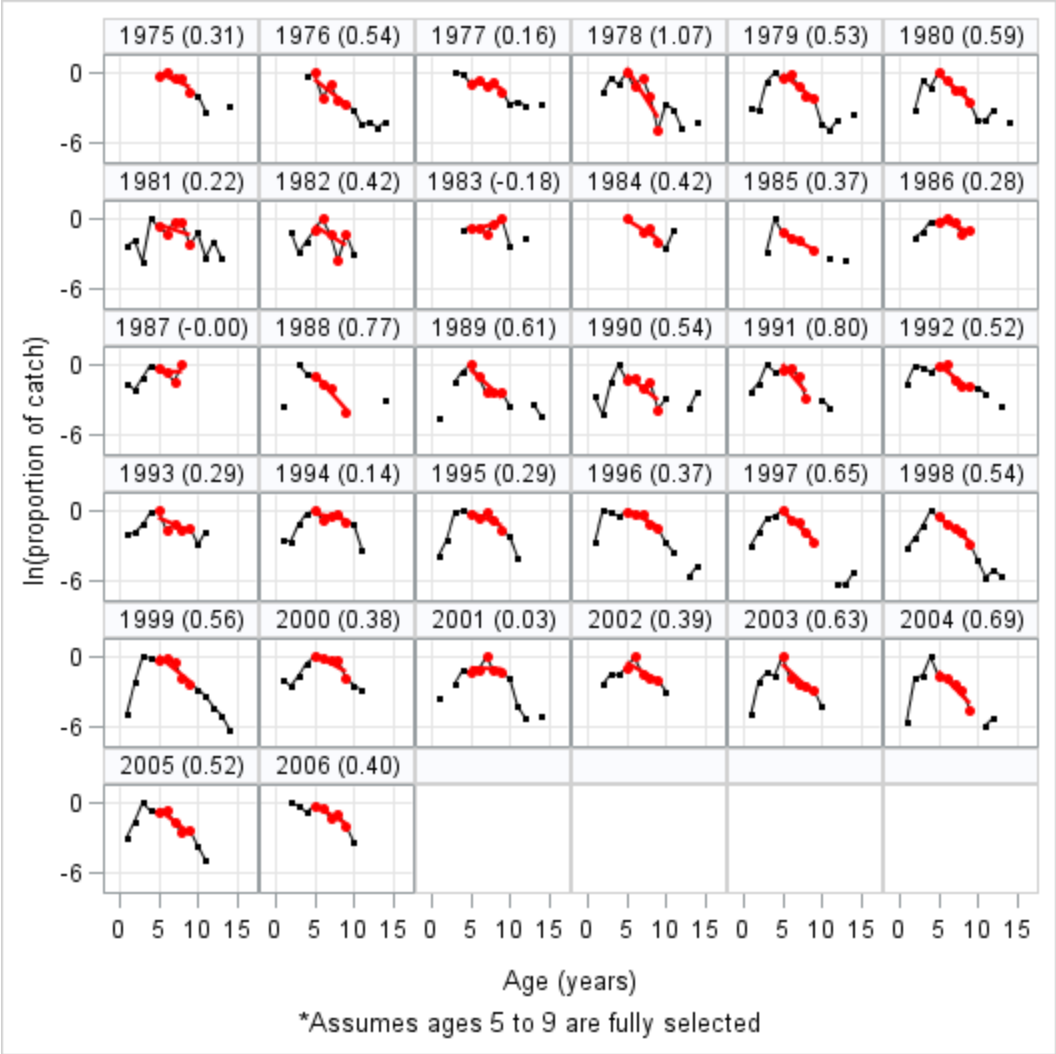

Figure B96. Witch flounder year class catch curves with a linear regression fitted to log-transformed age 5 to 9 (red circles) abundance-at-age (numbers/tow) data from the Northeast Fisheries Science Center spring bottom trawl survey. The corresponding slope of each regression line is shown next to the year class label above each plot. *Note that age 14 is a plus group.*

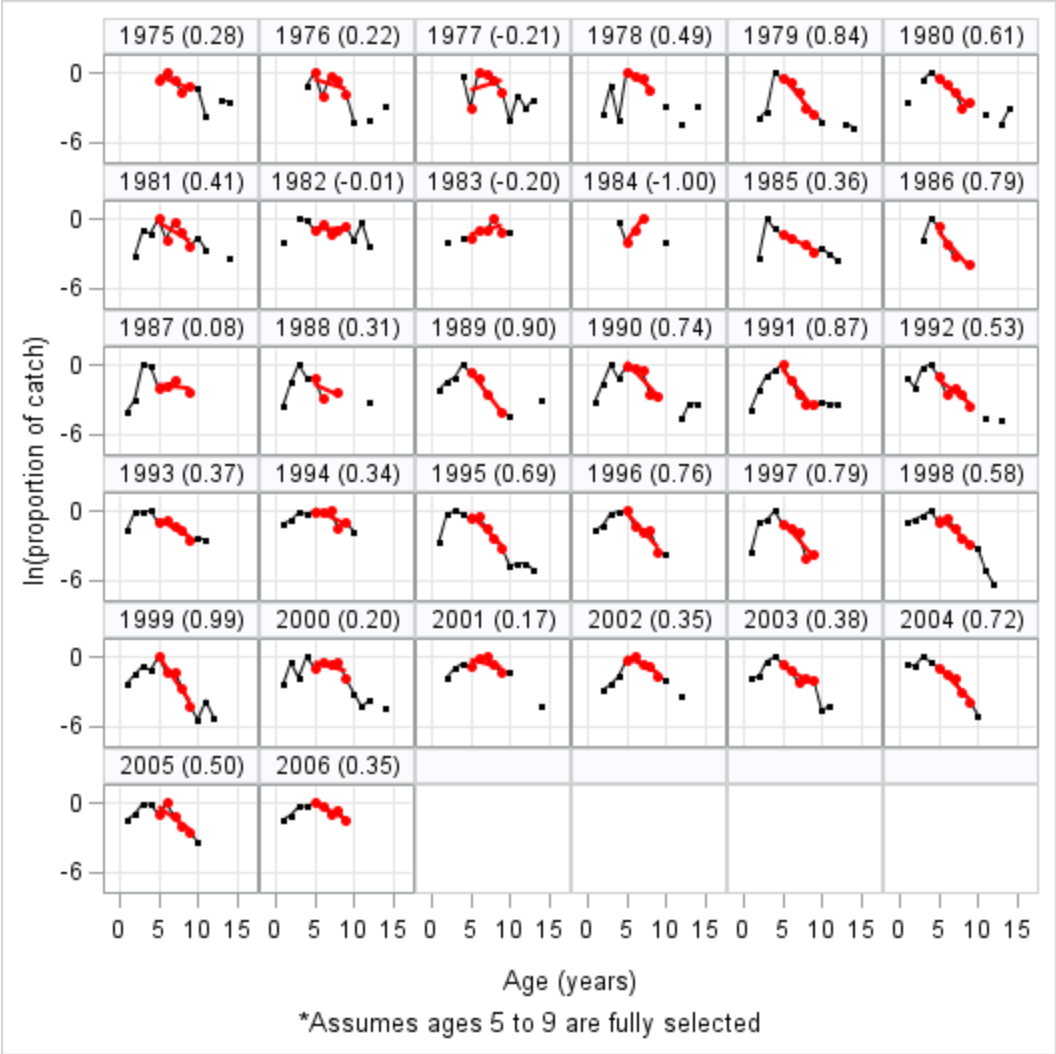

Figure B97. Witch flounder year class catch curves with a linear regression fitted to log-transformed age 5 to 9 (red circles) abundance-at-age (numbers/tow) data from the Northeast Fisheries Science Center fall bottom trawl survey. The corresponding slope of each regression line is shown next to the year class label above each plot. *Note that age 14 is a plus group.*

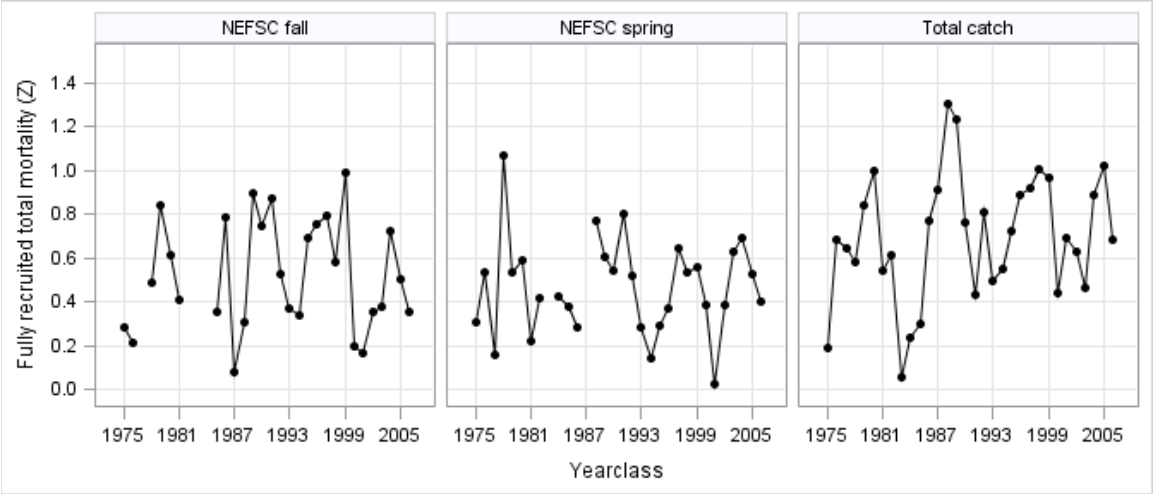

Figure B98. Plots of the annual estimates of witch flounder total mortality (Z) as estimated from the slope of the catch curve analysis of Northeast Fisheries Science Center (NEFSC) spring and fall bottom trawl surveys and total catch (landings and discards).

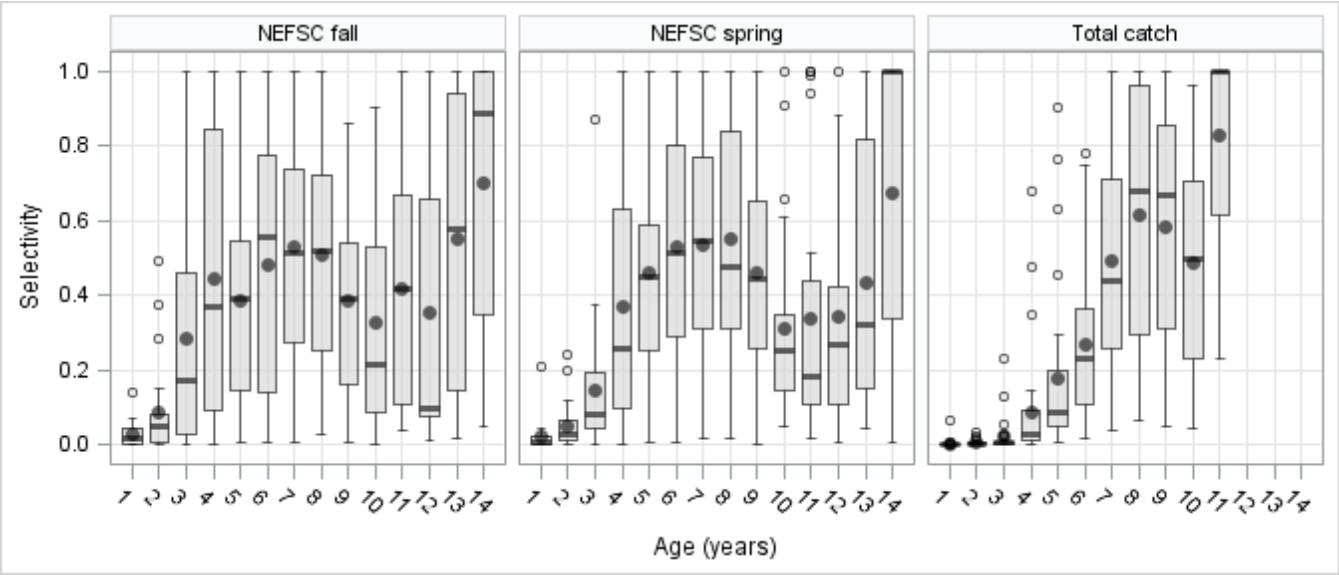

Figure B99. Distribution of catch selectivity-at-age as estimated from the residuals fits to the witch flounder catch curve analysis of Northeast Fisheries Science Center (NEFSC) spring and fall bottom trawl surveys and total catch (landings and discards). *Note that age 14 is a plus group in the NEFSC spring and fall survey data and age 11 is a plus group in the total catch data.*

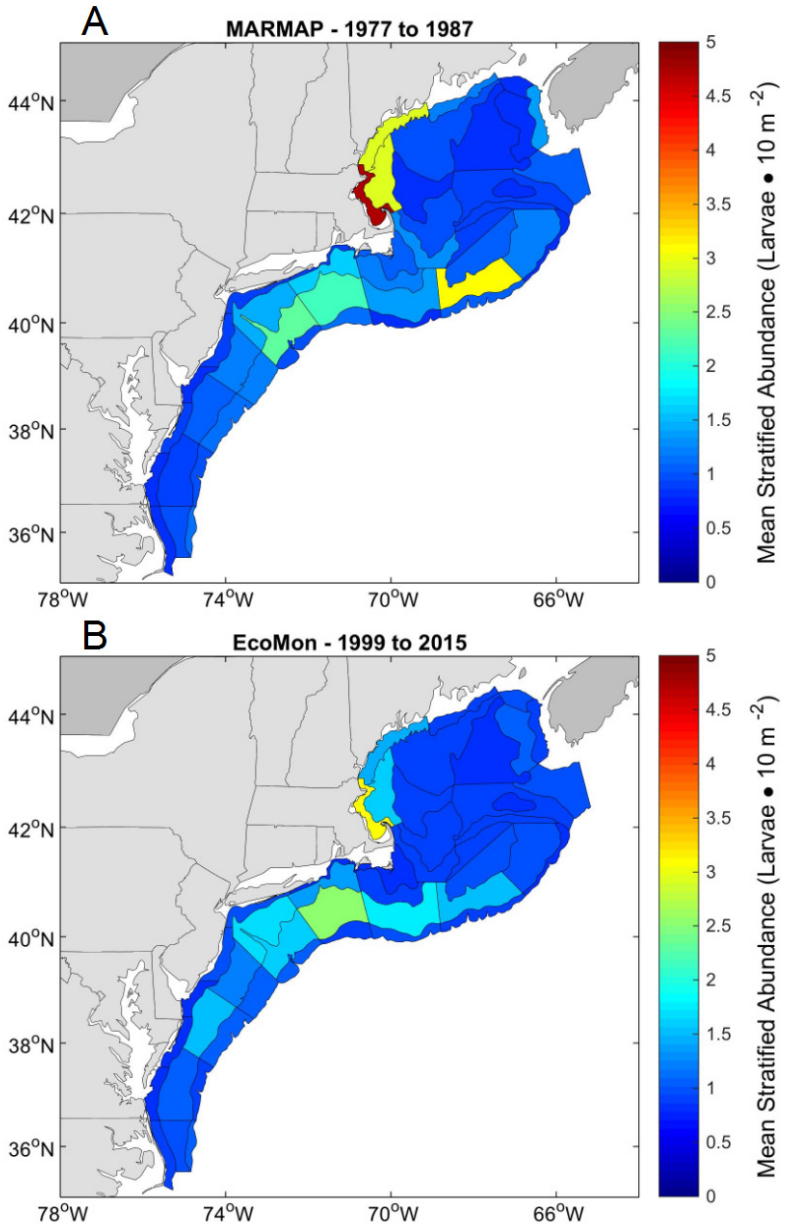

Figure B100. Larval witch flounder (*Glyptocephalus cynoglossus*) stratified mean abundance collected during Marine Resources Monitoring, Assessment and Prediction (MARMAP; A) and Ecosystem Monitoring (EcoMon; B) programs. Larval strata were originally developed using the stratum design of the bottom trawl survey.

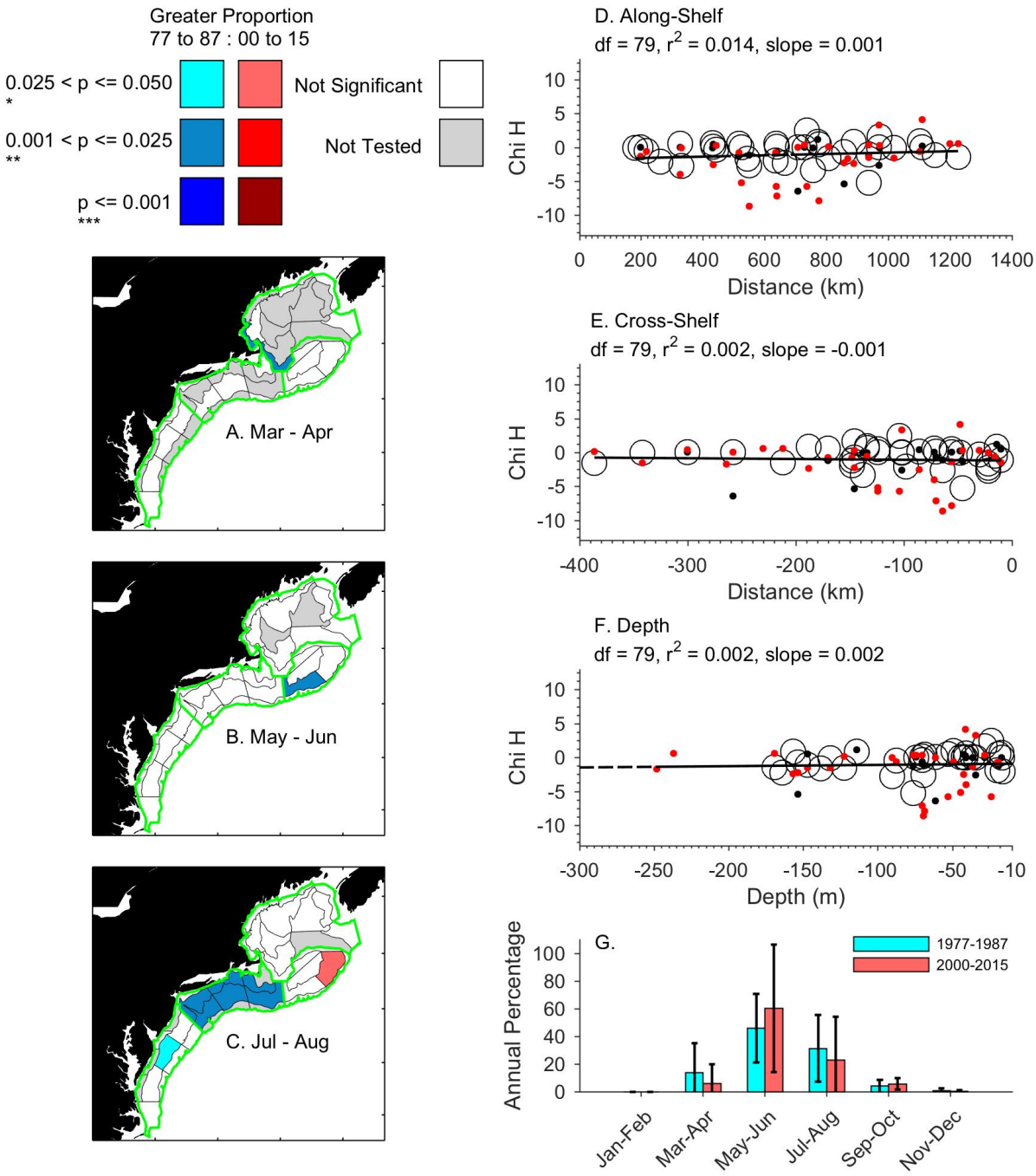

Figure B101. Spatial and seasonal distribution of larval witch flounder (*Glyptocephalus cynoglossus*) in the Northeast U.S. Shelf Ecosystem. Change in spatial distribution of larval in the March – April (A; •), May – June (B; O), and July – August (C; •) were examined in the along-shelf (D), cross-shelf (E), and depth (F) directions. Larval witch flounder did not shift significantly spatially or seasonally (G).

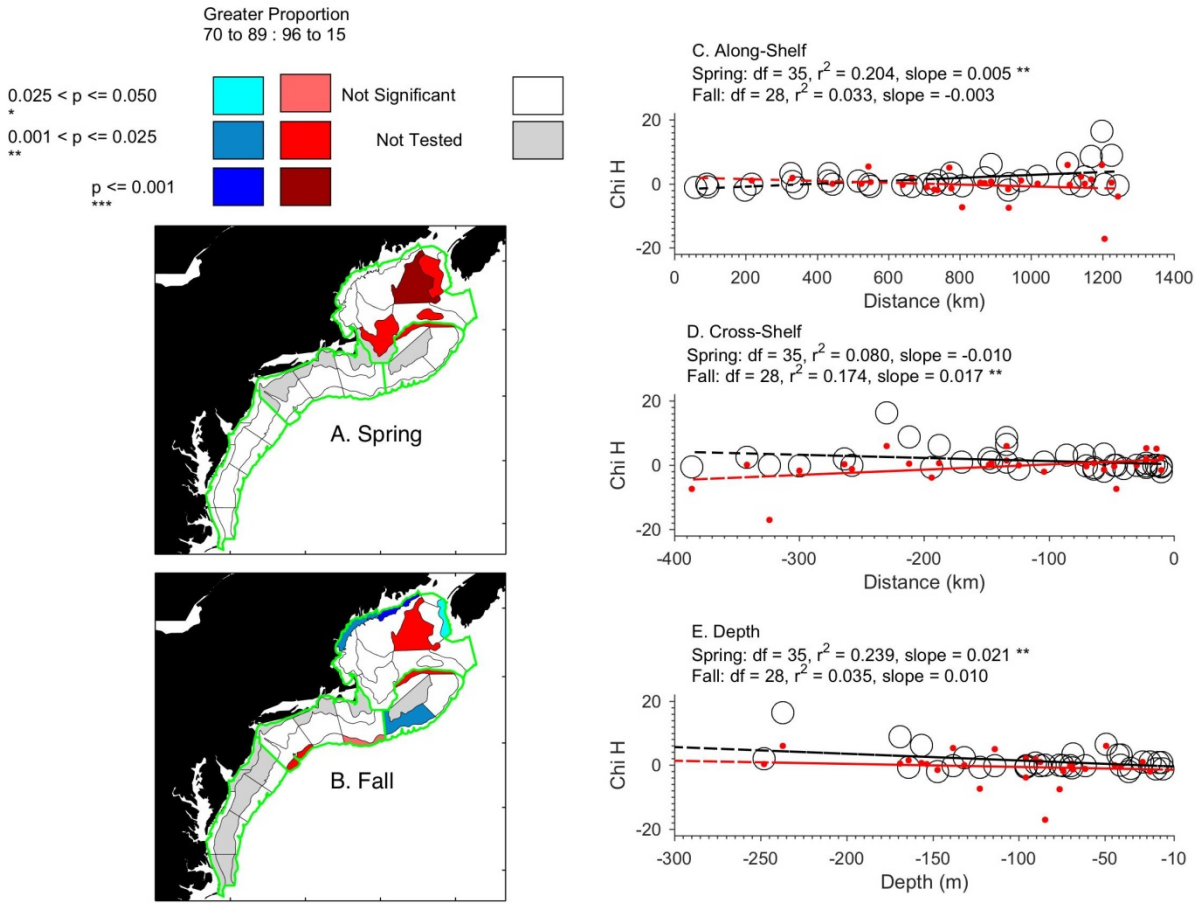

Figure B102. Spatial distribution of juvenile (< 30 cm) witch flounder (*Glyptocephalus cynoglossus*) in the Northeast U.S. Shelf Ecosystem. Change in distribution of juveniles in the spring (A; O) and fall (B; •) were examined in the along-shelf (C), cross-shelf (D), and depth (E) directions. Witch flounder juveniles shifted significantly northward (C) and deeper (E) in the spring, and offshore (D) in the fall.

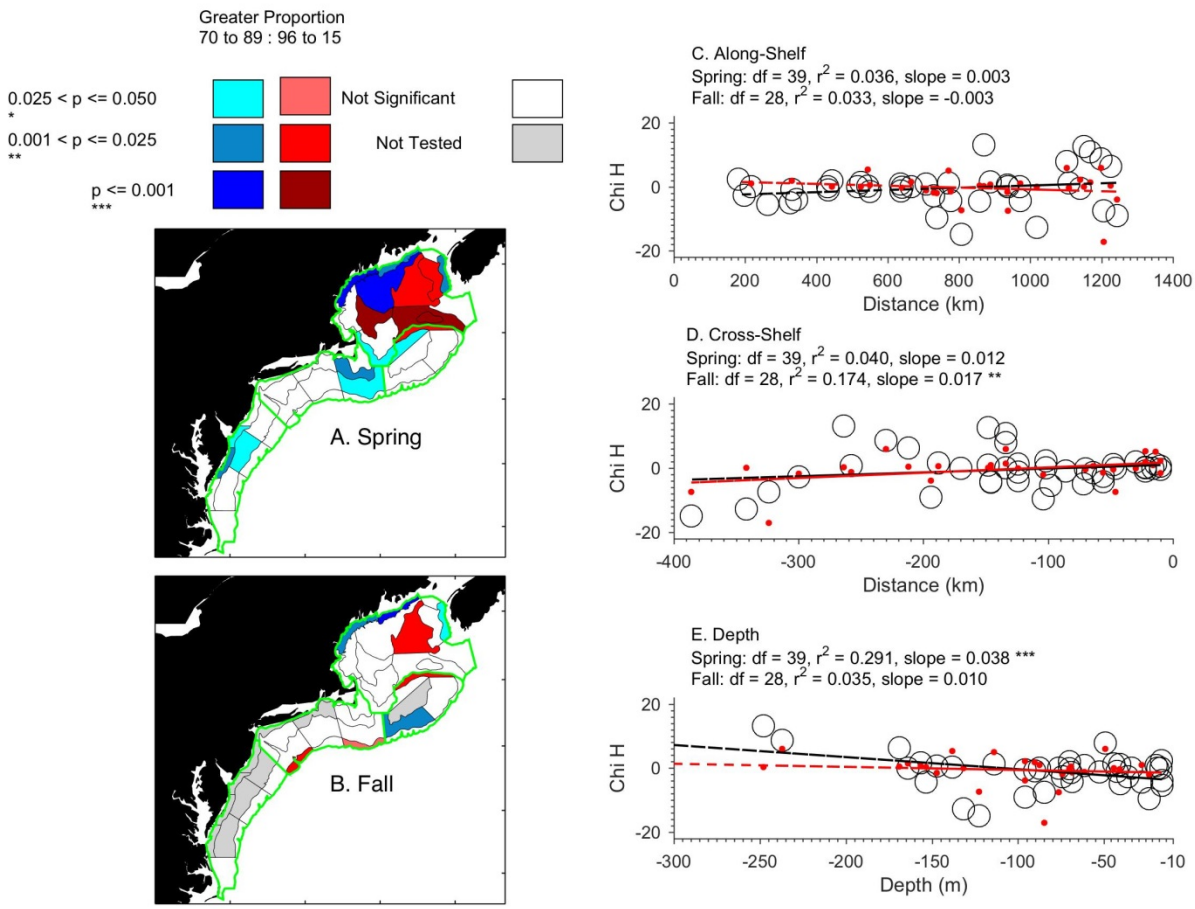

Figure B103. Spatial distribution of adult (>= 30 cm) witch flounder (*Glyptocephalus cynoglossus*) in the Northeast U.S. Shelf Ecosystem. Change in distribution of adults in the spring (A; O) and fall (B; •) were examined in the along-shelf (C), cross-shelf (D), and depth (E) directions. Witch flounder adults shifted significantly deeper (E) in the spring and offshore (D) in the fall.

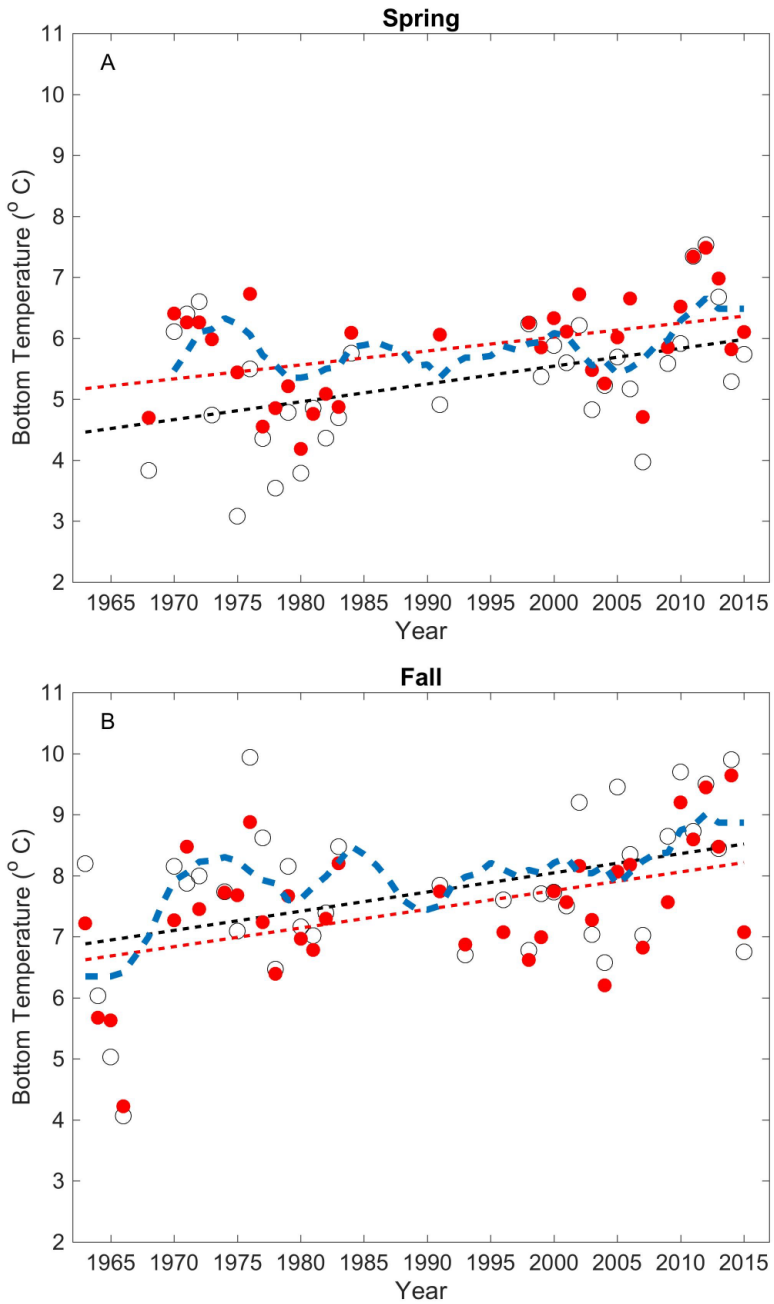

Figure B104. Stratified mean bottom water temperature (symbols) and linear trend (line) of juvenile (< 30 cm; O) and adult witch flounder (>= 30 cm; •) collected in the Gulf of Maine during the Northeast Fisheries Science Center spring (A) and fall (B) bottom trawl surveys. Mean bottom water temperature of all stations sampled in the region is shown as a 5-year moving average (---).

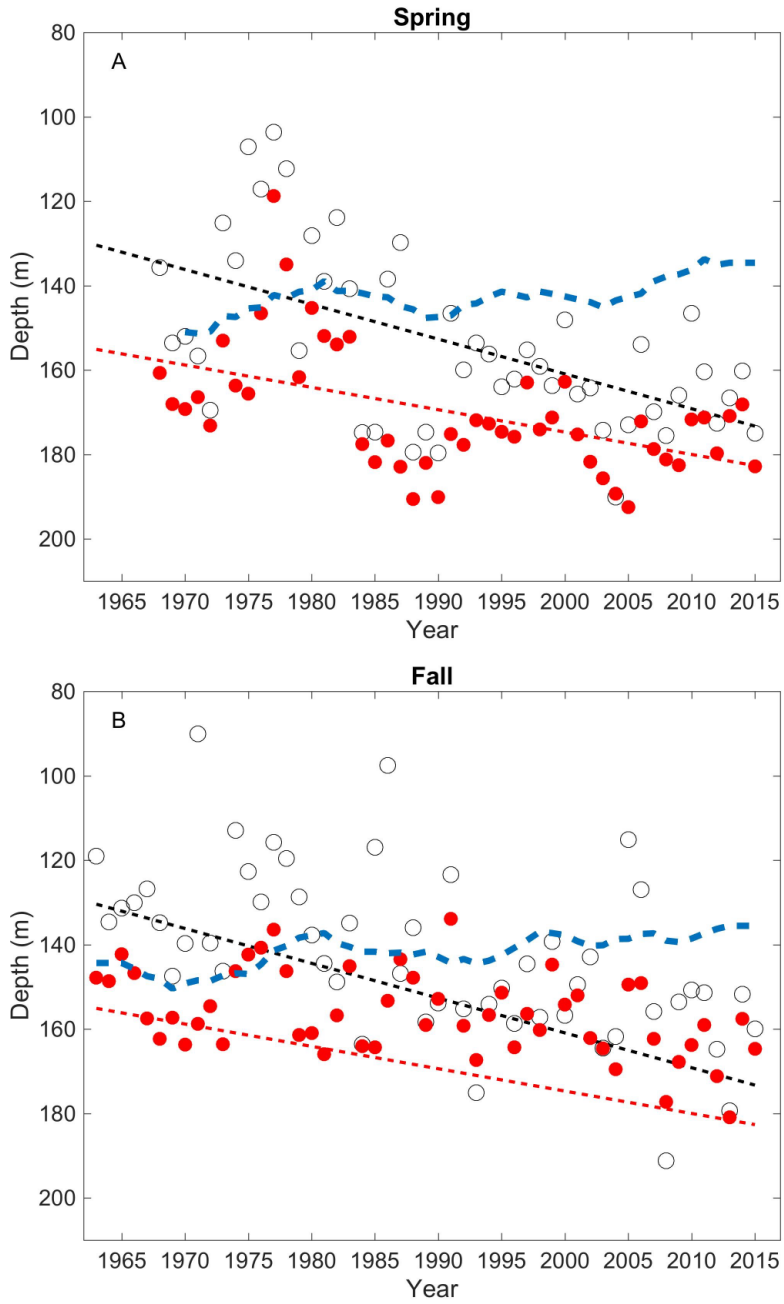

Figure B105. Stratified mean depth (symbols) and linear trend (line) of juvenile (< 30 cm; O) and adult witch flounder (>= 30 cm; •) collected in the Gulf of Maine during the Northeast Fisheries Science Center spring (A) and fall (B) bottom trawl surveys. Mean depth of all stations sampled in the region is shown as a 5-year moving average (---).

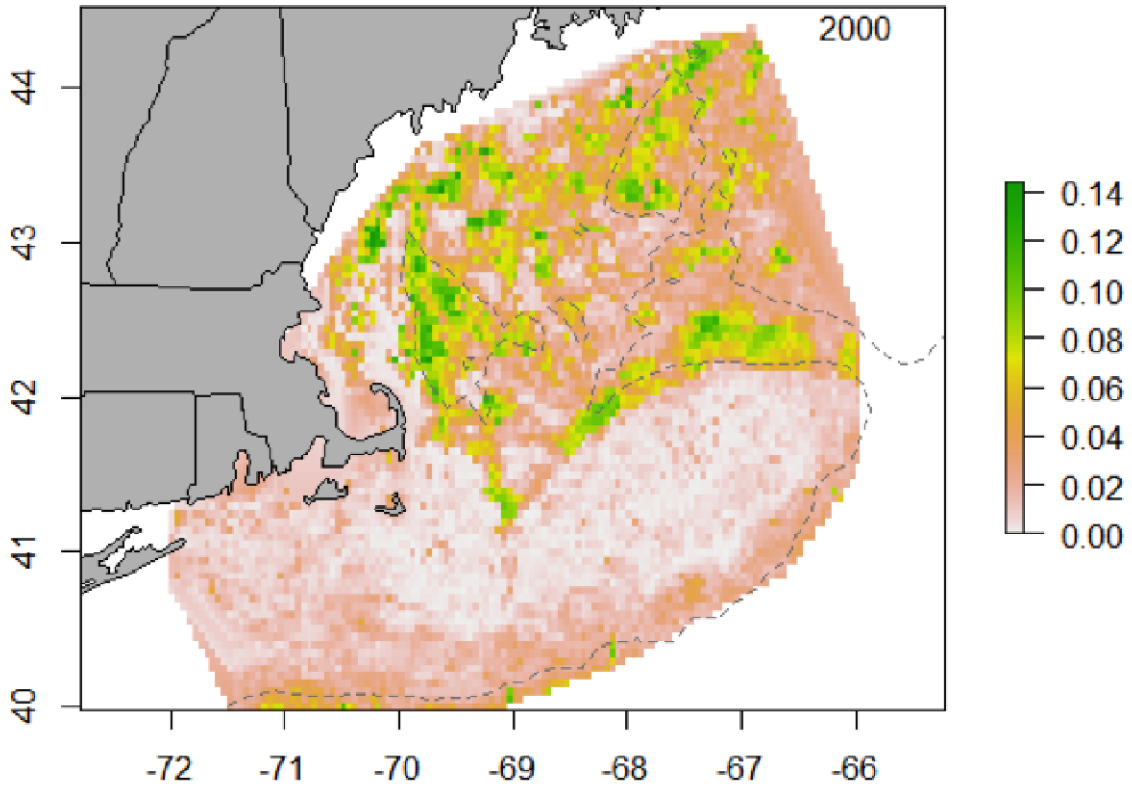

Figure B106. Estimated habitat map of witch flounder spring abundance (log) in the year 2000. Estimates were based on a regression model using Random Forrest models where depth was the most important habitat variable, and bottom temperature, bathymetric position index (BPI) and soft sediments were high contributors.

Figure B107. Trends in mean z-scores of witch flounder biomass based regression model habitat estimates using Random Forrest models were used to visualize changes from 2000 to 2015. A 5-point moving average was applied to the mean z-scores for the spring and fall survey periods.

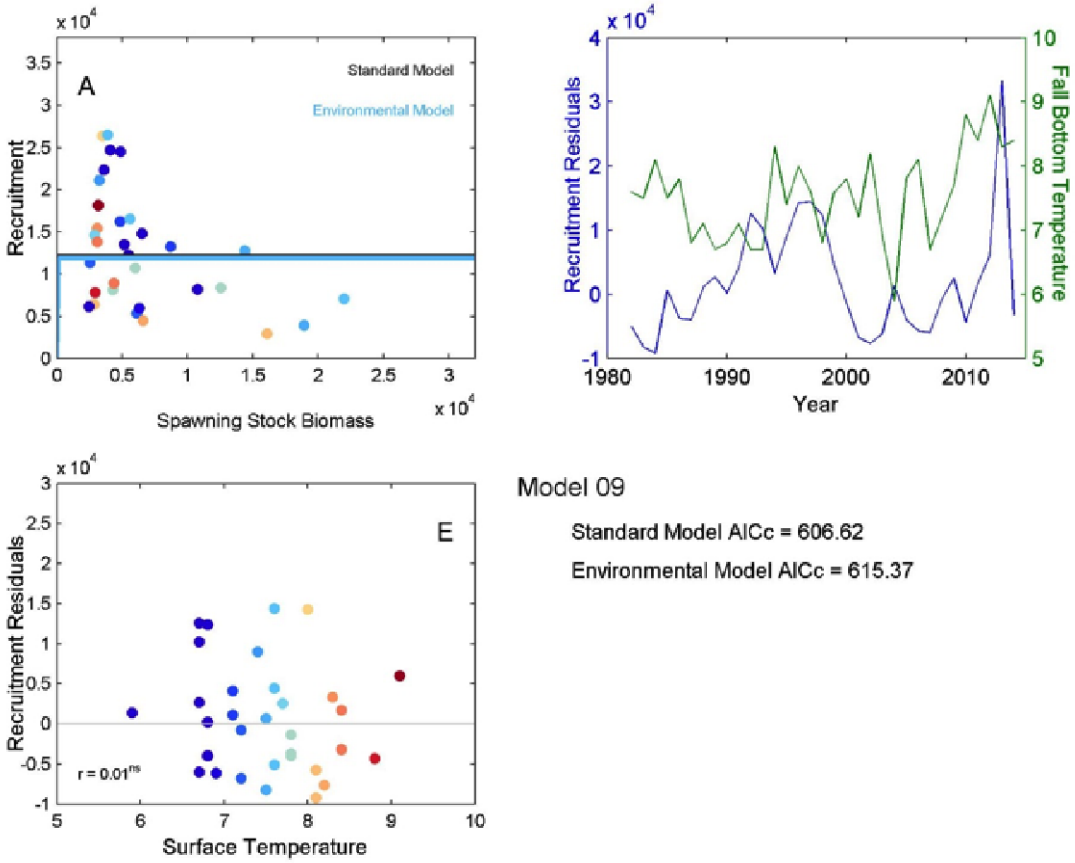

Figure B108. Stock-recruitment analyses for ASAP Model Output 09 using method described in Hare et al. 2016 working paper. ASAP Model Output 09 is the penultimate model run of Run 9_5_v2.

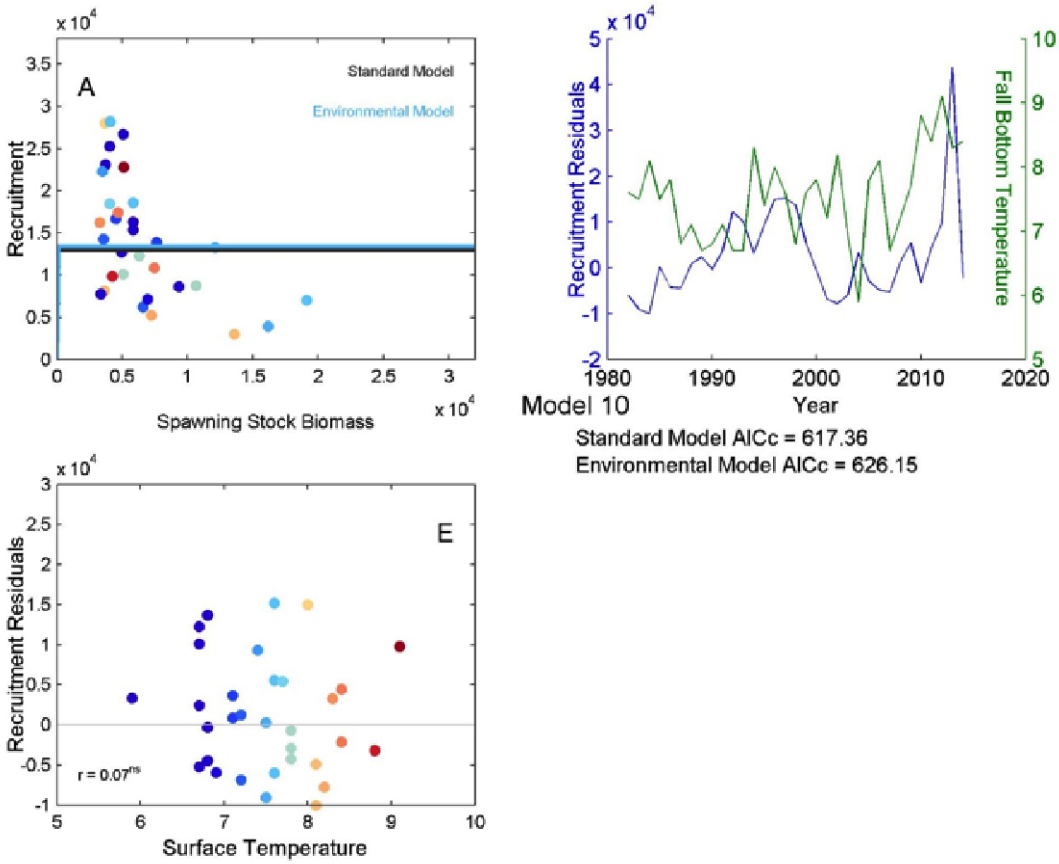

Figure B109. Stock-recruitment analyses for ASAP Model Output 10 using method described in Hare et al. 2016 working paper. ASAP Model Output 10 refers to a sensitivity run incorporating the LPUE40% tuning index.

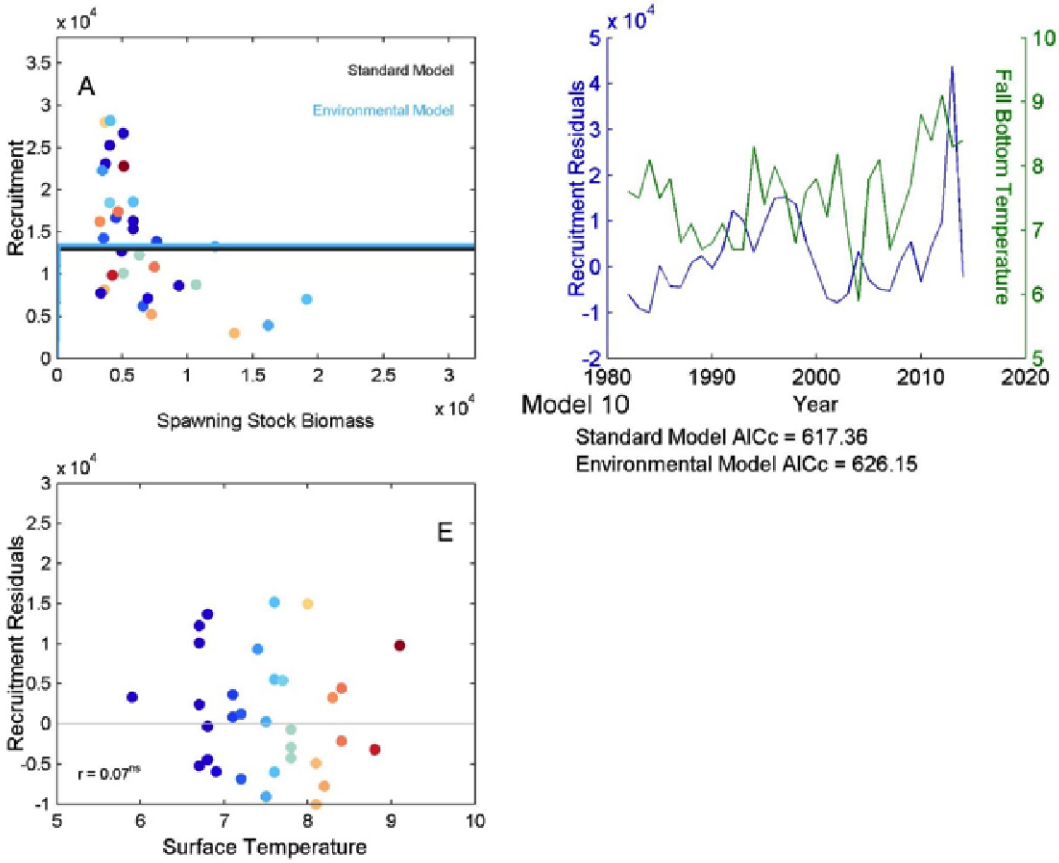

Figure B110. Stock-recruitment analyses for ASAP Model Output 15 using method described in Hare et al. 2016 working paper. ASAP Model Output 15 refers to a ASAP run with a catch multiplier of 4 for 2004 onward.

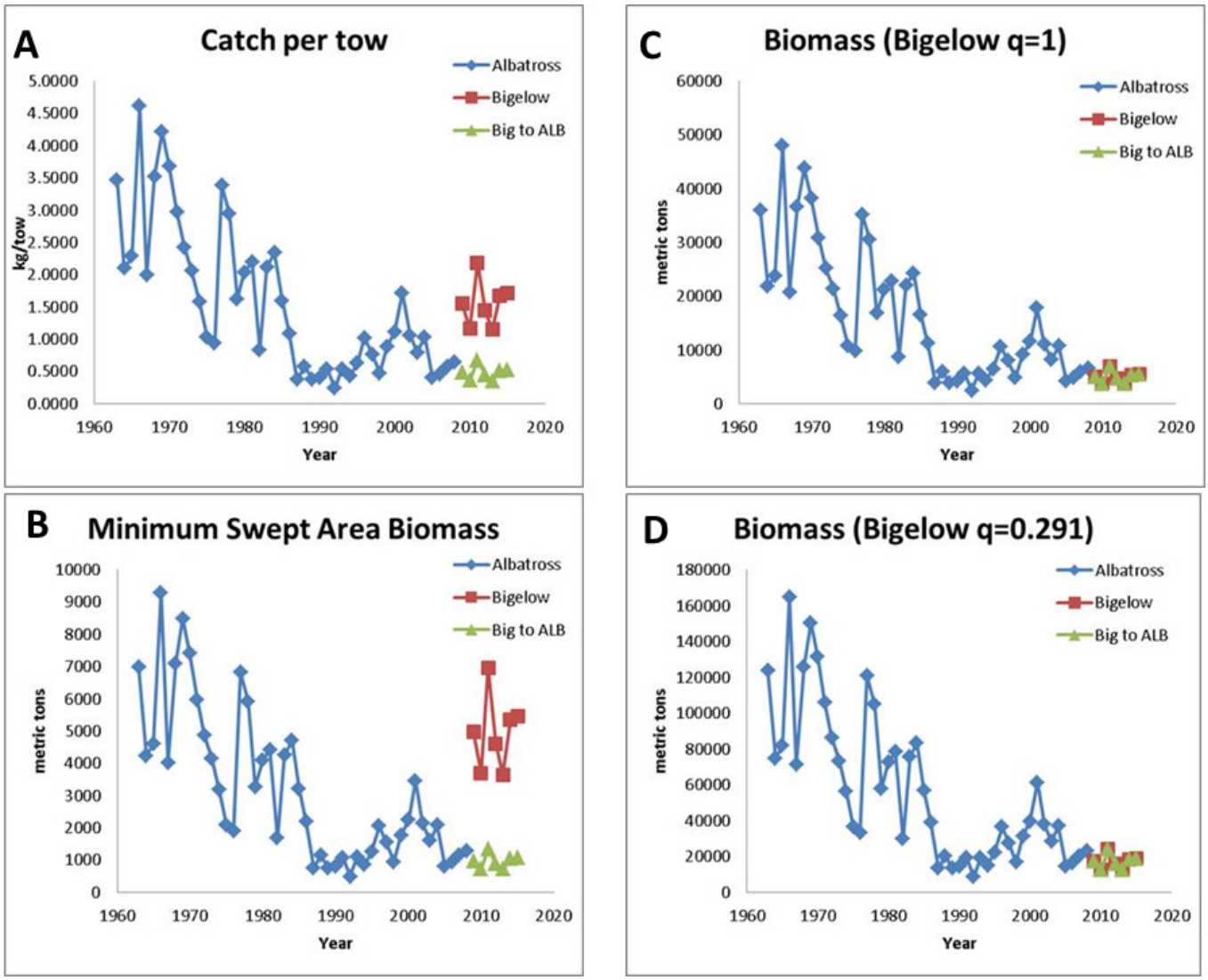

Figure B111. Trends in Northeast Fisheries Science Center autumn survey (kg/tow; A), minimum swept area biomass (mt; B), population biomass (mt; C) and population biomass accounting for net efficiency (mt, D) of witch flounder, 1963 – 2015.

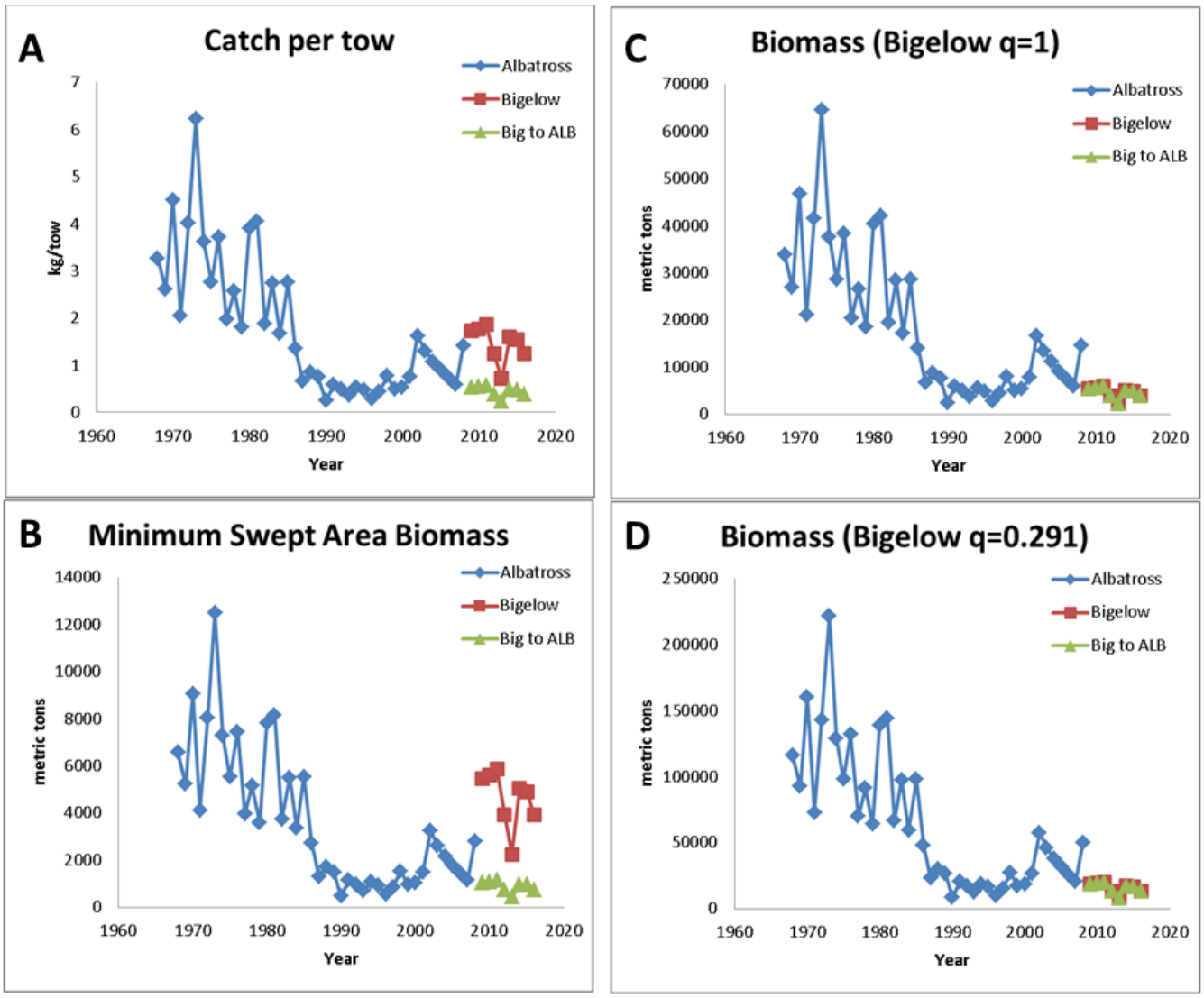

Figure B112. Trends in Northeast Fisheries Science Center spring survey (kg/tow; A), minimum swept area biomass (mt; B), population biomass (mt; C) and population biomass accounting for net efficiency (mt, D) of witch flounder, 1968 - 2016.

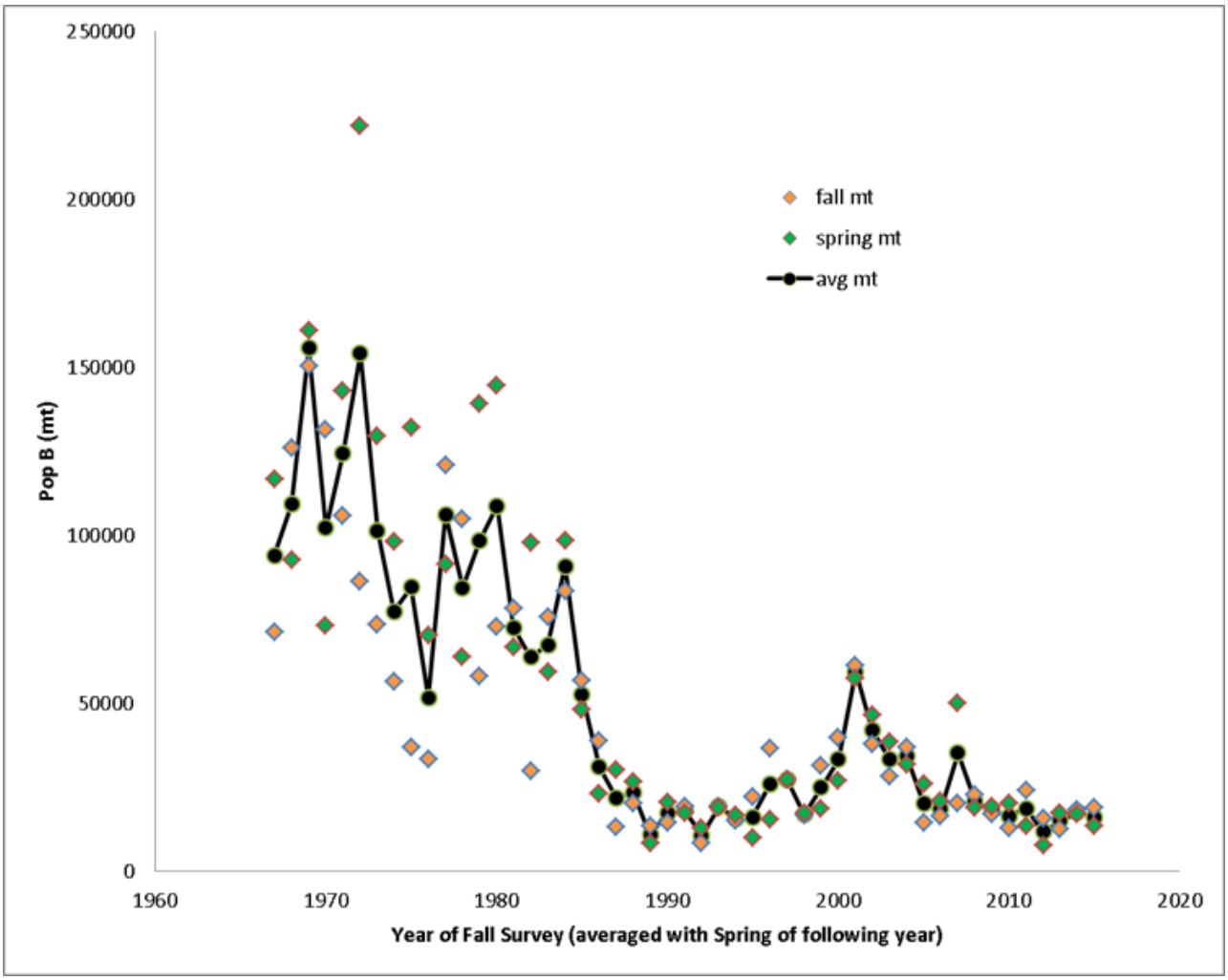

Figure B113. Trends in Northeast Fisheries Science Center autumn (pink diamond) and spring (green diamond) population biomass estimates (mt) and the average population biomass (mt; representing beginning year biomass; black line with solid circles) of witch flounder, 1969 – 2016.

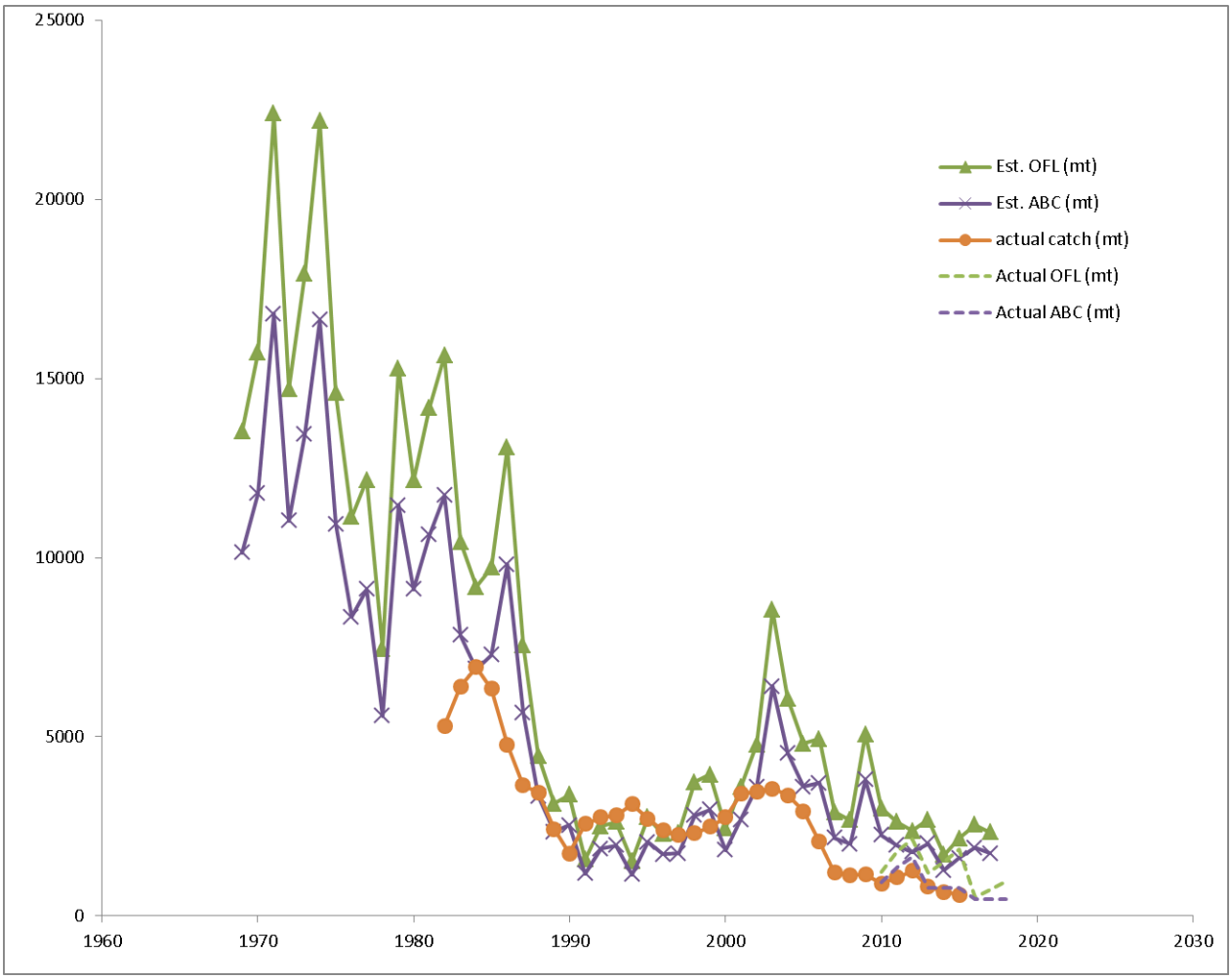

Figure B114. Estimated (solid lines) and actual (dashed lines) overfishing limit biomass (OFL; mt; green lines) and acceptable biological catch (ABC; mt; purple lines) and actual catch (mt; solid line with circles) of witch flounder, 1969 – 2018, using an assumed exploitation rate of 0.16.

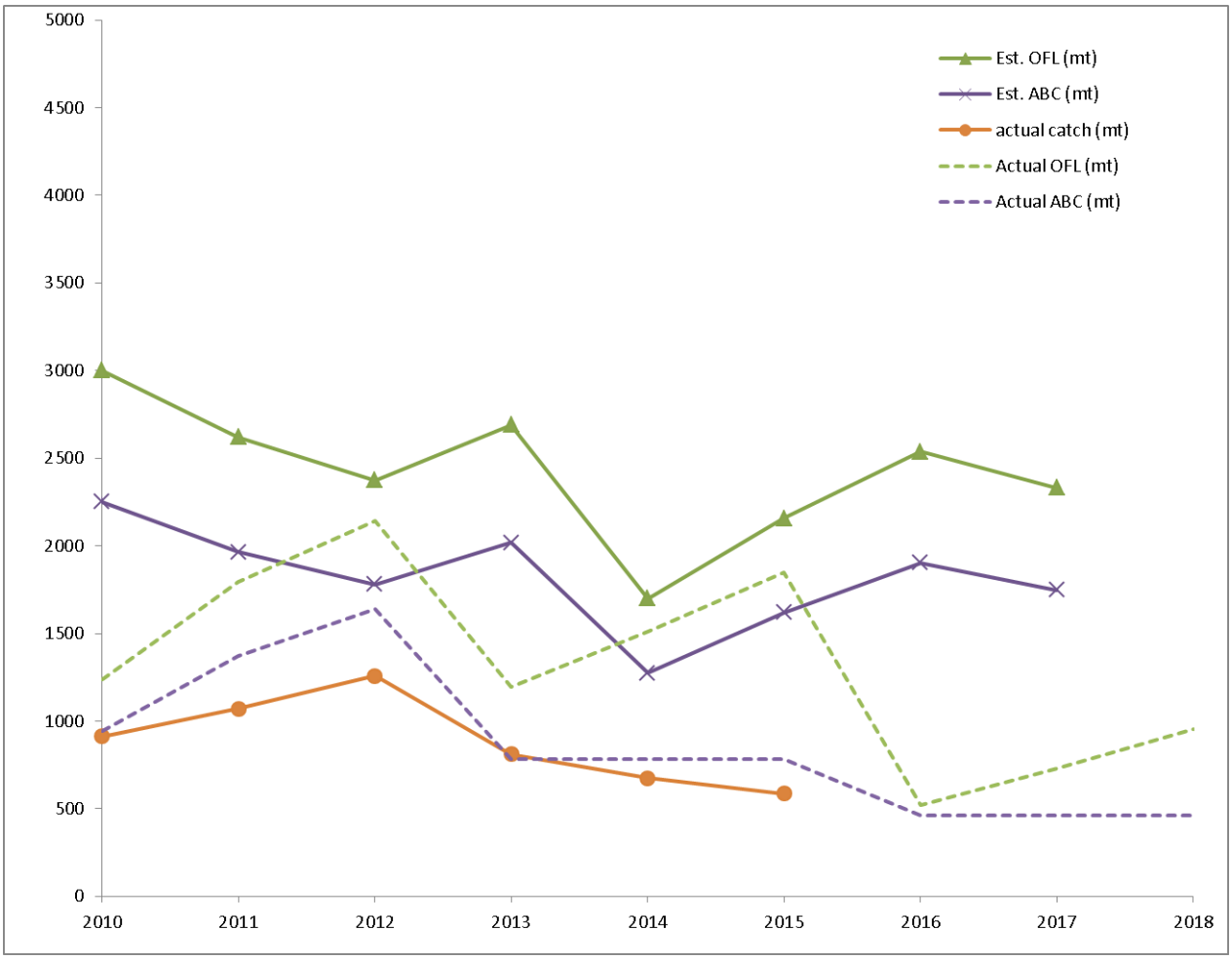

Figure B115. Estimated (solid lines) and actual (dashed lines) overfishing limit biomass (OFL; mt; green lines) and acceptable biological catch (ABC; mt; purple lines) and actual catch (mt; solid line with circles) of witch flounder for 2010 – 2018, using an assumed exploitation rate of 0.16.

.

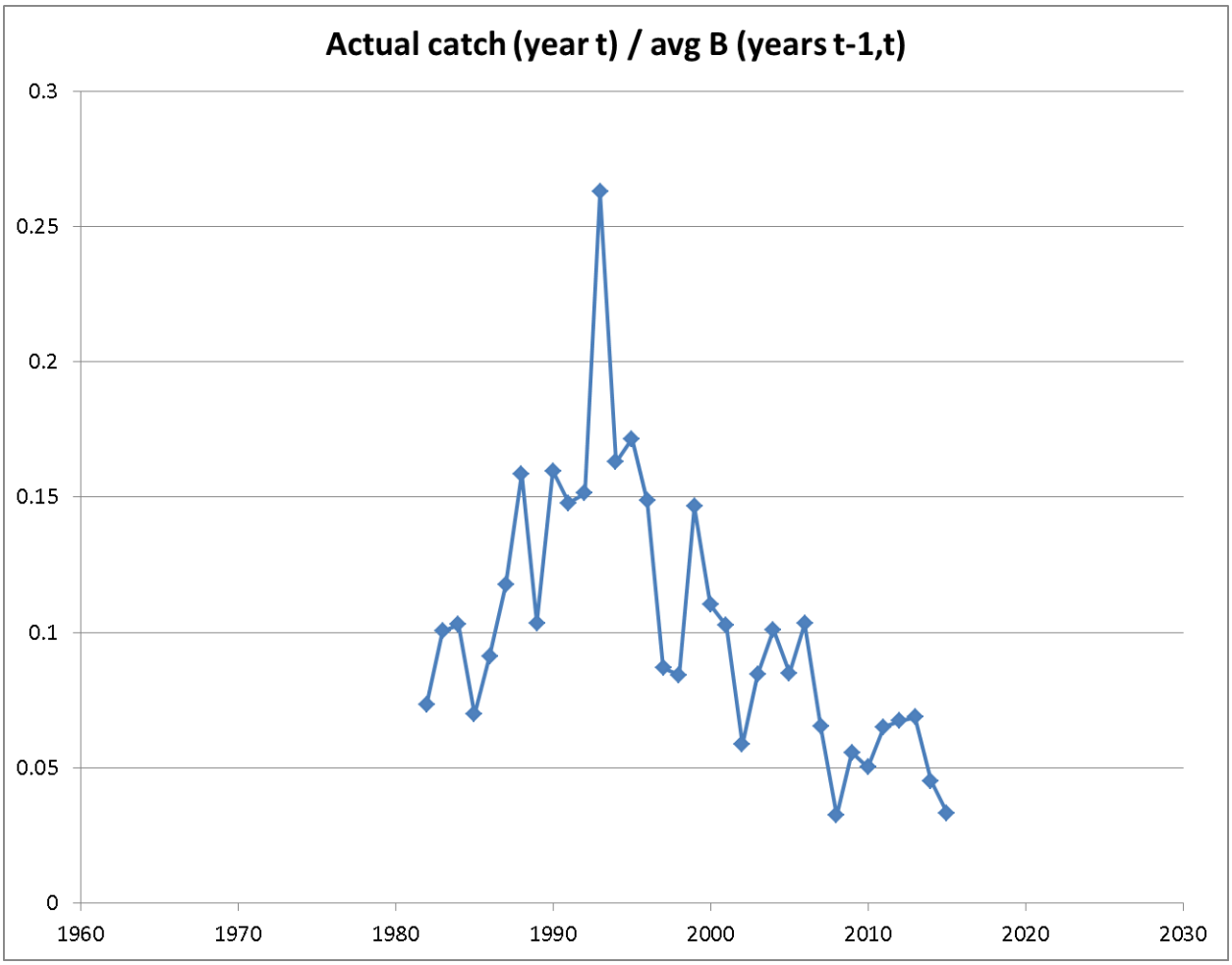

Figure B116. Historical exploitation rates of witch flounder derived from actual catch (year t) divided by average population biomass (years t-1 Autumn and t Spring), 1982 – 2015.

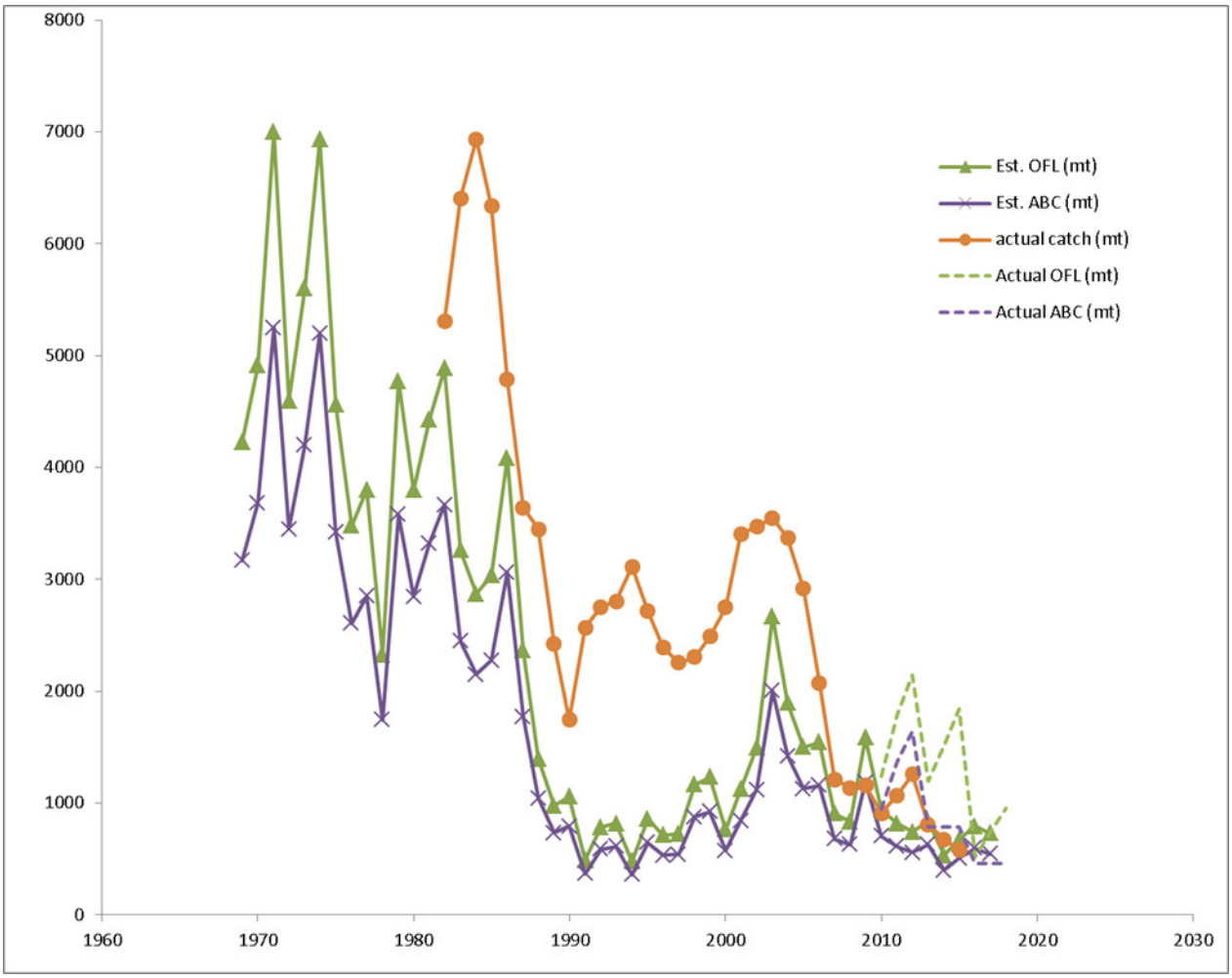

Figure B117. Estimated (solid lines) and actual (dashed lines) overfishing limit biomass (OFL; mt; green lines) and acceptable biological catch (ABC; mt; purple lines) and actual catch (mt; solid line with circles) of witch flounder, 1969 – 2018, using an assumed exploitation rate of 0.05.

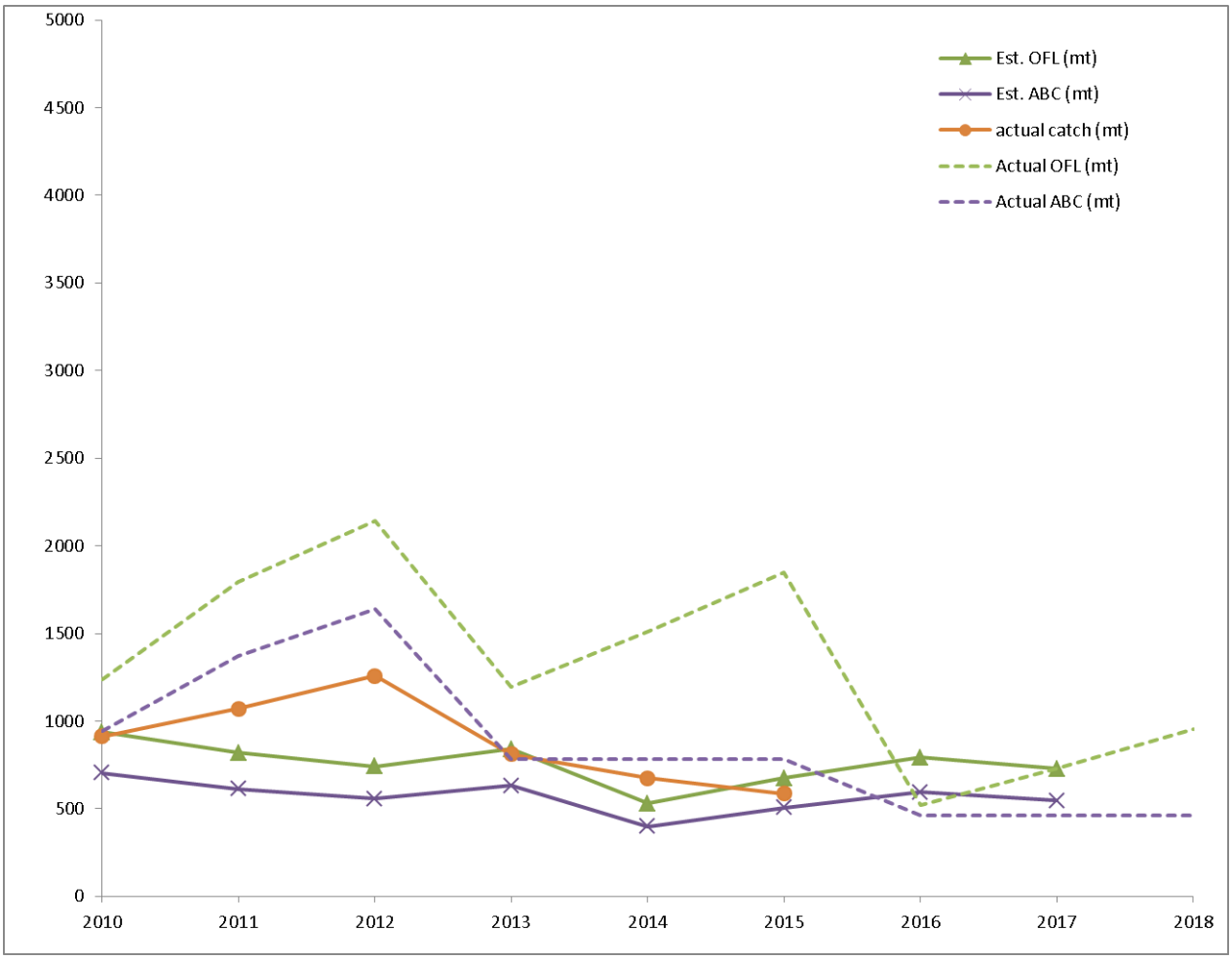

Figure B118. Estimated (solid lines) and actual (dashed lines) overfishing limit biomass (OFL; mt; green lines) and acceptable biological catch (ABC; mt; purple lines) and actual catch (mt; solid line with circles) of witch flounder for 2010 – 2018 using an assumed exploitation rate of 0.05.

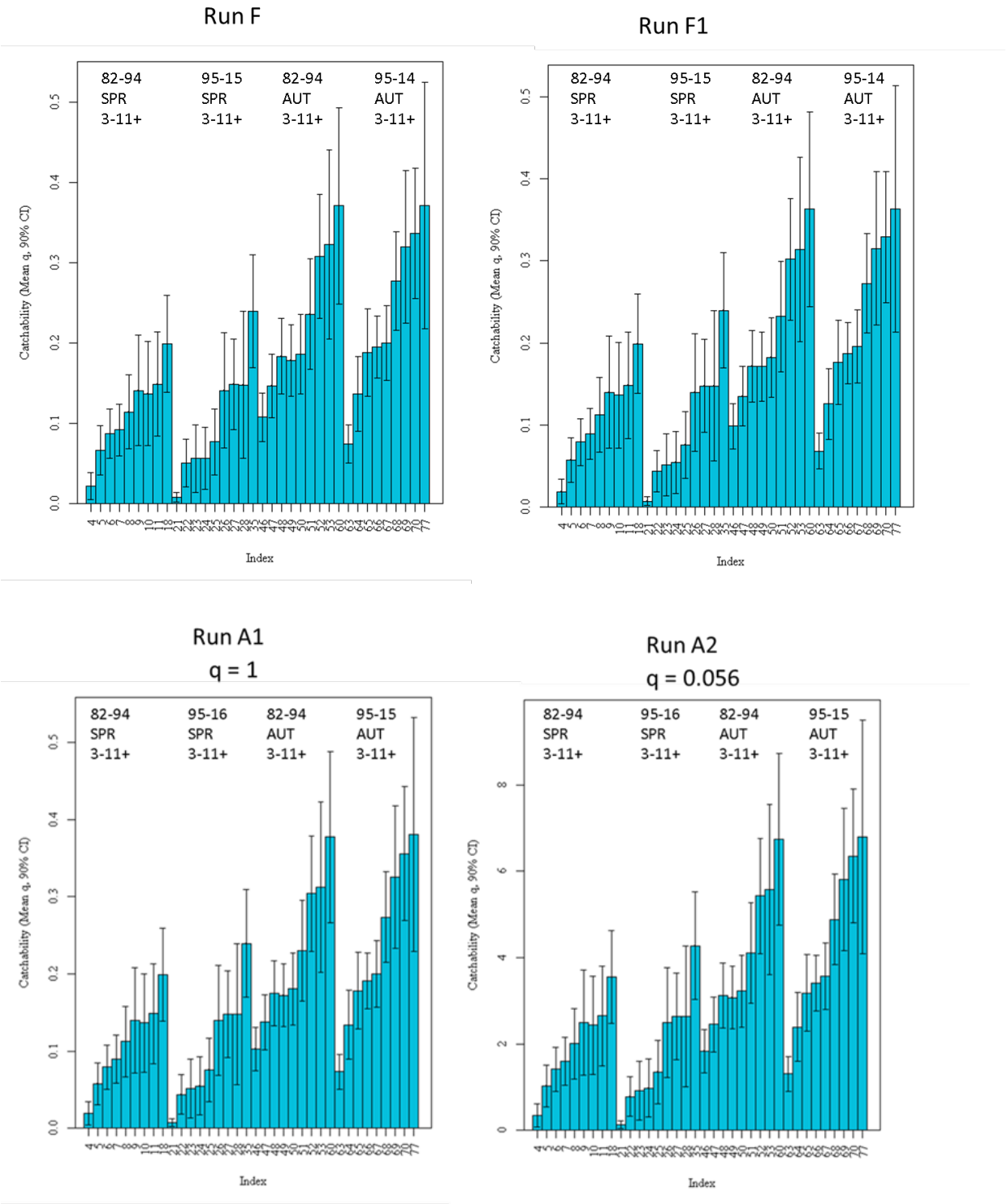

Figure B119. Northeast Fisheries Science Center swept-area survey catchabilities (q) by age (3 to 11+) and season (spring and autumn) from RUN F (2015 OA accepted run; top left), Run F1 (2015 OA with revised catch at age; top right), RUN A1 (q assumed to be 1) and RUN A2 (q = 0.056). Survey tuning indices split between 1994 and 1995.

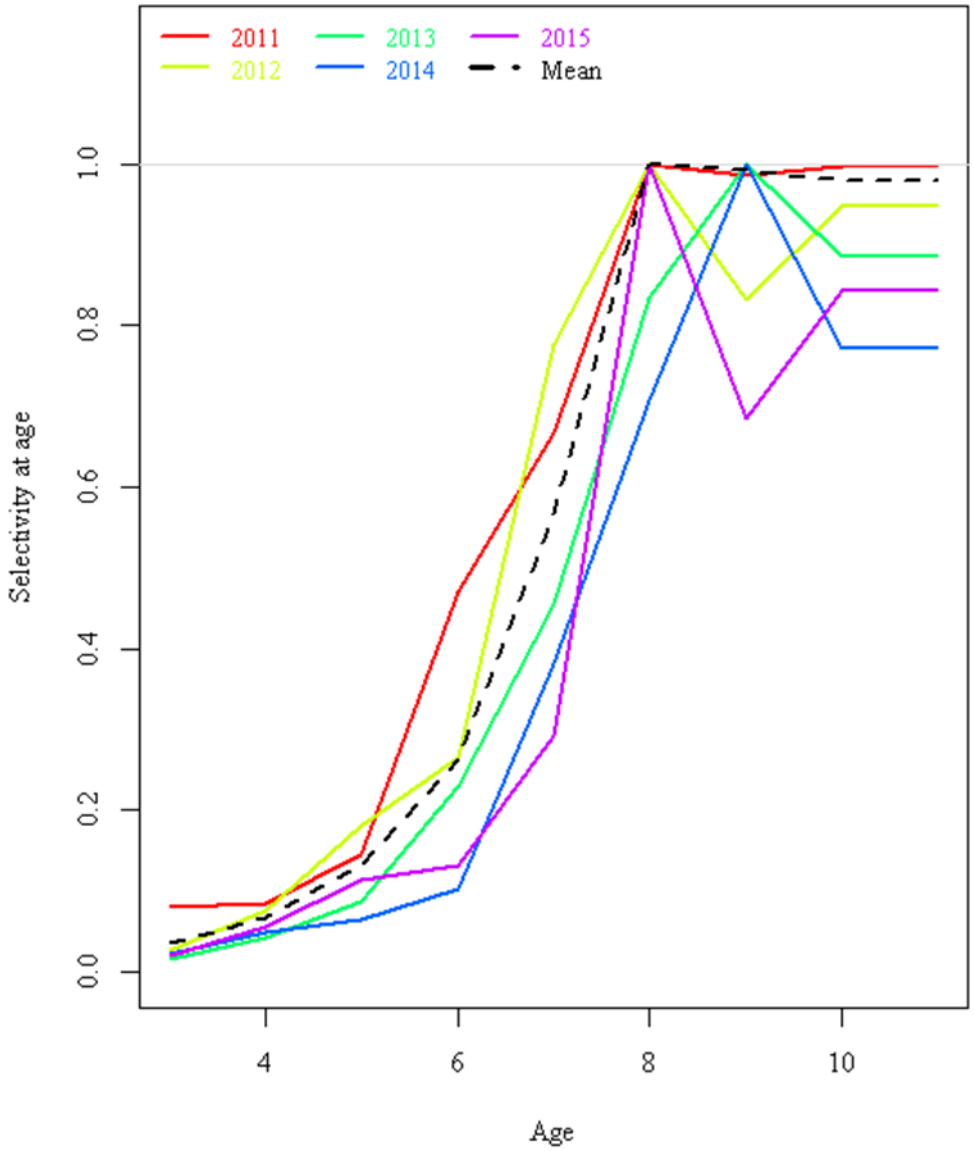

Figure B120. Model-estimated partial recruitment pattern of witch flounder for the five most recent years from Run A2, 1982-2015.

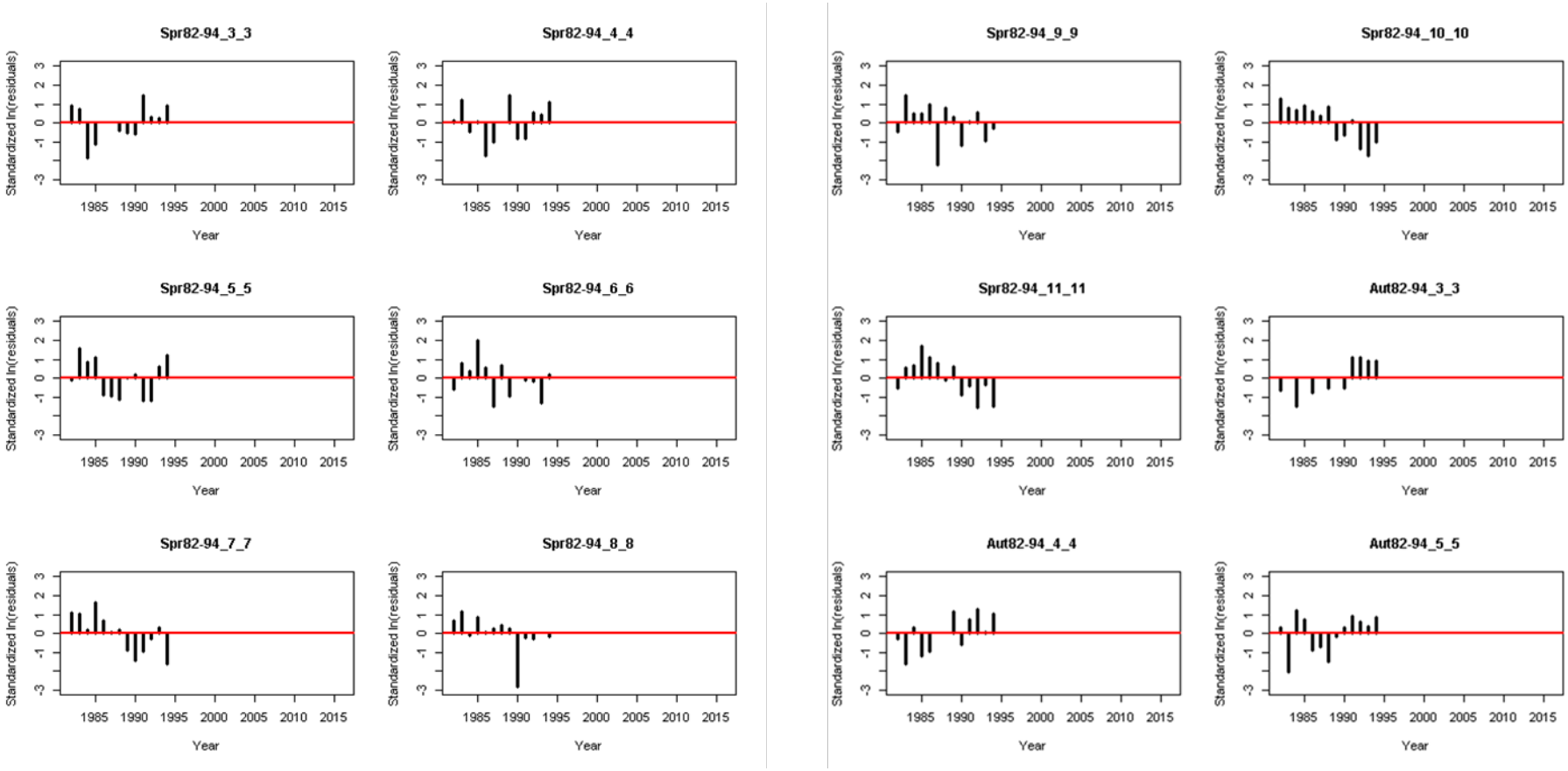

Figure B121. Witch flounder standardized residuals for Northeast Fisheries Science Center spring and autumn survey indices at age from RUN A2, 1982-2015.

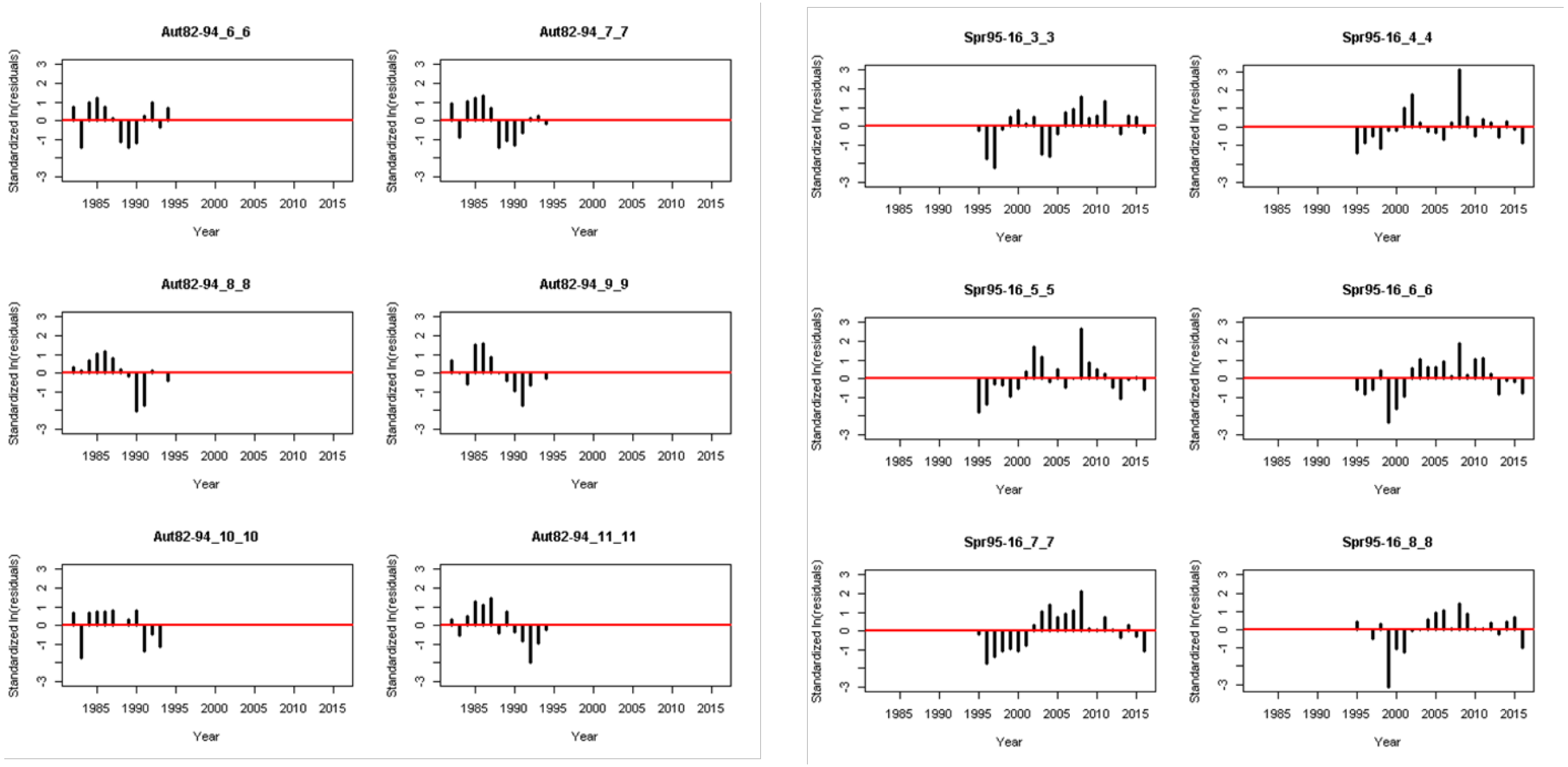

Figure B121, continued. Witch flounder standardized residuals for Northeast Fisheries Science Center spring and autumn survey indices at age (3 to 11+) from RUN A2, 1982-2015.

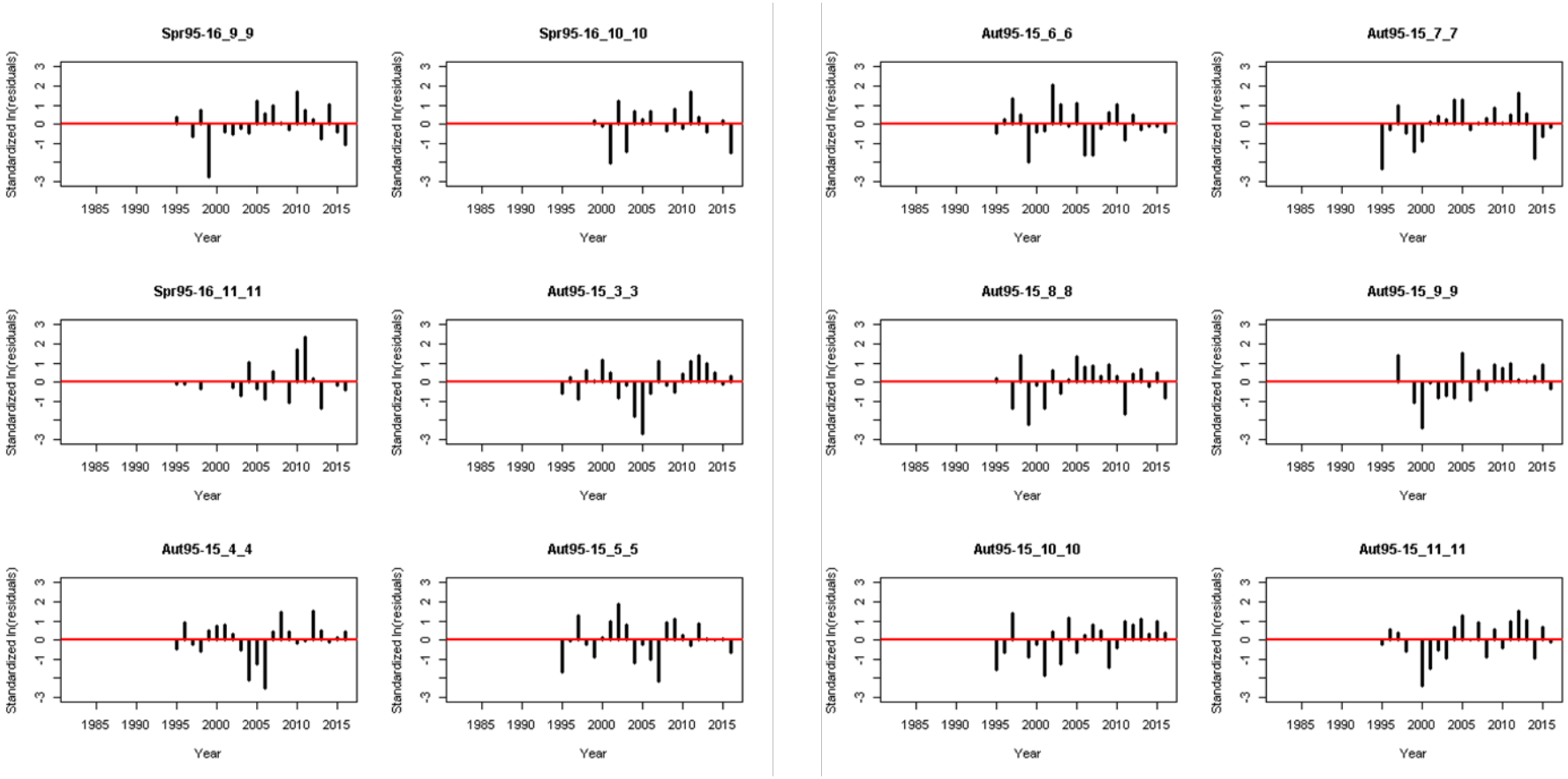

Figure B121, continued. Witch flounder standardized residuals for Northeast Fisheries Science Center spring and autumn survey indices at age (3 to 11+) from RUN A2, 1982-2015.

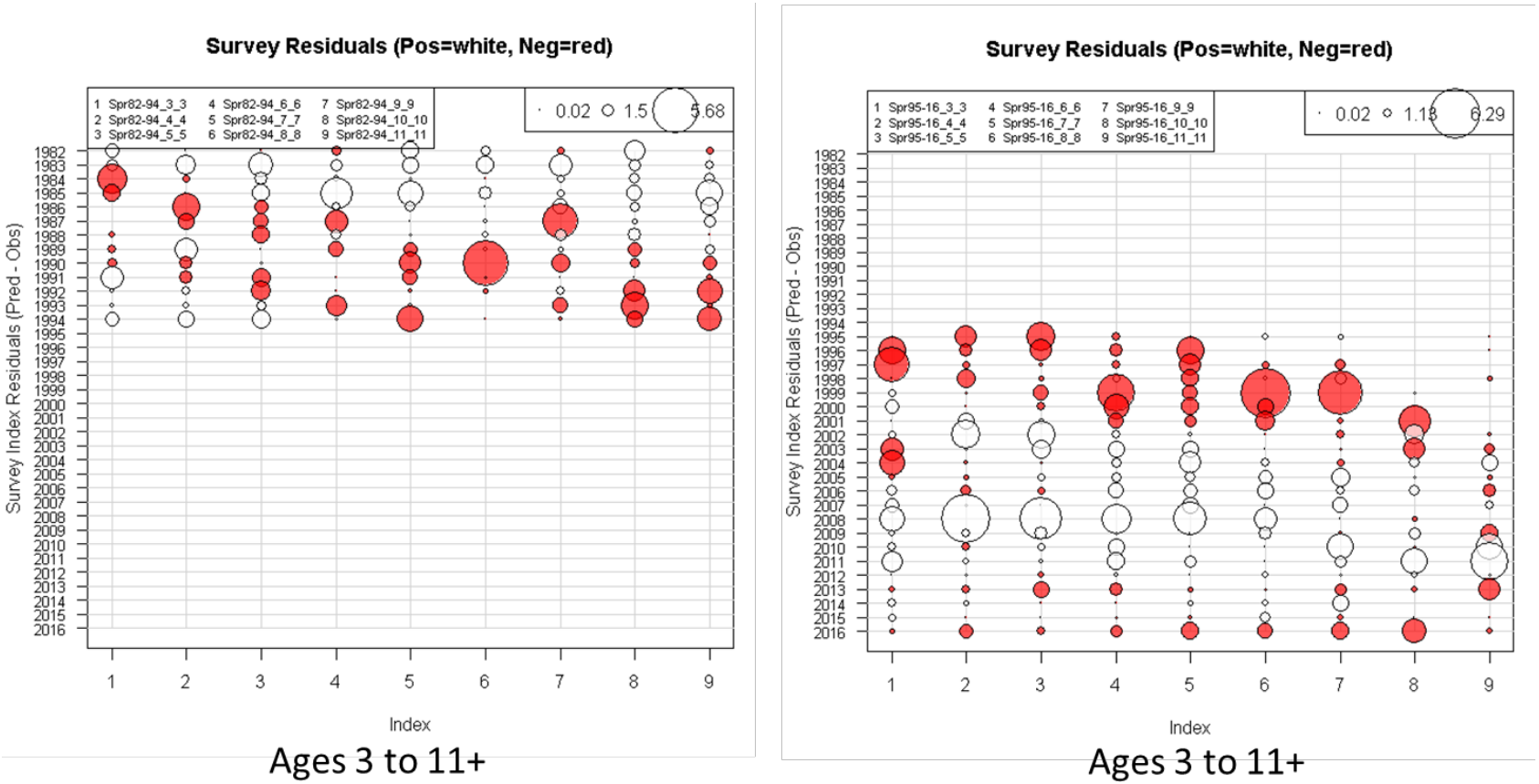

Figure B122. Witch flounder standardized residuals for Northeast Fisheries Science Center spring survey indices at age (3 to 11+) from RUN A2, 1982-2015.

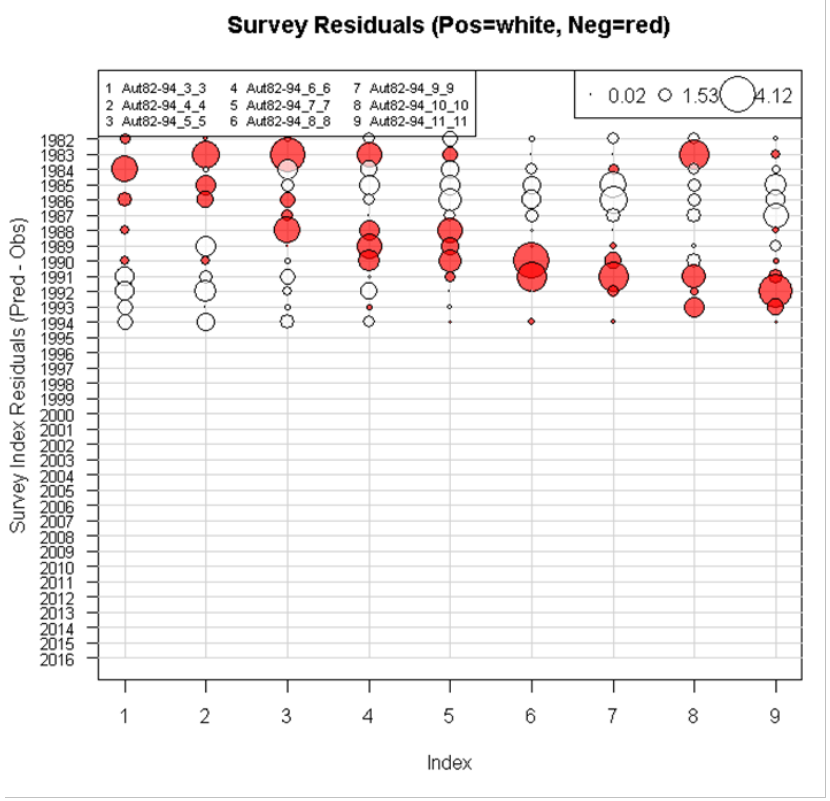

Ages 3 to 11+

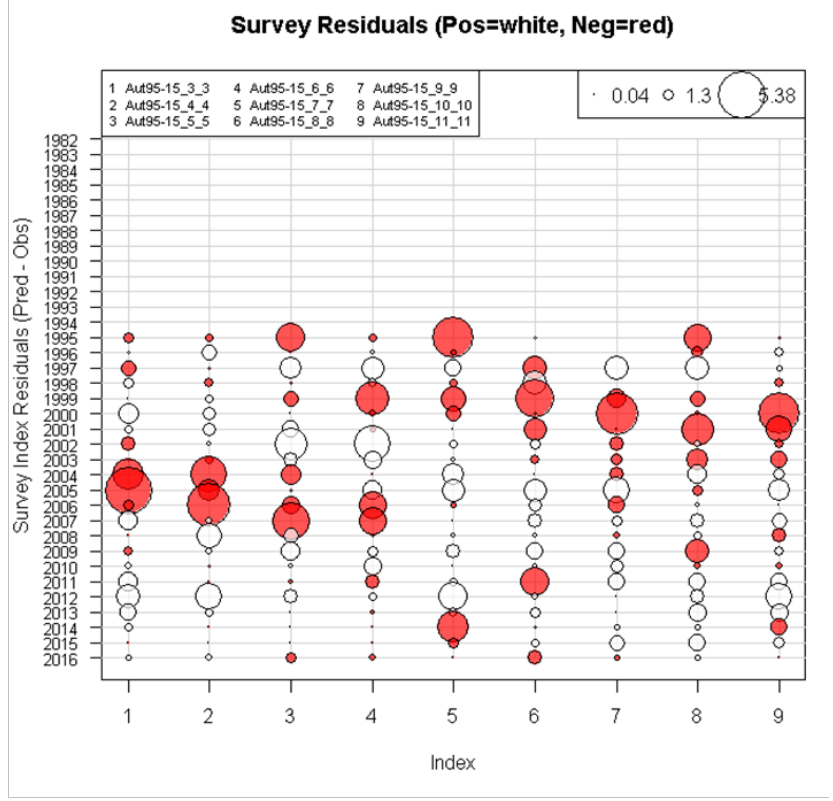

Ages 3 to 11+

Figure B122, continued. Witch flounder standardized residuals for Northeast Fisheries Science Center autumn survey indices at age (3 to 11+) from RUN A2, 1982-2015.

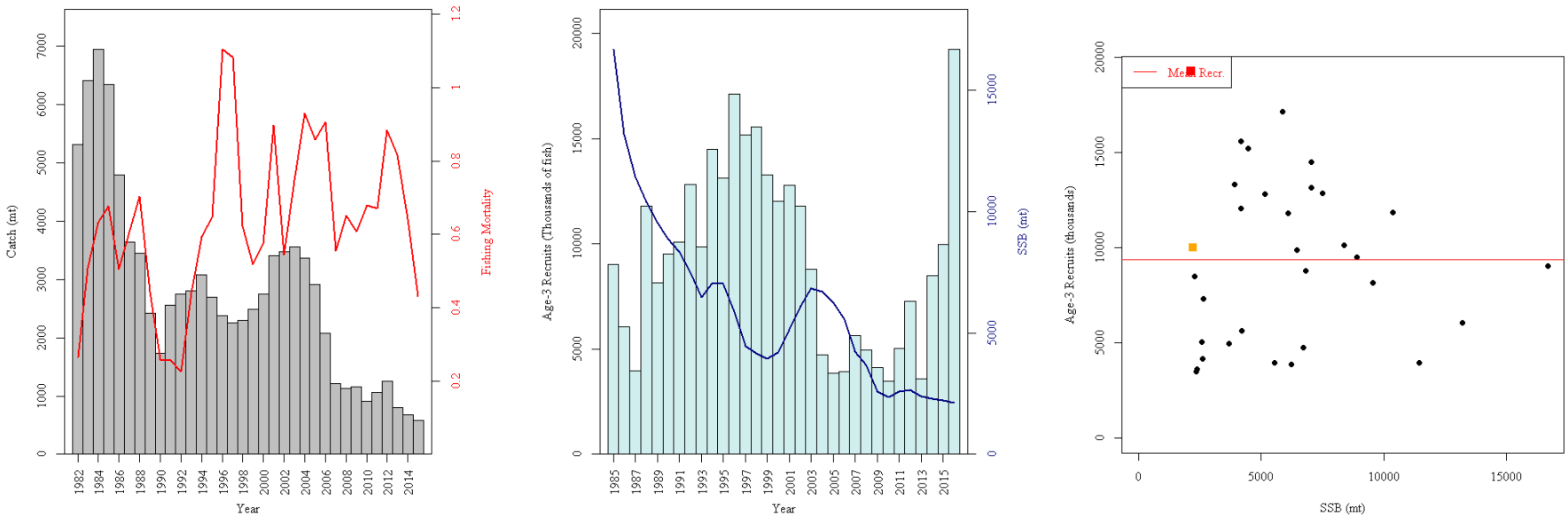

Figure B123. Trends of witch flounder total catch (gray bars) and fishing mortality (red line; left), Age 3 recruitment (light blue bars) and spawning stock biomass (dark blue line; middle), and spawning stock biomass and Age 3 recruits, 1982 – 2014 year classes (right) from RUN A2,1982 -2015. Red horizontal line represents mean recruitments; red and orange squares represent the 2012 and 2013 year classes (Age 3 in 2015 and 2016).

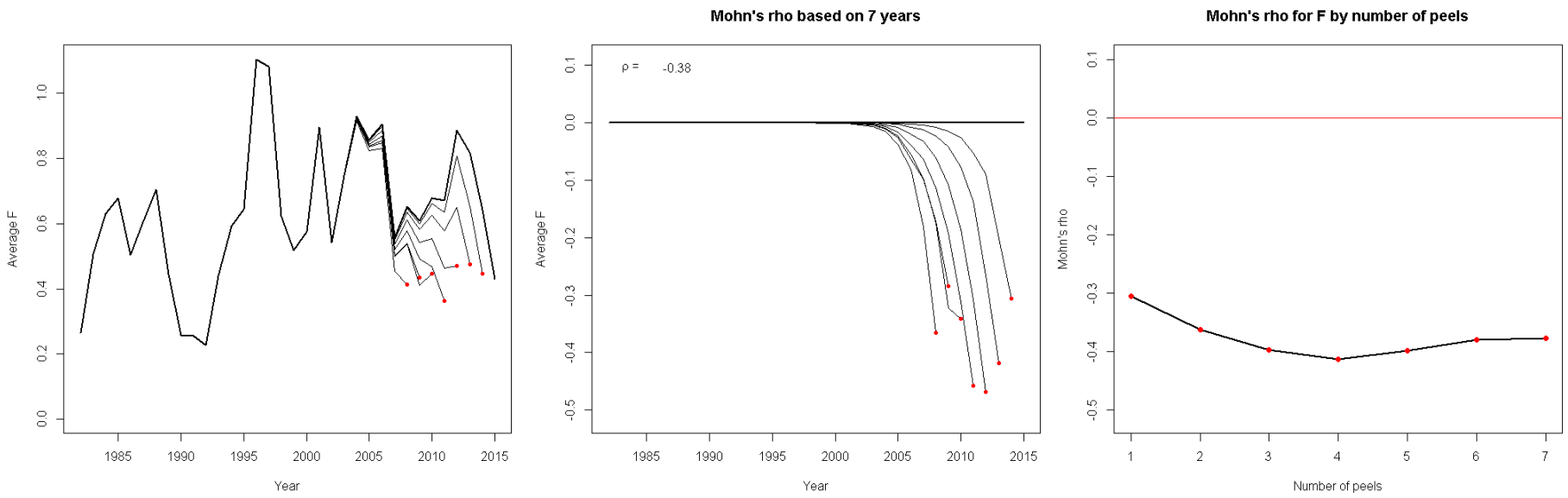

Figure B124. Retrospective analysis results of fishing mortality (left), relative difference of fishing mortality from the terminal year (middle) and Mohn's rho for each peel (right) from RUN A2, 1982 – 2015. Mohn's rho (average relative difference of 7 peels) is -0.38.

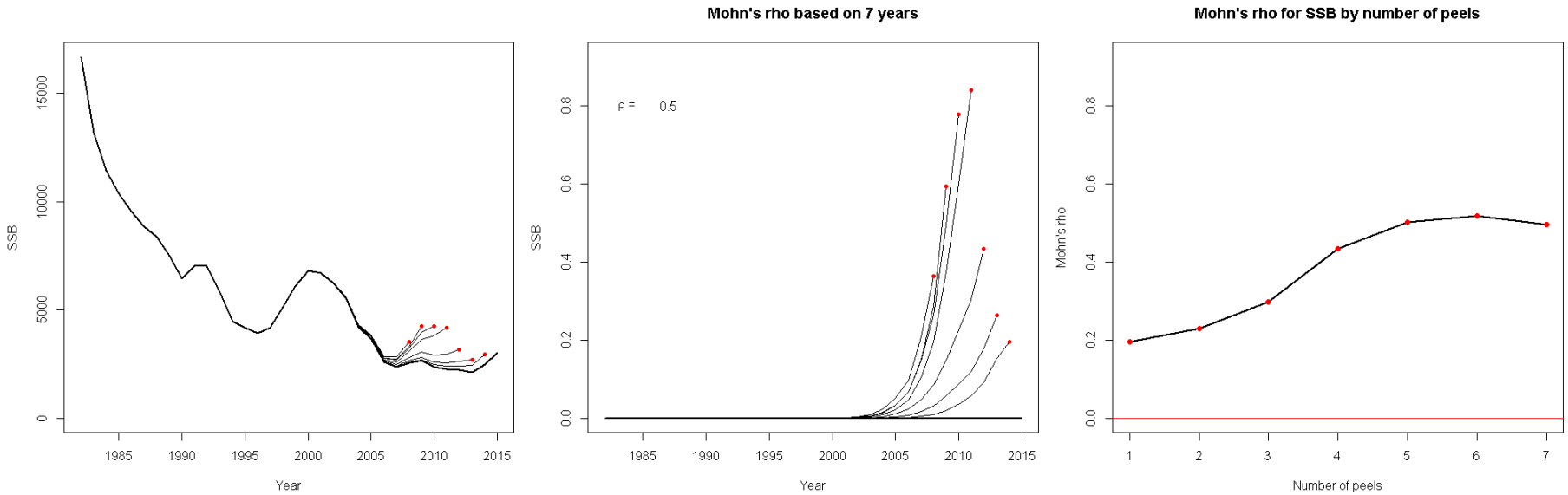

Figure B125. Retrospective analysis results of spawning biomass (left), relative difference of spawning biomass from the terminal year (middle) and Mohn's rho for each peel (right) from RUN A2, 1982 – 2015. Mohn's rho (average relative difference of 7 peels) is 0.50.

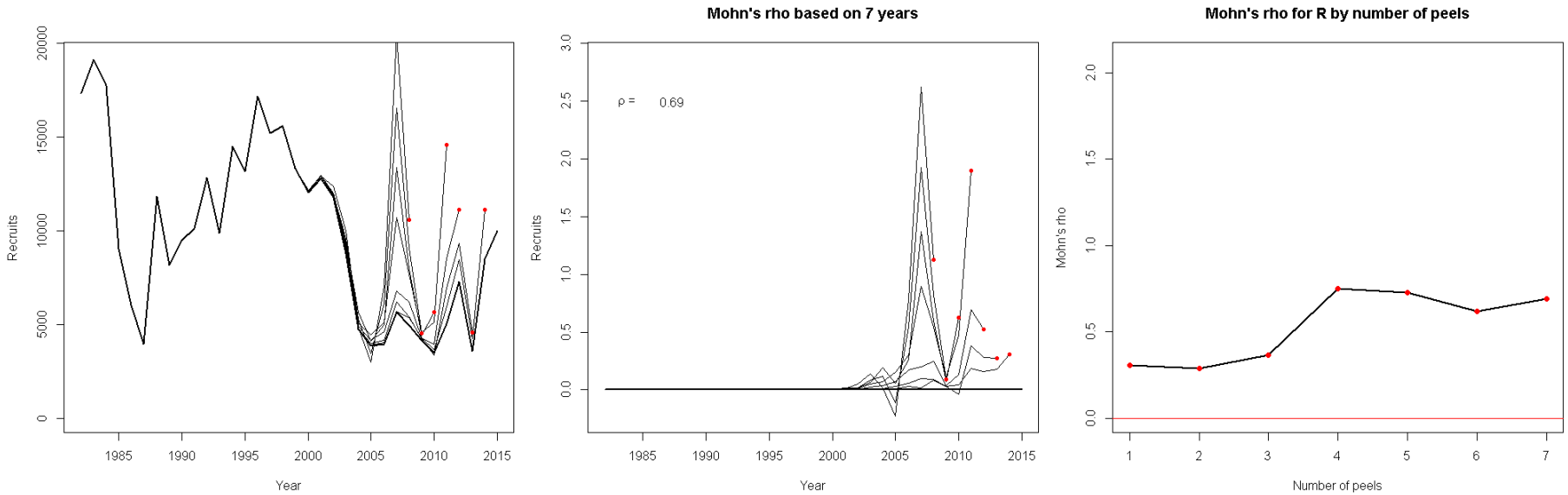

Figure B126. Retrospective analysis results of Age 3 recruitment (left), relative difference of Age 3 recruitment from the terminal year (middle), and Mohn's rho for each peel (right) from RUN A2, 1982 – 2015. Mohn's rho (average relative difference of 7 peels) is 0.693.

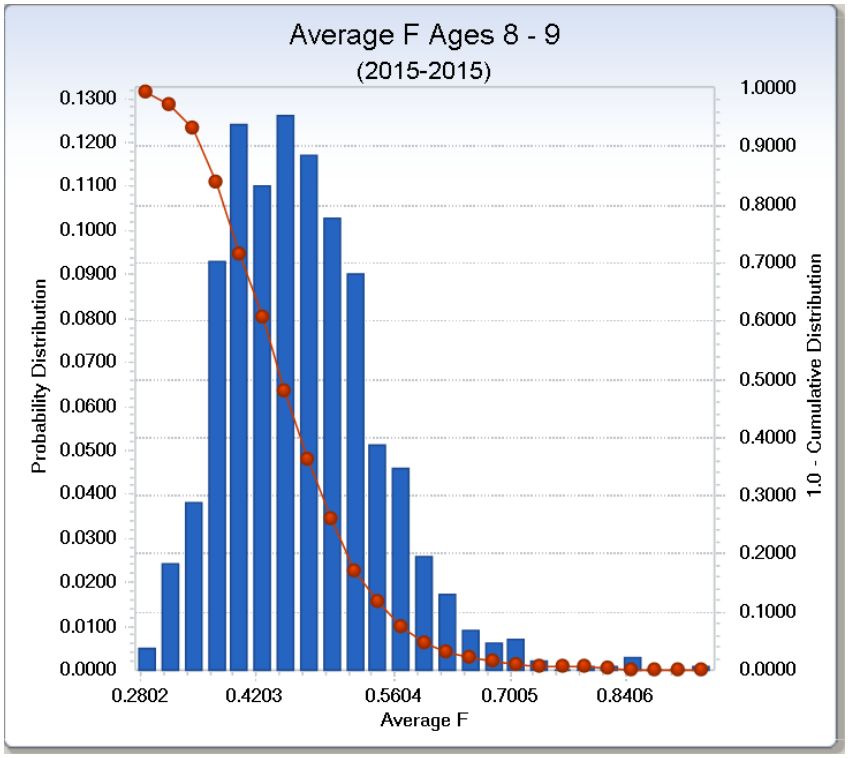

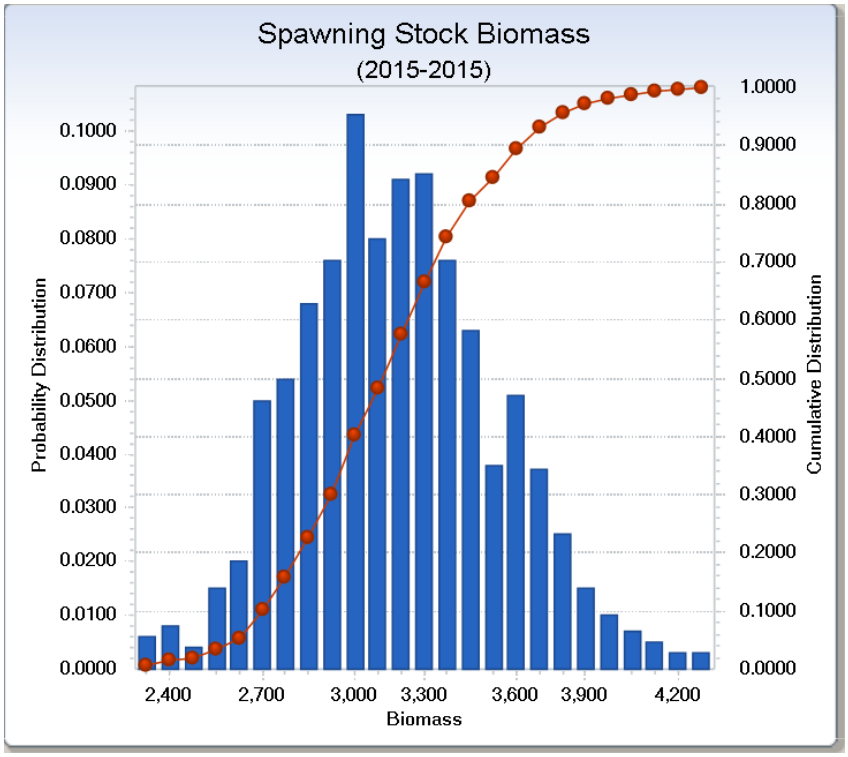

Figure B127. Precision estimates of fishing mortality (top) and spawning stock biomass (mt; bottom) in 2015 from RUN A2. Blue vertical bars display both the range of the bootstrap estimates and the probability of the individual values in the range.

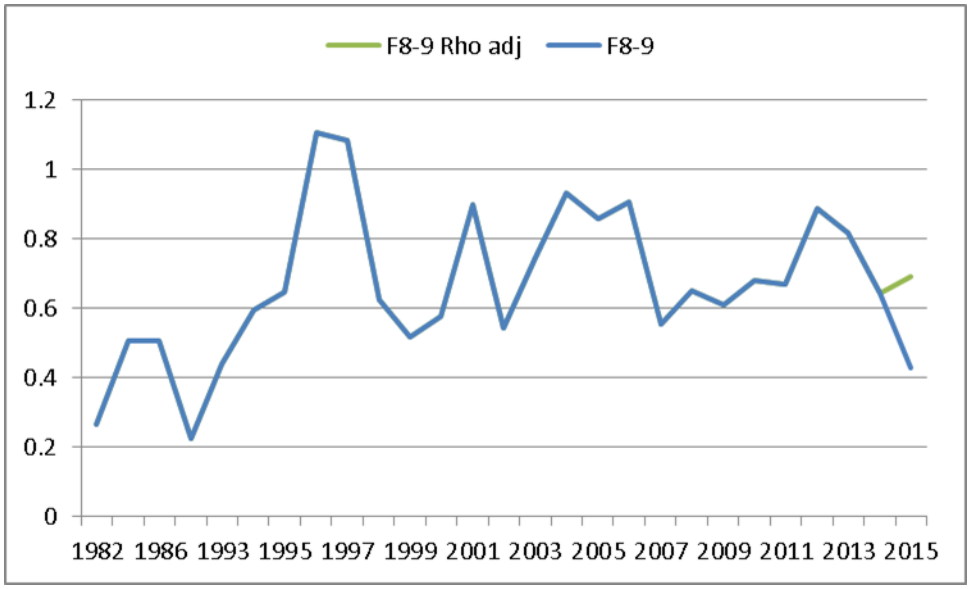

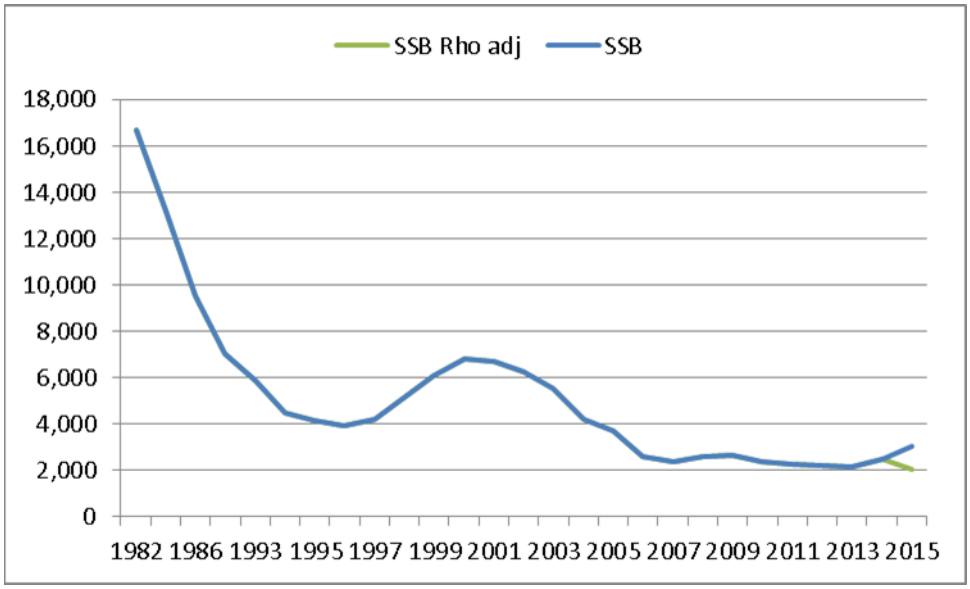

Figure B128 .Trends of witch flounder fishing mortality (top, blue line), and spawning stock biomass (bottom, blue line, mt), with a retrospectively adjusted 2015 values (green line); 1982 – 2015 year classes from RUN A2,1982 -2015.

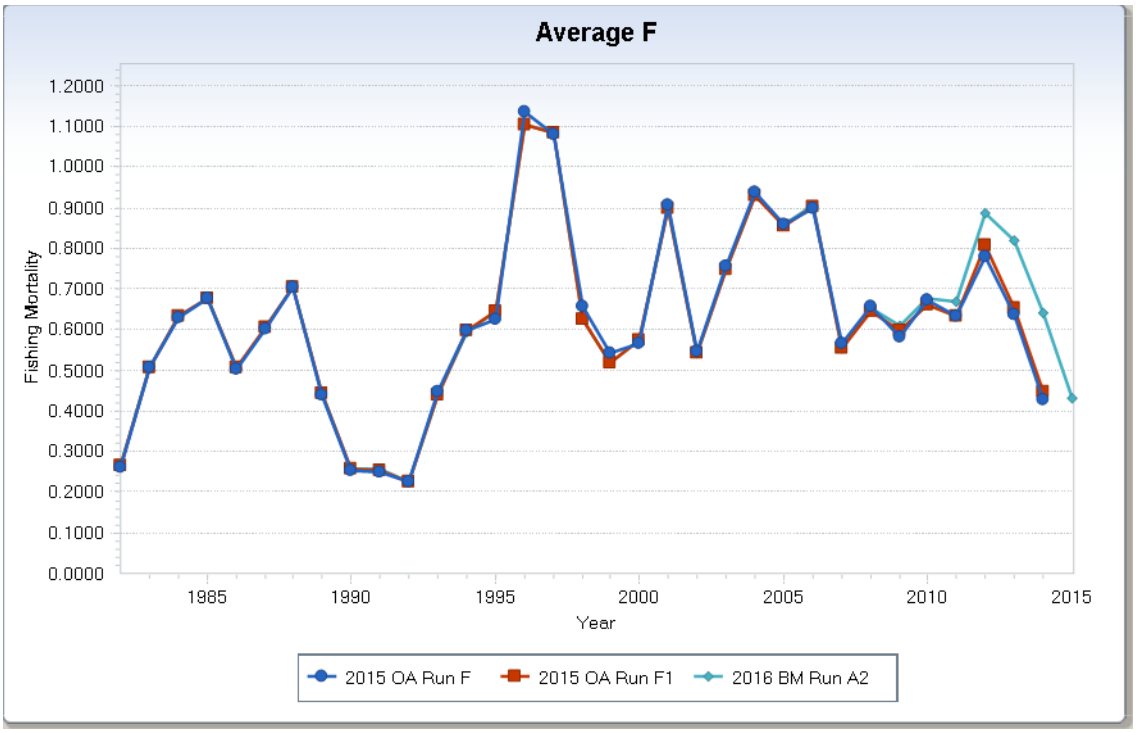

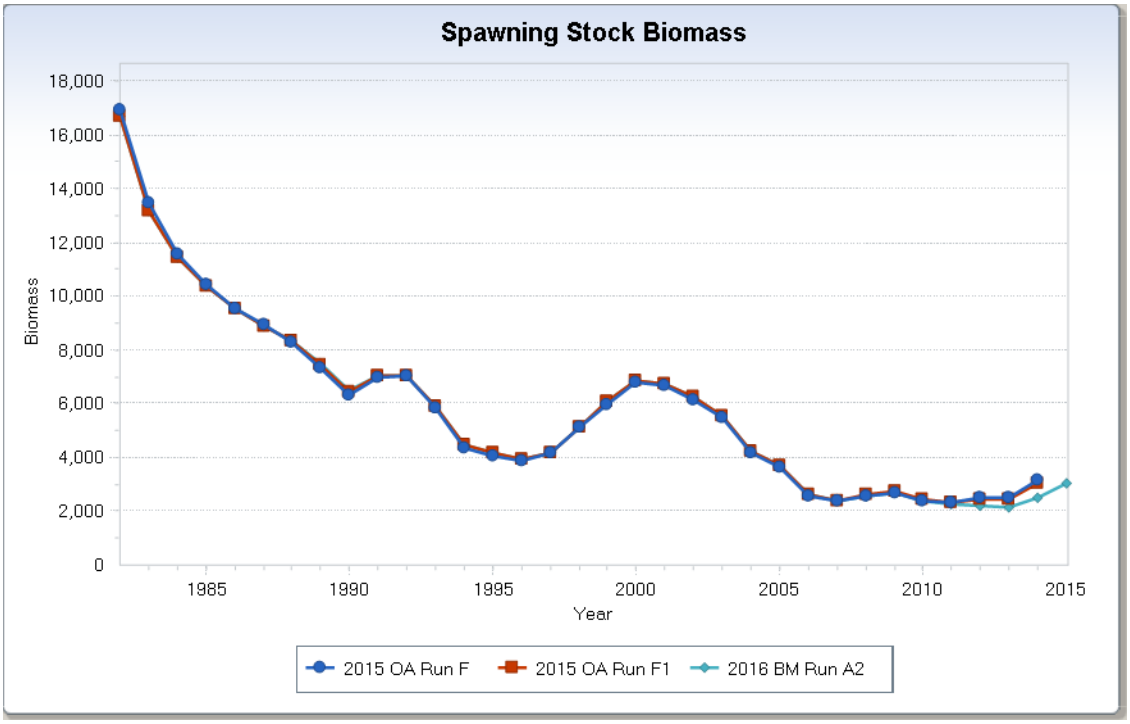

Figure B129. Comparison of trends in average fishing mortality (top), spawning stock biomass (middle),from the 2015 Operational Assessment (OA) RUN F (blue line with circles), 2015 OA with revised catch at age (RUN F1; red line with squares), and the 2016 benchmark (BM) RUN A2 (catch at age through 2015; cyan, small circles).

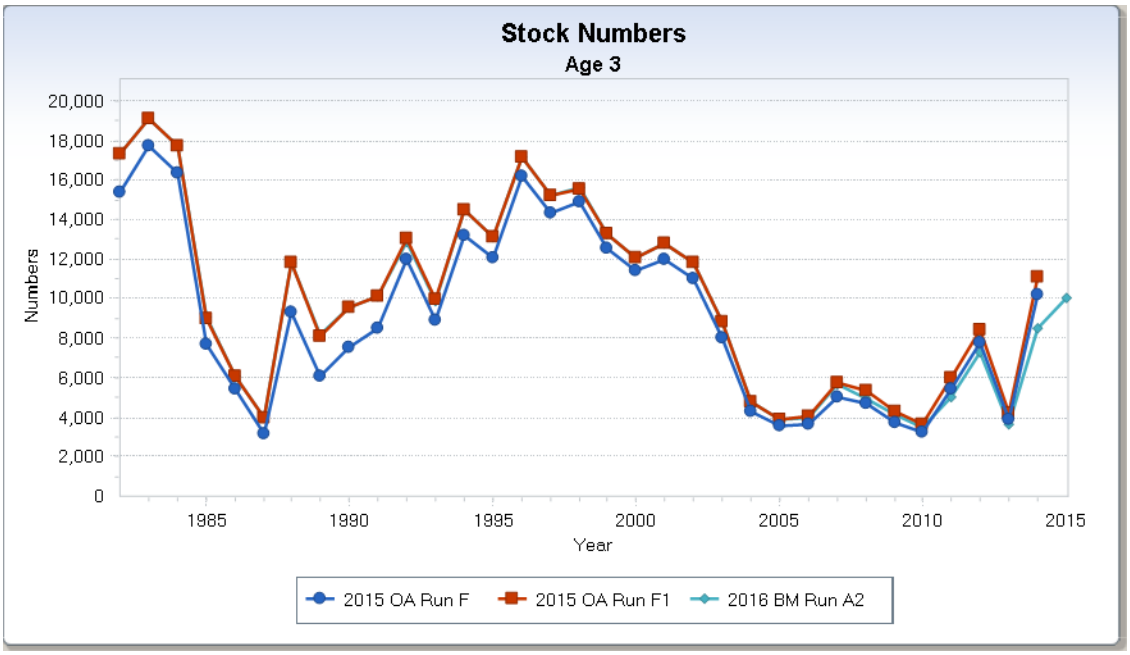

Figure B129 continued. Comparison of Age 3 recruits from the 2015 Operational Assessment (OA) RUN F (blue line with circles), 2015 OA with revised catch at age (RUN F1; red line with squares), and the 2016 benchmark (BM) RUN A2 (catch at age through 2015; cyan, small circles).

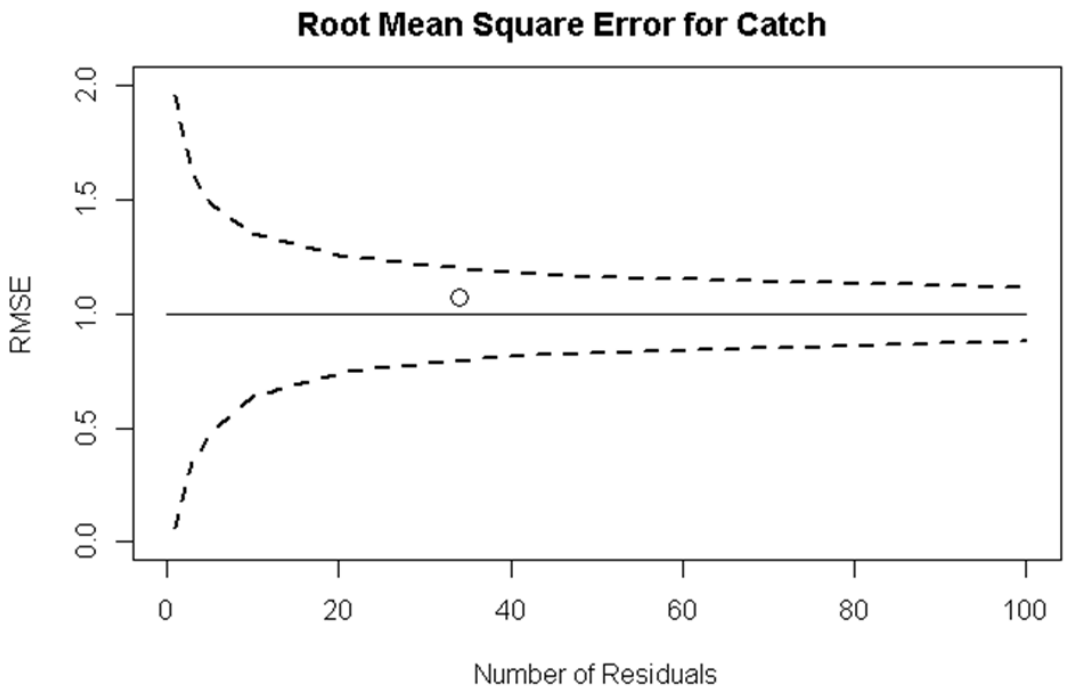

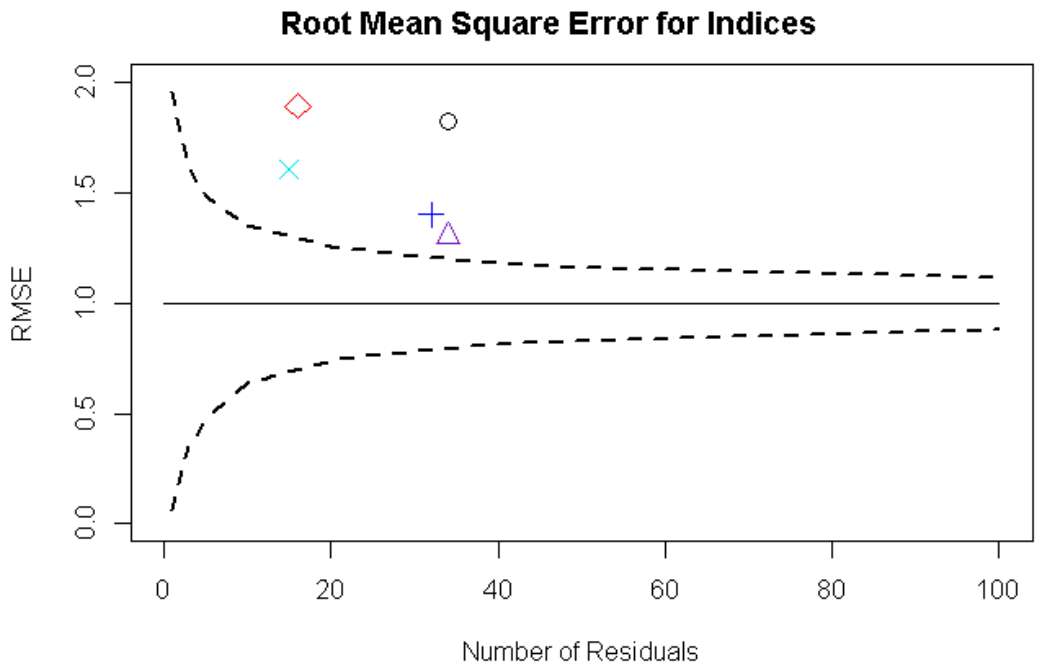

Figure B130. ASAP Run 9_5_v2 model fit root mean square error (RMSE) values for total catch (left) and survey indices (right) as a function of the number of residuals. The median and 80% confidence interval of the root mean square error from a normal distribution with mean zero and standard deviation one for a range of sample sizes is overlaid for reference.

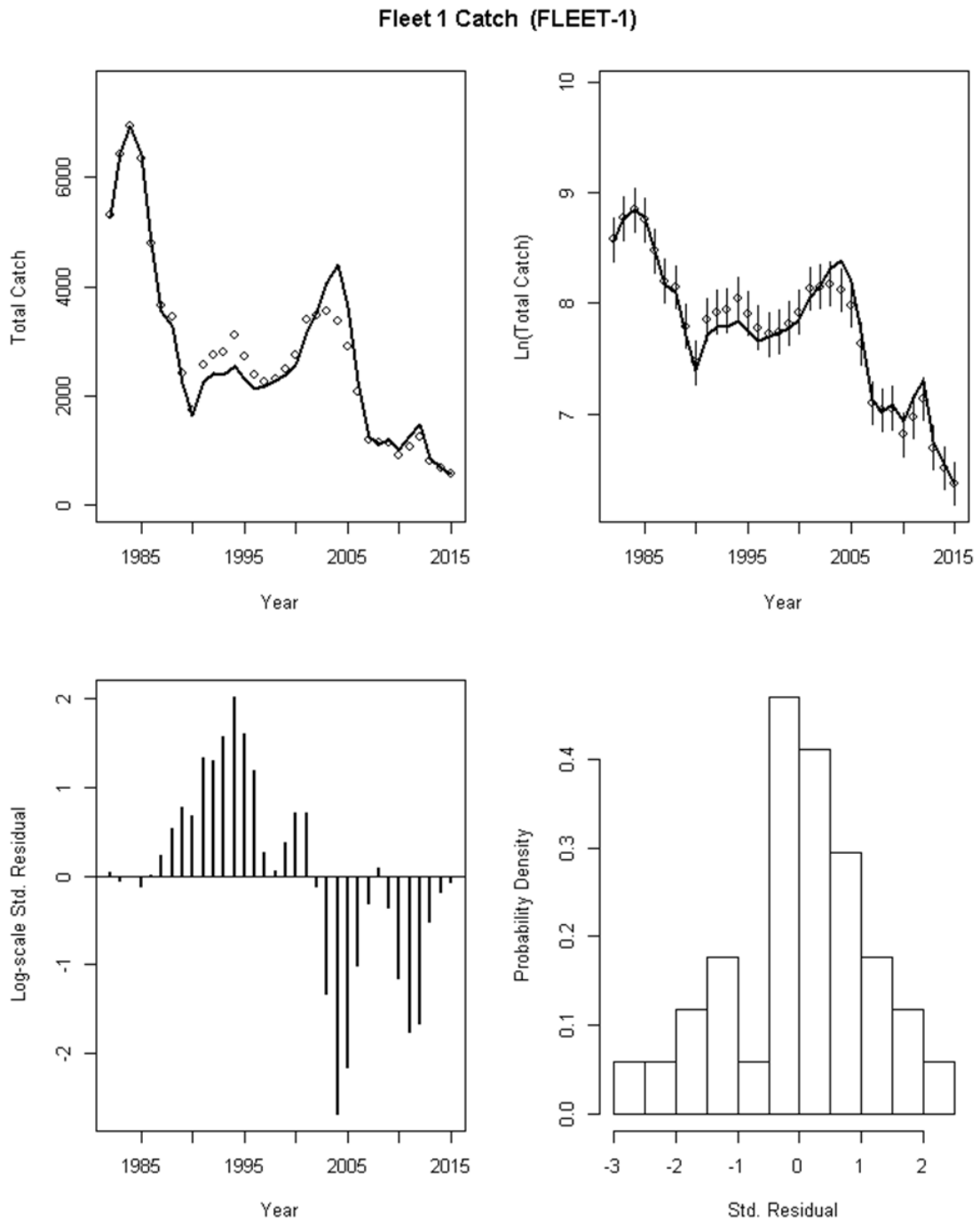

Figure B131. ASAP Run 9_5_v2 model fit to the total witch flounder catch (Fleet 1).

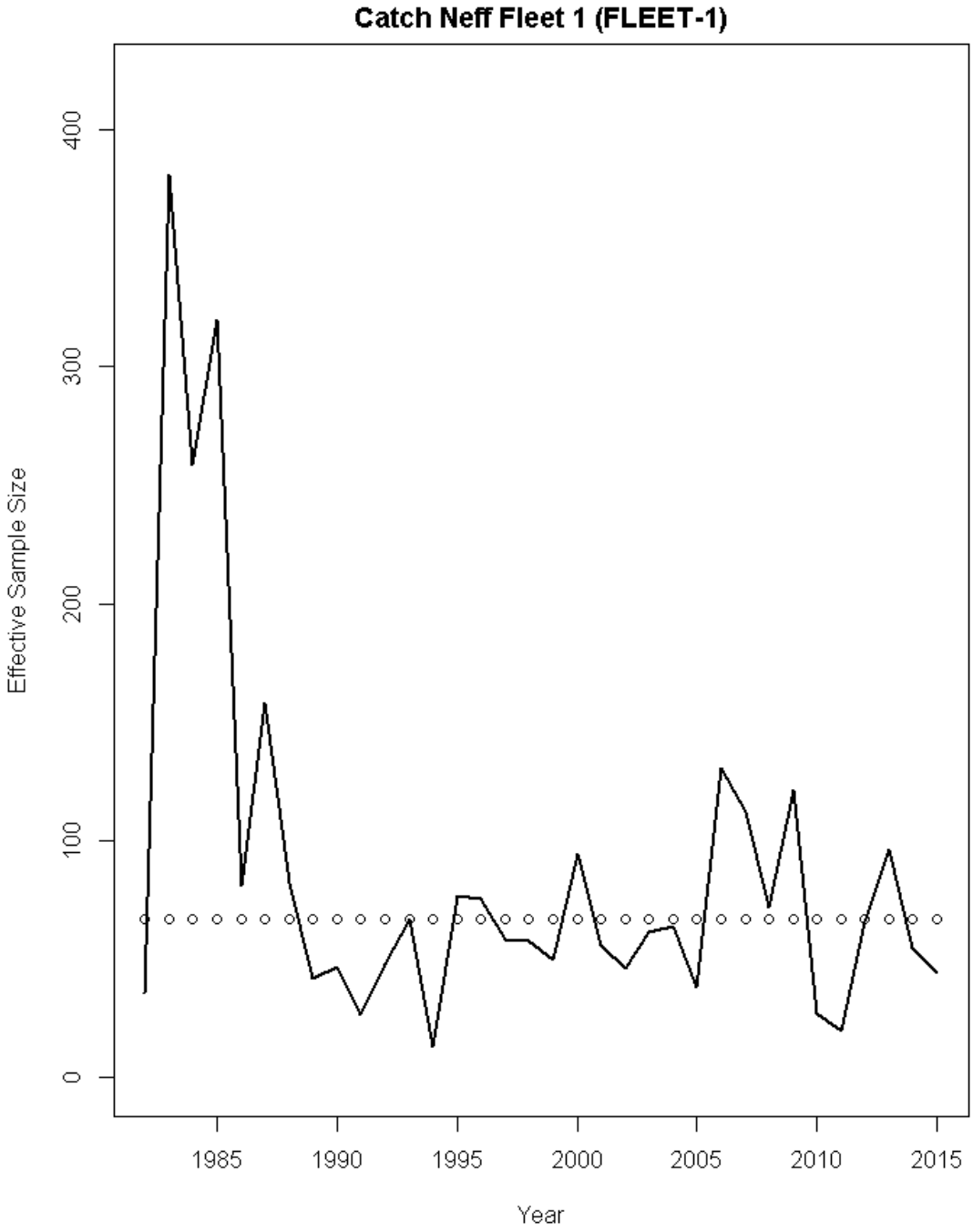

Figure B.132. ASAP Run 9_5_v2 model comparison of input effective sample size vs model estimated effective sample size for witch flounder catch (Fleet 1).

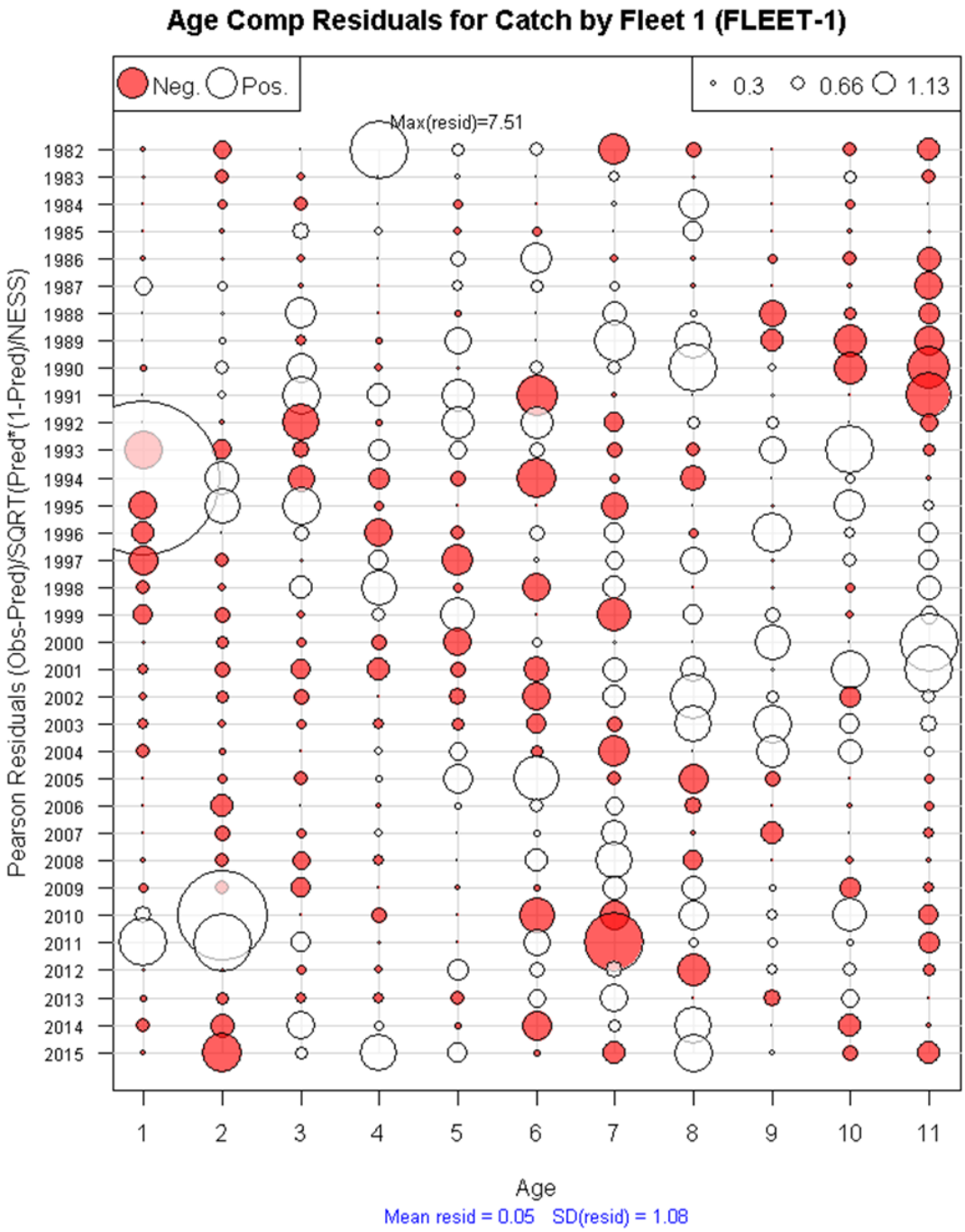

Figure B133. ASAP Run 9_5_v2 model fit residuals for the witch flounder catch (Fleet 1) at age.

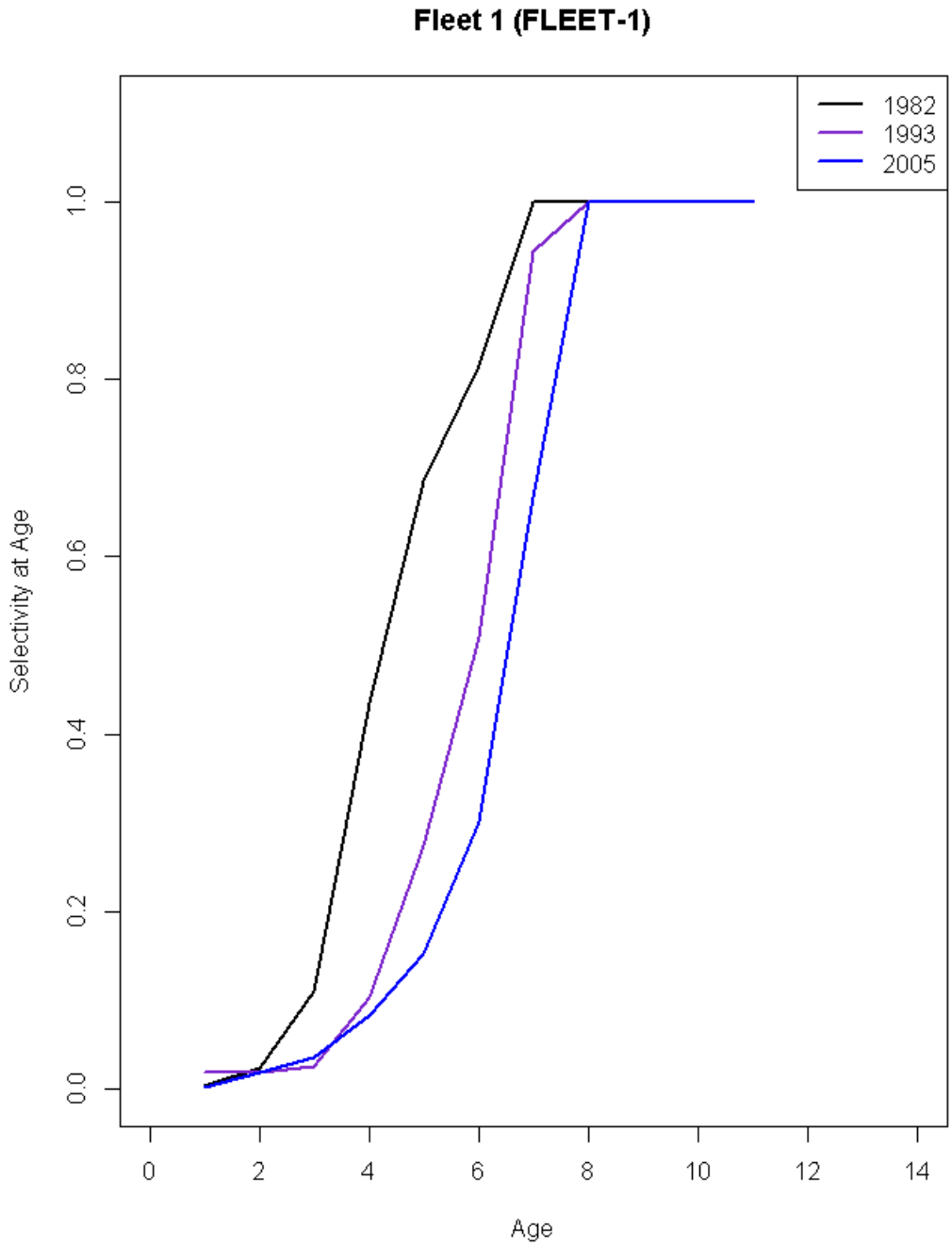

Figure B134. Witch flounder catch (Fleet 1) selectivity at age for block 1 (1982-1992), block 2 (1993-2004) and block 3 (2005-2015) as estimated by the ASAP Run 9_5_v2.

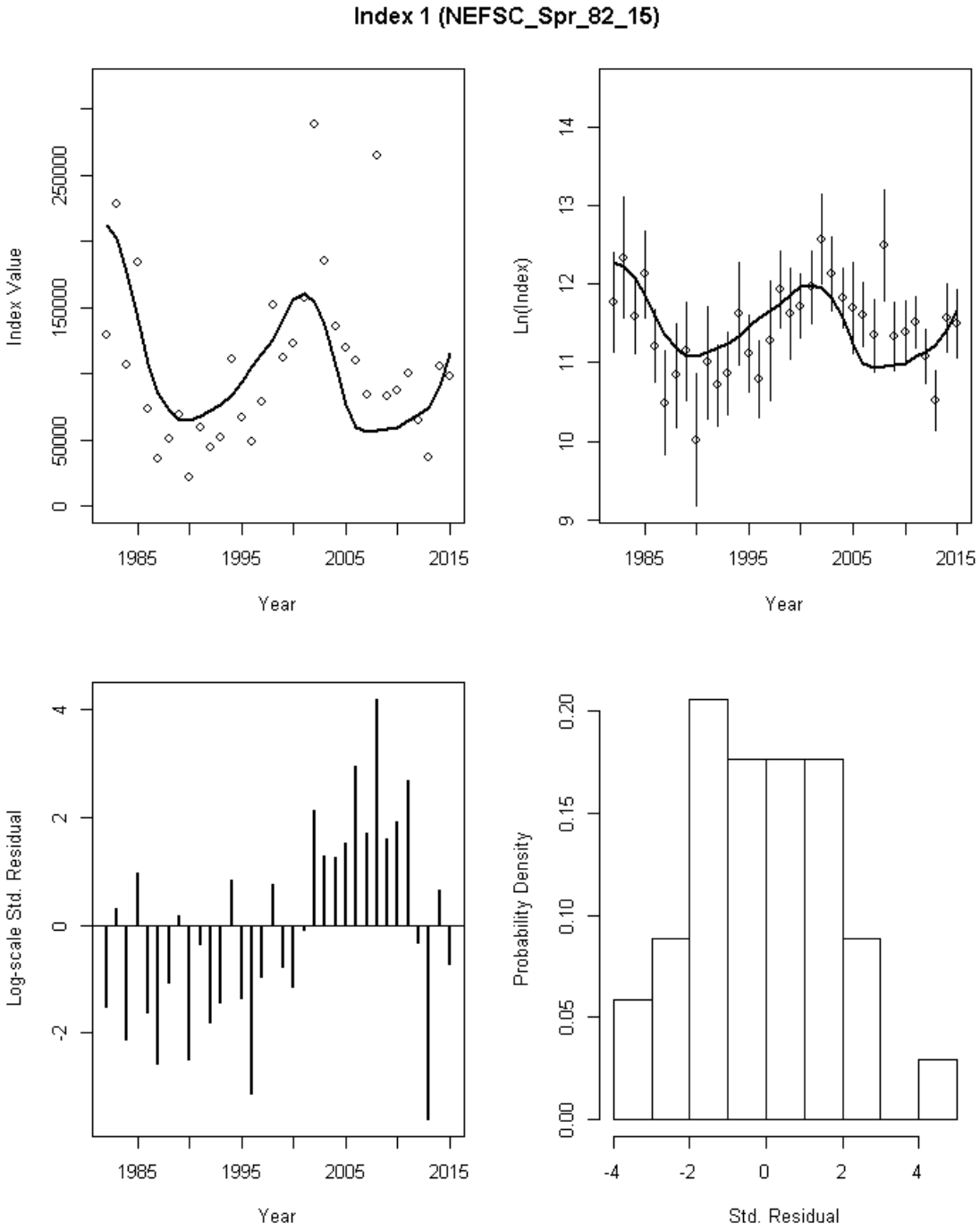

Figure B135. ASAP Run 9_5_v2 mode fit to the Northeast Fisheries Science Center spring survey witch flounder index (Index 1).

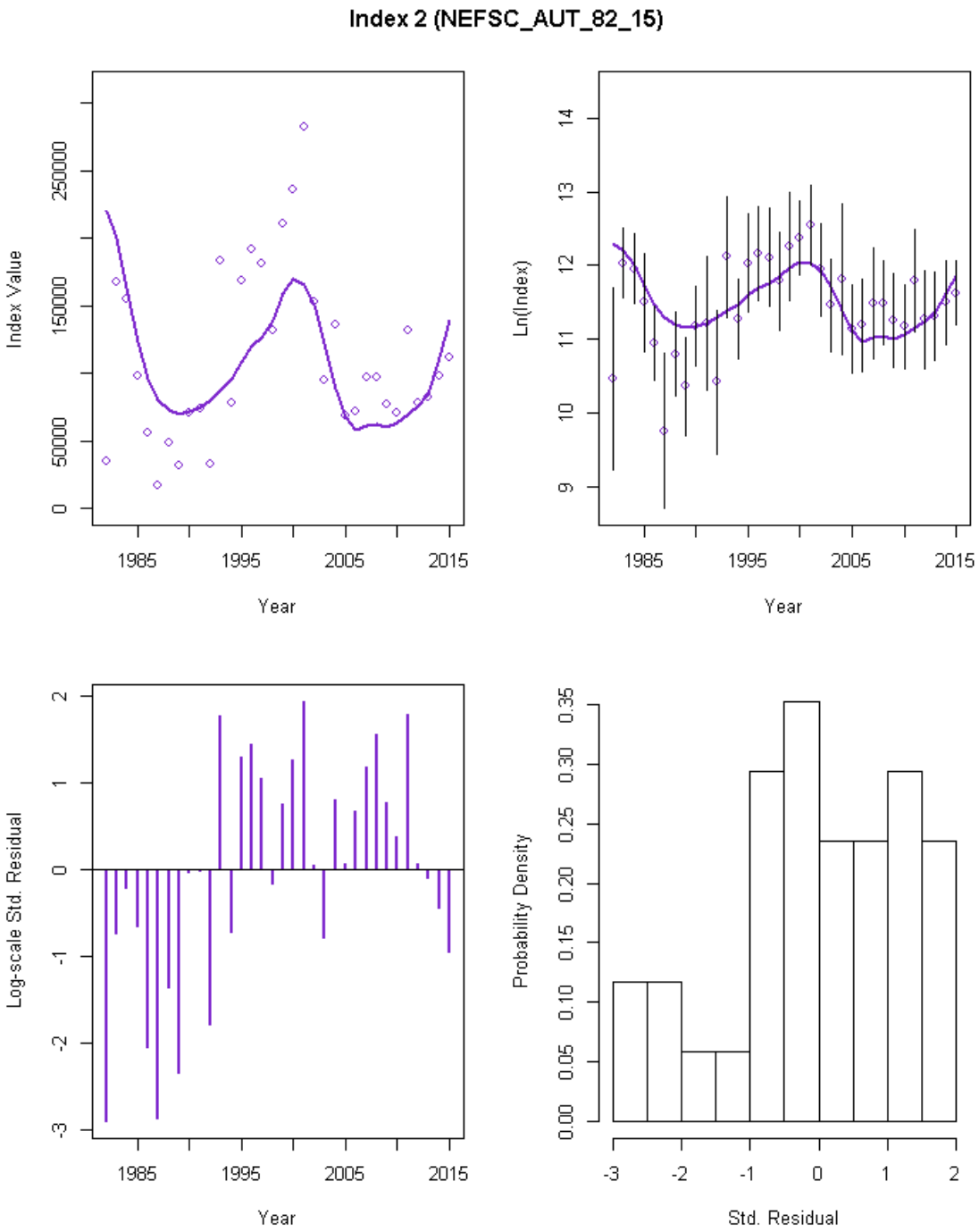

Figure B136. ASAP Run 9_5_v2 mode fit to the Northeast Fisheries Science Center autumn survey witch flounder index (Index 2).

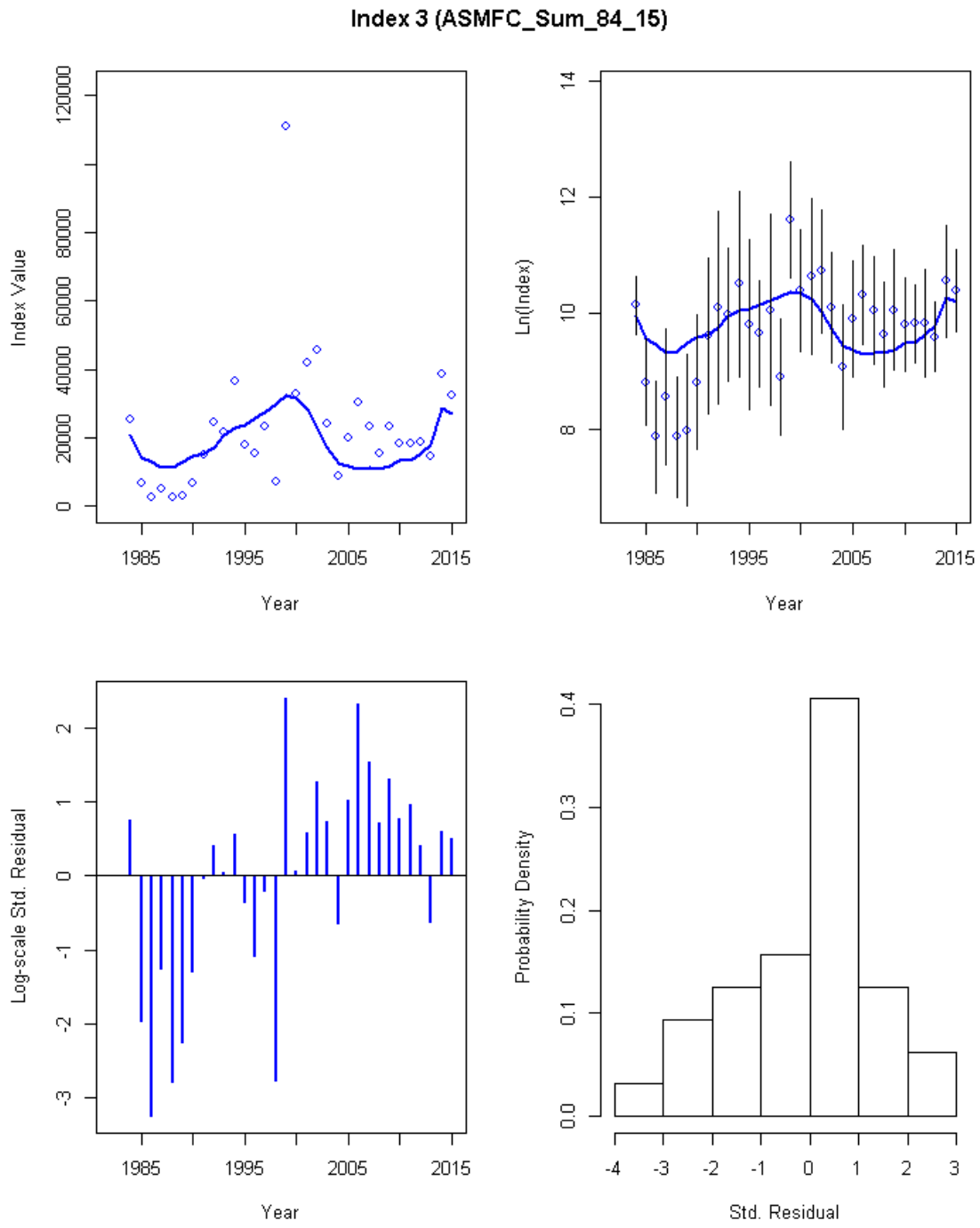

Figure B137. ASAP Run 9_5_v2 mode fit to the Atlantic States Marine Fisheries Commission summer survey witch flounder index (Index 3).

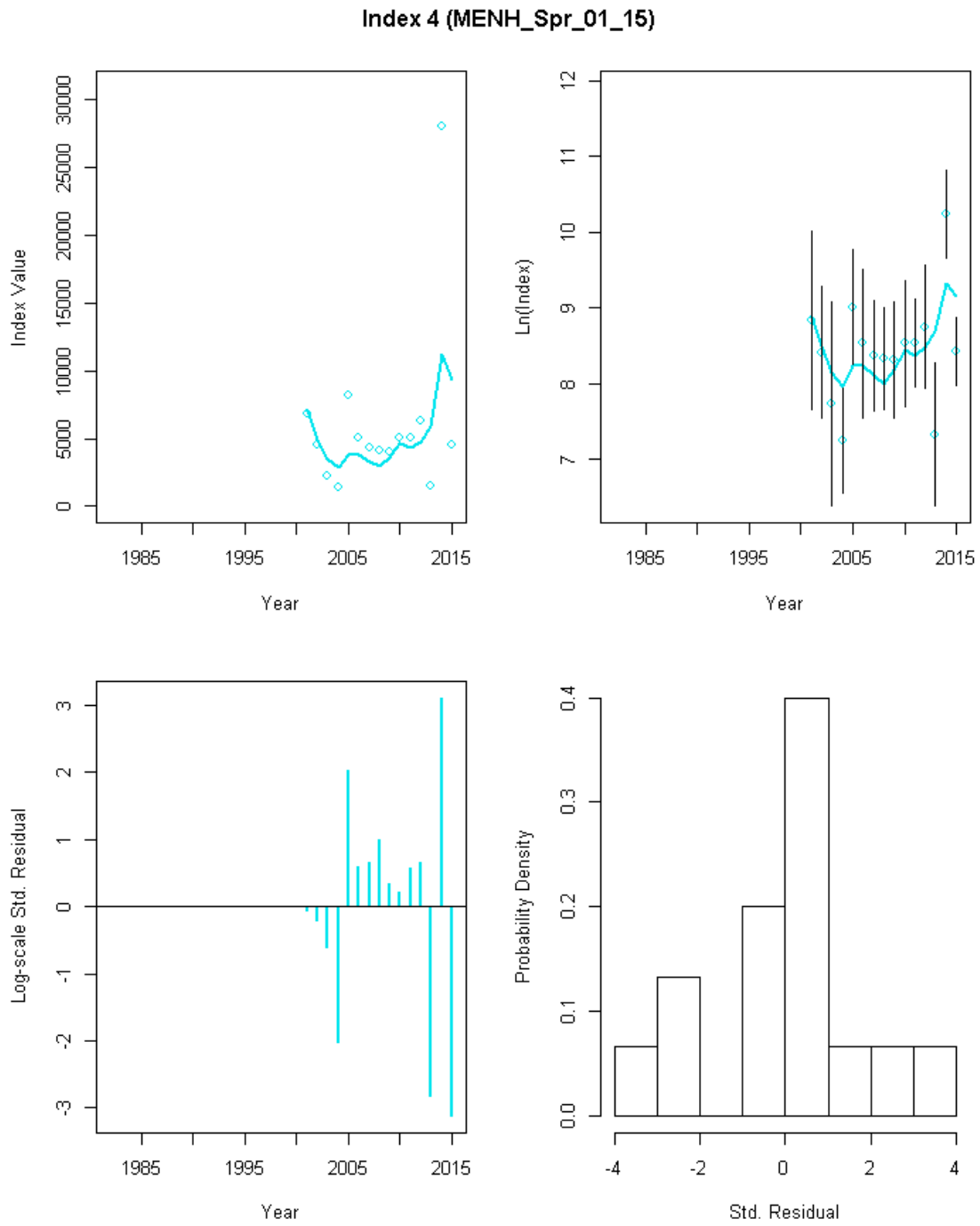

Figure B138. ASAP Run 9_5_v2 mode fit to the Maine-New Hampshire spring survey witch flounder index (Index 4).

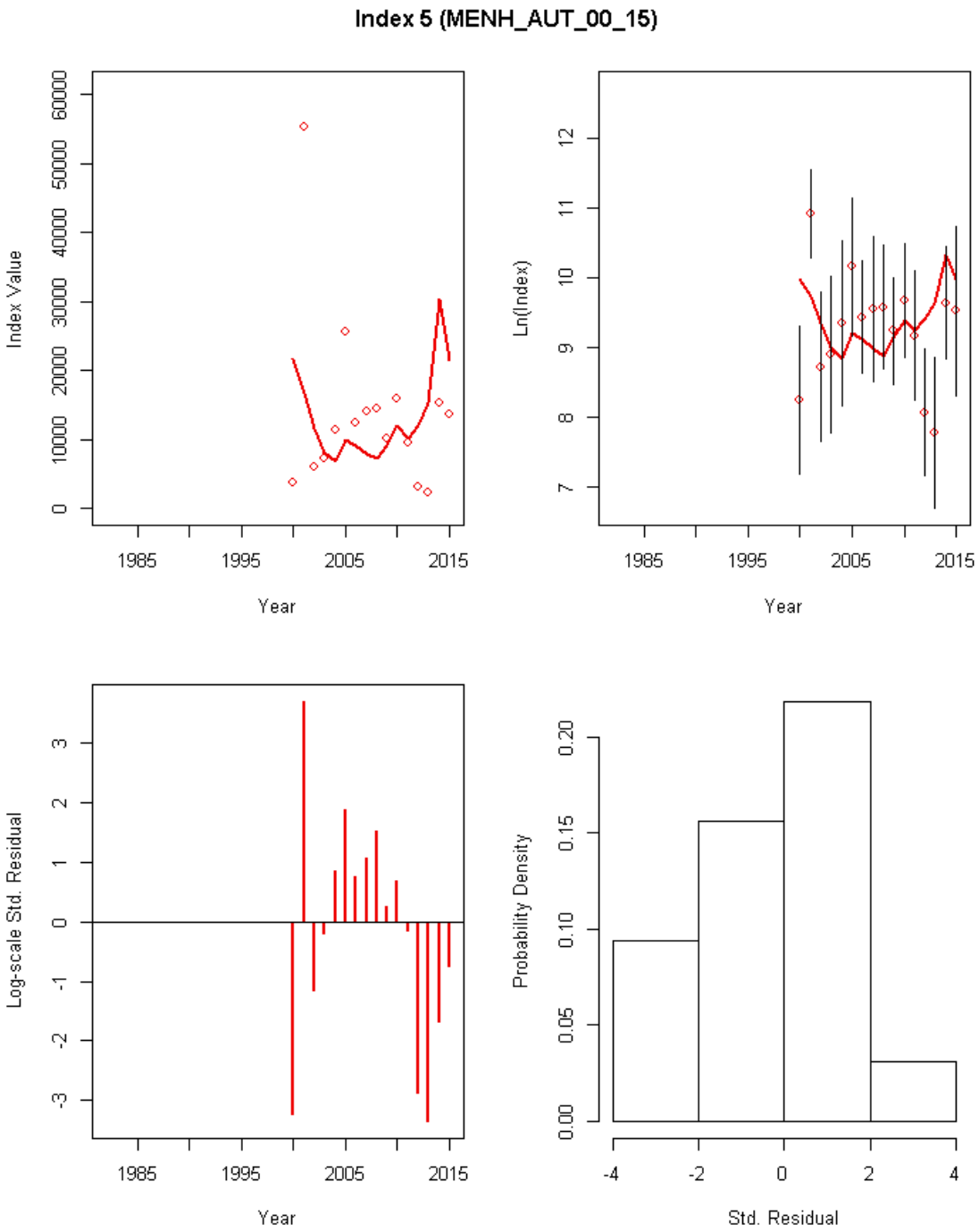

Figure B139. ASAP Run 9_5_v2 model fit to the Maine-New Hampshire autumn survey witch flounder index (Index 5).

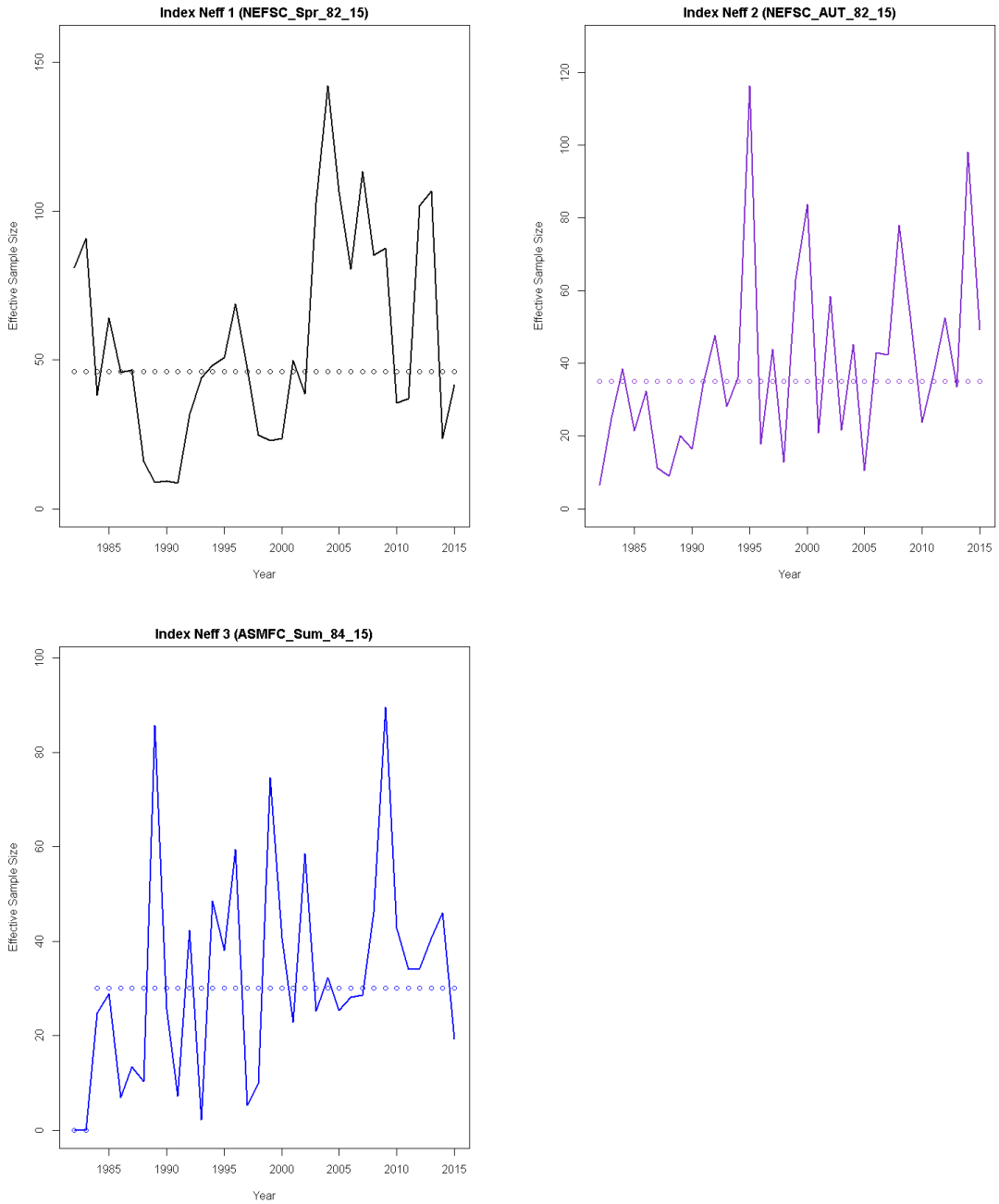

Figure B140. ASAP Run 9_5_v2 model comparison of input effective sample size vs model estimated effective sample size for Northeast Fisheries Science Center spring survey (Index 1) and autumn survey (Index 2), and Atlantic States Marine Fisheries Commission summer survey (Index 3).

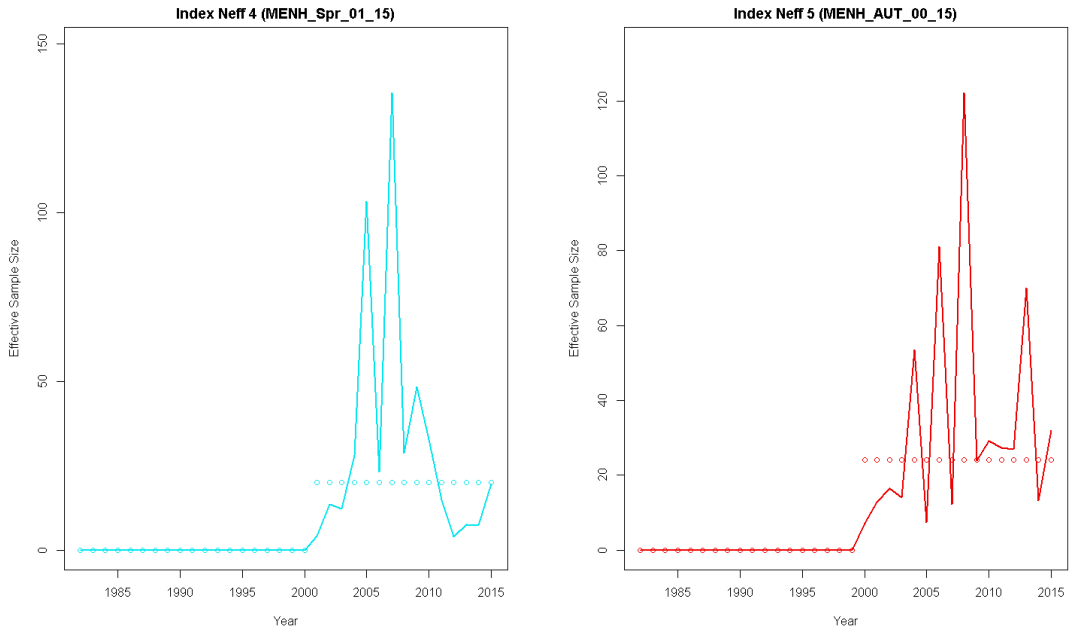

Figure B140, continued. ASAP Run 9_5_v2 model comparison of input effective sample size vs model estimated effective sample size for Maine-New Hampshire spring survey (Index 4) and autumn survey (Index 5).

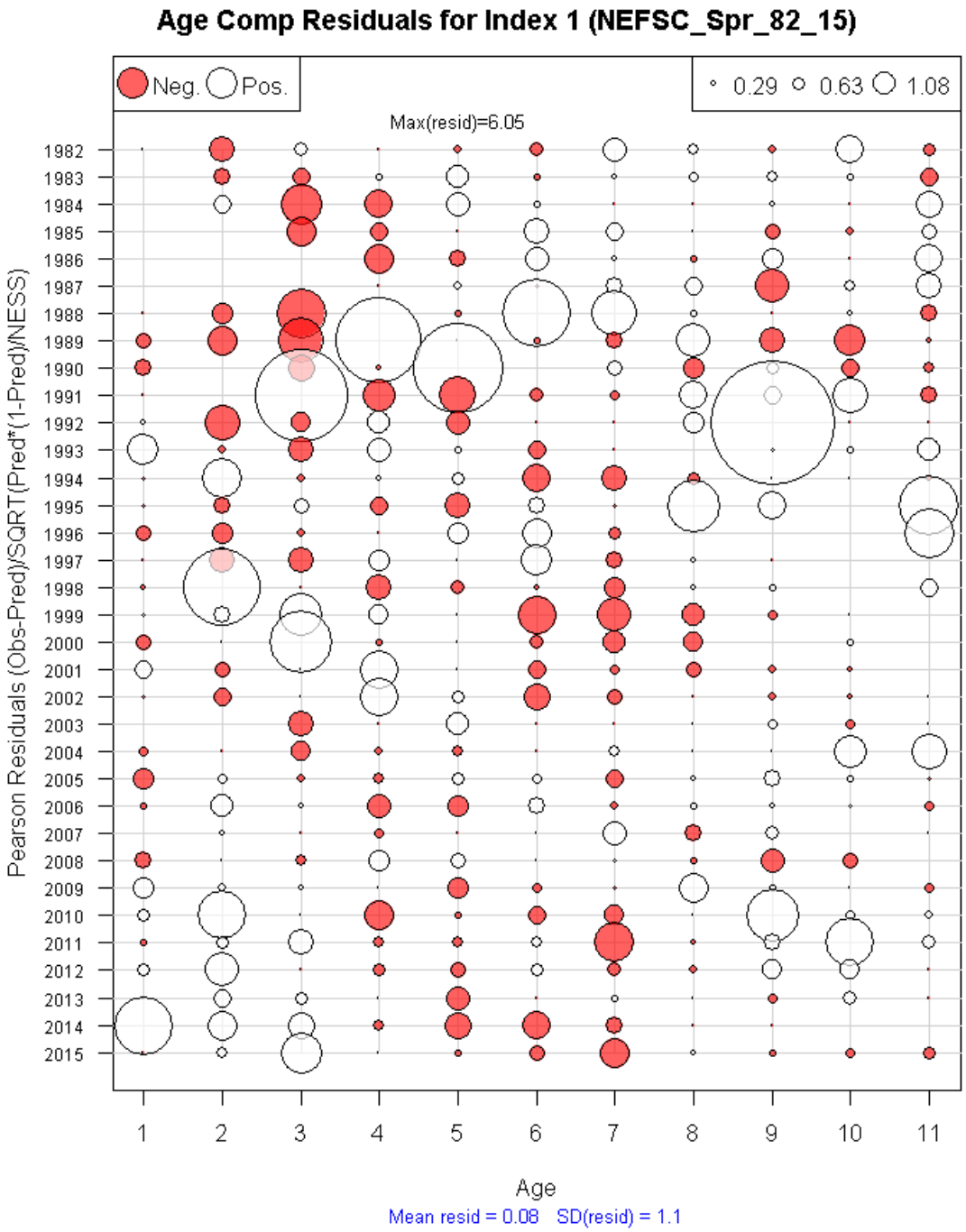

Figure B141. ASAP Run 9_5_v2 model fit residuals for the Northeast Fisheries Science Center spring survey witch flounder indices at age (Index 1).

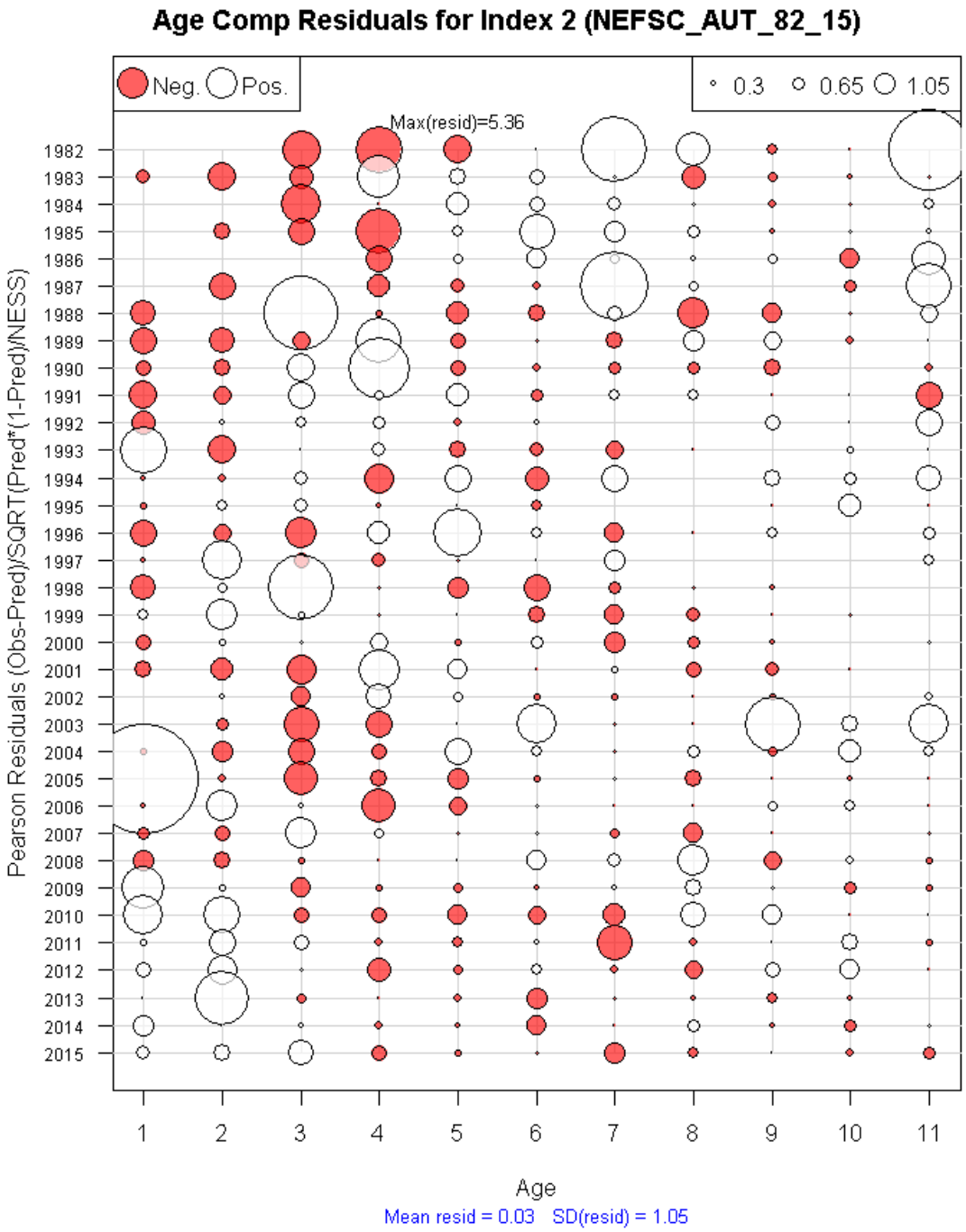

Figure B142. ASAP Run 9_5_v2 model fit residuals for the Northeast Fisheries Science Center autumn survey witch flounder indices at age (Index 2).

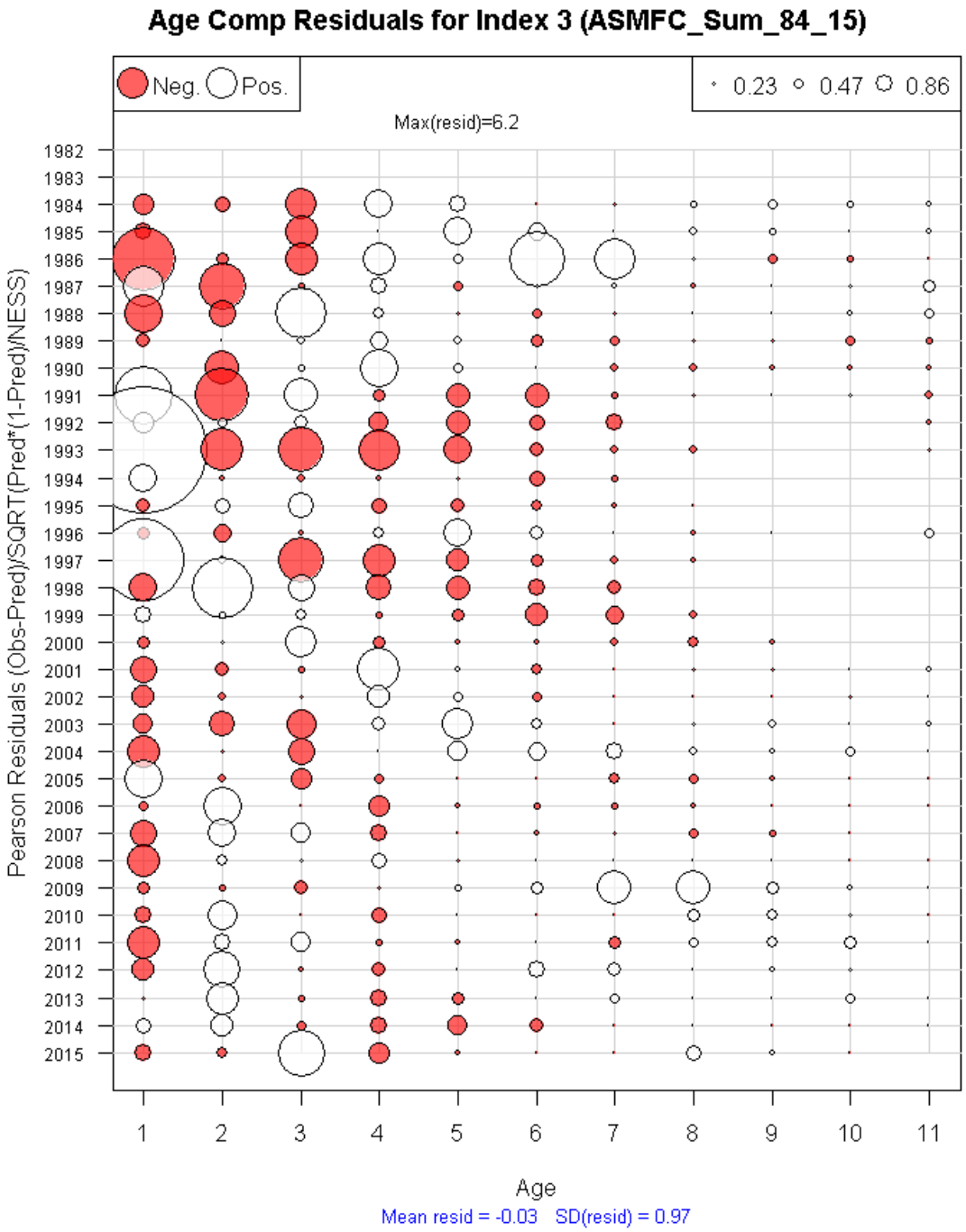

Figure B143. ASAP Run 9_5_v2 model fit residuals for the Atlantic States Marine Fisheries Commission summer survey witch flounder indices at age (Index 3).

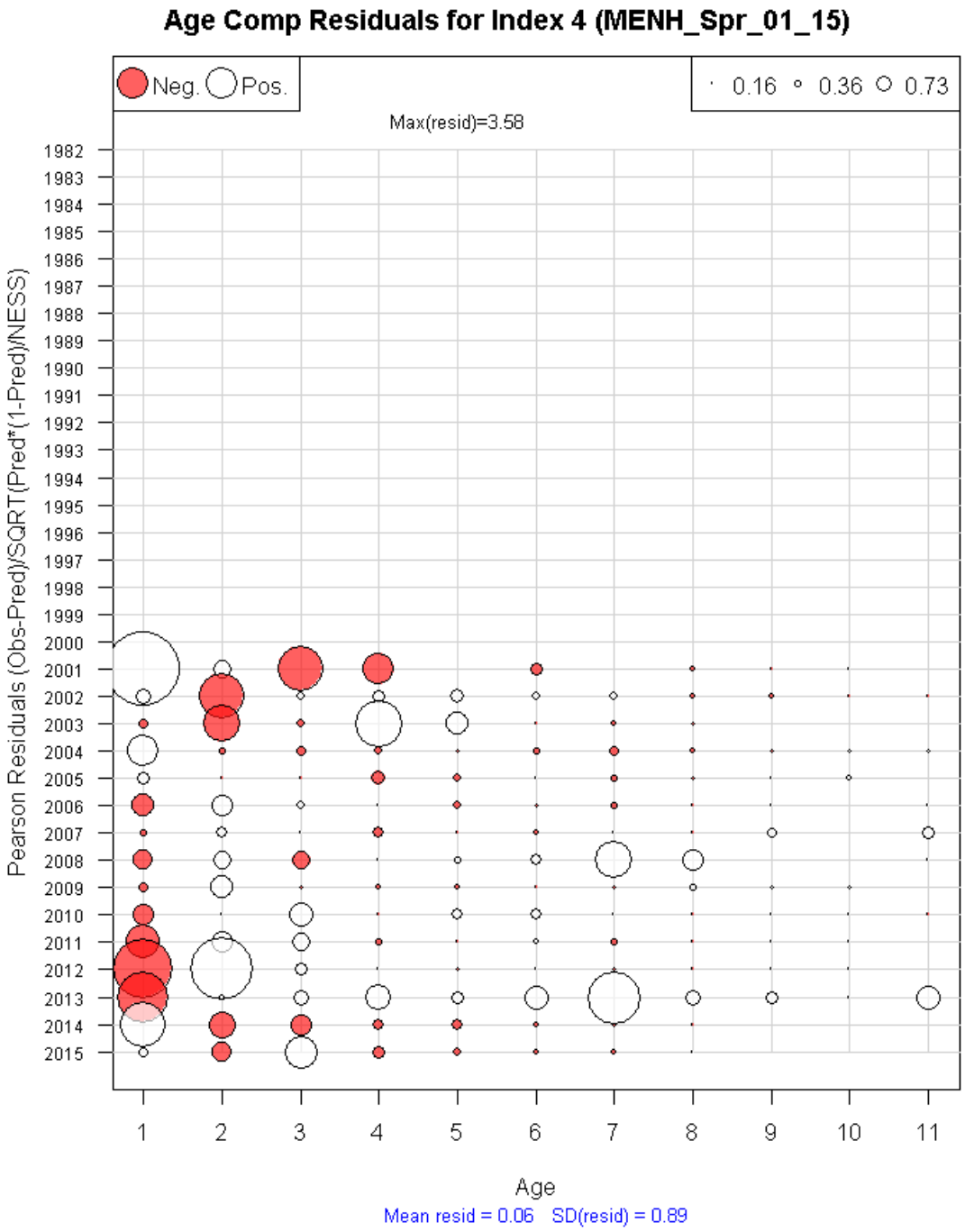

Figure B144. ASAP Run 9_5_v2 model fit residuals for the Maine-New Hampshire spring survey witch flounder indices at age (Index 4).

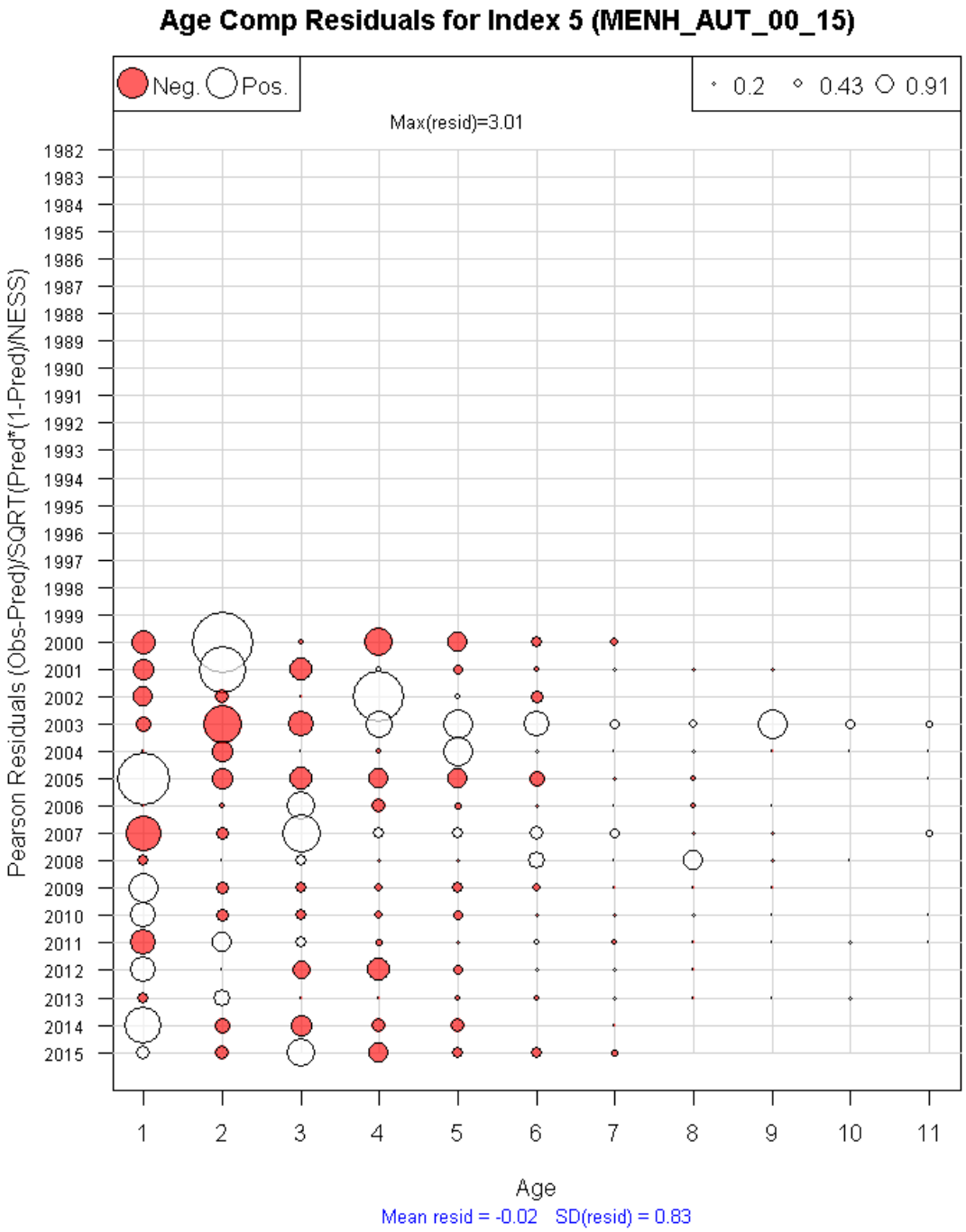

Figure B145. ASAP Run 9_5_v2 model fit residuals for the Maine-New Hampshire autumn survey witch flounder indices at age (Index 5).

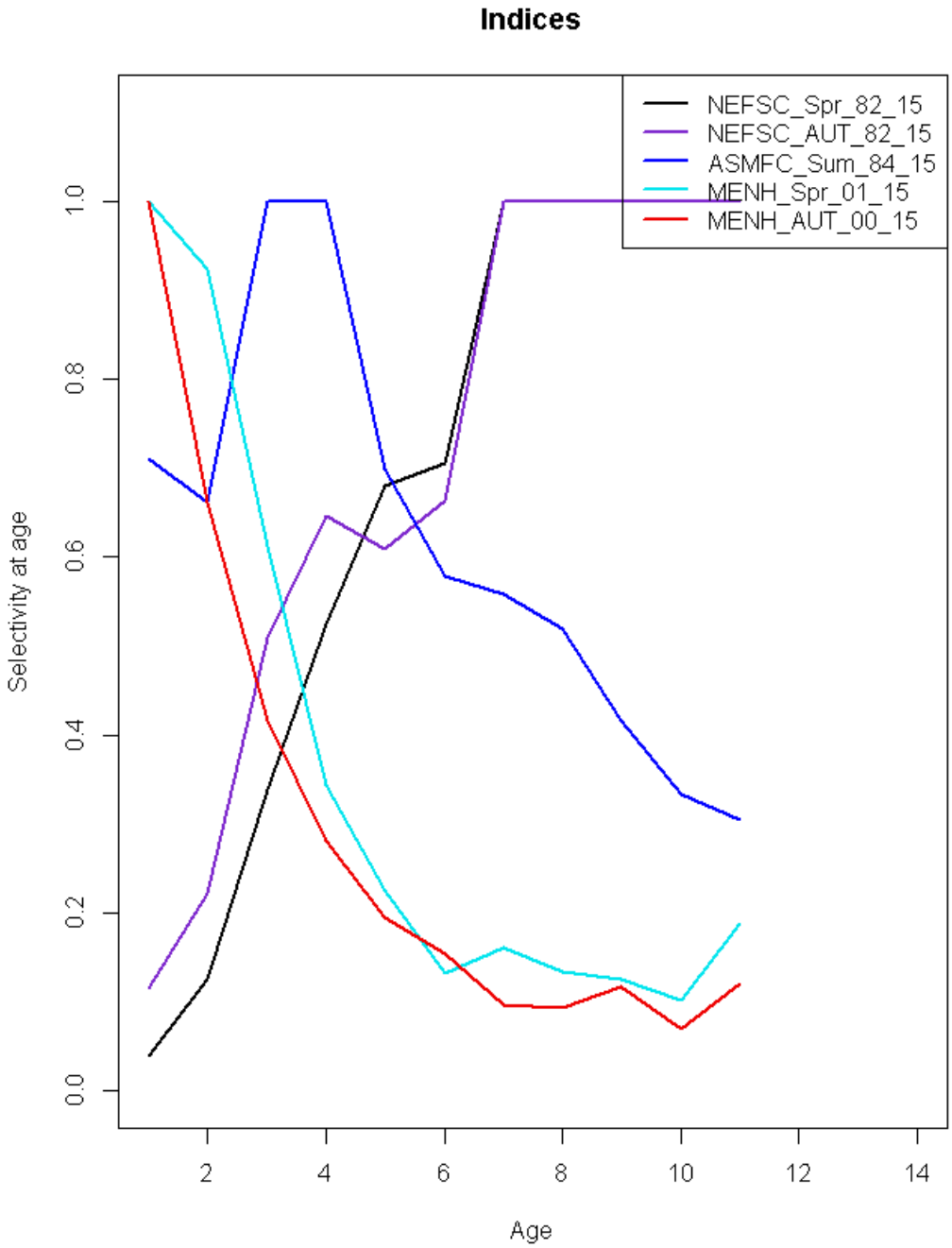

Figure B146. Witch flounder selectivity at age for the Northeast Fisheries Science Center spring (Index 1), autumn (Index 2), Atlantic States Marine Fisheries Commission (Index 3), Maine-New Hampshire spring (Index 4) and autumn (Index 5) surveys from ASAP Run 9_5_2v.

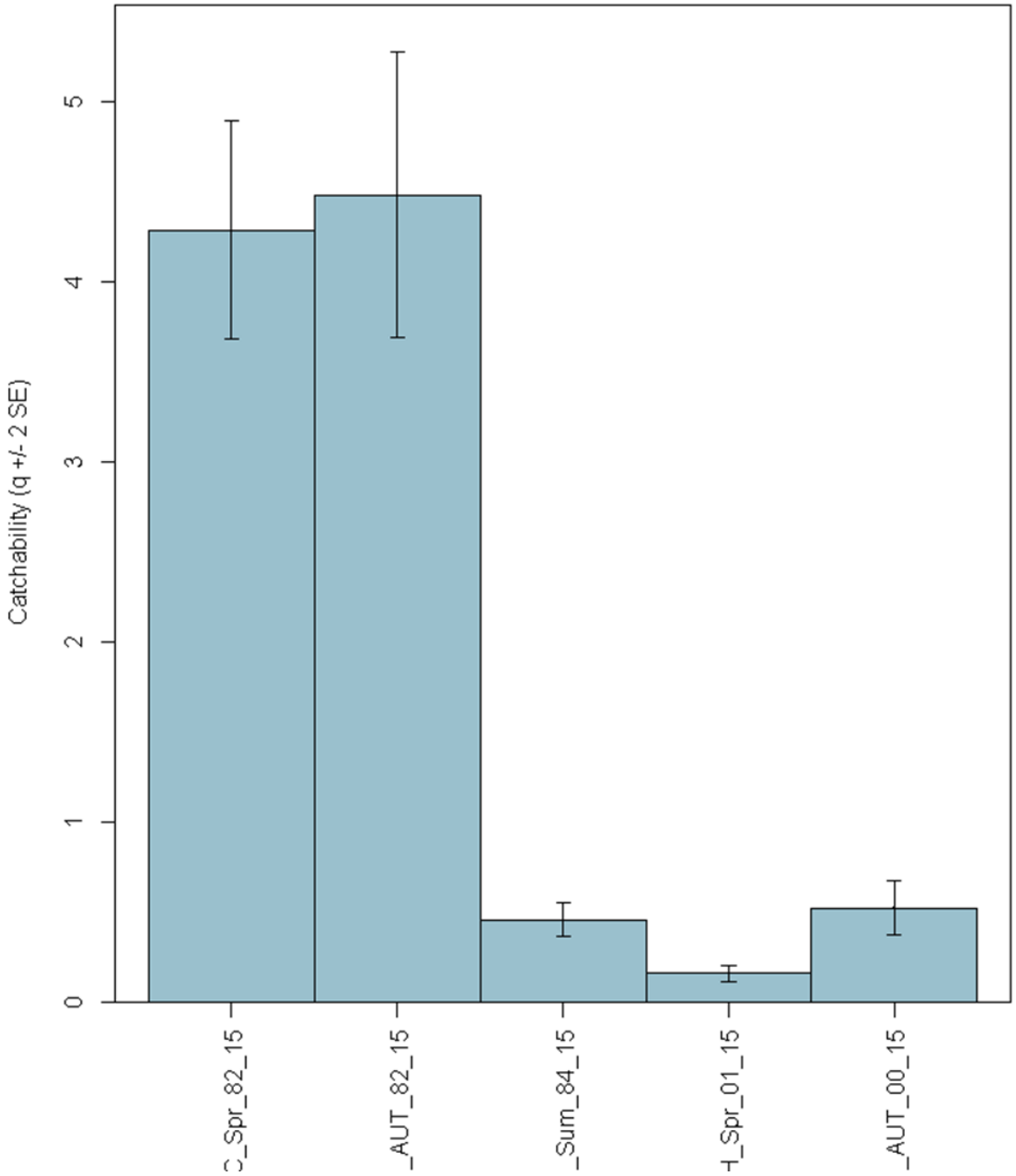

Figure B147. Witch flounder survey catchability, q, for the Northeast Fisheries Science Center spring (Index 1), autumn (Index 2), Atlantic States Marine Fisheries Commission (Index 3), Maine-New Hampshire spring (Index 4) and autumn (Index 5) surveys from ASAP Run 9_5_v2.

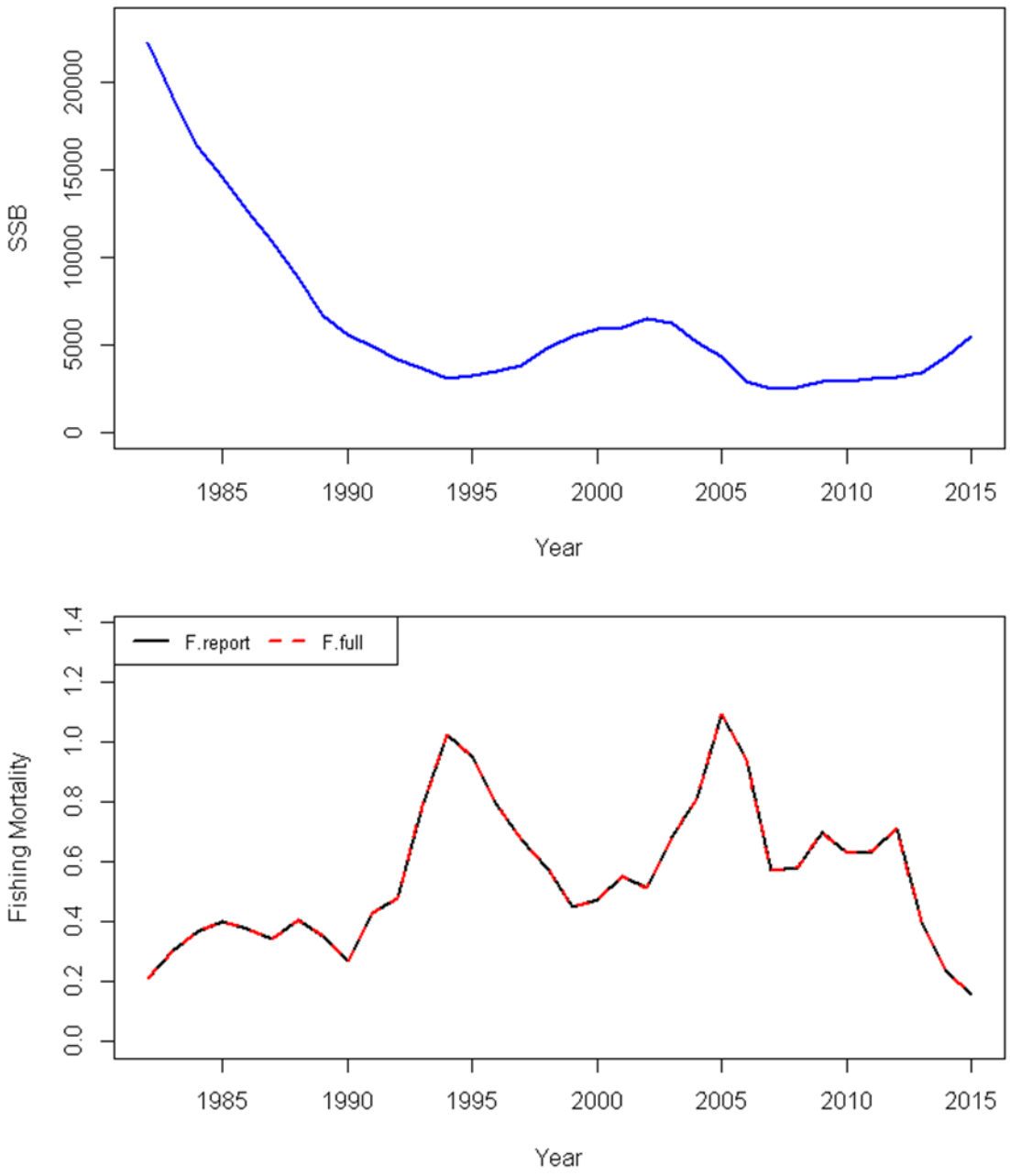

Figure B148. Trends in spawning stock biomass (top) and fishing mortality (bottom) estimates from ASAP Run 9_5_v2, 1982-2015.

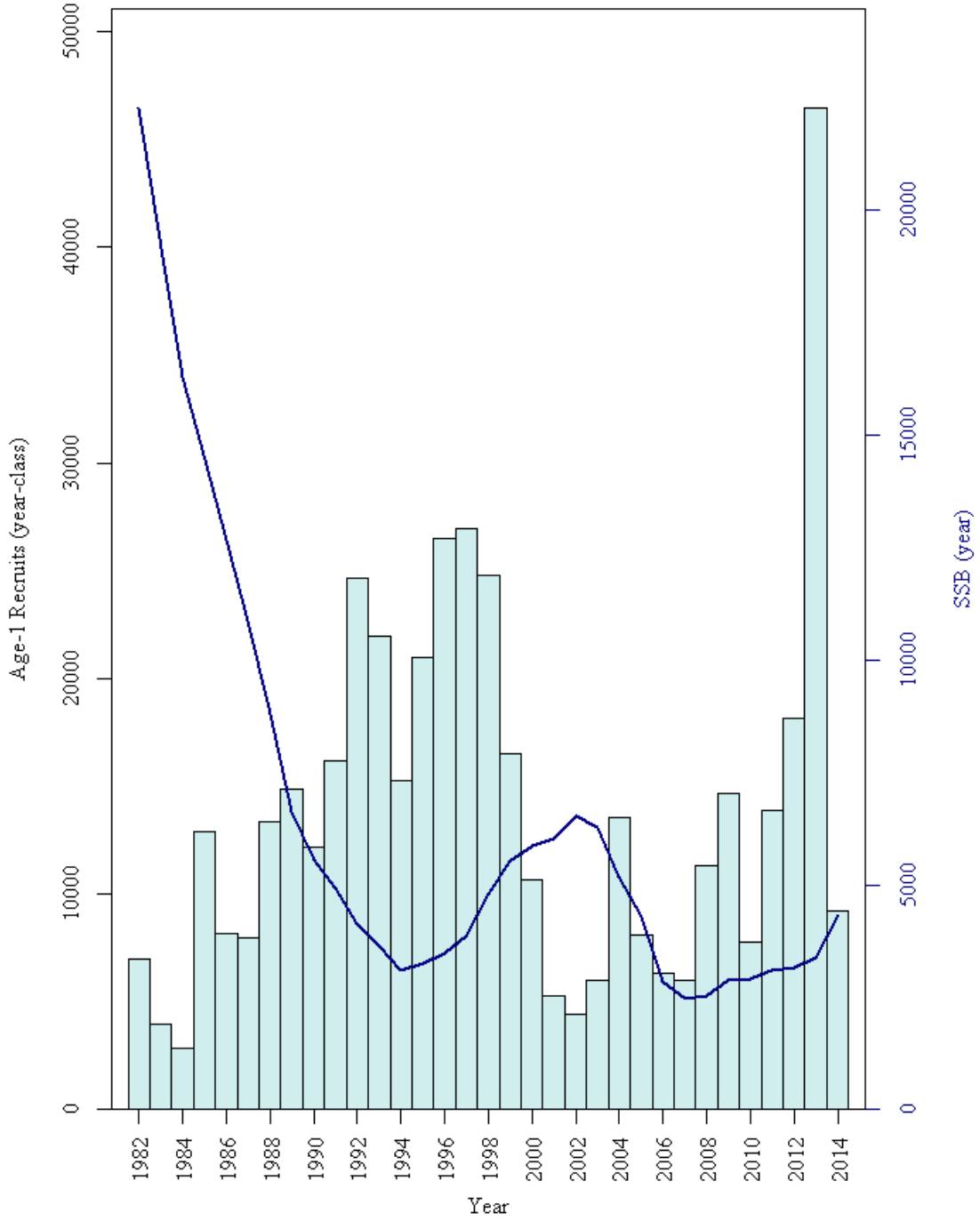

Figure B149. Trends in Age 1 recruitment year class (bars) and spawning stock biomass (mt; line) estimates from ASAP Run 9_5_v2.

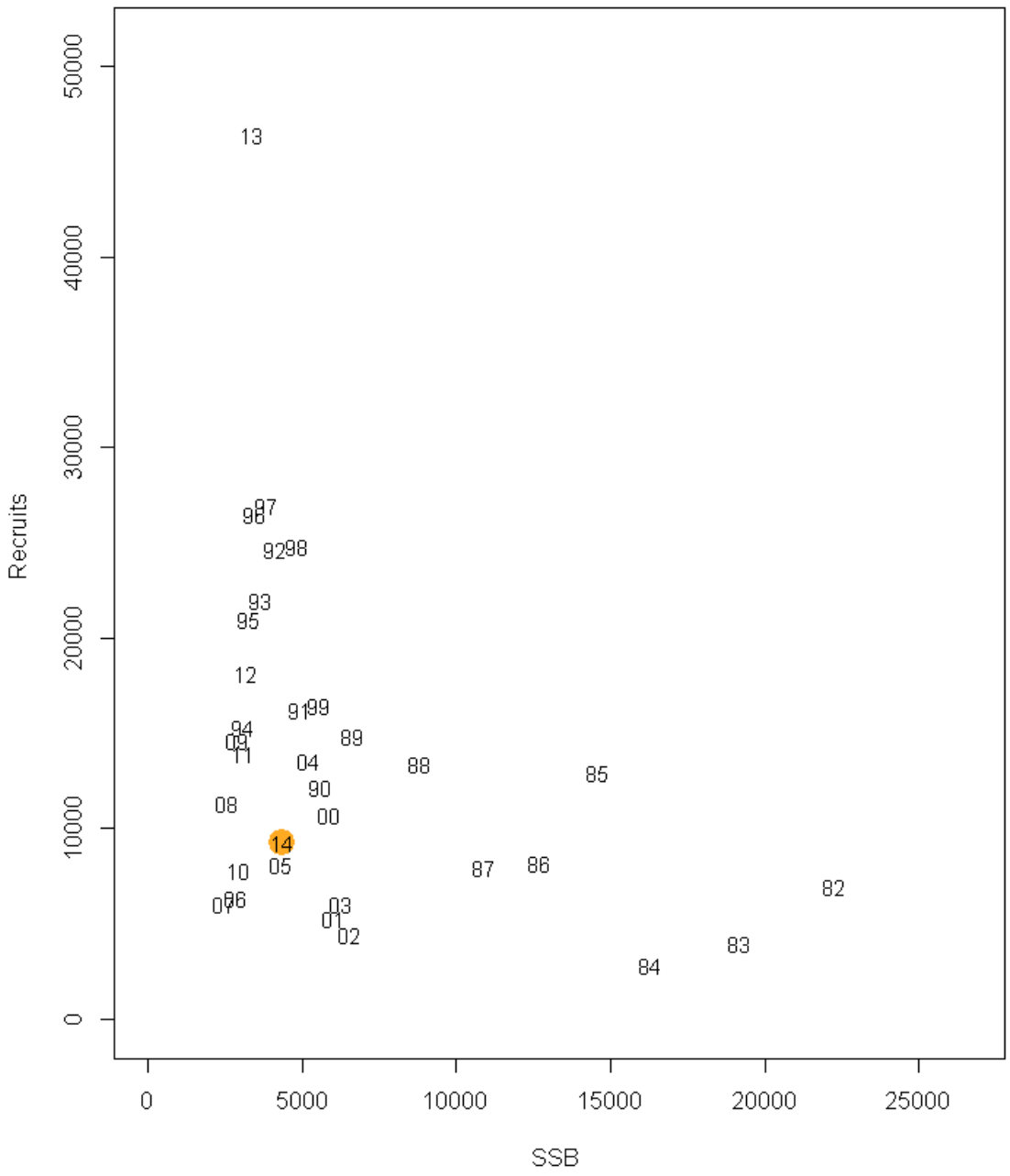

Figure B150. Witch flounder age 1 recruitment (000s) and spawning stock biomass (mt) estimated from ASAP Run 9_5_v2; year classes 1982-2014.

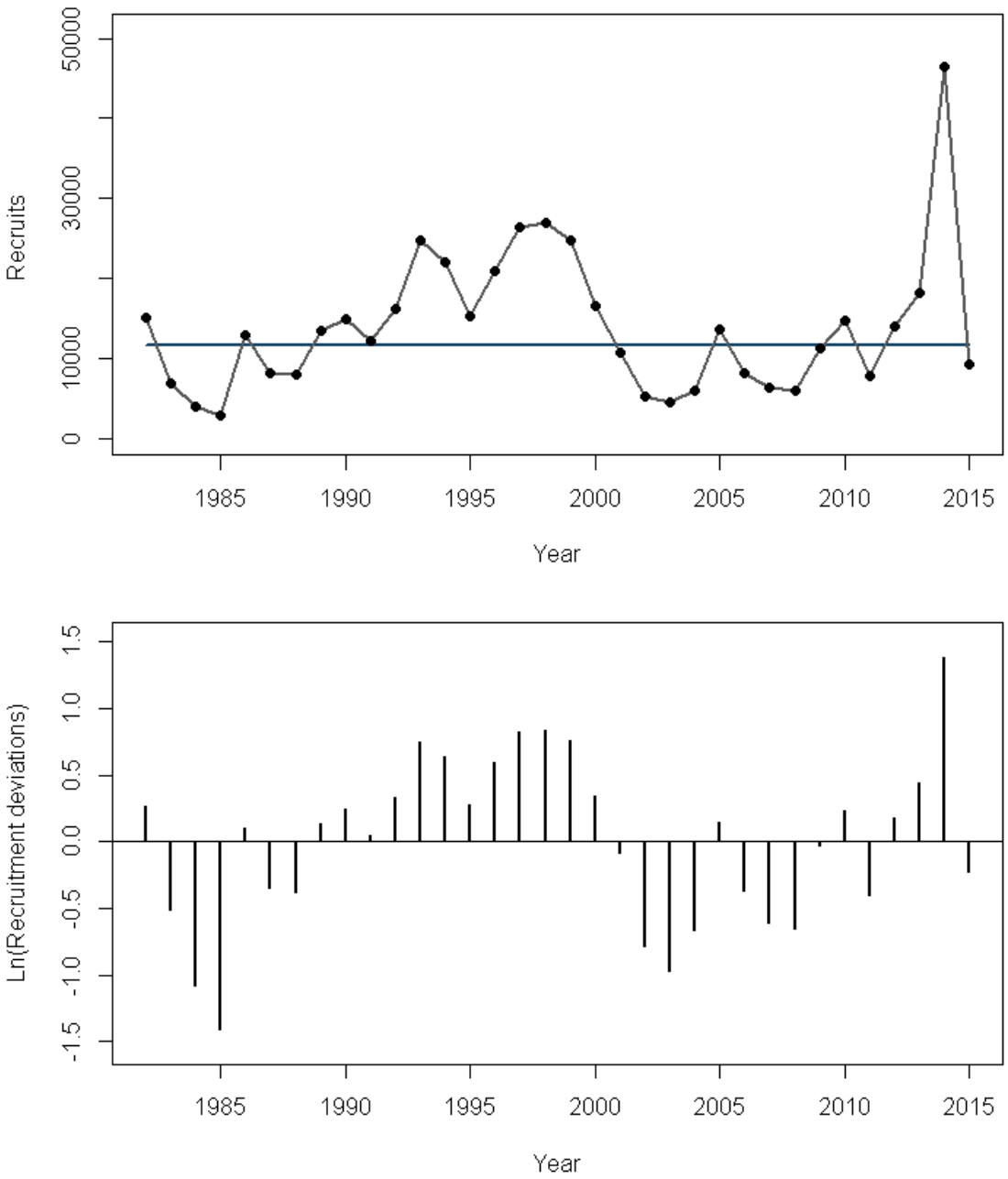

Figure B151. Estimated witch flounder age 1 recruitment (000s) and recruitment residuals from the geometric mean from ASAP Run 9_5_v2.

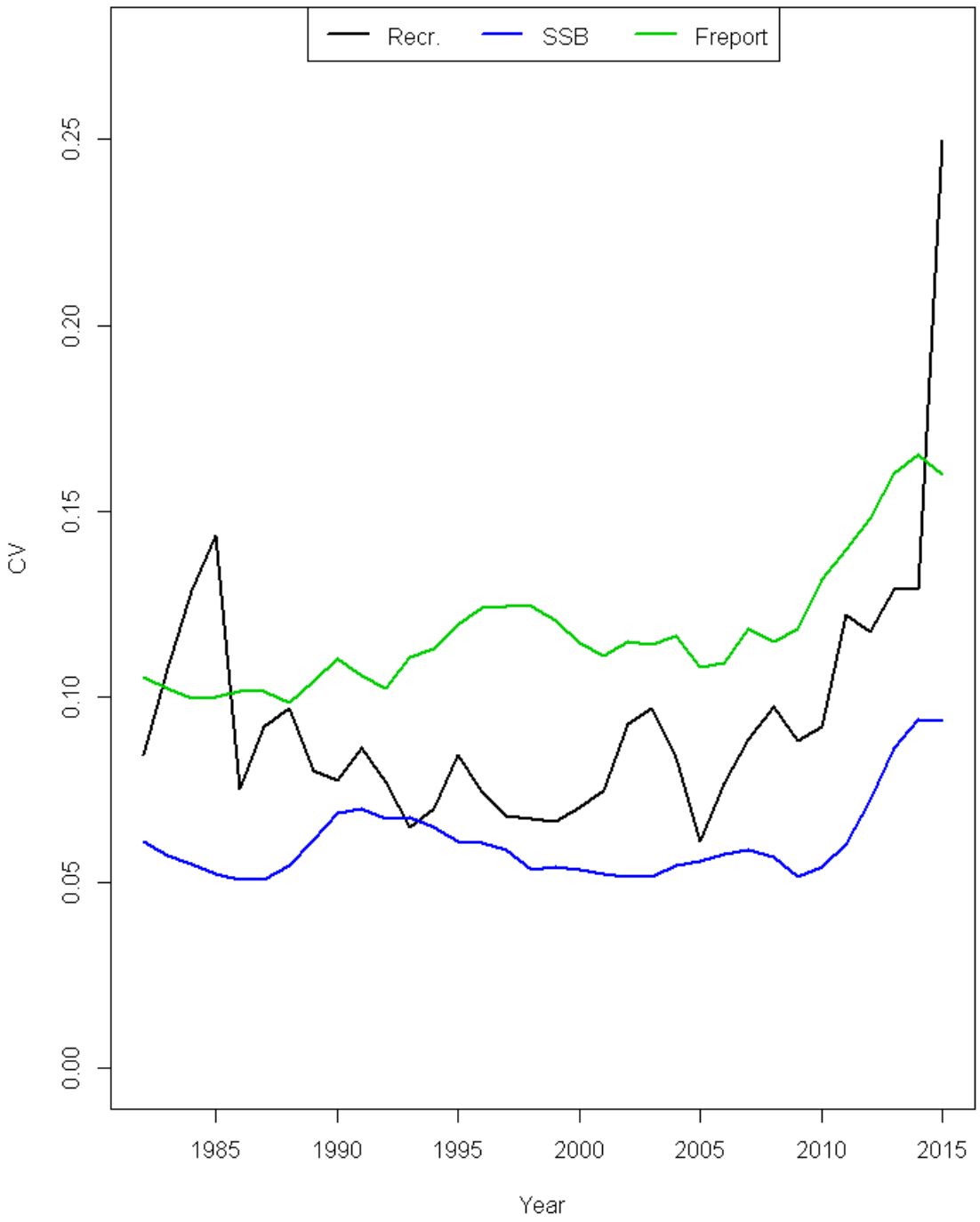

Figure B152. Hessian-based coefficients of variations (CV) estimates of witch flounder spawning stock biomass (SSB), fishing mortality ($F_{report} = F_{full}$) and age 1 recruitment (Recr) from ASAP Run 9_5_v2.

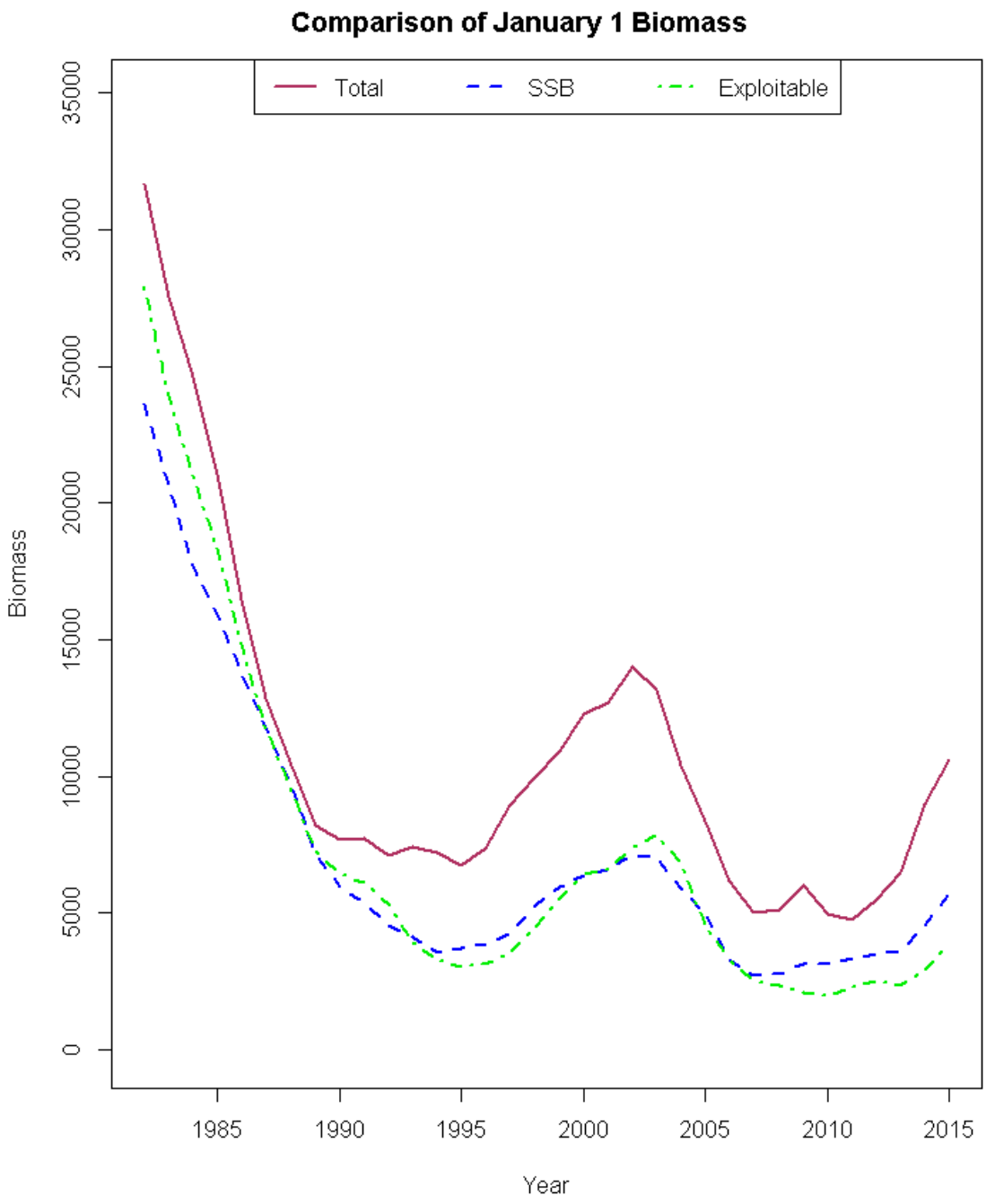

Figure B153. Comparison of ASAP Run 9_5_v2 estimates of witch flounder January 1 biomass after maturity ogive (SSB) and fleet selectivity ogive (exploitable).

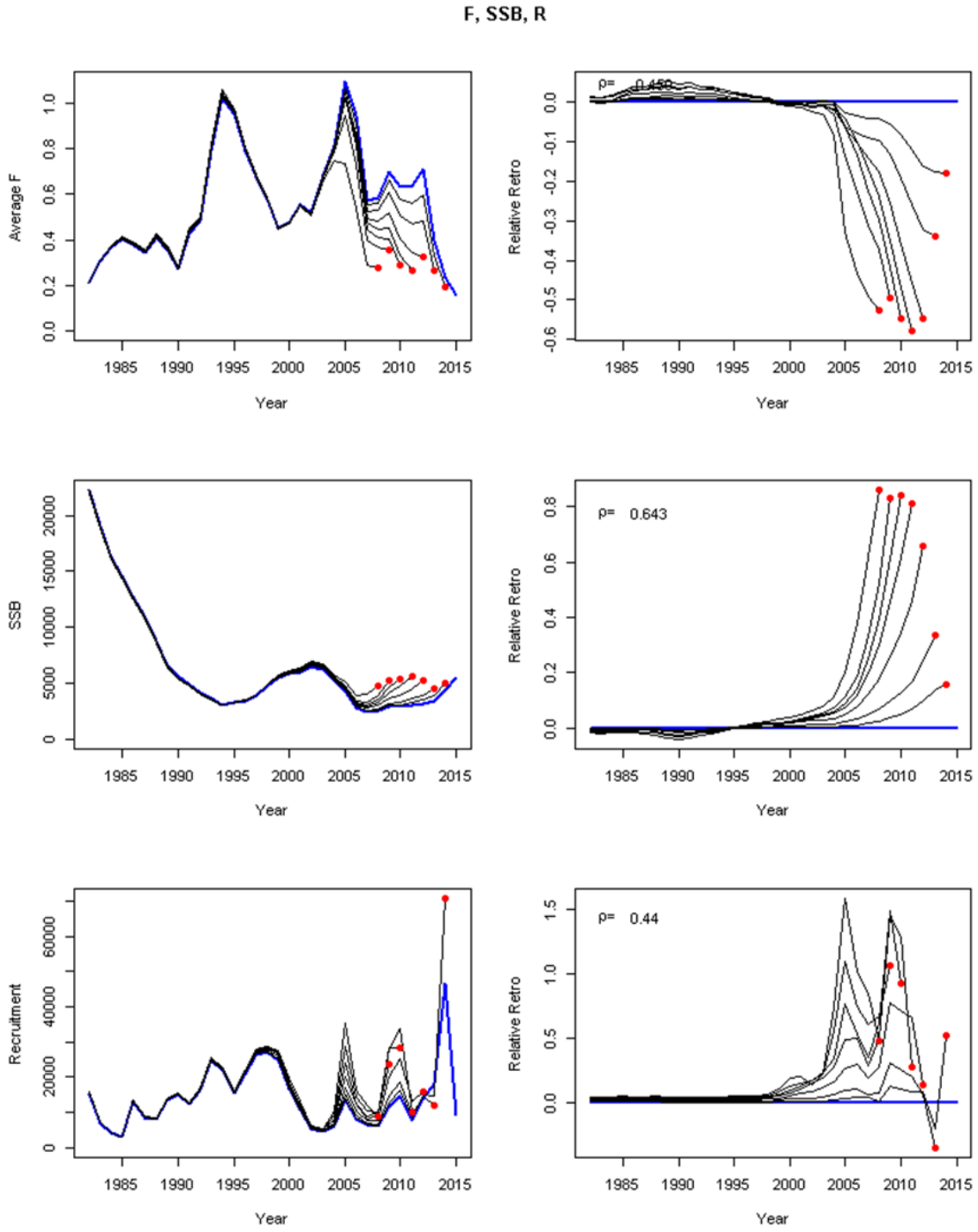

Figure B154. Retrospective patterns (absolute, left; relative, right) for witch flounder fishing mortality (top), spawning stock biomass (SSB; middle) and age 1 recruitment (bottom) from ASAP Run 9_5_v2. The Mohn's rho value based on 7 year peel is indicated.

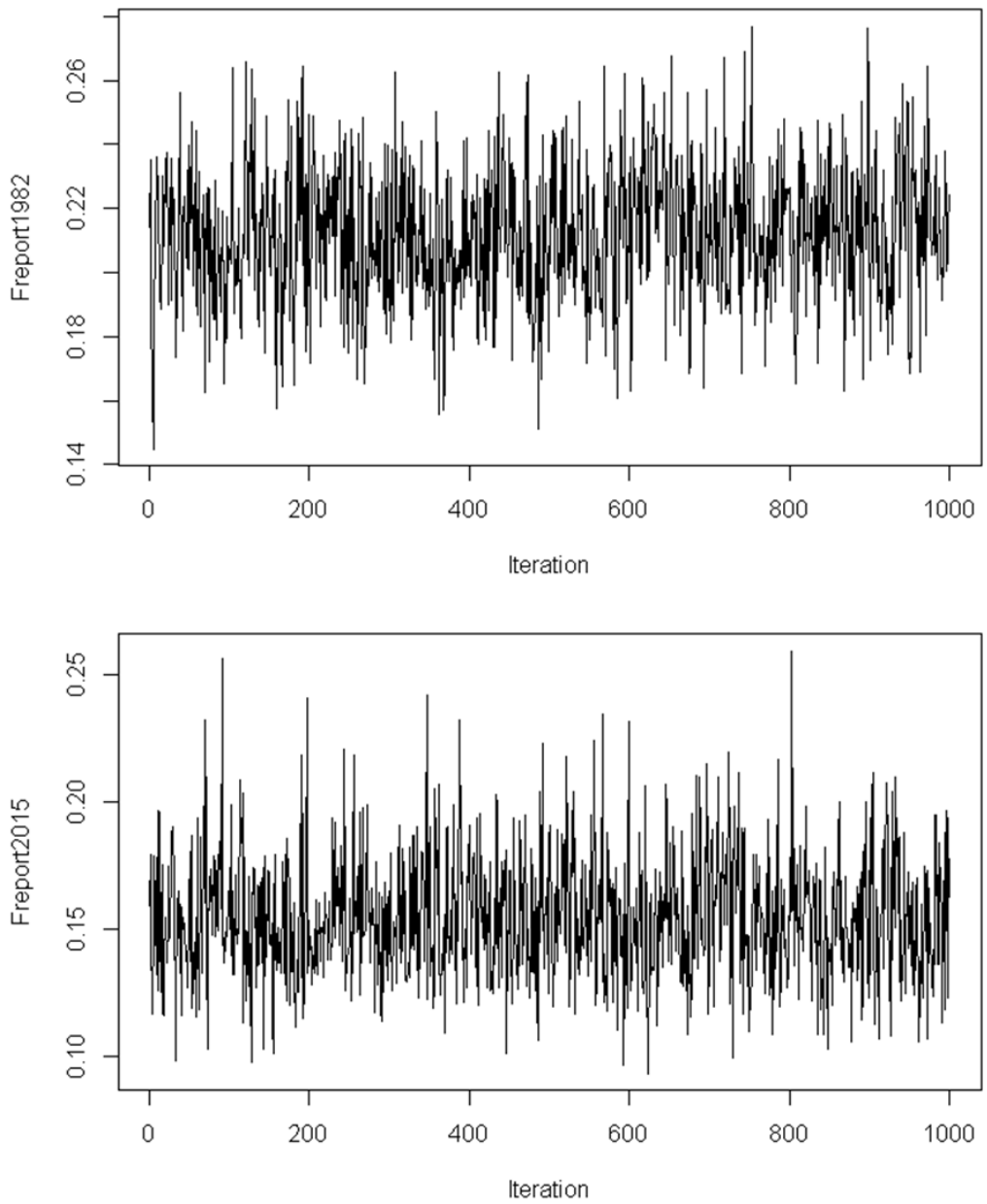

Figure B155. Trace of Monte Carlo Markov chains for witch flounder 1892 (top) and 2015 (bottom) fishing mortality from ASAP RUN 9_5_v2.

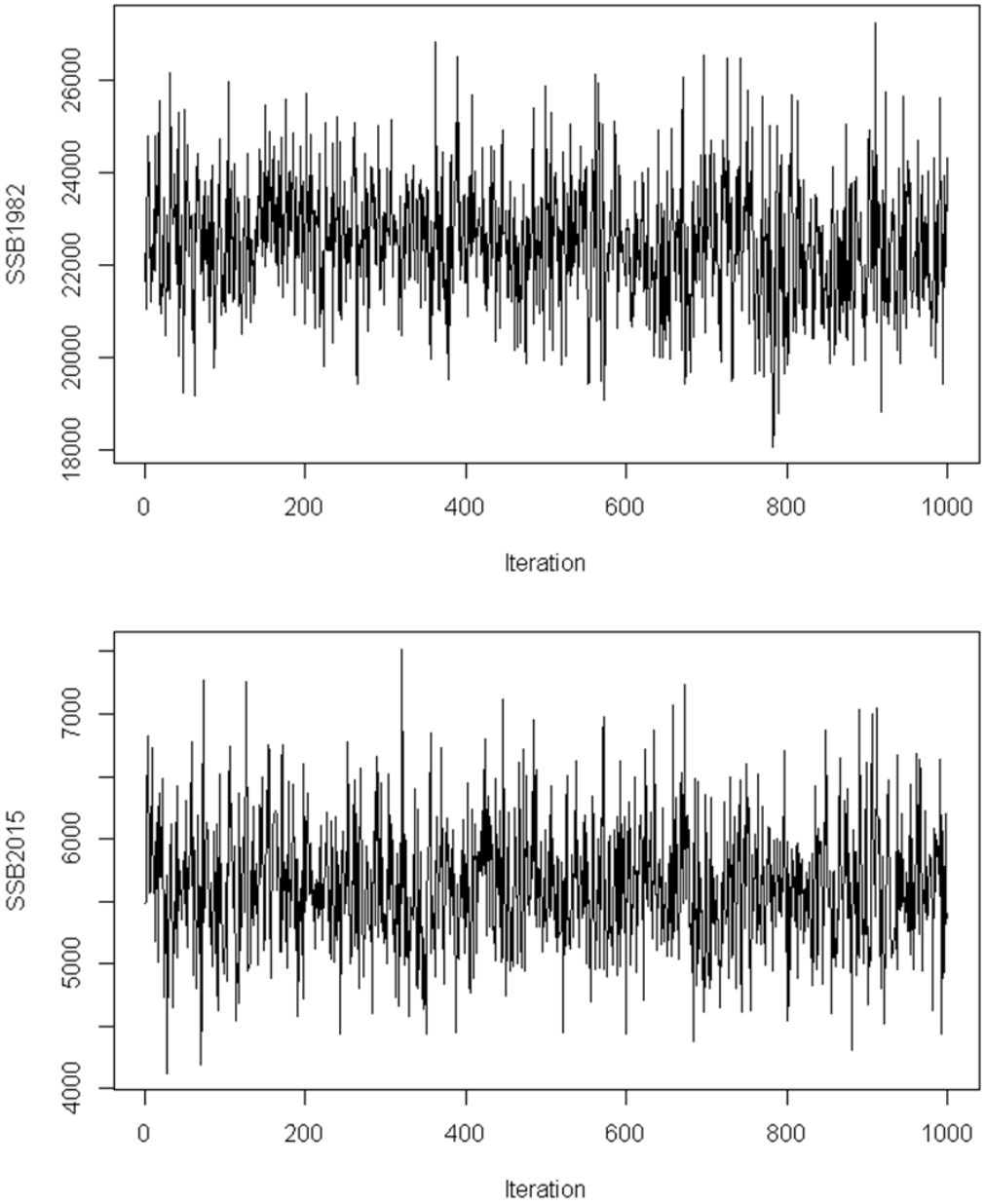

Figure B156. Trace of Monte Carlo Markov chains for witch flounder 1892 (top) and 2015 (bottom) spawning stock biomass from ASAP RUN 9_5_v2.

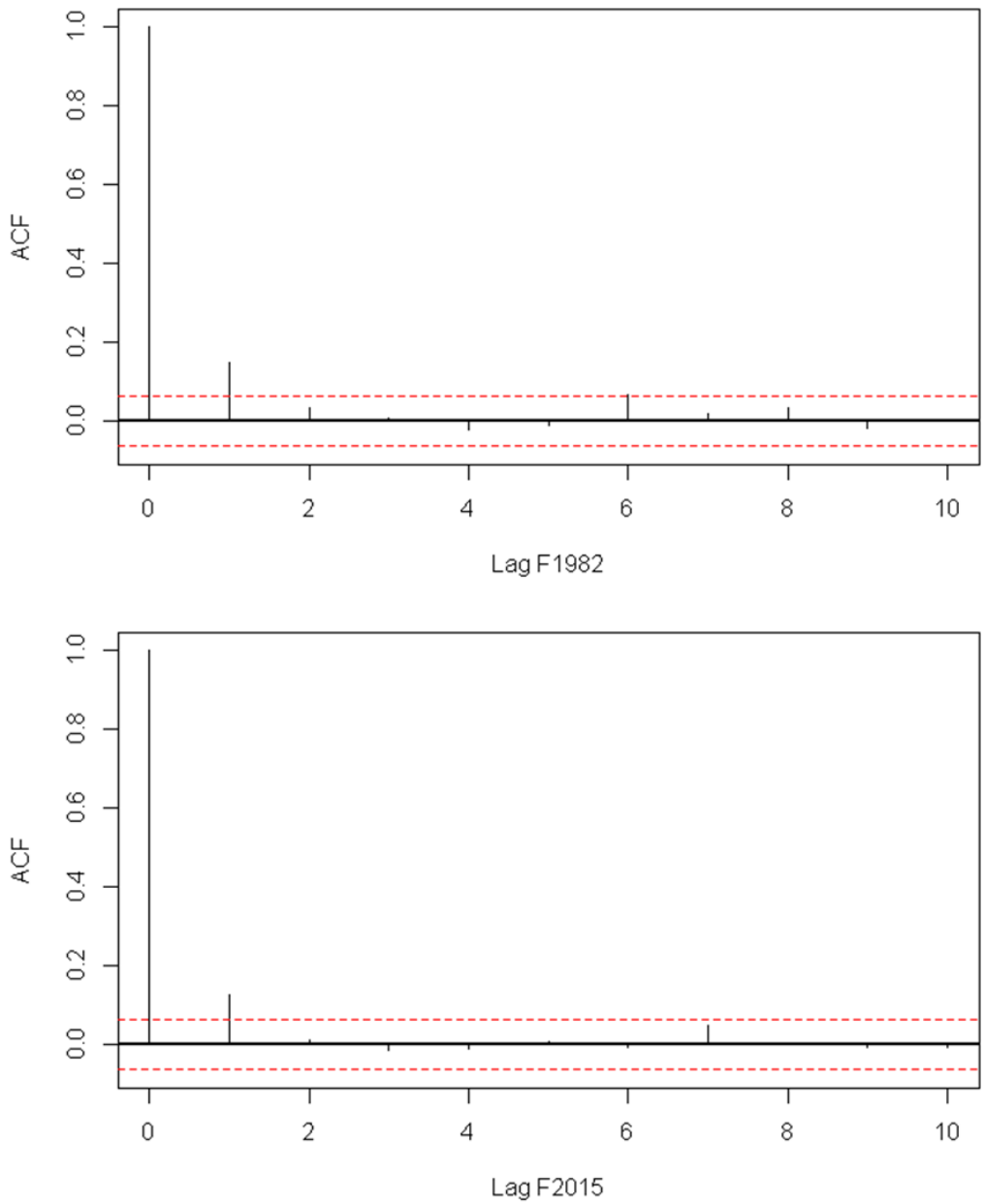

Figure B157. Autocorrelation within the 1982 (top) and 2015 (bottom) witch flounder fishing mortality Monte Carlo Markov chains from ASAP Run 9_5_v2.

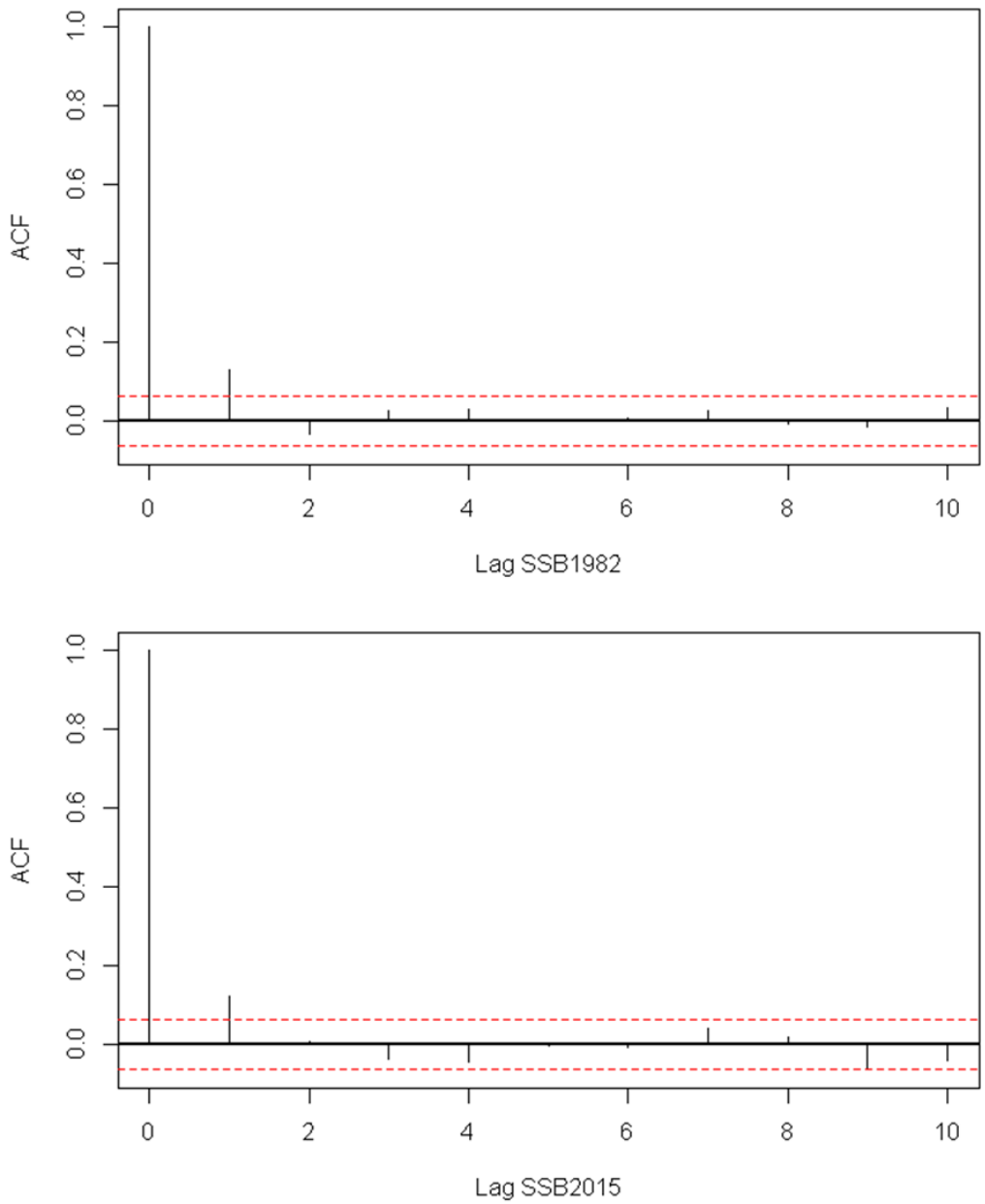

Figure B158. Autocorrelation within the 1982 (top) and 2015 (bottom) witch flounder spawning stock biomass Monte Carlo Markov chains from ASAP Run 9_5_v2.

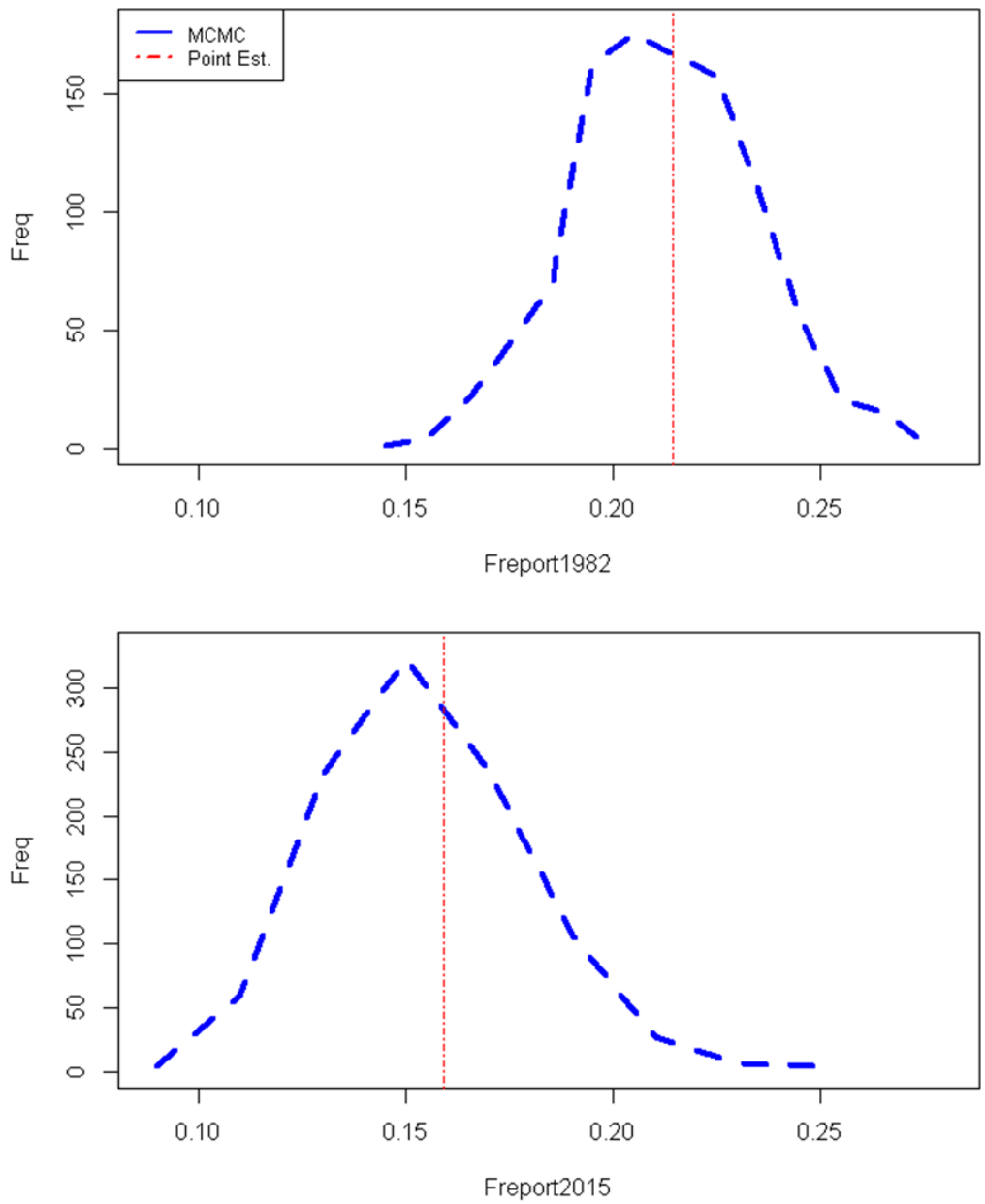

Figure B159. ASAP Run 9_5_v2 point estimates and MCMC distributions of fishing mortality.in 1982 (top) and 2015 (bottom).

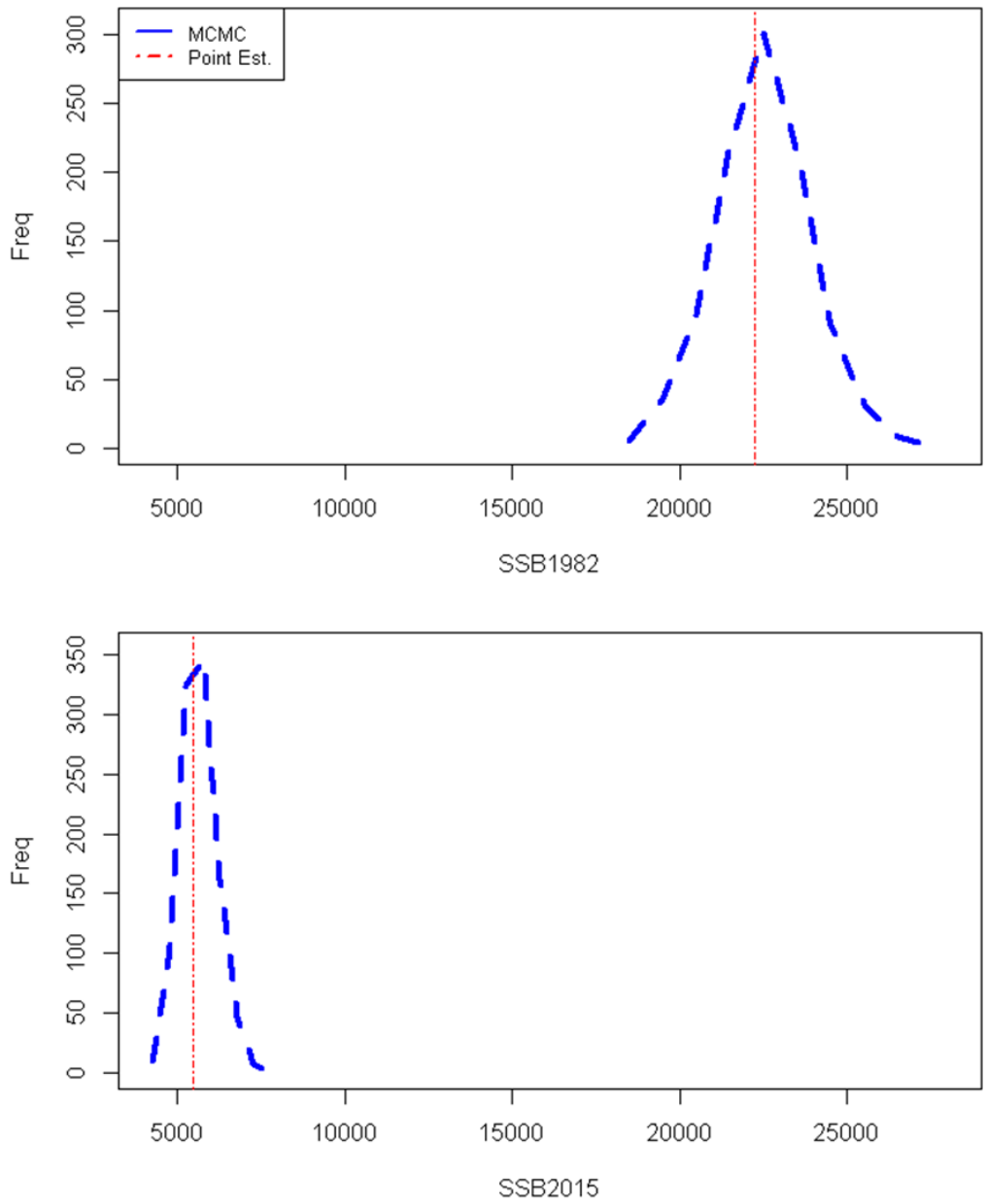

Figure B160. ASAP Run 9_5_v2 point estimates and MCMC distributions of spawning stock biomass (mt) in 1982 (top) and 2015 (bottom).

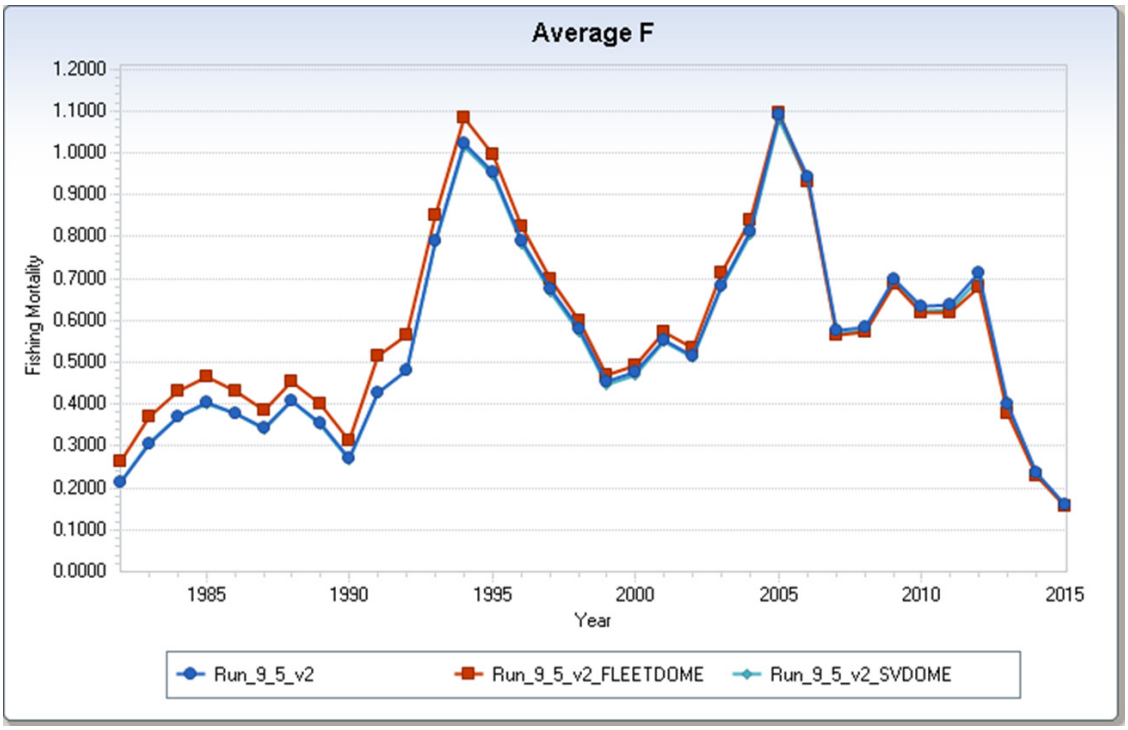

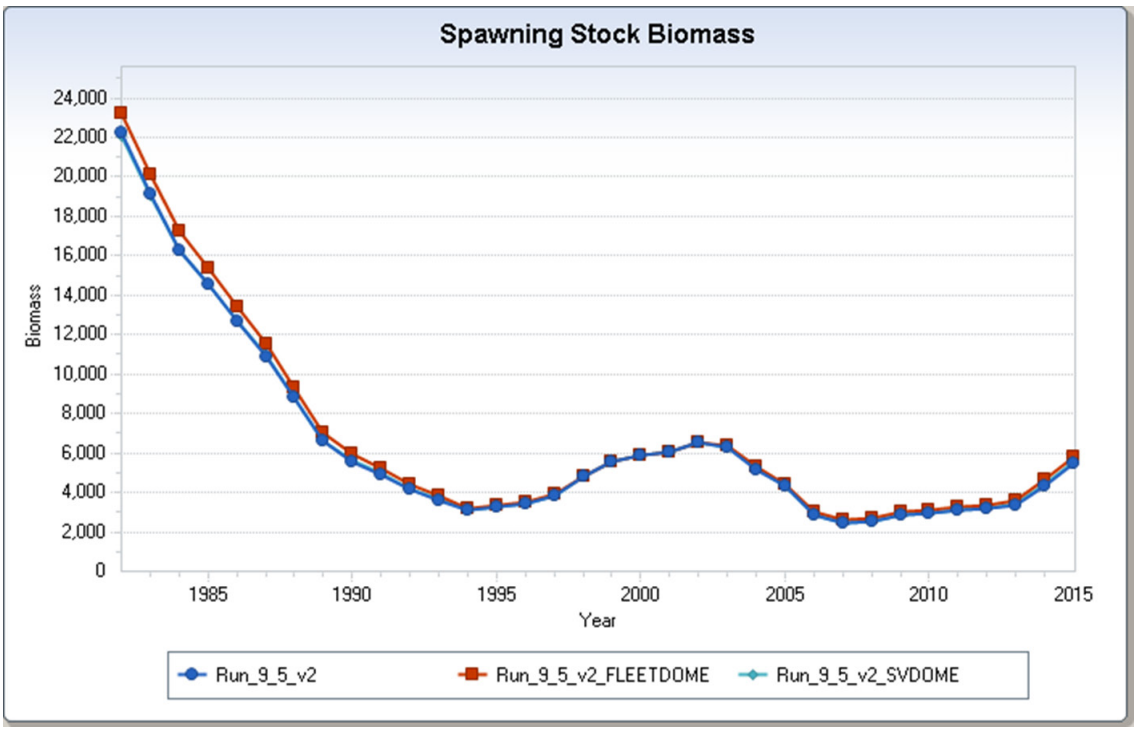

Figure B161. Comparison of witch flounder fishing mortality (top) and spawning stock biomass (mt; bottom) estimated from ASAP Run 9_5_v2, Sensitivity Run 1 (FLEET DOME), and Sensitivity Run 2 (SV DOME).

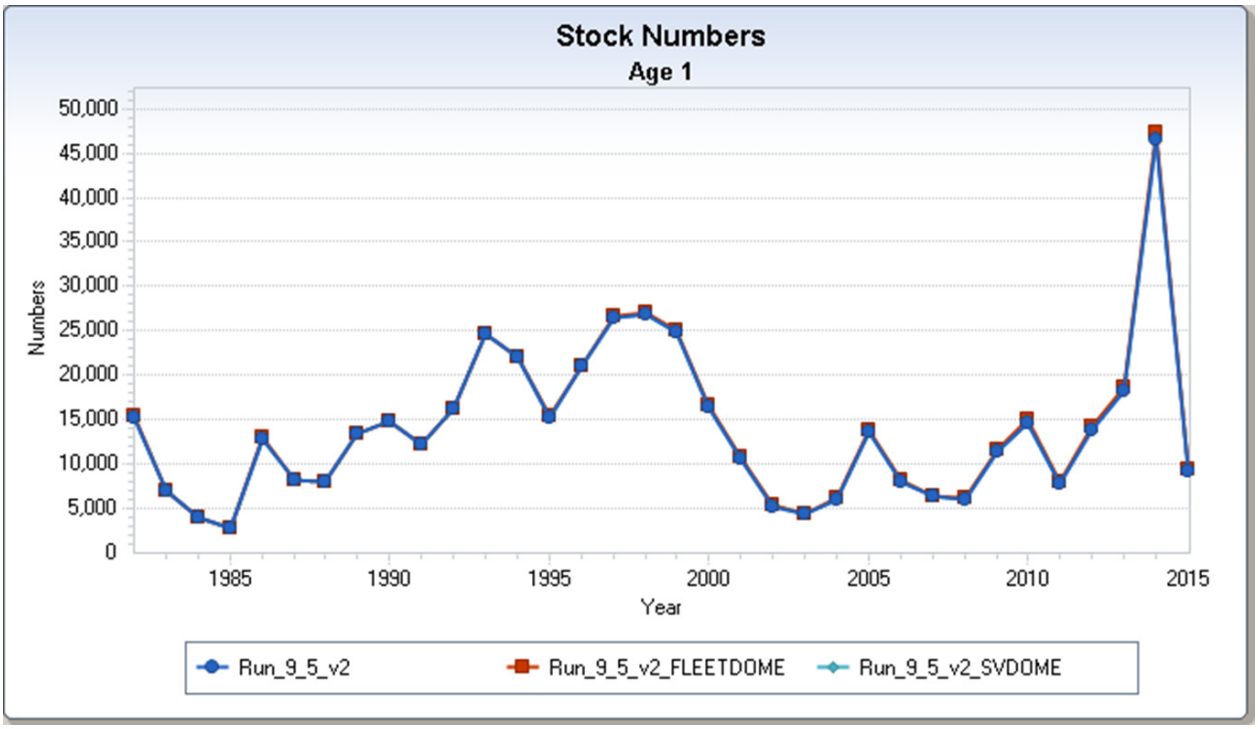

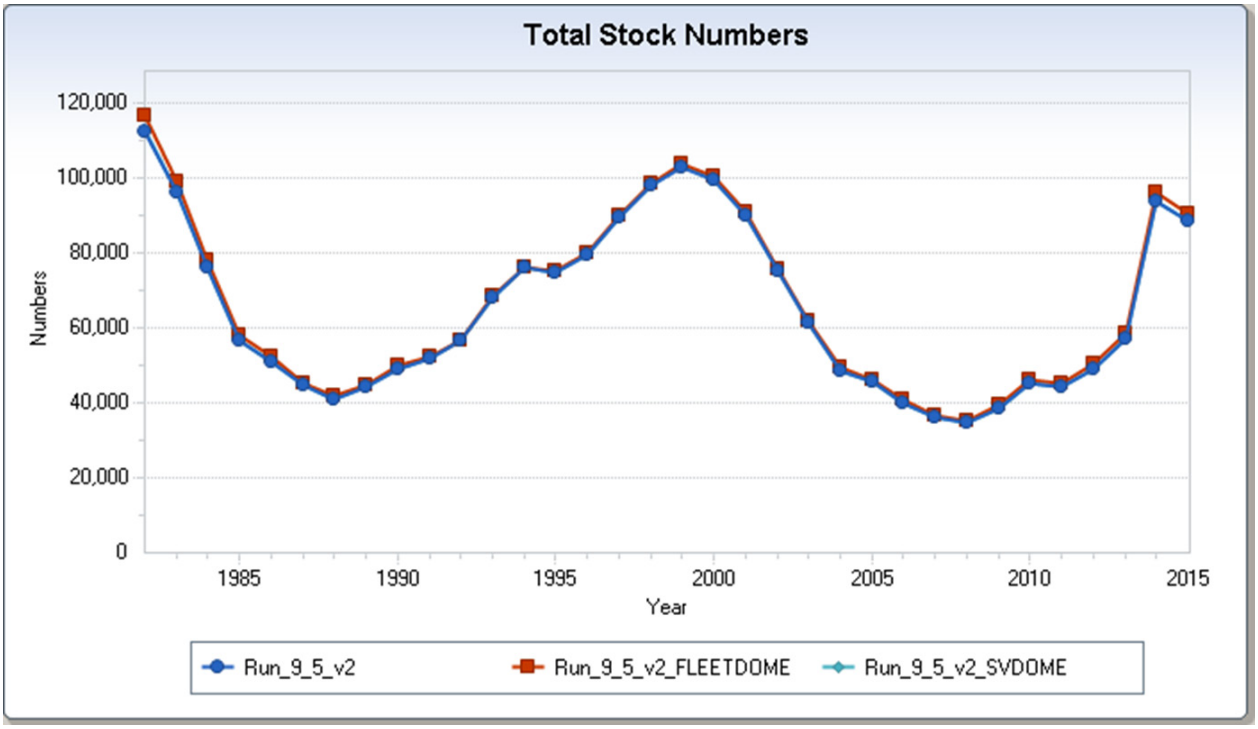

Figure B161, continued. Comparison of witch flounder stock numbers (Age 1, top; Total, bottom) estimated from ASAP Run 9_5_v2, Sensitivity Run 1 (FLEET DOME), and Sensitivity Run 2 (SV DOME).

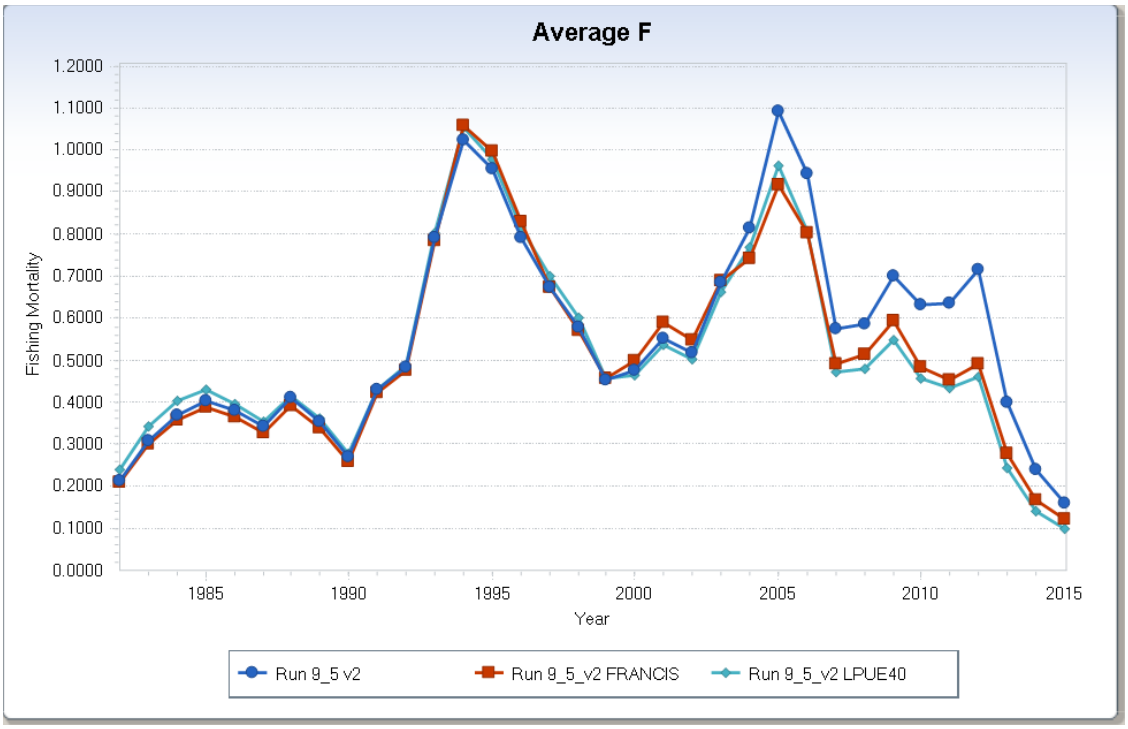

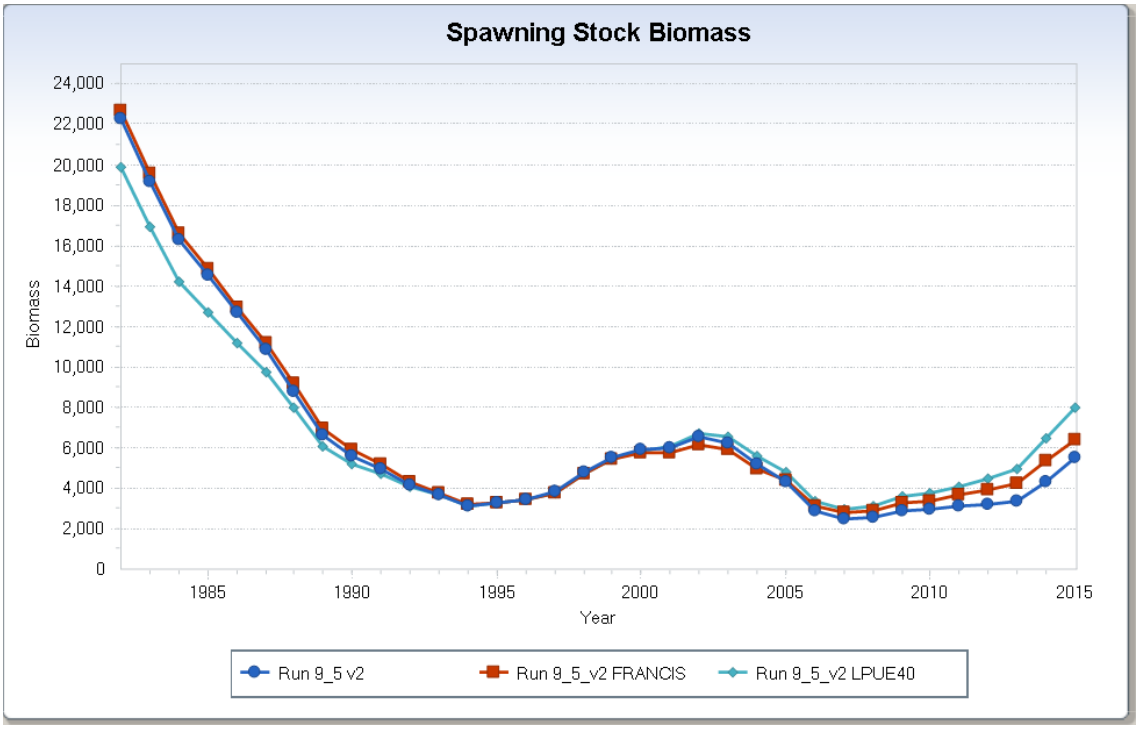

Figure B162. Comparison of witch flounder fishing mortality (top) and spawning stock biomass (mt; bottom) estimated from ASAP Run 9_5_v2, Sensitivity Run 3 (LPUE40) and Sensitivity Run 5 (FRANCIS Effective sample size)

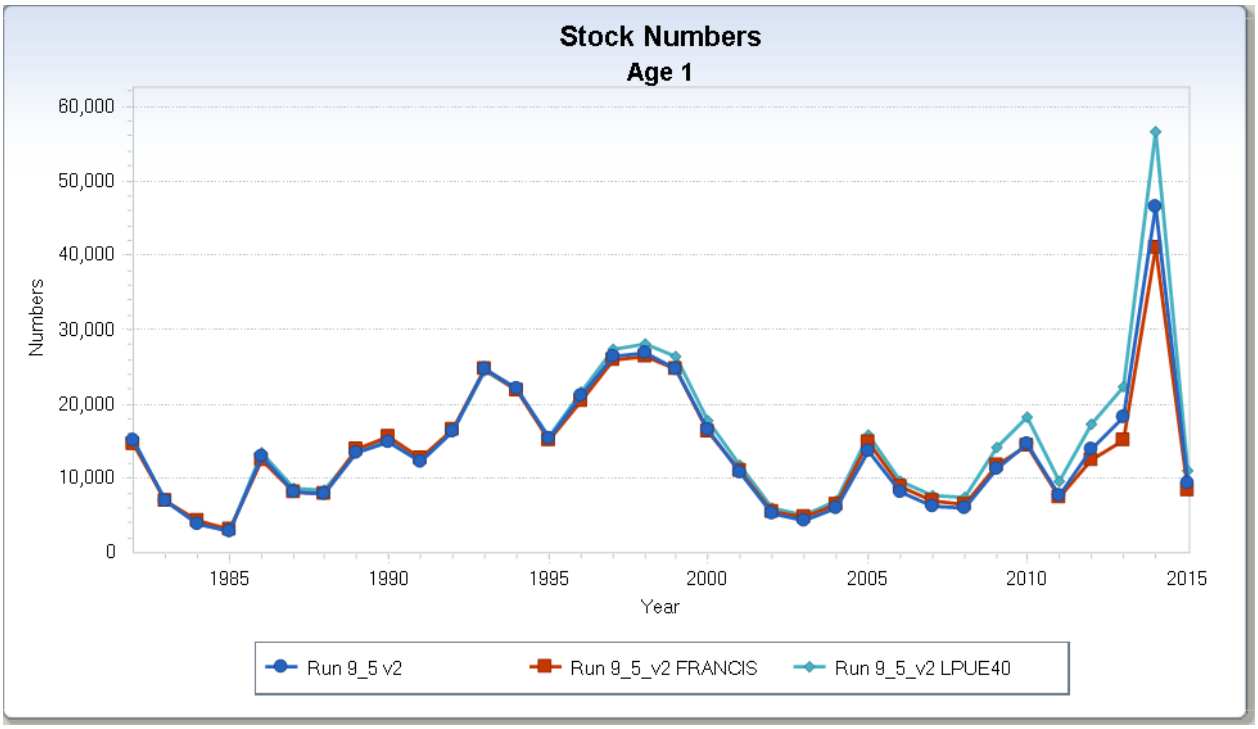

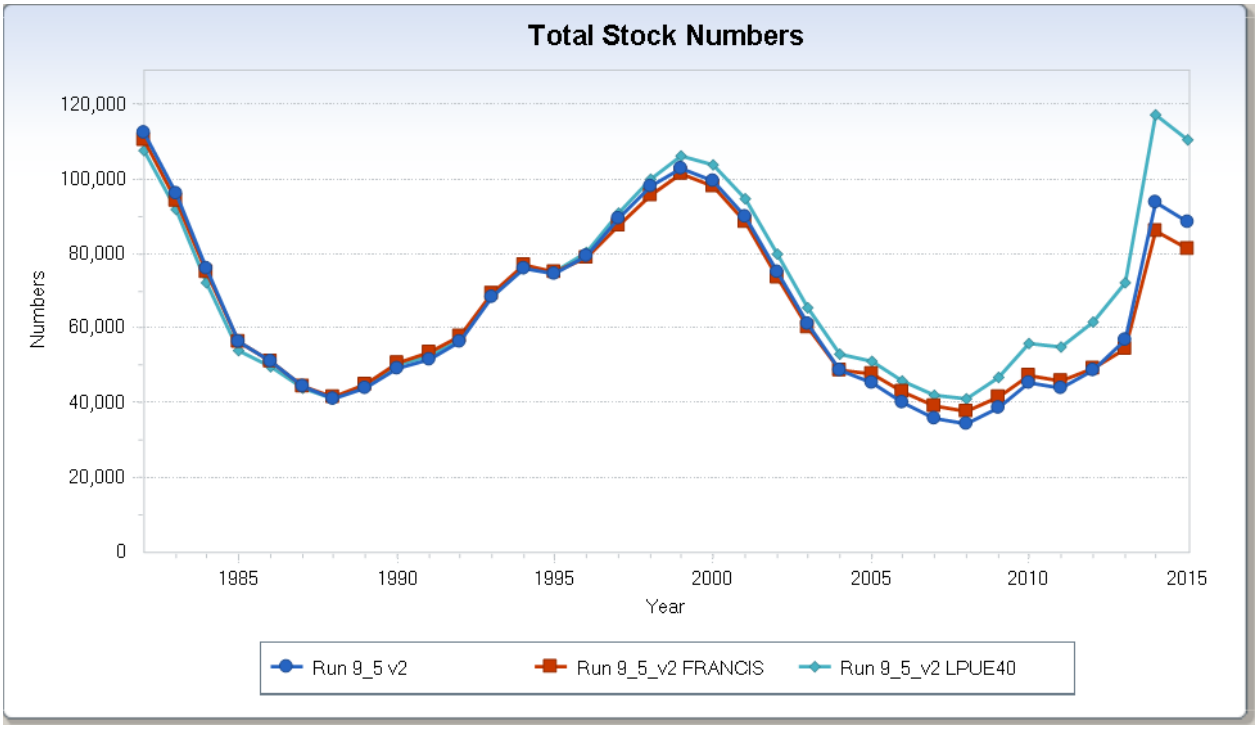

Figure B162, continued. Comparison of witch flounder stock numbers (Age 1, top; Total, bottom) estimated from ASAP Run 9_5_v2, Sensitivity Run 3 (LPUE40) and Sensitivity Run 5 (FRANCIS Effective sample size).

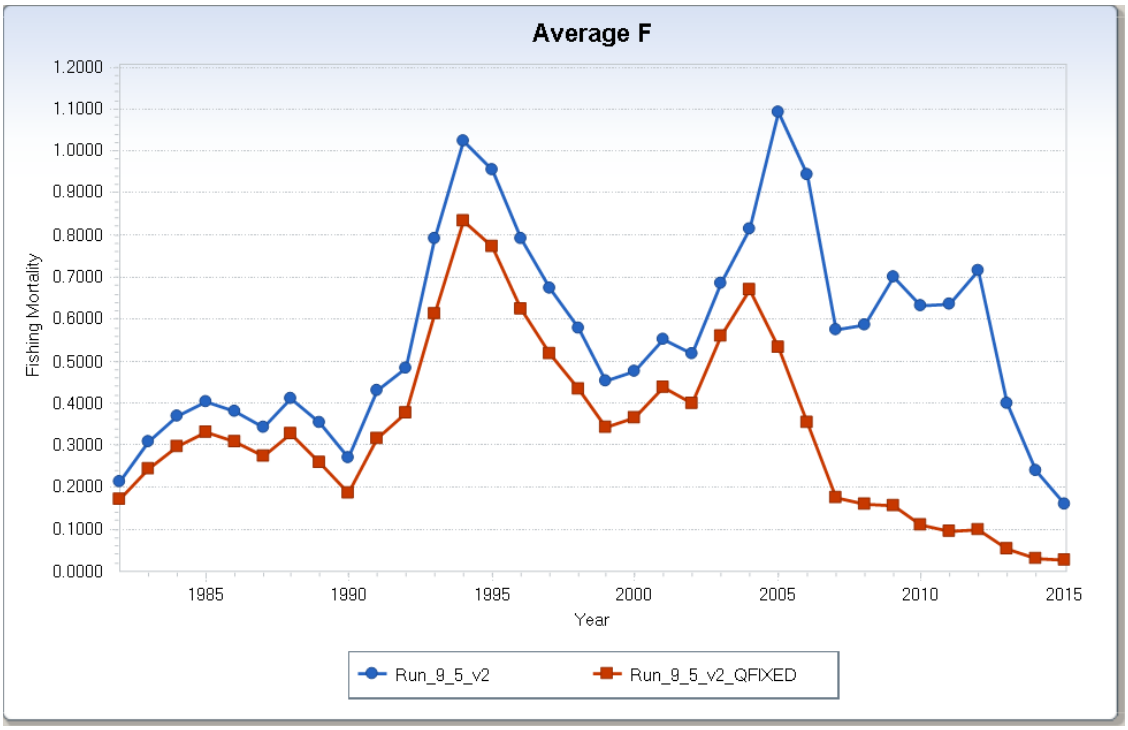

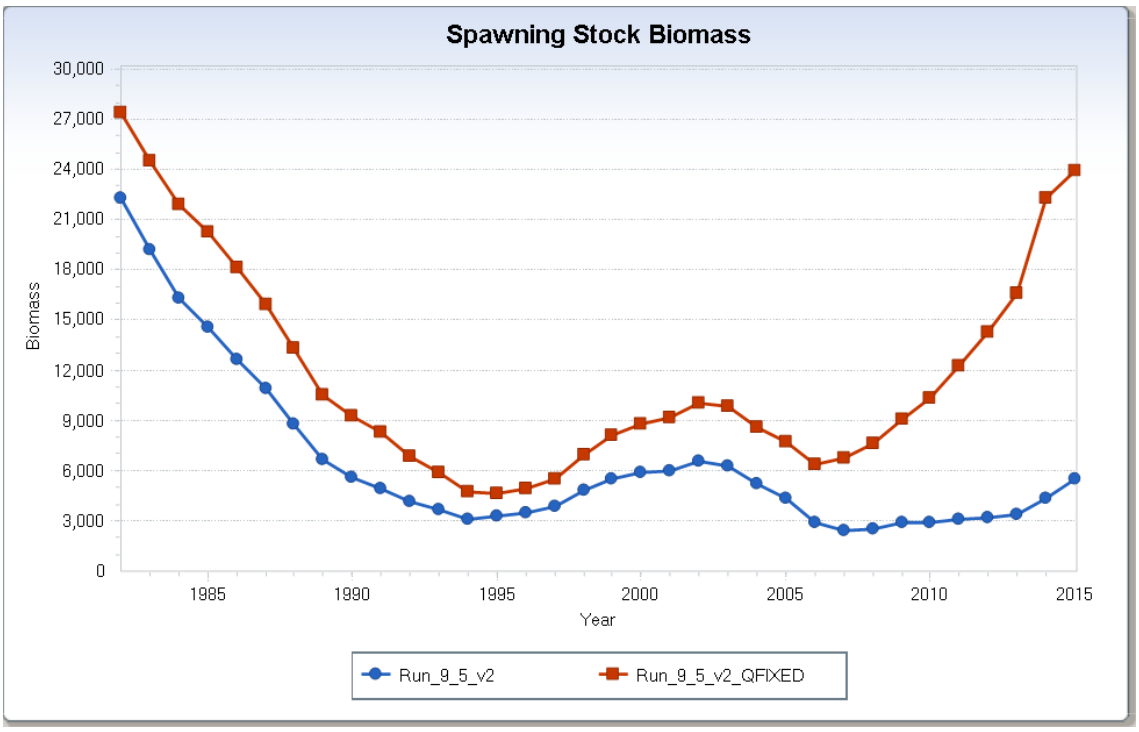

Figure B163. Comparison of witch flounder fishing mortality (top) and spawning stock biomass (mt; bottom) estimated from ASAP Run 9_5_v2 and Sensitivity Run 4 (QFIXED).

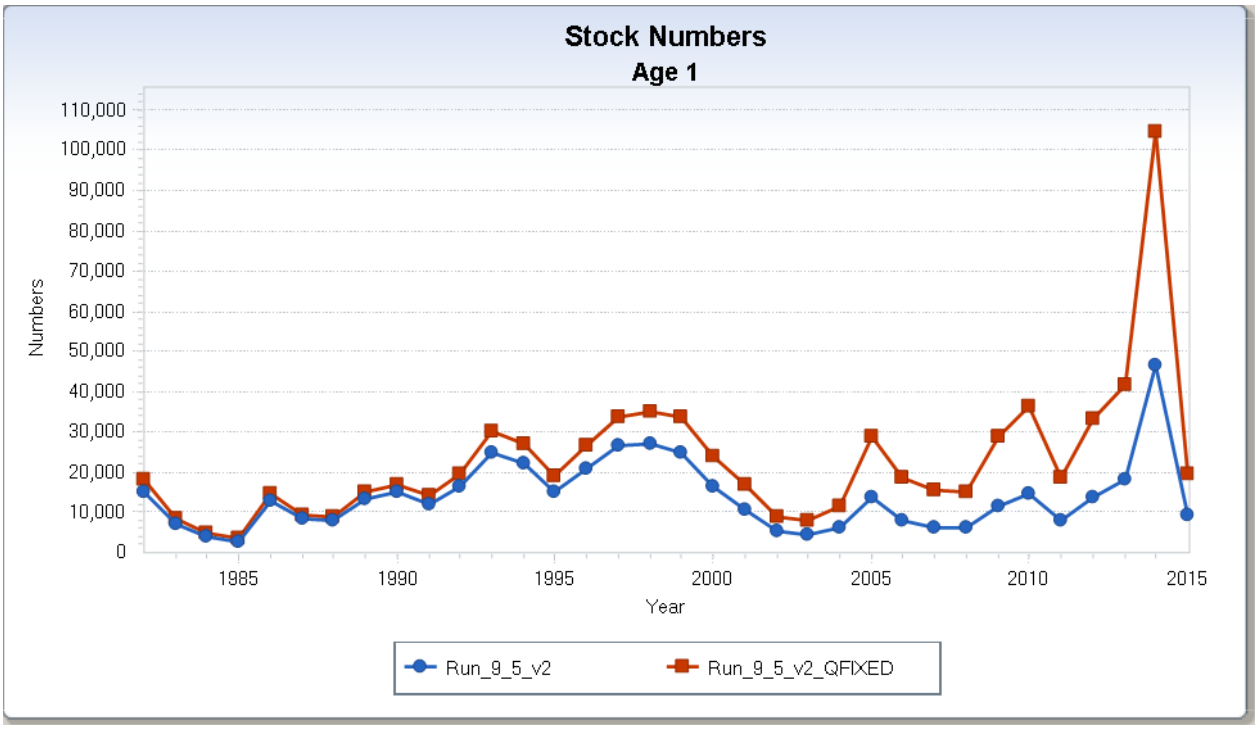

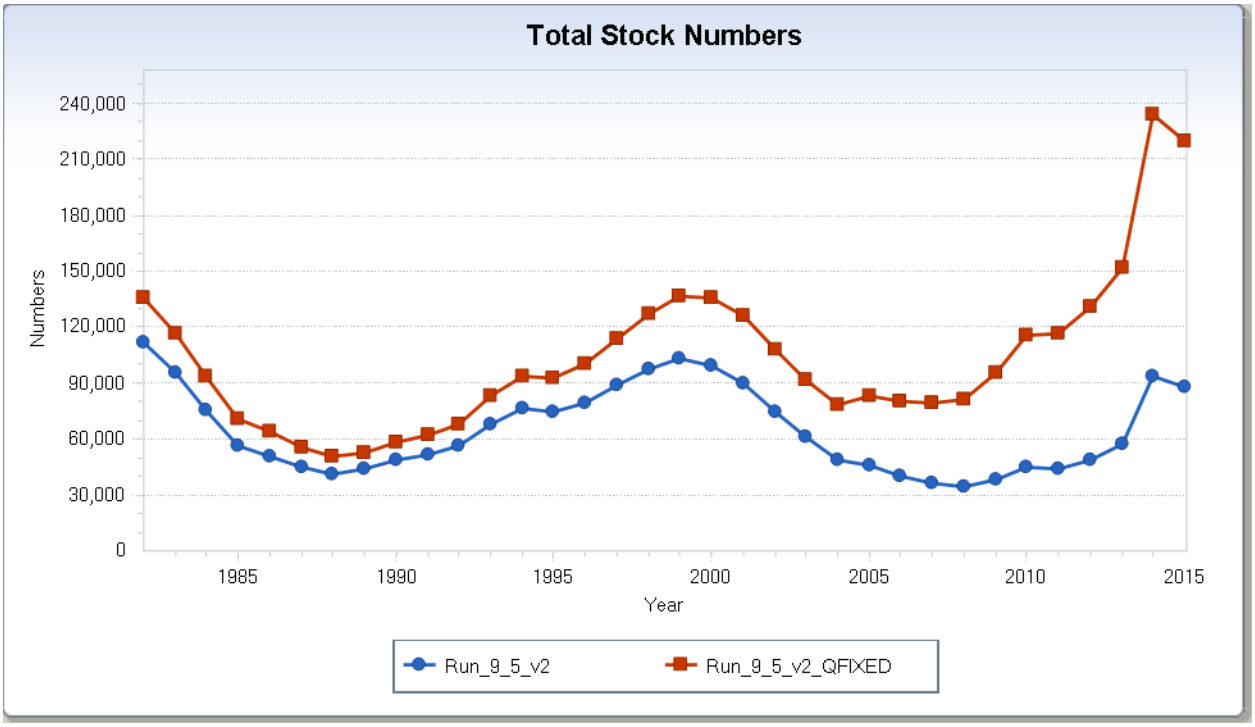

Figure B163, continued. Comparison of witch flounder stock numbers (Age 1, top; Total, bottom) estimated from ASAP Run 9_5_v2 and Sensitivity Run 4 (QFIXED).

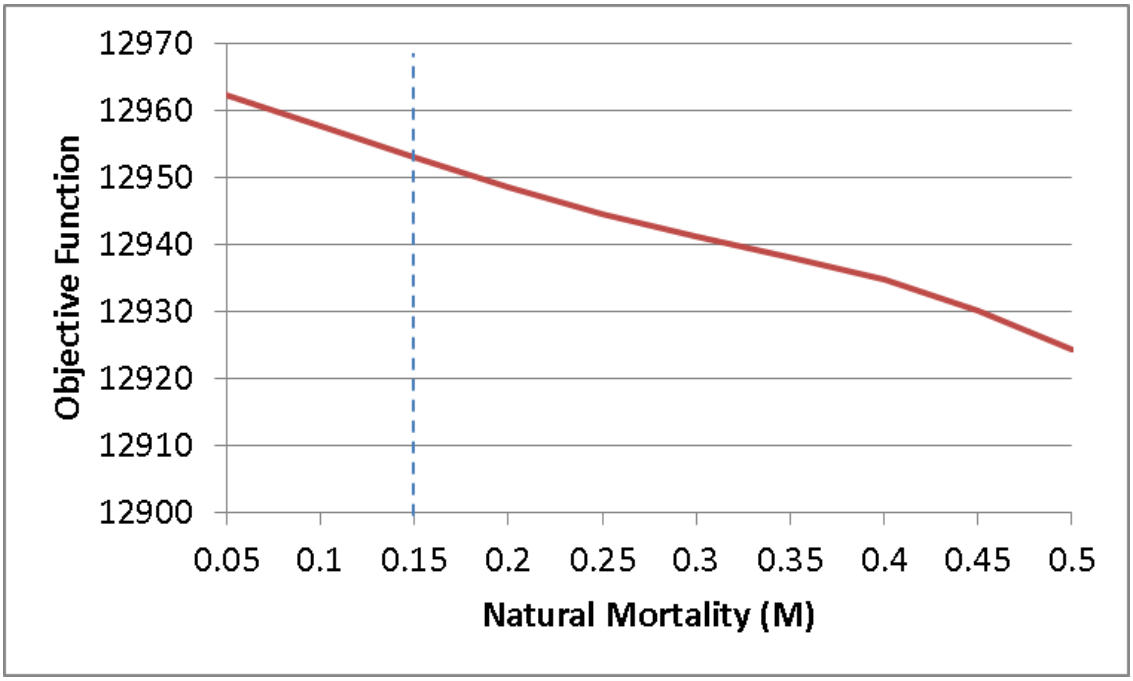

Figure B164. Response of the model objective function to profiling over a range of natural mortality values for ASAP Run 9_5_v2. Blue dashed line indicates M=0.15 assumption applied in ASAP Run 9_5_v2.

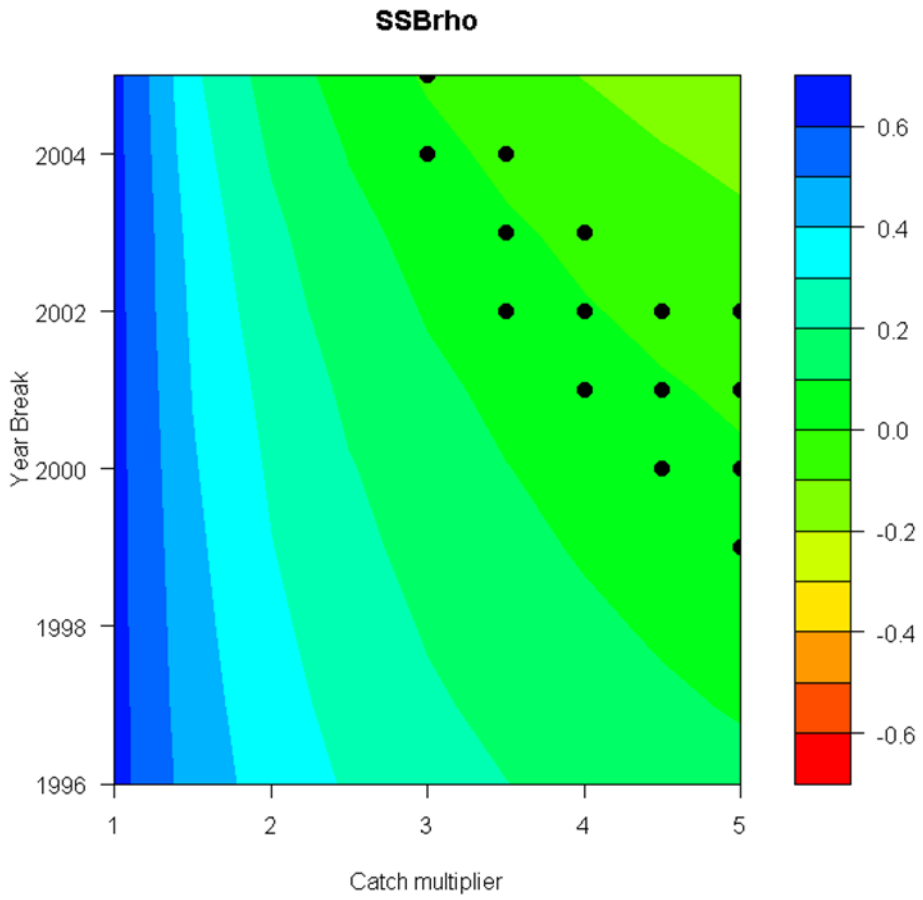

Figure B165. The value of the SSB rho (mean of Mohn's rho value on SSB based on 7 peels; color shading) as the catch multiplier ranges between 1 and 5 (x-axis) and year break (y-axis). The solid black dots denote combinations of year break and catch multiplier that resulted in |SSBrho| < 0.05, indicating multiple ways (combinations of catch multiplier and year break) to eliminate the SSB retrospective pattern in the witch flounder model.

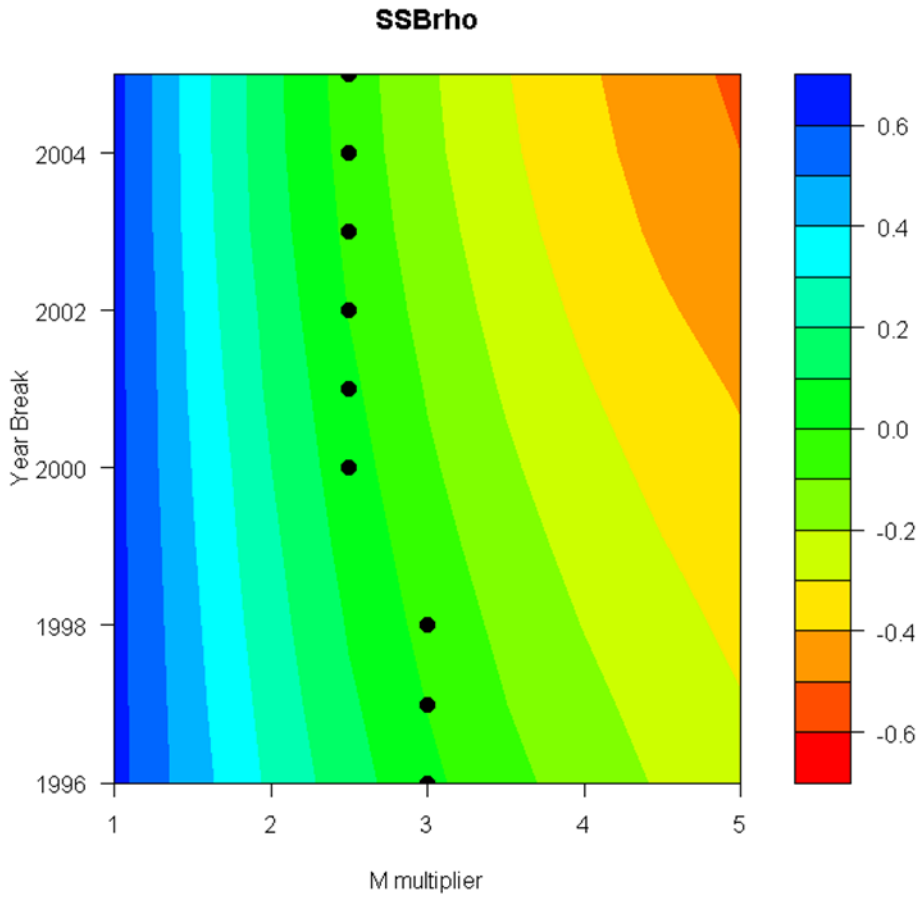

Figure B166. The value of the SSB rho (mean of Mohn's rho value on SSB based on 7 peels; color shading) as the natural mortality (M) multiplier ranges between 1 and 5 (x-axis) and year breaks between 1996 and 2005 (y-axis). The solid black dots denote combinations of year break and M multipliers that resulted in |SSBrho| < 0.05, indicating multiple ways (combinations of M multiplier and year break) to eliminate the SSB retrospective pattern in the witch flounder model.

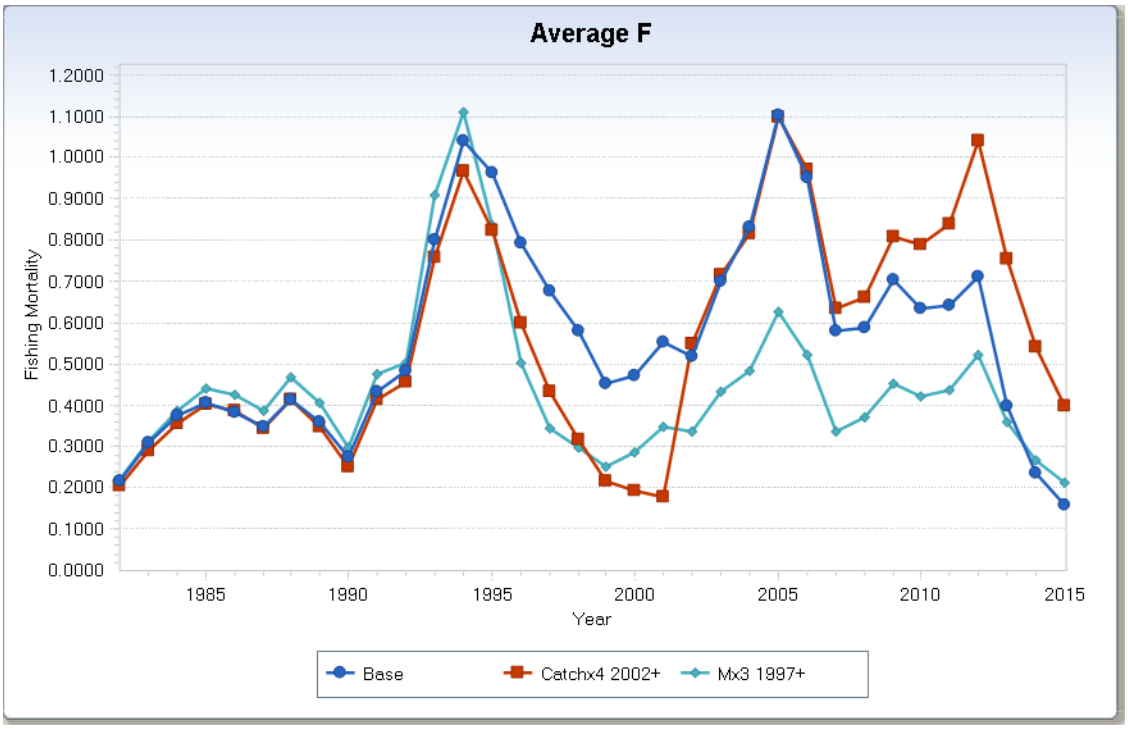

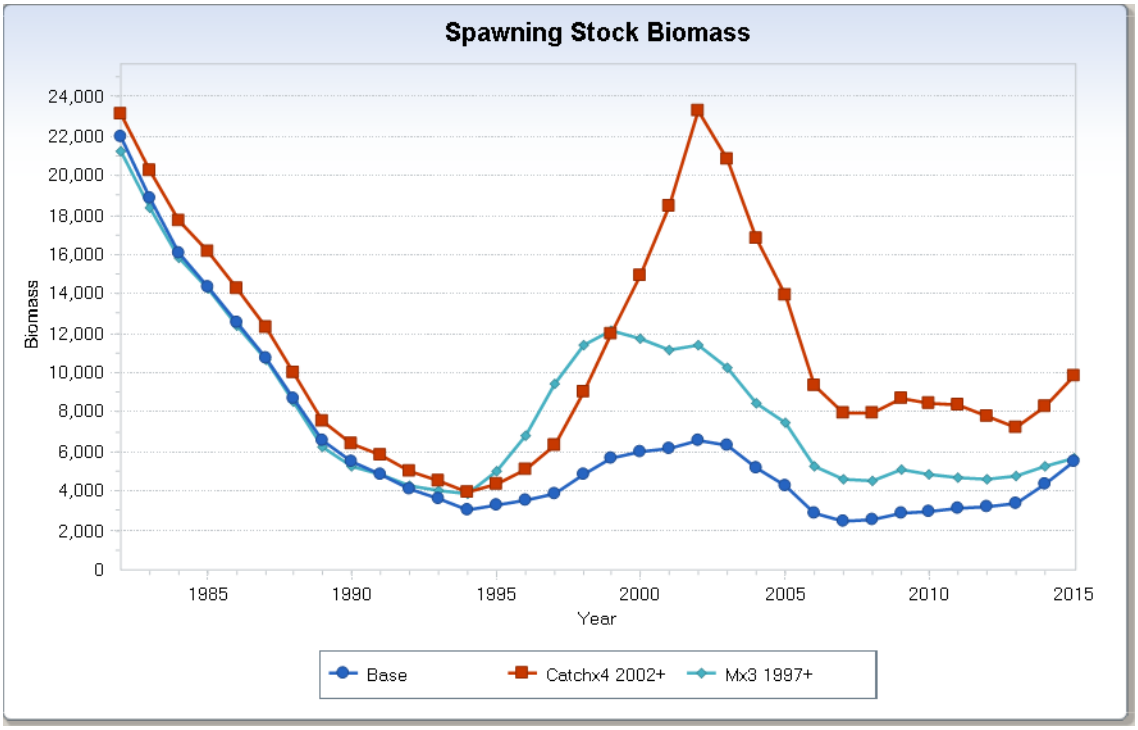

Figure B167. Trends in spawning stock biomass (top) and fishing mortality (bottom) resulting from the ASAP Run 9_5 (Base; blue circle), base run with catch increased by 4 times beginning in 2002 and onward (Catchx4 2002+; red square), and base run with natural mortality increased by 3 times beginning in 1997 and onward (Mx3 1997+; light blue diamond).

Figure B168. Trends in fishing mortality (top) and spawning stock biomass (mt; bottom) estimated from the VPA RUN A2 (dashed line) and ASAP Run 9_5_v2 (solid line) with +/- 2 standard deviation (dotted line).

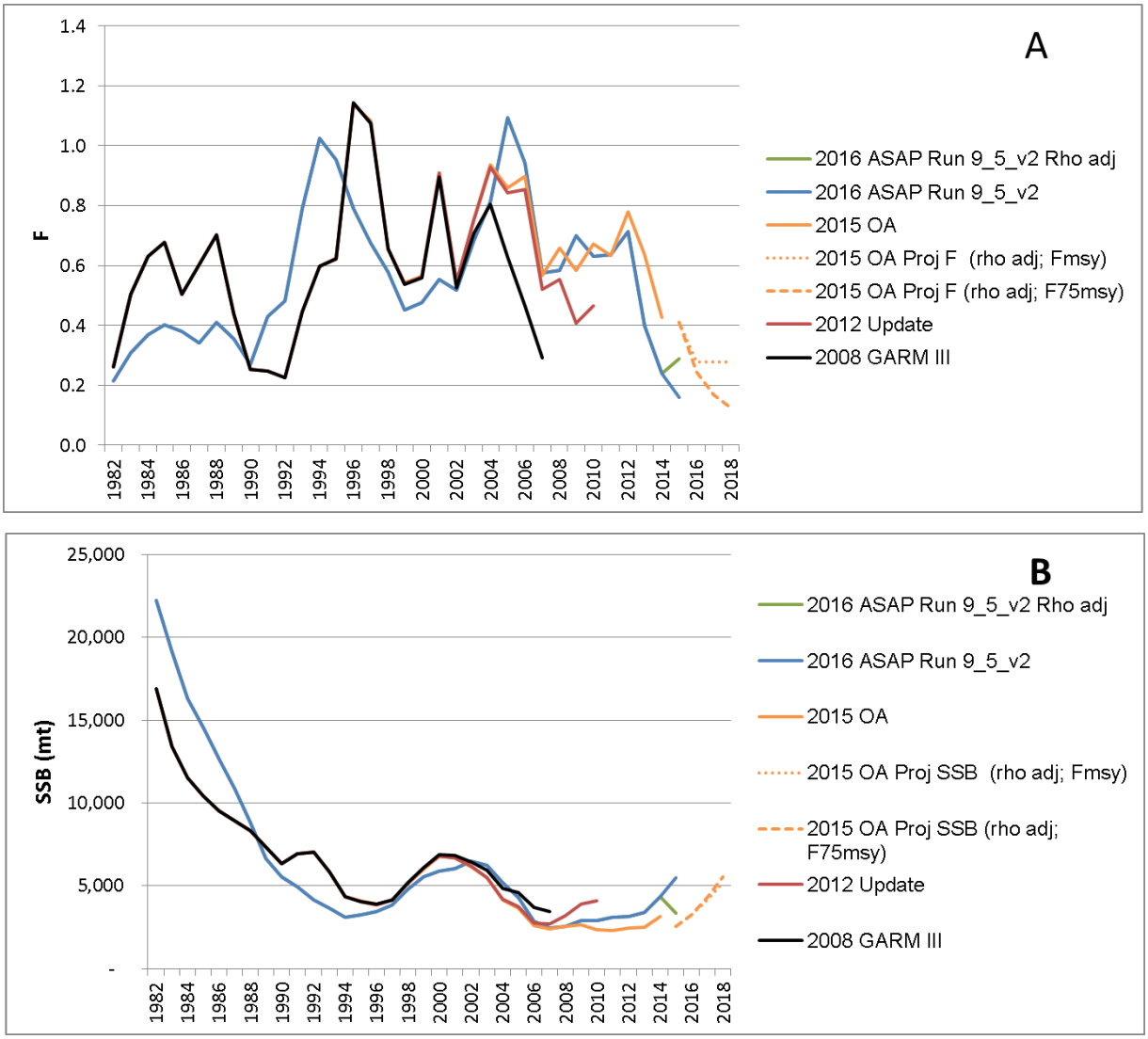

Figure B169. Trends in fishing mortality (top) and spawning stock biomass (mt; bottom) from the 2008 GARM benchmark, 2012 Update, 2015 Operational Assessment (OA), and ASAP Run 9_5_v2 in this assessment (solid lines). The 2015 OA projections are indicated with dashed lines.

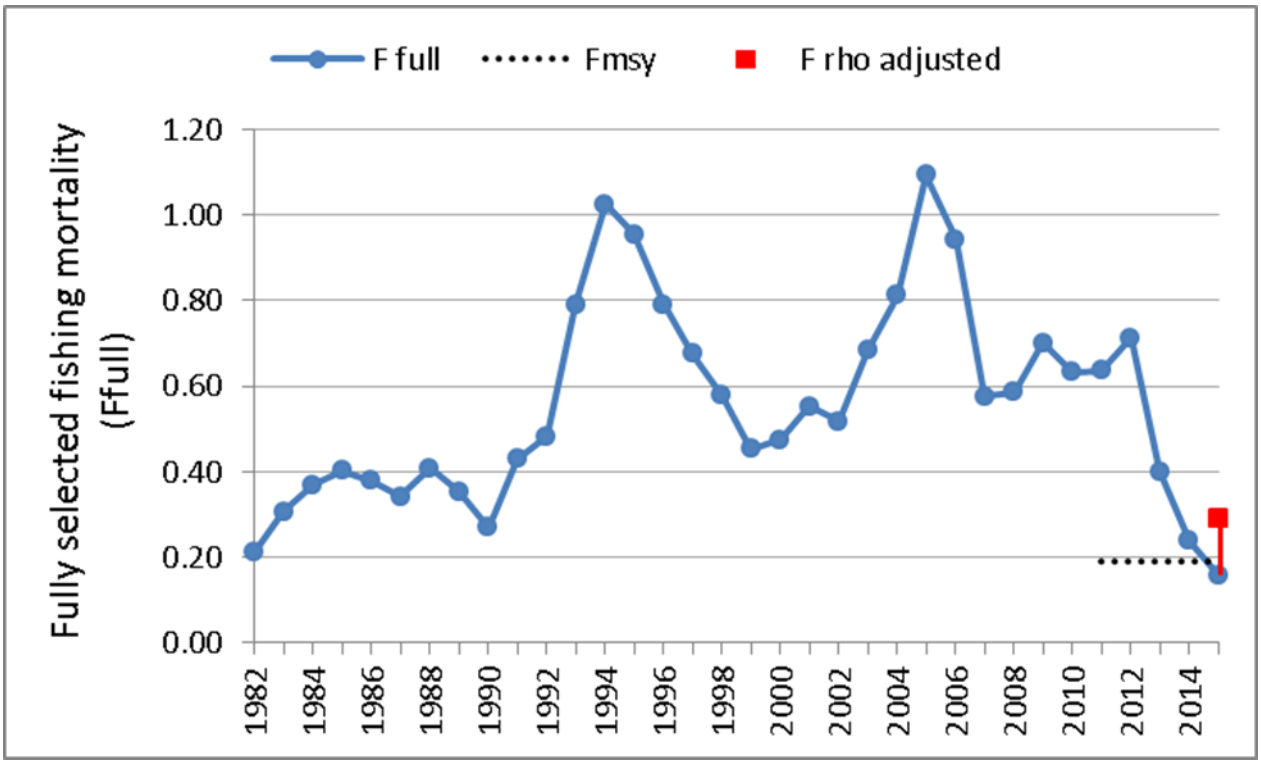

Figure B170**.** Estimated trends in the fully selected fishing mortality (F_{full}; blue line with circle) of witch flounder between 1982 and 2015, and the corresponding F_{MSY} (black dashed line) based on ASAP Run 9_5_v2. The 2015 retrospective adjusted F (F rho adjusted; red square) is also shown.

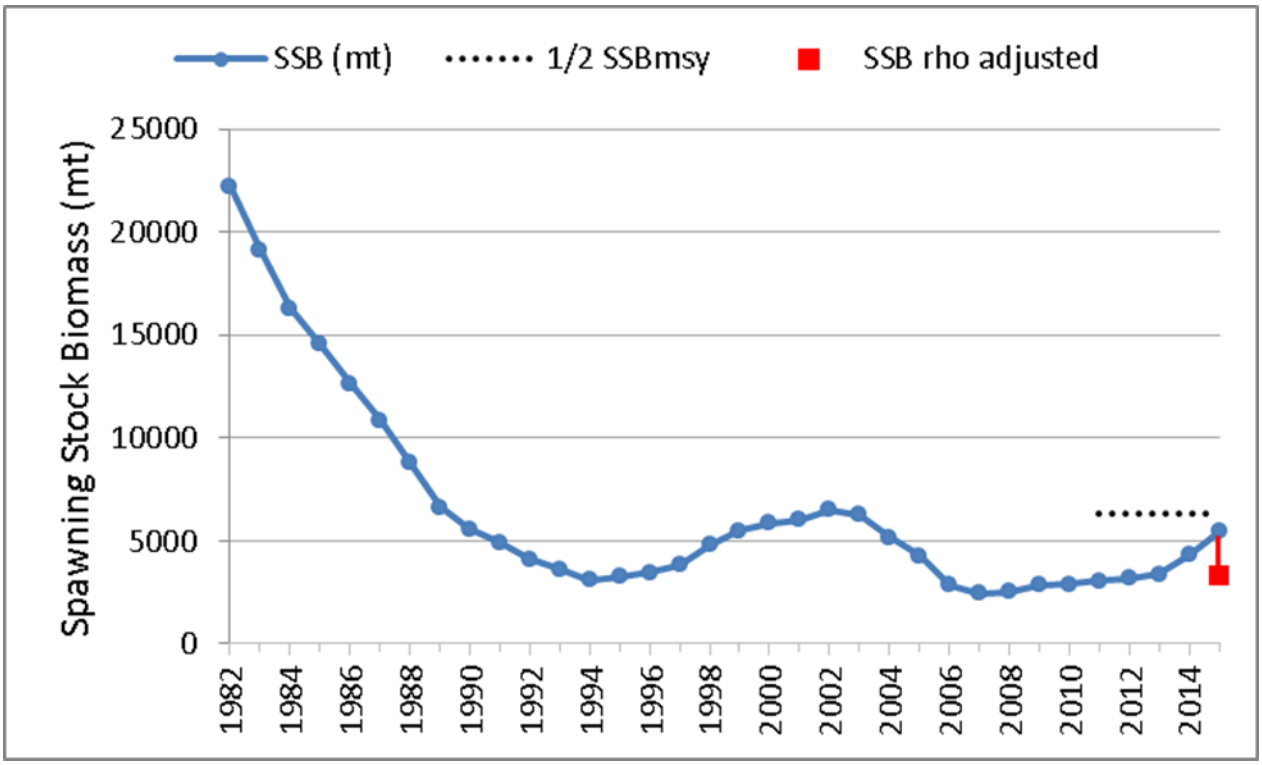

Figure B171. Estimated trends in the spawning stock biomass (mt; blue line with circle) of witch flounder between 1982 and 2015 and the corresponding $SSB_{threshold}$ (1/2 SSB_{MSY}; black dashed line) based on ASAP Run 9_5_v2. The 2015 retrospective adjusted SSB (SSB rho adjusted; red square) is also shown.

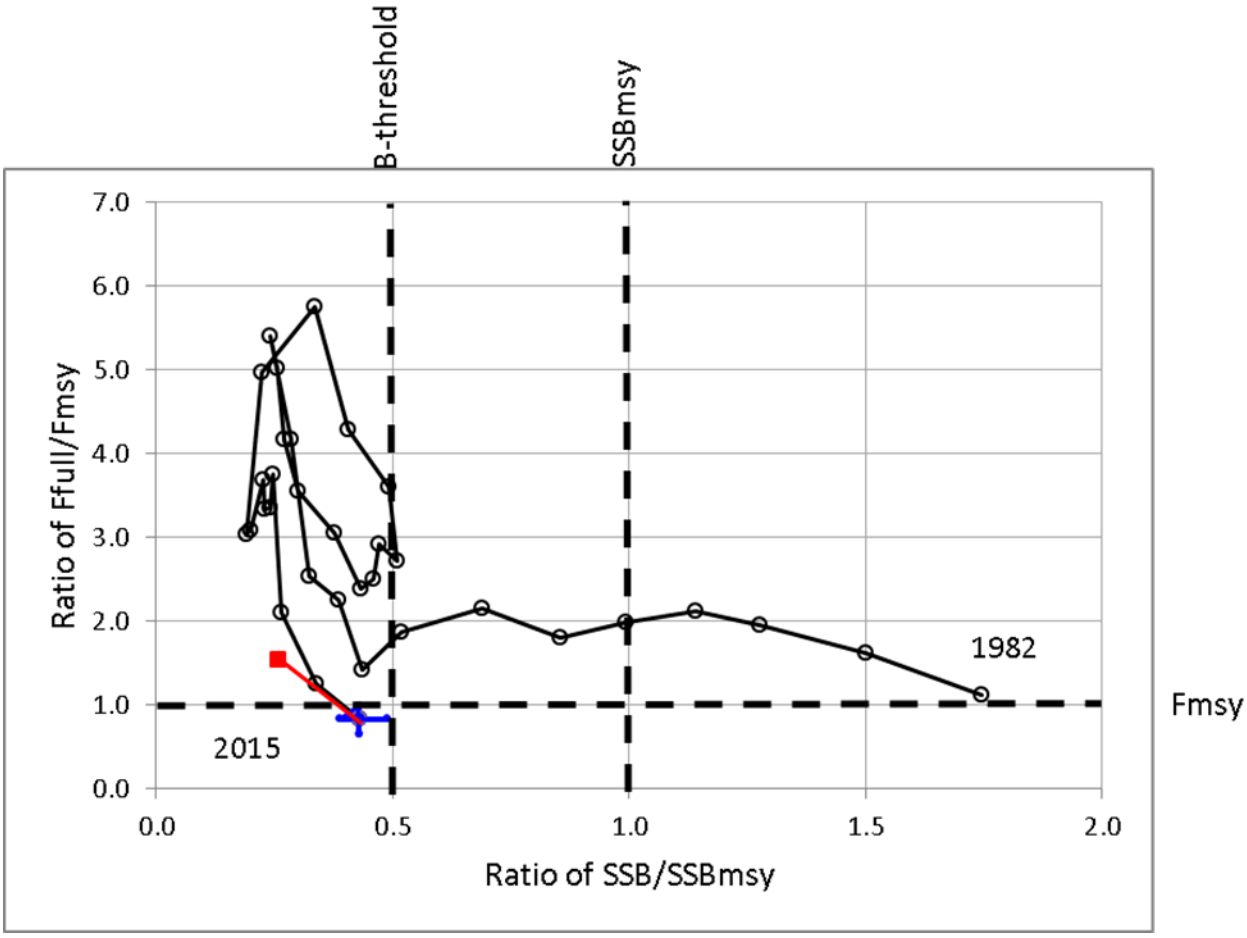

Figure B172. Time series plot of the witch flounder fully selected fishing mortality/F_{MSY} ratio relative to the spawning stock biomass/SSB_{MSY} ratio from 1982 to 2015 (black line with open circles) based on ASAP Run_9_5_v2. The retrospectively adjusted current stock status is indicated with a red solid square; the unadjusted stock status (blue solid circle) along with the corresponding 90% confidence intervals (blue lines) is also shown.

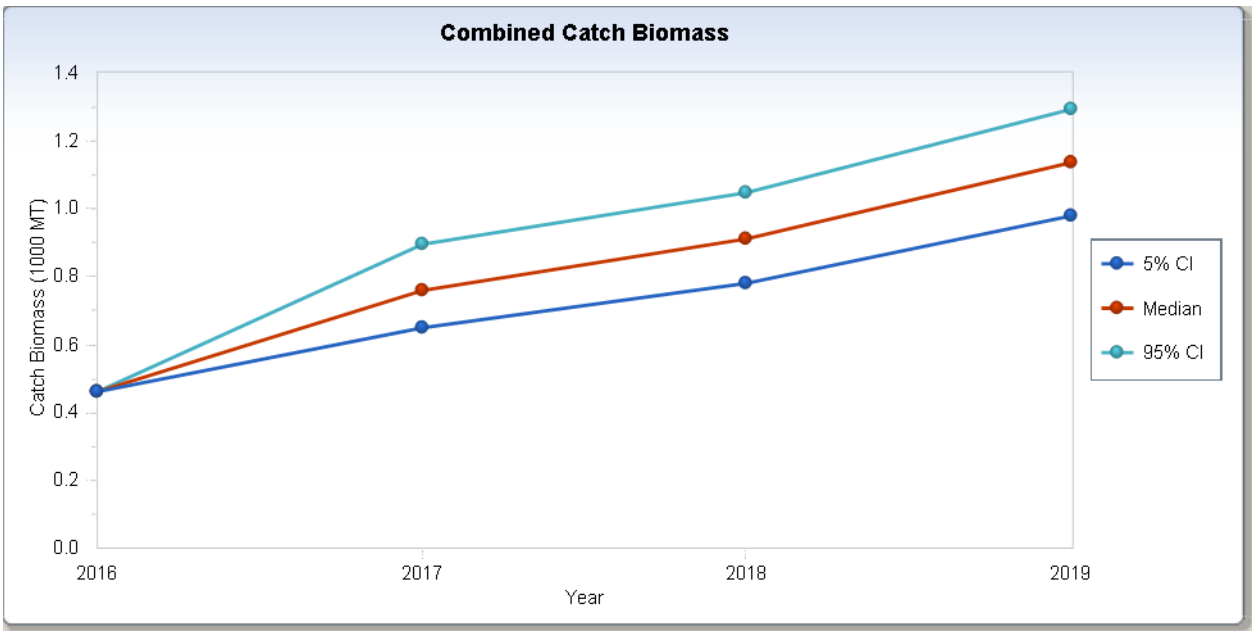

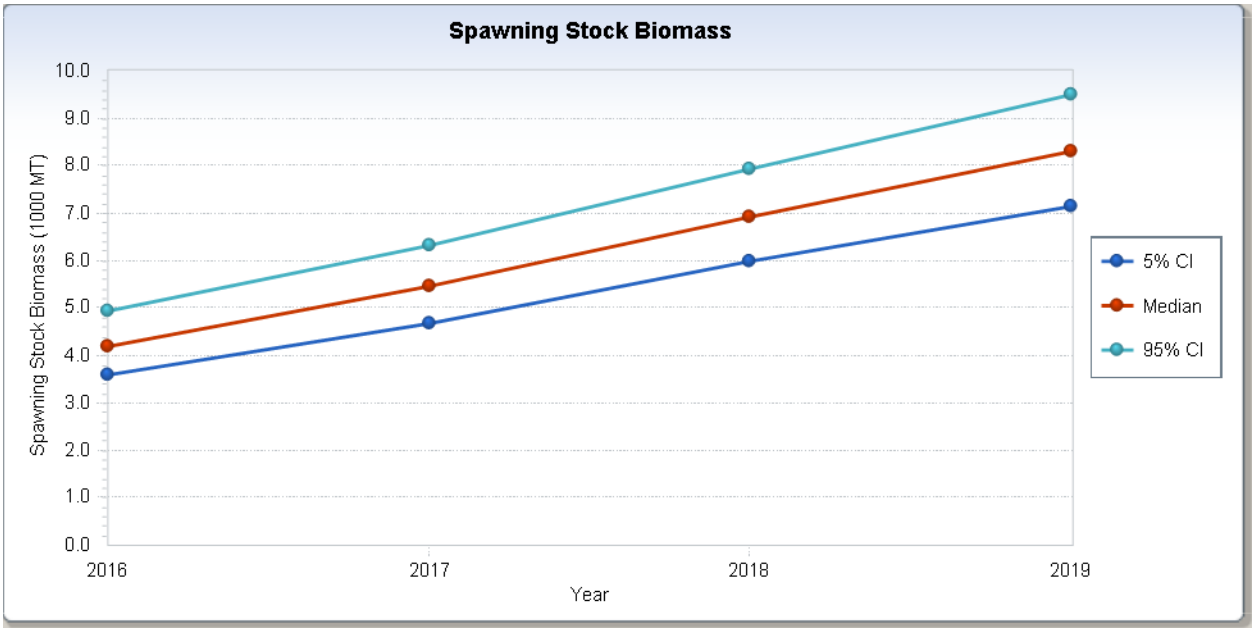

Figure B173**.** Short-term projections of total fishery yield (‘000s mt; top) and spawning stock biomass (‘000 mt; bottom) for witch flounder based on an assumed catch of 460 mt in 2016 and fishing at $F_{40\%}$ between 2017 and 2019. A retrospective adjustment (0.6608) was applied in the projections from ASAP Run_9_5_v2.

Appendix Figures

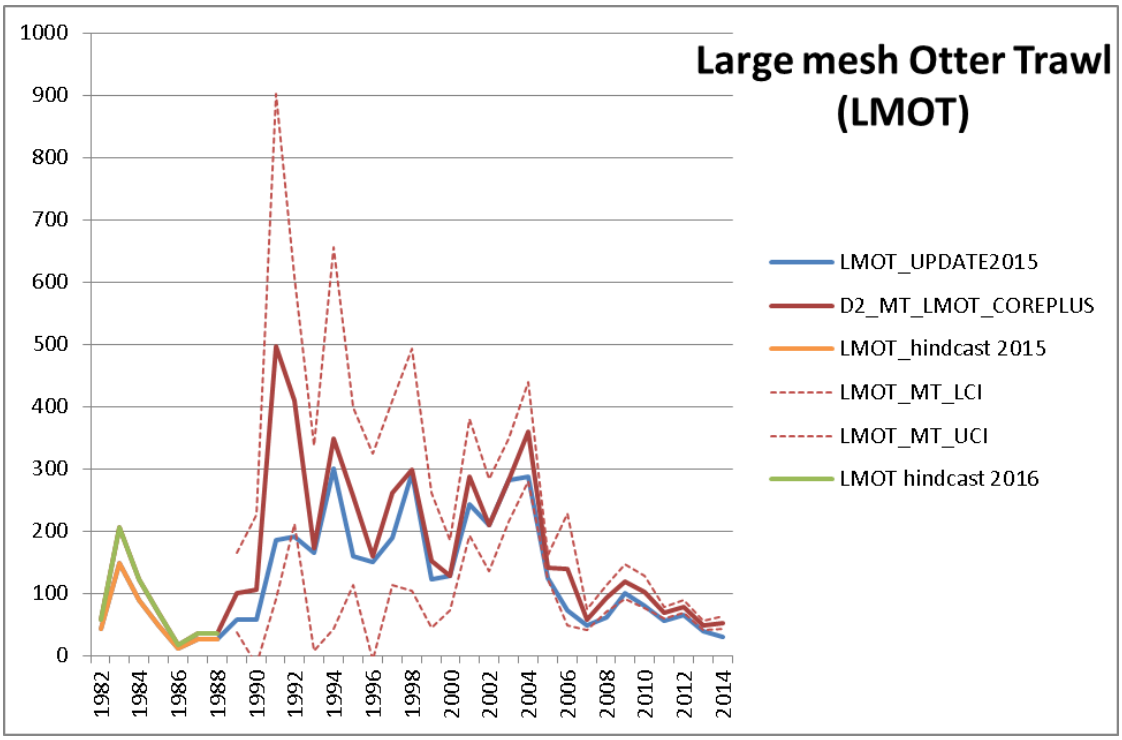

Appendix Figure B1. Witch flounder discards (mt; solid lines) with 95% confidence intervals (dashed lines) in the large mesh otter trawl fishery, 1982-2014.

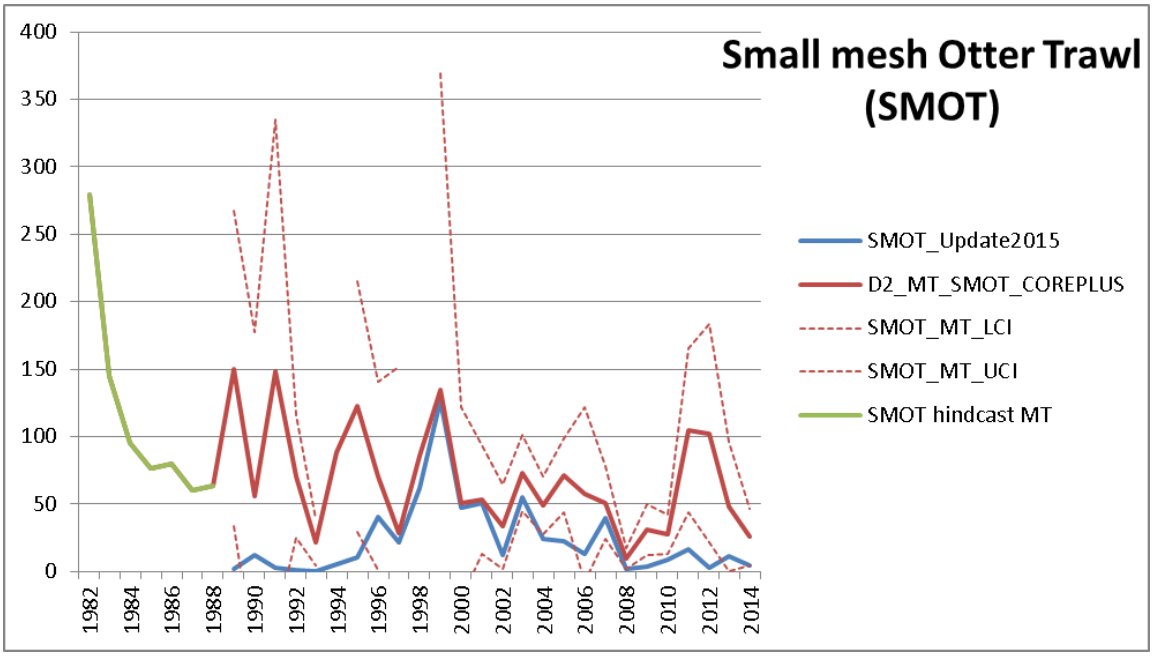

Appendix Figure B1. Witch flounder discards (mt; solid lines) with 95% confidence intervals (dashed lines) in the small mesh otter trawl fishery, 1982-2014.

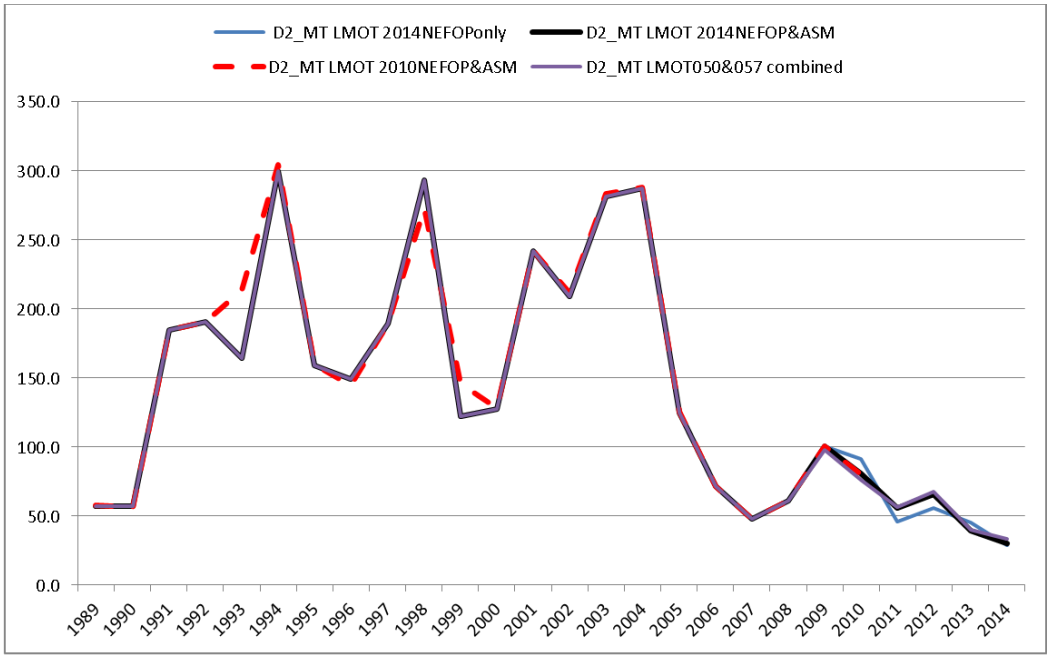

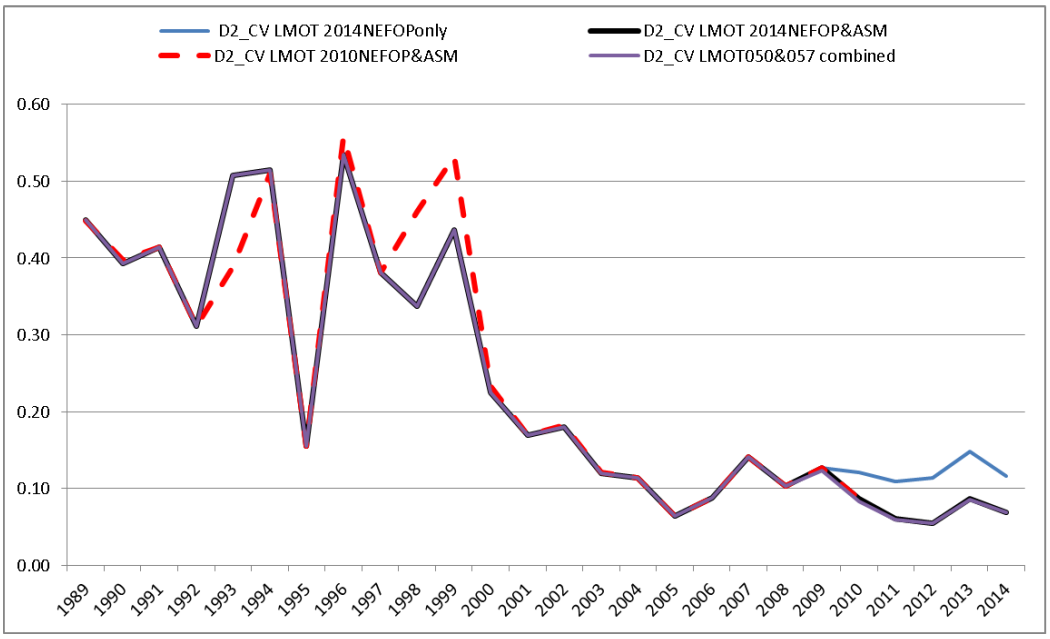

Appendix Figure B2. Comparison of large mesh otter trawl discards derived using Northeast Fisheries Observer Program (NEFOP) and At-Sea Monitoring (ASM) data (black line) and large mesh otter trawl and haddock separator trawl (combined) discards using NEFOP and ASM data (purple line) for the CORE region. Large mesh otter trawl discards using NEFOP only (blue line) and large mesh otter trawl discards using NEFOP and ASM data from the 2012 Update (red dashed line) are also given for perspective.

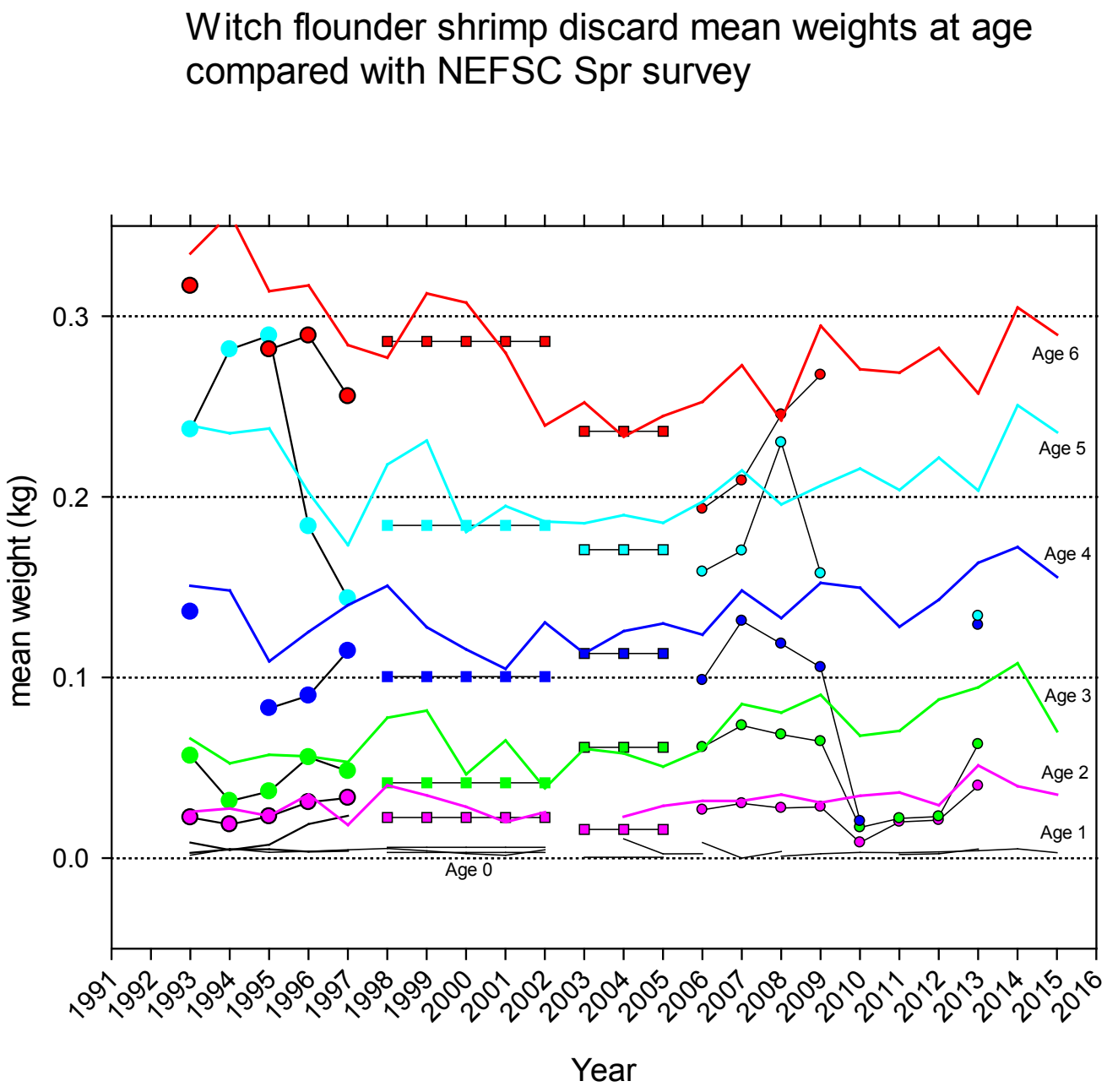

Appendix Figure B3. Witch flounder mean weight at age for discarded fish in the Gulf of Maine shrimp trawl fishery, 1993 – 2015. Means weights at age derived from Northeast Observer Program discard length frequency and Northeast Fisheries Science Center spring survey age data age are indicated with circles; average mean weights at age for 1989-2002 and 2003-2005 are derived using the 5 year weighted mean weights. Spring survey mean weights at ages (solid lines with no symbol) are also show for comparison purposes only.

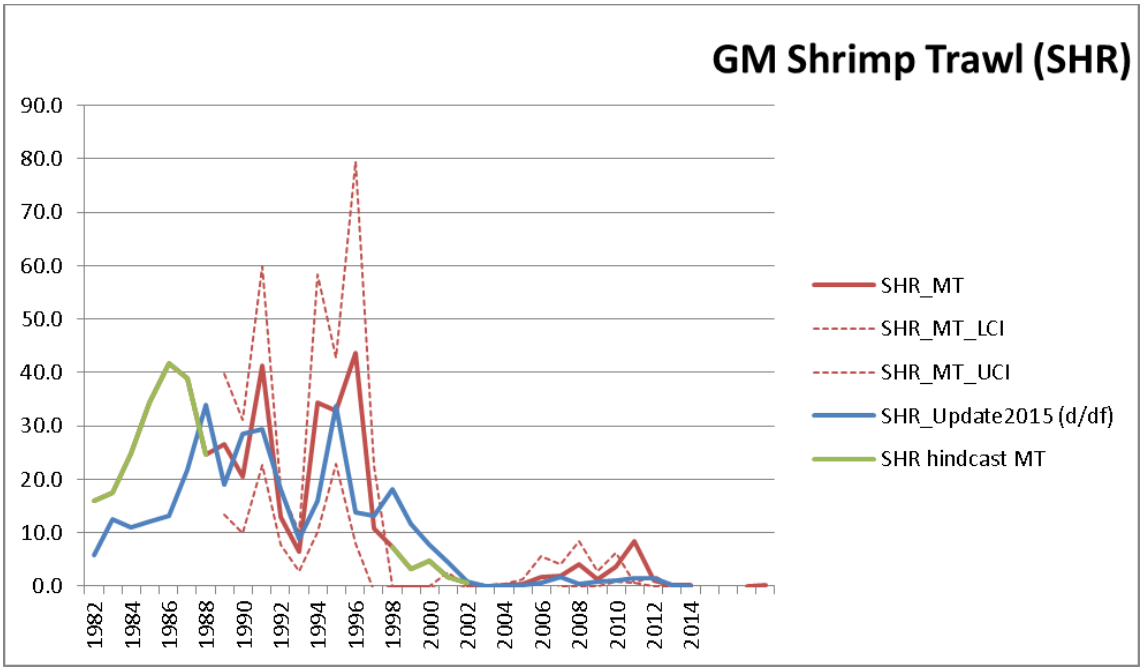

Appendix Figure B4. Witch flounder discards (mt; solid lines) with 95% confidence intervals (dashed lines) in the Gulf of Maine shrimp trawl fishery, 1982 to 2014.

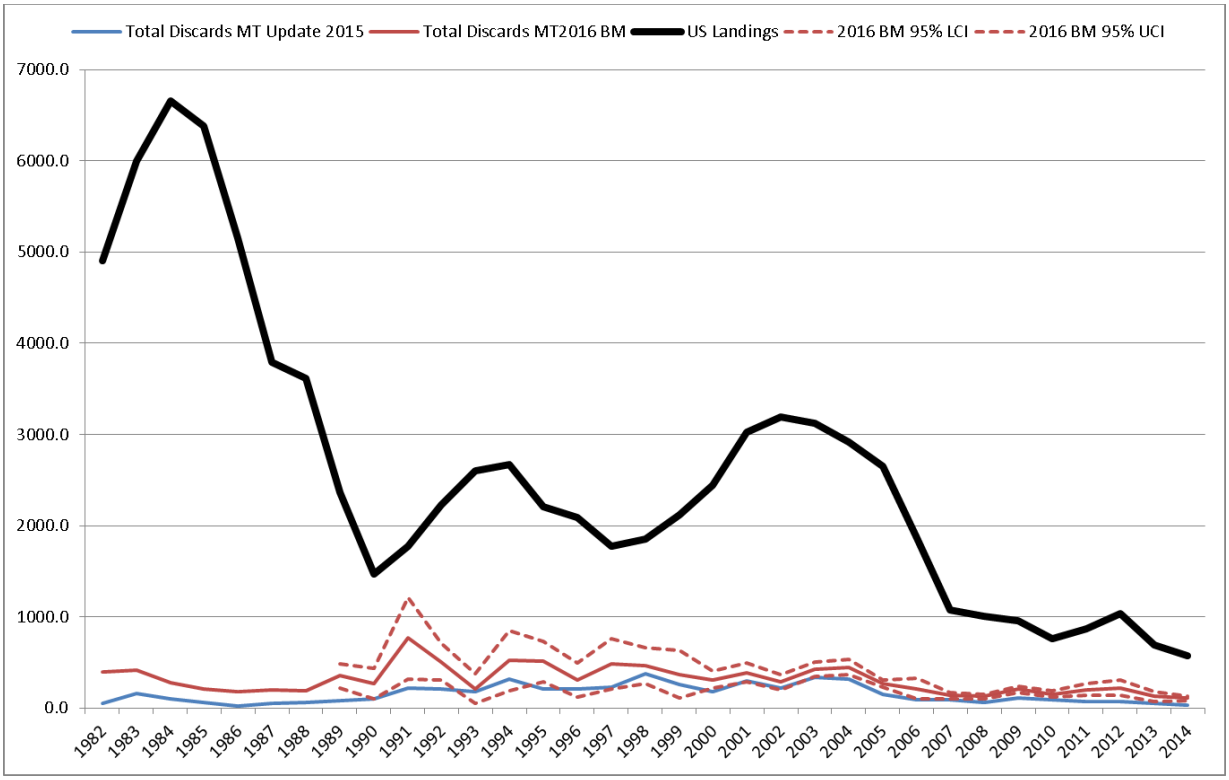

Appendix Figure B5. Witch flounder landings (mt; bold solid line) and total discards (mt; blue line) from the 2015 Update and total revised discards (mt; red line) with 95% confidence intervals, 1982 – 2014.